Characterisation of Novel Compounds as antagonists of Protease-Activated Receptor-2 (PAR2)

Taghreed Sabah Saeed Al-Rawi

A thesis submitted in the fulfilment of the requirements for the degree of Doctor of Philosophy

November 2018

Strathclyde Institute of Pharmacy and Biomedical Sciences (SIPBS)

Glasgow, UK

Acknowledgement

First, I would like to thank Allah for giving me this opportunity to pursue a Ph.D. degree in the United Kingdom. Also, this achievement would not be possible without the support of my parents back home who continuously prayed for this moment of time to come.

The research and work towards the degree for four years could not be accomplished without the supervision, guidance, advice, and patience of Professor Robin Plevin who supported me immensely. I am also in debt to Dr Kathryn McIntosh for her assistance in research and in proofreading of my thesis. Katy, you have always kept your doors open when problems arise for general discussions, directions in research and technical support.

My thanks to Dr Musab Bhutta and Dr Margaret Cunningham, who assisted, encouraged and solved a few technical issues in my research. Thanks to Dr Craig Jamieson who prepared GB88 and other relative compounds in the progression of my lab work. Thanks to my scientific partner Dr Shilan Jabbar. I like to pass my thanks to all members in Plevin's lab. I would also like to thank Dr Fakhir Al-Naeme who paved my path in science approaches, writing and moral support. His words made me an 'optimist' towards achieving my goal and opportunity towards the Ph.D. degree'.

I would like to extend my thanks to the Ministry of Higher Education in Iraq and University of Anbar for awarding me for this PhD scholarship and providing me with the financial support to study in the United Kingdom.

Poster Communications

Taghreed Saaed Al-Rawi, Kathryn McIntosh, Craig Jamieson, Robin Plevin, **Modulating PAR2 signalling by novel compounds based on GB88**. British Pharmacological Society meeting 15th -17th December /2016, London. UK.

Taghreed Saeed Al-Rawi, Kathryn McIntosh, Craig Jamieson, Robin Plevin, **Modulating PAR2 signalling by novel compounds based on GB88**. Research day University of Strathclyde. 11th November 2016. Glasgow UK

Abstract

Protease-activated receptor-2 (PAR2) is a G-protein coupled receptor that is activated through proteolytic cleavage of the N-terminus leading to the coupling to a number of defined second messenger systems though G-protein engagement. Early signalling events such as the mobilisation of intracellular Ca^{2+} and downstream cascades including ERK MAP kinase mediate an array of cellular effects stimulated through PAR2. Many studies have demonstrated the involvement of PAR2 in a number of disease pathologies including arthritis, GI disorders and inflammatory pain. However, treatments for these and other conditions have been limited by the lack of potent and selective small-molecule antagonists. Recently, a number of new putative antagonists including GB88 and AZ8838 have been proposed to be effective in cells and *in vivo*. However, given the relative lack of information about these compounds this thesis examined the characteristics of these compounds in a number of PAR2 mediated cellular assays.

In Chapter 3 it was found that 2f-LIGRLO-NH$_2$ and trypsin activated NFκB-transcriptional activity in a PAR2 overexpressing cell line with potencies as expected from other studies. Somewhat surprisingly, GB88 and a number of derivatives generated in-house, behaved as partial agonists compared to synthetic peptide 2f-LIGRLO-NH$_2$ in stimulating reporter activity with reduced efficacy but moderate potency. They were largely ineffective as antagonists. In HEK293 where PAR2 expression was moderate, GB88 derivatives also stimulated the phosphorylation of ERK again with reduced efficacy and lower what compared with synthetic peptide. Moreover, intracellular calcium mobilisation mediated by PAR2 coupling to $G_{q/11}$ as determined by treatment with YM254890 was also activated by GB88 and related compounds with similar characteristics. In neither assay did GB88 act as a antagonist compound.

Studies in chapter four examined the effect of the novel PAR2 antagonist, AZ8838 both as a racaemic mixture and as a pure compound. It was found to inhibit PAR2

induced NFκB-transcriptional activity in NFκB-Reporter cells in a concentration dependent manner confirming its identification as an allosteric modulator. AZ8838 also decreased ERK and p38 MAP kinase stimulated by either 2f-LIGRLO-NH$_2$ or trypsin in NFκB-Reporter cells as well as inhibiting phosphorylation of ERK in HEK293 cells. In addition, AZ8838 had the ability to reduce PAR2-mediated calcium mobilisation in a time dependent fashion with maximum inhibition observed following preincubation for 30 minutes or more. These effects were consistent for the S-AZ8838 isomer whilst R-AZ8838 is not.

Taking together these studies suggest that GB88 may have different pharamcological prpoerties in different systems but that AZ8838 has the potential to be a truly breakthrough compound. If the ADMET properties of AZ8838 are good this compound could be used in clincal studies for the treatment of inflammatroy disorders.

Abbreviations

ANOVA	Analysis of variance
AP	Activating peptide
APC	Activated Protein C
APS	Ammonium Persulphate
ATP	Adenosine triphosphate
BSA	Bovine Serum Albumin
Ca^{2+}	Calcium ion
CNS	Central Nervous System
CVS	Cardiovascular system
DAG	Diacyleglycerol
DMEM	Dulbecco's Modified Eagle Medium
DMSO	Dimethyl sulfoxide
DTT	Dithiothreitol
ECL	Enhanced chemiluminescence
ECL2	Extracellular loop 2
EGFR	Epidermal growth factor receptor
ERK	Extracellular Signal-regulated Kinase
FVIIa	Activated factor VIIa
Fxa	activated factor X
GDP	Guanosine diphosphate
GM-CSF	Granulocyte monocyte-colony stimulating factor
GPCR	G-protein coupled receptor
G-Protien	GTP-binding protien
Grb2	Growth factor receptor-bound protein 2
GRK	G-protein coupled receptor kinase
GTP	Guanosine triphosphate
HEK	Human Embryonic Kidney
ICL	Intracellular loop
IkB	Inhibitory kappa B
IKK	inhibitory kappa kinase B

IL-6	Interleukin-6
IL-8	Interleukin-8
IP$_3$	Inositol 1,4,5-triphosphate
kDa	Kilo dalton
KO	Knockout
MAPK	Mitogen activated protein kinase
MCP-1	Monocyte chemotactic protein-1
NAM	Negative allosteric modulators
NFκB	Nuclear Factor Kappa B
NO	Nitric oxide
OA	osteoarthritis
OR	Opioid receptor
PAM	Positive allosteric modulators
PAR	Protease activated receptor
PBMC	Human peripheral blood mononuclear cells
PGE2	Prostaglandin E$_2$
PKC	Protein kinase C
PLC	Phospholipase C
PTX	Pertussis toxin
RT	Room temperature
SDS	Sodium Dodecyl Sulphate
SDS-PAGE	Sodium dodecyl sulphate polyacrylamide gel electrophoresis
siRNA	Small interfering RNA
TEMED	N,N,N',N' tetramethendiaamine
TF	Tissue factor
TH2	T helper cytokine-2
TL	Tethered Ligand
TLR4	Toll-Like Receptor 4
TM	Transmembrane
TNFα	Tumour Necrosis Factor-alpha
WT	Wild-type

Table of Contents

List of figures

List of table

Chapter One

General Introduction

1.1 G-protein coupled receptors

A major group of receptors within the mammalian system are the G-protein coupled receptors (GPCRs). These are primarily cell surface receptors found on the plasma membrane and comprise of seven transmembrane domains (Audet and Bouvier, 2012). GPCRs mediate many biological events through activation of downstream signalling pathways in cells and are the focus of intense study since the majority of medicines interact with this class of receptor. Transducing signals are transmitted from external stimuli across the plasma membrane to the cytoplasmic region, which then allows the initiation of cellular signalling events (Lagerstrom and Schioth, 2008, Kruse *et al*., 2013). There are two basic paradigms involved in the activation of GPCRs by extracellular ligands; firstly, by reversible binding of a soluble agonist with extracellular and transmembrane domains of the receptor, secondly, by irreversible activation when proteases cleave the receptor within the extracellular-N-terminal forming a new N-terminal ligand, which binds to the receptor. This latter model is confined to very few GPCRs. Upon receptor activation, intracellular second messenger signalling is initiated by binding of the receptor to heterotrimeric G proteins or β-arrestins linking these receptors to a vast array of downstream pathways (Congreve *et al*., 2011, Kruse *et al*., 2013).

There are have approximately 800 receptors of GPCRs encoded within the human genome (Lagerstrom and Schioth, 2008). The rhodopsin GPCRs are divided into sub-classes which comprises six receptors; rhodopsin, β1 and β2 adrenergic, adenosine A_{2A}, CXCR4, and dopamine D3 receptors (Congreve *et al*., 2011). There are four major subfamilies of human GPCRs that are classified based on the sequence conservation including rhodopsin-like family (Class A), secretin and adhesion family (Class B) (Archbold *et al*., 2011), glutamate family (Class C) (Kniazeff *et al*., 2011), and frizzled family (taste receptor)(Class F) (Fredriksson *et al*., 2003, Krishnan and Schioth, 2015), as illustrated in figure 1.1.
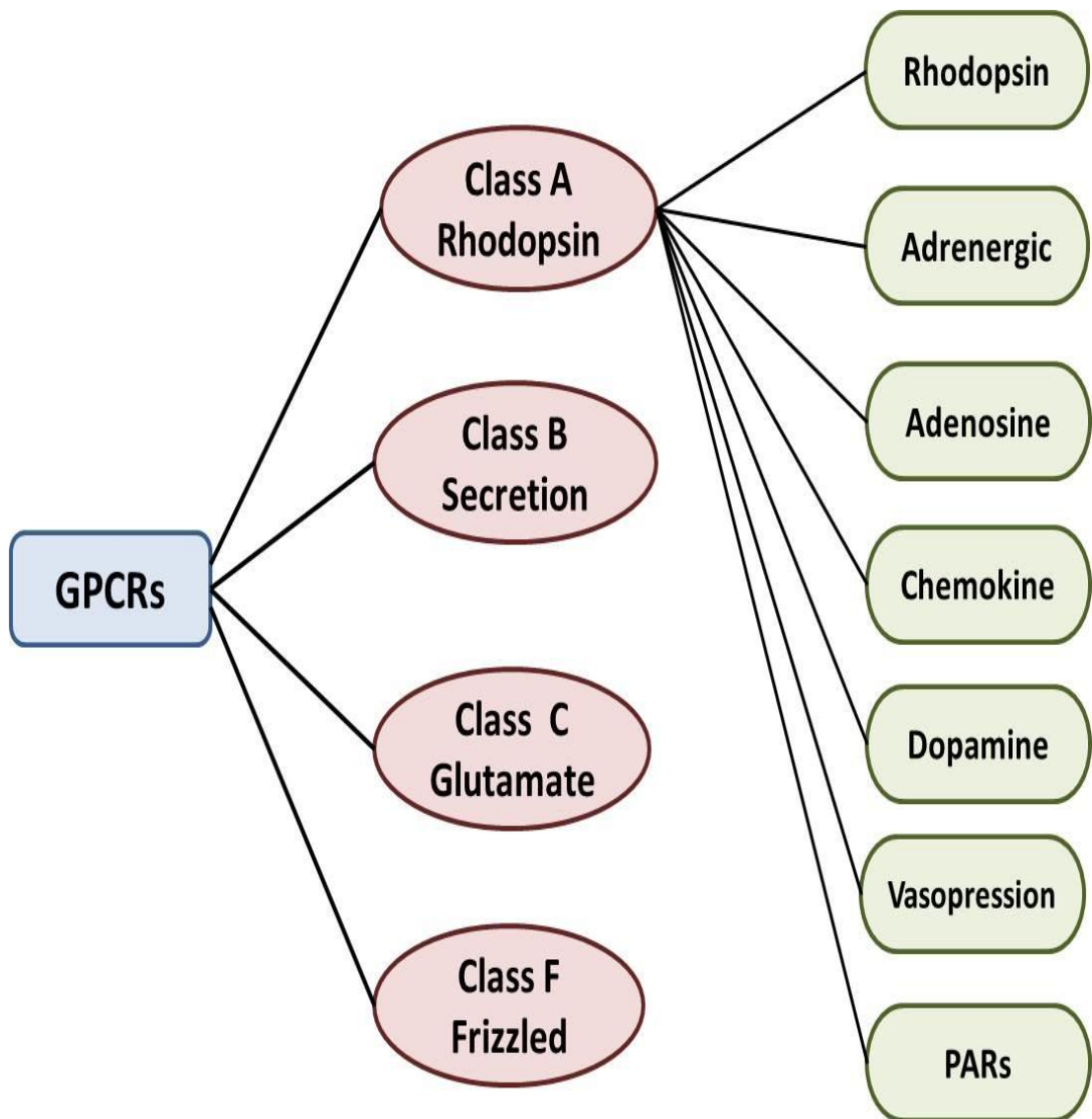
Figure 1. 1 Flowchart depicted the families of GPCR and the sub-families of rhodopsin GPCR.

The largest and most advanced GPCR subfamily in the mammalian genome is the Class A (Rhodopsin), rhodopsin is the first structure investigated by X-ray crystallography in 2000 (Palczewski *et al*., 2000). Class A is also subdivided to 19 groups (A1-A19) (Joost and Methner, 2002) and whilst the crystal structures of a number of these receptors have recently been resolved, this is only in the inactive state (Stenkamp *et al*., 2002). Class A GPCRs are stimulated by small molecules such as purine, amines, fatty acids, prostaglandins and glycoproteins (Hopkins and Groom, 2002). The structure of Class A receptors consists of an extracellular NH_2-terminal domain, seven transmembrane helices (TM1-TM7) with three intracellular hydrophilic loops (ICL1-ICL3) and three extracellular loops (ECL1-ECL3). The binding between ECL2 and TM3 is through a disulphide bridge; also, the C-terminal in the cytoplasm is parallel to the cell membrane containing an α-helix (Rosenbaum *et al*., 2007). The structure of Class A GPCR monomers was first demonstrated by Whorton and colleagues who identified monomeric β2-adrenergic receptors activated by coupling to G proteins (Whorton *et al*., 2007).

Class A GPCRs have very short NH_2-terminus domains, making them unable to bind with other molecules. There are many members of Class A GPCRs, including; $β_2$-adrenergic receptor, the sphingosine-1-phosphate (S1P) receptor, serotonin receptor (5-HT) and aminergic receptors. Another divergent subclass for class A GPCRs exist, which includes; vasopression receptors (V_{1A}, V_{1B}, V_2), oxytocin receptor (OT), prokineticin receptors (PKR1 and PKR2), melanocortin receptors (MC1-5) and protease-activated receptors (Akers *et al*.) (Gruber *et al*., 2010, Catania *et al*., 2004, Coughlin, 2000).

The second subfamily of GPCRs is the Secretin and Adhesion family (Class B) comprised of a seven-transmembrane structure linked to a very long NH_2-terminal (Yona *et al*., 2008). It consists of 15 receptors with a NH_2-terminal structure and these receptors are stimulated by large peptide hormone ligands such as glucagon-like peptides (GLP1), calcitonin and glucagon (Congreve *et al*., 2011). The main aspect of the Secretin family is the presence of orphan receptors (receptors for which

a ligand has not been determined) and for this reason drug discovery for this subclass has stalled.

Another member of GPCRs family is Class C or known as the glutamate family. This family consists of amino acids glutamate receptor γ-aminobutyric acid (GABA) receptor, calcium sensing receptor and taste receptors (Pin *et al*., 2003).

The ligands for GPCRs are catalogued depending on chemical structure; aminergic, lipidergic or synthetic small molecules and are classified based on whether they are peptides or organic compounds. Another classification of GPCR ligands depends on the mode of action; agonist or antagonist (Przydzial *et al*., 2013). Agonists usually bind to a specific region on GPCRs leading to receptor activation. In comparison, antagonists bind to the receptor blocking the activation site used by agonists. More specifically, GPCRs have an orthosteric ligand binding pocket which is located in the extracellular half of the helix bundle and comprises of helices III, VI and VII residues. The site of orthosteric binding in class A GPCRs is within the middle of the 7TM helical bundle, between the middle plane of the membrane and the extracellular loops (Dror *et al*., 2011). The orthosteric binding site facilitates binding of the endogenous ligand.

In some instances ligands bind to GPCRs at a site distinct from the orthosteric site, in this case the ligand is known as an allosteric modulator, as it binds to the allosteric site (Keov *et al*., 2011). There are two types of allosteric modulators; positive allosteric modulators (PAMs) and negative allosteric modulators (NAMs). The interaction of the allosteric modulator with the orthosteric site is not direct, it occurs via the function of the allosteric ligand; NAM or PAM. A ligand is referred to as a bitopic ligand when the agonists or antagonists can bind to both the allosteric and orthosteric site of the receptor (Christopoulos *et al*., 2014).

The activating GPCRs bind to small G proteins or arrestins resulting to intracellular signalling pathways. For example, when the receptor binds to G proteins primarily via a range of G-protein alpha subunits (G_α), second messengers are liberated usually

through enzymatic activation of a substrate. Well-recognised second messengers include; cAMP, Ca^{2+}, IP_3, and diacylglycerol (Schaffhauser *et al*.). When the receptor binds to the $G_{\beta\gamma}$ sub-unit, downstream signalling events such as ion channel regulation, phospholipase activation, and receptor kinases are also activated (Rasmussen *et al*., 2011). Additionally, GPCRs interact with a family of proteins called beta-arrestins which facilitates internalisation and desensitisation and in some instances mediates MAP kinase signalling (Kang *et al*., 2015). This will be discussed in more detail with reference to PAR2 later in the chapter.

At a structural level signals are activated via G-proteins when GTP binds to G-proteins at TM3, TM5, TM6, while the signalling via arrestin works within the spatially distinct TM1, TM2 and TM7 loops (Liu *et al*., 2012). The third TM loop is considered the most critical helix in the GPCR structure as it confers ligand binding and receptor activation (Venkatakrishnan *et al*., 2013).

Group A GPCRs differ from Class B and C as they have the ability to engage with ligands in both the orthosteric and allosteric sites, known as dualsteric ligands (Congreve *et al*., 2011). The formation of the orthosteric ligand binding pocket is via residue helices III, VI and VII and is placed in the extracellular half of the bundle. The helix V for β-adrenoceptors is a residue helices which gives specific ligand contacts then leads to essential determinant for ligand efficacy (Warne and Tate, 2013).

1.2 GPCRs as a drug target

GPCRs have long been a major and attractive pharmaceutical target for drug design and therapeutic intervention, the reason being that GPCRs have effects on many physiological and pathological outcomes including the allergic response, control of blood pressure, kidney function, central nervous function, inflammatory disorders and cancer (Luo *et al*., 2009). Whilst major advances have been based on developing agonists and antagonists which compete for binding to the orthosteric site, the field has now become more advanced. Currently the drug discovery field for GPCRs is

focused on modulating the activity of GPCRs via two methods; either using small molecule positive allosteric modulators (PAMs) which increase the activity of the orthosteric agonist for the receptor or by negative allosteric modulators (NAMs) which decrease the potency of the orthosteric ligand for the receptor (Bridges and Lindsley, 2008). In fact reappraisal of current drugs have identified that one third of those on the market actually target the receptor in this way and could be further optimised (Rask-Andersen *et al*., 2011). The development of new selective allosteric modulators discovered by modern pharmacology techniques have the potential to expand the field further in addition to developing traditional agonists or antagonists (Valant *et al*., 2012). Further, more allosteric modulators have the ability to direct downstream signalling via binding with specific G-proteins or β-arrestin activated pathways and this may be an additional benefit (Reiter *et al*., 2012).

Development of new drugs targeting GPCRs is a lengthy and expensive process and requires a multitude of steps. A key advantage is for a drug to have a high "drug target value" based on a heterogeneous distribution of the receptor which allows selective targeting (Jacoby *et al*., 2006). There are also many elements, which contribute to drug effectiveness and safety; these elements include absorption, distribution, metabolism, excretion, and toxicity (ADMET). The compounds must be designed within the upper limits of Lipinski's rules that are associated with molecular weight and lipophilicity. During drug development, it should decrease the risk of ADMET properties that assist for its clinical application (Lipinski *et al*., 2001). The clinical failure occurs via the cross-reactivity and toxicity which increases with both molecular weight and increasing lipophilicity compounds (Leeson and Springthorpe, 2007, Empfield and Leeson, 2010).

Another key advantage is having a high resolution 3D structure of the protein in the active state and bound to an appropriate ligand usually derived from X-ray crystallography (Lee *et al*., 2015). This allows close interrogation of both orthosteric and allosteric binding pockets. This advance has enabled further development in drug design for example, the 3-D structures of two types of serotonin receptor (5-HT$_{1B}$ and 5-HT$_{2B}$) were evaluated in terms of drug design with the effective creation of an

antimigraine drug (ergotamine) which binds effectively to both 5-HT$_{1B}$ and 5-HT$_{2B}$ receptors (Wacker *et al*., 2013).

Another issue, which is relevant in drug discovery, is the emergence of bias agonists/antagonists (Liu *et al*., 2012). These act by directing signalling down one pathway whilst blocking another, important physiological functions directed by the receptor can be maintained while only certain signalling aspects responsible for the undesirable effects in disease can be blocked. This type of approach also reduces the side effects often seen with blanket inhibition of receptor function (Tautermann, 2014). However to date, no bias ligands are used clinically to treat disease.

According to a study by Congreve *et al*; 63 drugs were discovered and marketed from the period (2000-2009), however most of these drugs target family A GPCRs (Congreve *et al*., 2011). Up to 2013, published pharmaceutical compounds consisted of; 20 class A, 2 class B, one class C and one frizzled class drug (Stevens *et al*., 2013). It seems to be more of a challenge to develop drugs for Class B and Class C GPCRs, as low druggability is a feature of both classes (Tautermann, 2014, Lee *et al*., 2015).

Lafferty-Whyte *et al* has identified more than 100 human genes encoding GPCRs for clinical development and approximately 400 small molecules as current therapeutic drugs (Lafferty-Whyte *et al*., 2017). About 50% of solved Class A GPCRs have been exploited in drug development and pharmacology. Some of these include the muscarinic receptor antagonists, 3-quinuclidinyl-benzilate (QNB) and tiotropium, and carazolol that act as a partial inverse agonist for β$_2$AR. Resolution of the dopamine D3 has underpinned the development of eticlopride and for PAR1, vorapaxar (Katritch *et al*., 2013, Tautermann, 2014).

Plavix is one of the anti-thrombotic GPCR related drugs that is activated as a prodrug in the liver (Beitelshees and McLeod, 2006). Other GPCR-related drugs are Maraviric (NAM) for the class A chemokine receptor CCR5, this drug is used in HIV therapy as an inhibitor for entry of the virus. Another drug; plerixafor acts to

decrease the activity of the chemokine receptor CXCR4, it is used in lymphoma and multiple myeloma patients to mobilize autologous stem cells for transplantation. In addition, cinacalcet is a PAM (class C GPCR) acting on the calcium-sensing receptor and is used to treat hyper-parathyreodism. Recent GPCR modulators that have been discovered include; Naloxegol which is an opioid receptor (OR) antagonist and functions by restraining intestinal absorption by blocking the adverse effects of systemic opiates (Zhang *et al*., 2014). In addition; many GPCR directed drugs have been reported as sleep condition remedies; for example, Suvorexant acts as an antagonist for the orexin receptor and is used to treat insomnia (Cox *et al*., 2010). Another drug approved for treatment of insomnia is BMS-214778 (tasimelteon) which acts on the melatonin receptor (Vachharajani *et al*., 2003). Clearly, examination of GPCRs still has the potential to generate new targets and molecules including members of the protease-activated receptor (PAR) family.

1.3 Protease-activated receptors

Protease-activated receptors (Akers et al.) are Class A GPCRs and were first discovered in the early 1990s (Vu *et al*., 1991). PARs have the classic seven transmembrane domain and couple to heterotrimeric G-protein G(α) subunits; G$\alpha_{q/11}$, Gα_s, Gα_i , G$\alpha_{12/13}$, leading to intracellular signalling (Rohatgi *et al*., 2004, Sokolova and Reiser, 2007, Steinhoff *et al*., 2005, Wang and Reiser, 2003). PARs have a distinctive mechanism of activation; they are enzymatically activated by a variety of serine proteases via cleavage of the receptor at a specific site within the extracellular N-terminus resulting in exposure of a new tethered ligand (TL), as shown in figure 1.2. The new tethered ligand interacts with the second extracellular loop (ECL2) (Coughlin, 2000). A conformational change of the receptor initiates downstream intracellular signalling and functional responses (Adams *et al*., 2011, Macfarlane *et al*., 2001).

Four members of the PAR family have been described; PAR1, PAR2, PAR3 and PAR4 (Hollenberg and Compton, 2002). Different types of proteases activate PARs, for example, PAR1, PAR3, and PAR4 are activated by the coagulation protease thrombin (Grand *et al*., 1996, Cirino *et al*., 2000, Naldini *et al*., 2002, Oganesyan *et al*., 2002), while PAR2 is cleaved by mast cell tryptase (Molino *et al*., 1997a) and trypsin (Nystedt *et al*., 1994), amongst others. PAR4 can also be activated by trypsin (Xu *et al*., 1998, Hollenberg, 1999), although with a lower affinity compared to PAR2. PARs have important roles in cellular mechanisms, for example in clotting and inflammation. The expression of PARs is widespread and includes; endothelial cells, fibroblasts, exocrine glands, epithelial cells, mast cells, smooth muscle cells, keratinocytes, platelets, and others (Macfarlane *et al*., 2001).
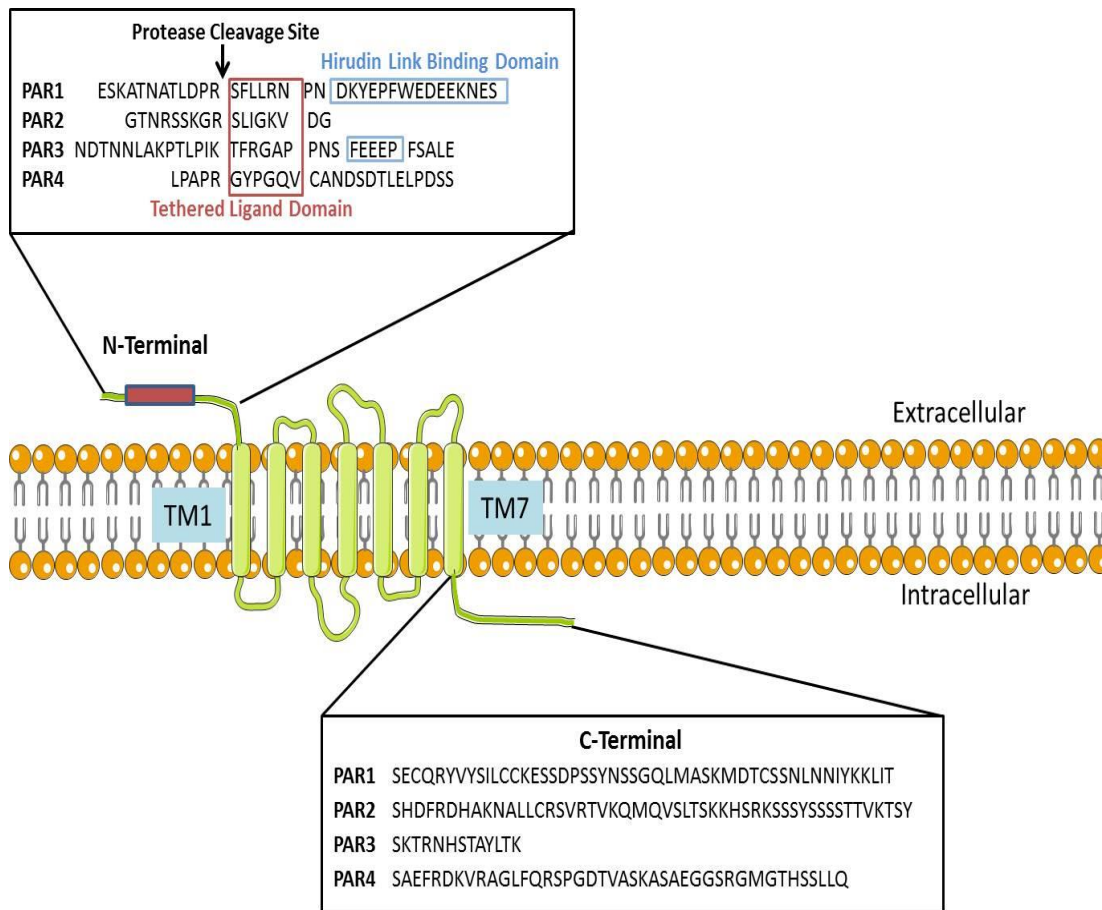
Figure 1. 2 Protein structure of PARs 1, 2, 3 and 4

Adapted from (Macfarlane *et al*., 2001).

The figure identifies the amino acid sequences within the N-terminal for all PARs and identifies the activating peptide and the C-terminus which identifies heterogeneity and potential differences in coupling to intracellular signalling pathways.

1.4 Protease activated receptor-1 (PAR1)

The first protease activated receptor (PAR1) was conceptualised by studying the coagulation process; thrombin was found to have cellular effects which could not be explained by its action within the coagulation cascade (Davey and Luscher, 1967). However, the identification of PAR1 as the cognate receptor for thrombin was only made possible through the work of Shuan Coughlin and co-workers who cloned and characterised the receptor (Vu *et al*., 1991). Thrombin is not just produced in coagulation, for example it has been isolated from brain tissue in parkinsonism-dementia and Alzheimer's diseases giving rise to the potential of PAR1 to have widespread effects out with the circulatory system (Arai *et al*., 2006). The PAR1 gene contains two exons and is localised on chromosome 5q13 (Schmidt *et al*., 1997). Exon 2 encodes the receptor, which comprises of 425 amino acids and the seven transmembrane (TM) structure. The receptor is comprised of a 41 amino acid extracellular amino-terminal, three extracellular loops (ECL regions 1, 2, 3), three intracellular loop (ICL regions 1, 2, 3), and an intracellular carboxyl terminal domain that has a small additional eighth helix of 50 residues. Significantly, PAR1 contains a hirudin-like binding domain within the N-terminus to facilitate high affinity thrombin binding (Macfarlane *et al*., 2001). There is a disulphide linkage connecting ECL2 with TM3, this bond is conserved in all types of GPCRs and has an important role structurally in the stability of the receptor (Hamm, 2001).

1.4.1 PAR1 activation

As indicated above PAR1 is activated by thrombin via cleavage of the exodomain N-terminus at the site (LDPR^{41}↓S^{42}FLLRN) (Ishii *et al*., 1995). This new tethered ligand sequence encompasses an active peptide, SFLLRN, which can be used to directly stimulate the receptor (Vu *et al*., 1991). A number of modifications of this peptide have been made including the addition of an N-terminal amino group to generate the more potent agonists, SFLLRNPN, SFLLRNP-NH$_2$, and SFLLRN-NH$_2$ (Scarborough *et al*., 1992). Over the last 20 years high affinity PAR1 drugs have been developed with clinical utility. These will be examined in more detail in Section 1.9.1.

1.4.2 PAR1 signalling

PAR-mediated signal transduction is considered to be similar to that of other GPCRs. PAR1-mediated signal transduction is through intracellular coupling to specific heterotrimic G proteins subunits. (Defea, 2008). When PAR1 is activated, it couples to one of the G-proteins $G_{\alpha12/13}$, $G_{\alpha i}$ or $G_{\alpha q}$, resulting in different major downstream signalling pathways that mediate an array of physiological outcomes (Soh *et al*., 2010). PAR1 couples to $G_{\alpha q/11}$ to activate phospholipase C (PLC) that catalyses the formation of diacylglycerol (Schaffhauser et al.) and inositol 1,4,5-triphosphate (IP_3) from inositol 4,5-biphosphate. IP_3 mediates calcium mobilization released from the endoplasmic reticulum into the cytosol, whilst DAG binds and activates protein kinase C (PKC) (Hung *et al*., 1992). This signalling pathway mediates cellular responses in a number of instances such as aggregation in platelets (Benka *et al*., 1995) and transcriptional activity in endothelial cells (Offermanns *et al*., 1997). A second signalling pathway mediated by PAR1 is a decrease in adenylyl cyclase activity via coupling of PAR1 to $G_{\alpha i}$, (Kanthou *et al*., 1996, Hung *et al*., 1992).

PAR1 has also been reported to couple to $G_{\alpha12/13}$ (Offermanns *et al*., 1994) leading to Rho-activated kinase activity (Fukuhara *et al*., 1999), Rho-dependent cytoskeletal responses such as migration in endothelial cells (Vouret-Craviari *et al*., 1998) and platelet shape change (Klages *et al*., 1999). PAR1 can also couple to Gβγ subunits to stimulate phosphoinositide-3-kinase (PI-3) (Stoyanov *et al*., 1995), and K^+ channels (Clapham and Neer, 1997).

In addition, PAR1 regulates cell growth, proliferation, and differentiation (van Biesen *et al*., 1996, Blenis, 1993) via activation of the MAP kinase pathway. This signalling occurs predominantly via coupling to different G-proteins or can be via a G-protein independent mechanism depending on the context. For example, PAR1 binds to $G_{q/11}$ initiating PKC activation, which then activates and phosphorylates Raf-kinases, which stimulates MAP kinase via a Ras-dependent pathway (L'Allemain *et al*., 1991, Molloy *et al*., 1996, Shock *et al*., 1997). In human platelets, activated PAR1 couples to G_{13} leading to Rho activation and platelet aggregation (Huang *et al*., 2007).

The activation of MAP kinase through PAR1 in astrocytes occurs in two ways; firstly by pertussis toxin-sensitive $G_{\beta\gamma}$, PI-3 kinase mediated activation of Raf and secondly by pertussis toxin-insensitive PKC-directed and Raf phosphorylation (Wang *et al*., 2002). Several other signalling pathways can link to PAR1, for example, the activation of NFκB by PAR1 occurs through $G\alpha_q$ dependent signalling or through $G\beta\gamma$ signalling involving PI3-kinase, depending on the cell type.

The role of PAR1 in activating the MAP kinase pathway can also be attributed to its interaction with the epidermal growth factor receptor (EGFR) resulting in transactivation. The PAR1 receptor is able to dimerize with EGFR leading to tyrosine auto-phosphorylation in the intracellular domain and activation of ERK (Darmoul *et al*., 2004). In addition, PAR1 agonists are able to activate the Shc-Grb2-SOS complex leading to ERK/MAP kinase activation. Thus, PAR1 can couple to growth-factor receptor tyrosine kinase signalling to regulate cell differentiation and growth (Chen *et al*., 1996).

1.4.3 Expression and distribution of PAR1

PAR1 is widely distributed across many cells and tissues including but not limited to; endothelial cells, platelets, T-cells, fibroblasts, monocytes, epithelial cells, smooth muscle cells, neurons, glial cells and cancer cells (Arena *et al*., 1996, Colotta *et al*., 1994, Grandaliano *et al*., 1994, Jenkins *et al*., 1993, Nierodzik *et al*., 1996, Vu *et al*., 1991, Weinstein *et al*., 1995). PAR1 is also expressed in fibroblasts, smooth muscle cells, and endothelium of human arteries and is linked to atheroma, atherosclerosis and inflammatory processes prevalent in cardiovascular disease. (Nelken *et al*., 1992) In addition, abundant PAR1 levels have been detected in rheumatoid and osteoarthritis (OA) patients within the synovial membrane (Morris *et al*., 1996, Shin *et al*., 1995). High levels of PAR1 expression have also been observed in neurons of the cortex via immuno-histochemical analysis of the rat brain and *in situ* hybridization (Nierodzik *et al*., 1996) suggesting a role in the CNS in addition to a function with the central vasculature. In addition, the PAR1 has been expressed in human brain; human astrocytes and glioblastoma cells. PAR1 activation is mediated

the increasing of intracellular Ca^{+2} and hydrolysis of PI leading to glial tumour (Junge et al., 2004)

1.4.4 The physiological and pathophysiological roles of PAR1

Within a given tissue system, PAR1 activation can lead to both physiological outcomes and pathophysiological effects dependent on the context. PAR1 is well recognised to mediate platelet aggregation and is a strong vasoconstrictor but has also been shown to mediate acute pro-inflammatory events such as vasodilatation, vascular permeability, and increased cell adhesion, all of which contribute to the normal repair process following damage (Gudmundsdottir *et al.*, 2008, Alberelli and De Candia, 2014). Activation of PAR1 in a rat models also leads to an immediate increase in vascular permeability to albumin with resultant paw oedema through formation of IP_3 and Ca^{2+} mobilisation (Cirino *et al.*, 1996). In addition, PAR1 activation has an important role during vascular injury in mediating the recruitment of monocytes by inducing the expression of chemo-attractants in human peripheral blood mononuclear cells (PBMC). This includes monocyte chemotactic protein-1 (MCP-1) a specific chemotactic agent expressed in endothelial cells which promotes monocyte recruitment during acute injury to tissues (Colotta *et al.*, 1994). These types of cellular event combined within a specific tissue organ system in a given context to mediate a number of outcomes categorised below.

Cardiovascular (Chen et al.) system - PAR1 is well expressed within the CV system including smooth muscle cells, fibroblasts and endothelial cells. Activation of PAR1 on smooth muscle cells leads to activation of calcium and muscle contractility (Antonaccio *et al.*, 1993). In contrast, the activation of PAR1 via agonist peptides has been shown to cause hypotension *in vivo* (Damiano *et al.*, 1999). In vascular injury, PAR1 activation leads to regrowth of endothelial tissue, also, PAR1 mediates vessel growth and increased density of carotid cells (Cheung *et al.*, 1999). Cardiac inflammation is also a feature of PAR1 activation increasing production of the local monocyte chemoattractant proteins MCP-1, MCP-3, and MCP-5 and increasing macrophage infiltration (Chen *et al.*, 2008). However, contradictory outcomes have

also been recorded; activated protein C (APC)-mediated cardiac protection is abolished in PAR1 deficient mice in a model of myocardial ischemia-reperfusion injury (Loubele *et al*., 2009). Local activation of PAR1 also results in nitric oxide (NO) release and subsequent endothelium-dependent relaxation of the arterial rings in the human and rat internal mammary artery suggesting a local protective role (Ballerio *et al*., 2007). Furthermore, PAR1 activation in monocytes stimulates plague stability through atherogenesis by decreasing macrophage accumulation through the inhibition of transendothelial migration in mice (Seehaus *et al*., 2009).

A number of studies also suggest a negative role for PAR1 in sepsis via the APC pathway. Under normal conditions, signalling of APC mediated through PAR1 has a protective effect on the vascular barrier in human endothelium. APC can in turn, significantly change the vascular barrier function in response to PAR1 activation and helps to maintain vascular barrier integrity in sepsis (Schuepbach *et al*., 2009). Interestingly in mice, systemic inhibition of PAR1 by hirudin leads to enhanced blood perfusion and lower mortality rates (Pawlinski and Mackman, 2004). This study supports another report, which indicates that vascular damage, (predominantly sepsis) is mediated by PAR1 in mice. The damage is inhibited using PAR1 inhibitors to treat sepsis and involves cross-talk with PAR2 (Kaneider *et al*., 2007). Furthermore, vascular leakage induced by inflammation can be prevented by PAR1 activation and by the endothelial cell PC receptor (EPCR) through the APC pathway, whereas vascular hyper-permeability mediated by PAR1 is increased via the blockade of APC (Niessen *et al*., 2009) suggesting a direct interaction between these receptors.

Respiratory System- PAR1 is widely expressed in cells and tissues of the lung and airways and is required for normal respiratory functions and response to infection and injury. Studies have shown stimulation of vagal lung C-fibres mediated by PAR1 in the mouse trachea. This is a due to a direct effect on nerve cell activity (Kwong *et al*., 2010). In the lung, PAR1 mediated IL-13 signalling causes neutrophil chemotaxis and degranulation, events relevant in asthma. An experiment using a

PAR1 KO model has shown the receptor to be protective against N-formyl-L-methionyl-L-leucyl-L-phenylalanine (fMLP) induced emphysema and goblet cell metaplasia (Atzori *et al.*, 2009). An important role for PAR1 has been shown in response to injury to the airway epithelium. In primary rat distal lung epithelial cells, activation of PAR1 results in the reduction of chloride channel-dependent, trans-epithelial resistance while epithelial permeability is increased (Moraes *et al.*, 2009). This suggests that within the lungs PAR1 plays a protective role.

Central Nervous system (CNS)- Within the central nervous system, PAR1 is widely expressed and an important correlation between expression levels and its effect on the brain has been observed. High expression of PAR1 mRNA is found in the cortex, and dorsal root ganglia of the rat, therefore, the function of nervous system is influenced through the activation of PAR1 in brain locations (Niclou *et al.*, 1994). The morphology of astrocytes changes following PAR1 activation to a more epithelial and flatter shape (Beecher *et al.*, 1994), thrombin mediates this effect by the release of vasoconstriction endothelin-1 (Ehrenreich *et al.*, 1993) and an increase in the secretion of nerve growth factor (Neveu *et al.*, 1993). In addition, there is a correlation between Alzheimer's disease and PAR1; it seems thrombin mediates a reduction in the neurotoxicity of β-amyloid protein which is a component in the development of Alzheimer's disease (Pike *et al.*, 1996). In addition, the expression of PAR1 in rat astrocytes leads to GRO/CINC-1 release, the rat orthologue of the human cytokine IL-8 suggesting a role in brain inflmmation (Wang *et al.*, 2007b).

PAR1 stimulation also enhances neuroprotective disorders in various conditions. In mouse cortical neurons, PAR1 has been shown to reduce N-methyl-D-aspartate (NMDA) mediated apoptosis (Guo *et al.*, 2004). There is also an important role for PAR1 expression in gliosis, which is correlated with the pathogenesis of Parkinson's disease. Dopamine expression is reduced via PAR1 activation leading to damage of the neuronal nigrostriatal pathway (Lee *et al.*, 2010). The same study demonstrated that the neuronal protein α-synuclein contributes to Parkinson's disease and this was revealed using inhibitors of PAR1. They show that α-synuclein upregulated matrix metalloproteinases (MMPs) mediated via PAR1, and IL1-β, TNF-α, and NO as well

as other species of reactive oxygen (Lee *et al*., 2010). PAR1 has been also implicated in CNS inflammation mediated by the serine protease mesotrypsin (Grishina *et al*., 2005). Mesotrypsin has been observed to induce Ca^{2+} mobilisation mediated through PAR1 in primary rat astrocytes and rat retinal ganglion cells (RGC-5), suggesting a crucial role for mesotrypsin in the protection of brain cells (Wang *et al*., 2006b). Another study has indicated an increased sensitivity to pain in PAR1 knock-out mice through chemical stimuli (Martin *et al*., 2009).

Intestinal system- A role for PAR1 in the gastrointestinal system has also been established. Studies have shown that activation of PAR1 affects intestinal epithelium functions, such as colonic permeability, which is disrupted via narrow junctions (Cenac *et al*., 2004). The activation of PAR1 by agonist peptides mediates chloride secretion in non-transformed human SCBN epithelial cells; while in mouse colon tissue, chloride secretion is reduced (Buresi *et al*., 2005). The chloride secretion mediated by PAR1 happens through stimulation of submucosal secretomotor neurons in mice cecum (Ikehara *et al*., 2010). Intestinal inflammation and enhanced colitis is affected by PAR1 activation also (Nguyen *et al*., 2003, Vergnolle *et al*., 2004). PAR1 presents the endogenous modulatory function; colitis induced by oxazolone is mediated by the pro-inflammatory cytokines IL-4, IL-10, TNFα, and lymphocyte T helper cytokine-2 (TH2). Activation of PAR1 inhibits oxazolone-mediated colitis as well as inflammatory cytokine release indicating the anti-inflammatory response associated with TH2-mediated colitis in mice (Cenac *et al*., 2005).

Cancer- Important roles for PAR1 have been uncovered in relation to cancer with effects on angiogenesis, metastasis, and tumor formation. For example; high levels of PAR1 expression is found in tumor cells, breast carcinoma biopsy specimens, and invasive cells (Wojtukiewicz *et al*., 1995, Even-Ram *et al*., 1998). PAR1 is found in breast tumor cells. A relationship has been discovered between PAR1 over-expression in normal cells and metastases. The assessment of human epithelial growth factor receptor (HER1) mediated by PAR1 occurs by many techniques including immunohistochemistry, immunoblotting and flow cytometry (Hernandez *et al*., 2009), also PAR1 is expressed in pulmonary metastasis (Nierodzik *et al*., 1998).

Other studies have reported that activation of PAR1 drives matrix metalloproteinase (MMP)-1 mediated invasion and tumorigenesis of breast cancer cells (Boire *et al*., 2005) and breast cancer cell migration (Nguyen *et al*., 2006). Survival, tumor growth, and invasion are all mediated by PAR1 activation through the mitogenic activity of thrombin. Reducing PAR1 expression in metastatic melanoma A375SM cells leads to reduced xenograft tumor vascularisation, formation, cell growth and invasion *in vitro* (Salah *et al*., 2007).

1.5 PAR 3 & 4

Similar to PAR1, PARs 3 and 4 localise to the plasma membrane and they have the typical seven-transmembrane structure of GPCRs. This consists of an N-terminus, seven transmembrane domains, ECL1-3, ICL1-3, a C-terminus, and both have the disulphide linkage between ECL2 and TM3 to give the stability of the receptor structure (Hamm, 2001).

The PAR3 gene contains two exons and it localises to chromosome 5q13 (Schmidt *et al*., 1997). PAR3, like PAR1, has a hirudin-like binding domain within the NH_2-terminus which promotes high affinity thrombin binding (Macfarlane *et al*., 2001). Similar to PAR1, PAR3 requires low concentrations of thrombin for cleavage and activation of the receptor (Coughlin, 1998). Thrombin cleaves and activates PAR3 at the $LPIK^{38}{\downarrow}T^{39}FRG$ site to expose the new N-terminus (TFRGAP) (Ishihara *et al*., 1997, Vu *et al*., 1991). PAR3 has a very short C-terminus, which restricts the ability of the receptor to couple to G proteins and β-arrestins to regulate the range of intracellular signalling pathways noted for other PARs (Nakanishi-Matsui *et al*., 2000).

Protease activated receptor-4 (PAR4) was first cloned in 1998 by Xu and colleagues (Xu *et al*., 1998) although previous studies had implicated a second thrombin activated PAR in PAR1 knockout mice. The PAR4 gene contains two exons and it localises to a different chromosome (19p12) compared to the other PARs (Kahn *et*

al., 1998). PAR4 contains a dual proline motif P[45]APR instead of a hirudin-like binding domain and therefore requires higher concentrations of thrombin to cleave and activate the receptor compared to PAR1 or PAR3 (Xu *et al*., 1998). PAR4 can also be activated weakly via trypsin. PAR4 has also been shown to couple to a number of well-known signalling cascades but does not display the range noted for PAR1 (Coughlin, 2000).

1.5.1 The physiological and pathophysiological role of PAR3 and PAR4

Unlike PAR1 and PAR2, the short C-terminus for PAR3 leads to restriction signalling for the receptor and incapable to couple to G proteins or arrestines, therefore, there were limited studies for the roles of PAR3 in diseases.

The strong association between the expression of PAR4 and thrombo-inflammation have been illustrated through many stimuli such as thrombin, angiotensin II, and sphingosine-1-phosphate (S1P) and this expression could be operated when needed. In addition, PAR4 has a role in vascular disease, atherosclerosis, and cardiac post-infraction remodelling (Fender *et al*., 2017). Examination of PAR4 antagonist YD-4 provides protective effect in transfected cells for flux of Ca^{+2} and the releasing of IP3 mediated the platelet aggregation (Edelstein *et al*., 2014). Proliferation, migration, and inflammatory responses mediated by PAR3 and PAR4 in human vascular SMC. The down-regulation of PAR3 by vasodilatory prostaglandins (PGI2/PGE2) is occurring in SMC (Schror *et al*., 2010). A recent study has discussed an important role of PAR4 in mouse cardiac fibroblasts that is regulated by extracellular glucose *in vitro* and contributes to cardiac remodelling in mice (Kleeschulte *et al*., 2018). In addition, the myocardial ischaemia reperfusion injury mediated by PAR4 is inhibited by the antagonist tc-YPGKF in mice models (Strande *et al*., 2008).

PAR4 has an effect on visceral pain and nociception and modulated the colonic hypersensitivity and nociception, and is confirmed by PAR4 knockout mice studies

that explained the sensitivity to pain increases with mustard oil (Bradesi, 2009). Moa and co-workers have explained the role of PAR4 deficiency to protect animals from cerebral reperfusion. In mouse models after middle cerebral artery occlusion (MCAO), the cerebral oedema, leukocyte, neuronal death and cerebral infraction have determined. The significant enhanced in neurologic and reduction of infract volume were found in PAR4 deficient mice compared to wild-type mice. The adhesion of both leukocytes and platelets are inhibited in PAR4 deficient and can decrease the cerebral oedema (Mao *et al*., 2010). The anti-apoptosis signalling is mediated by PAR3 in mice cortical neurons. The apoptosis downstream activated by N-methyl-D-aspartate (NMDA) is blocked by activate APC. Therefore, the reduction of apoptosis is through the decreasing of the signalling of PAR3 via PAR3 antibody or PAR3 deletion to reduce APC activation (Guo *et al*., 2004).

The expression of PAR3, (but not PAR4), has been demonstrated in lung fibrosis in patients as well as in mice through induced mesenchymal transition. The expression of PAR3 mediates epithelial-EMT in primary mouse alveolar type II cells (AT II). The morphological aspects, expression changes of epithelial markers and functional changes, were evident to EMT (Wygrecka *et al*., 2013).

As other PARs, PAR3 and PAR4 have roles in inflammatory and swelling. The inflammation factors such as the internalisation of calcium, ERK phosphorylation and releasing of IL-8 are mediated by PAR3 in HEK293-PAR3 cells, human lung epithelial and astrocytoma (Ostrowska and Reiser, 2008). The crucial role of PAR4 has been explained in the inflammation regulation. The neutrophil migration mediated inflammation induced by carrageenan or neutrophil chemoattractant CXCL8 is inhibited by PAR4 antagonist YPGKF-NH$_2$ in mice (Gomides *et al*., 2014). The expression of PAR4 contributes to inflammation and vessel injury, is activated by S1P in human monocytes. The activation of ERK, p38 MAPK, Akt, and COX-2 are the signalling responses for this expression leading to promote the up-regulation and cell migration. The inhibitor of PI3K (LY) inhibits the activation of COX-2 mediated by PAR4. S1P improves the chemo-attracted for PAR4 and can be inhibited with siRNA PAR4 studies (Mahajan-Thakur *et al*., 2014). The increasing of

IL-6 in mice serum has proved that the expression of PAR4 mediated arthritis. The paw oedema is decreased by PAR4 knockout mice studies (Busso *et al.*, 2008).

The expression of PARs is widely in the CNS. Studies using knockdown PAR3 cells have established the invasion in human pancreatic adenocarcinoma (PANC-1). The expression of invasion is determined through the cell division control protein 42 homolog (CDC42) which means that CDC42 expression is reduced by PAR3 activation by agonists (Segal *et al.*, 2014). PAR4 mediates ERK MAP kinase the tumour cell migration in hepatocellular carcinoma cells (HCC) that is inhibited by the antagonist trans-cinnamoyl-YPGKF-NH$_2$ (Kaufmann *et al.*, 2007). The expression of PAR3 has been also found in primary cultures of human renal cells carcinoma (RCC). The expression has been evaluated by RT-PCR and confocal fluorescence techniques. PAR4 has not been expressed in RCC cells (Kaufmann *et al.*, 2002). In addition, PAR4 has a role in tumour suppressor in oesophageal squamous cell carcinoma Cells (ESCC). The expression of PAR4 induces apoptosis and decreases the cell proliferation through the activation of p38 and ERK MAPK (Wang *et al.*, 2018). The activation of PAR4 relates to the phosphorylation of ERK in colorectal cancer cells is capable of promoting the proliferation in colon tumour, while the proliferation decreases with PAR4 deficient in HT29 cells (Zhang *et al.*, 2018). The expression of PAR4, however, mediates the tumour proliferation in MCF-7 and MDA-MB-231 breast cancer cells. This expression is determined by the decreasing of ERK and the block of PKC which contributes to angiogenesis and breast cancer progression (Jiang *et al.*, 2017).

1.6 Protease-activated receptor-2 (PAR2)

The second member of the PAR family is protease activated receptor-2 (PAR2). PAR2 localises on the plasma membrane and can be found in intracellular pools within the cytoplasm. The receptor is expressed in a wide variety of cells, particularly of epithelial and endothelial origin as well as immune cells. The PAR2 gene comprises of two exons (similar to PAR1) and is localised on chromosome 5q13 (Schmidt *et al*., 1997). Mouse PAR2 was originally identified by Nystedt *et al* (Nystedt *et al*., 1994) followed by human PAR2 by probing a genomic DNA Library using a hybrisation probe derived from the 3' prime region of mouse PAR2 (Nystedt *et al*., 1995a). The molecular weight of PAR2 is approximately 50 kDa dependent upon post-translational modification, it is composed of 397 amino acids and comprises seven putative transmembrane (TM) helices. The extracellular amide terminal domain has 25 residue peptides and an 11 amino acid pro-domain, three extracellular loops (ECL 1-3), three intracellular loops (ICL 1-3) and the intracellular carboxyl terminus domain that is a small eight helix of 50 residues. The connection between TM4 and TM5 is ECL2, which is bound with TM3 via a disulphide bond. The disulphide bond with a cysteine residue in GPCRs facilitates the stability of the receptor structure (Hamm, 2001).

A number of studies have demonstrated that PAR2 couples to multiple G-proteins; $G_{\alpha i}$, $G_{\alpha q/11}$, or $G_{\alpha 12/13}$, or alternatively G protein-independent signalling via β-arrestin 1/2 (DeFea *et al*., 2000, Seatter *et al*., 2004, Nichols *et al*., 2012) leading to subsequent downstream signalling and physiological responses (Ramachandran *et al*., 2012a). These concepts are examined in more detail later in this chapter.

1.6.1 Endogenous PAR2 activators

PAR2 is activated at the N-terminus specifically within the $SKGR^{36}{\downarrow}S^{37}LIGR$ sequence. The exposed tethered ligand, SLIGRL in rodent or SLIGKV in human, is then free to interact and activate the receptor extracellular loop 2 (Bohm *et al*., 1996, Adams *et al*., 2011, Nystedt *et al*., 1995b). Unlike the other PARs, PAR2 is cleaved at its N-terminus by an extensive number of extracellular serine proteases such as;

trypsin, tryptase (Molino *et al.*, 1997a), the TF-FVIIa complex (Camerer *et al.*, 2000), kallikreins and human leukocyte elastase (Barry *et al.*, 2006, Ramachandran *et al.*, 2012b) (for a full list see table 1.1). However, despite these discoveries it is unclear which serine protease is the endogenous activator in different tissues systems. Trypsin is assumed to be produced endogenously to activate epithelial cells (keratinocytes, enterocytes), T cells, myocytes, endothelial cells and several cancer cell (al-Ani *et al.*, 1995, Bohm *et al.*, 1996, Corvera *et al.*, 1997, Howells *et al.*, 1997, Hwa *et al.*, 1996, Kong *et al.*, 1997, Mari *et al.*, 1996, Mirza *et al.*, 1996, Saifeddine *et al.*, 1996, Santulli *et al.*, 1995).

Trypsin I and II are serine proteases found mainly in the gastrointestinal system which have the potential to activate PAR2 in this location (Cottrell *et al.*, 2004, Rinderknecht *et al.*, 1984). PAR2 "specific" proteases can also be found in the brain such as trypsin IV (Sawada *et al.*, 2000), and neurotrypsin (Gschwend *et al.*, 1997), which also actives PAR2 in the breast and ovary (Anisowicz *et al.*, 1996).

P22 is another endogenous agonist for PAR2; it is a trypsin-like serine protease of 22 kDa, and is able to activate PAR2 in human glioblastoma cells (A172 cells) leading to transient intracellular calcium mobilisation (Sawada *et al.*, 2000). PAR2 is also activated by the protease neurosin, which cleaves the peptide bond within the N-terminal of the receptor at the $Arg^{36} \downarrow Ser^{37}$ site (Oikonomopoulou *et al.*, 2006). Furthermore, there are also enzymes derived from bacterial protease classes that are able to activate PAR2 for example; bacterial cysteine gingipains (Uehara *et al.*, 2005), house dust mite cysteine protease Der P1, Der P3 and Der P9 (Adam *et al.*, 2006, Asokananthan *et al.*, 2002), and chitinase derived from *Streptomyces griseus* (Hong *et al.*, 2008). Certain proteases can also cleave the receptor and disarm PAR2 signalling pathways (Ramachandran *et al.*, 2011). More proteases have been discovered which inactivate or disarm PAR2 and are listed in table 1-1.

PAR2 activated proteases	PAR2 dis-activated proteases
• Trypsin	• Protease 3
• Tissue factor:	• Plasmin
▪ Factor Xa	• Cathepsin G
▪ Factor VIIa	• Elastase
• Mast cell tryptase	• Calpain
• Pen C 13	
• matriptase/MT-SP1	
• Der P1, Der P2, Der P3	
• Trypsin IV (Mesotrypsin)	
• Bacterial gingipains	
• Kallikrein 2, 4, 5, 6, 16	
• Granzyme A	
• Matriptase	
• KLK5, KLK6 and KLK14	
• TMPRSS2	
• Acrosin	
• Chitinase	
• Pen C 13	
• Neurosin	
• human airway trypsin-like protease (HAT)	

Adapted from (Adams *et al*., 2011).

Table 1. 1 Proteases which activate or inactivate PAR2

1.7 PAR2 agonists

1.7.1 Synthetic agonist peptides

As with PAR1, cleavage of the N-terminal of PAR2 generates a peptide sequence, which can be synthesised synthetically. SLIGKV (human) and SLIGRL (mouse/rat) act to mimic the tethered ligand sequence of the receptor and can therefore bind directly without the need for receptor cleavage (Bohm *et al*., 1996, Nystedt *et al*., 1995a, Nystedt *et al*., 1994, Nystedt *et al*., 1995b, Macfarlane *et al*., 2001). SLIGKV and SLIGRL can be modified by adding an amino group to give SLIGKV-NH$_2$ and SLIGRL-NH$_2$. The purpose for modification is to allow the new peptides to be more potent from the original sequence and less prone to degradation (Hollenberg *et al*., 1996, Kawabata *et al*., 2000).

The creation of PAR2 agonist peptides with greater potency than the synthetic PAR2 agonists SLIGKV and SLIGRL, was achieved by the modification and substitution of the N-terminal serine with a 2-furoyl group to produce 2-furoyl-Leu-Ile-Gly-Lys-Val (2f-LIGKV-OH) (ASKH95) and this has greater potency than SLIGRL-NH$_2$ *in vitro* and *in vivo* (Ferrell *et al*., 2003). Using the mouse sequence with modification gives 2-furoyl-LIGRL-NH$_2$ with further improved potency (Kawabata *et al*., 2004). Further modification by the addition of an ornithine group as evidenced by Kawabata *et al*, 2004 who created 2-furoyl-LIGRLO-NH$_2$ resulted in 300 times greater potent than SLIGRL-NH$_2$ (McGuire *et al*., 2004). In addition, the three peptides derived from the mouse TL domain (SLIGRL-NH$_2$); S-p-fFIARL-NH2, SLIARK-NH$_2$, and SL-Cha-ARL-NH$_2$ were found to be far more potent in the activation of PAR2 than the original peptide (Maryanoff *et al*., 2001).

Recently Barry *et al*., 2007, have discovered more than 50 peptide agonists with increased potency for PAR2 through modification of the agonist SLIGRL-NH$_2$. Some of these modifications include new peptides, which consist of seven or eight residues instead of six leading to an increase in potency of approximately 8-fold. Another modification is replacing the sixth residue (leucine) with an aromatic amino acid, which results in a gain in potency compared to the aliphatic group. The

interaction suggested between PAR2 and the aromatic ring is via a π-π bond (Barry *et al*., 2007). The partial agonist 3-mercapto-propionyl-Phe-Cha-Cha-Arg-Lys-Pro-Asn-Asp-Lys amide (G186-65) activates PAR2 in HEKs but also interacts with PAR1 in some cell types (Kawabata *et al*., 1999).

1.7.2 Non-peptides agonists

Despite the discovery of several peptide agonists for PAR2, many of these compounds are still not suitable for use *in vivo* because of poor bioavailability and lack of potency. Therefore, focus has turned to the generation of non-peptide PAR2 agonists. Seitzberg's studies have reported that the non-peptide agonist AC-55541 is a full agonist and AC-98170 a partial agonist. The methyl group bound to hydrazone in the agonist AC-55541 gives an increase in the potency compared to hydrogen or another larger alkyl group such as an ethyl group. AC-55541 is weakly soluble in organic solvents as well as aqueous phosphate buffers with a good metabolic stability in human and rat microsomes suggesting the potential to be used *in vivo* (Seitzberg *et al*., 2008). AC-55541 and AC-264613 are more potent agonists, with increased activity compared to the synthetic peptide SLIGRL and due to their selectivity for PAR2 are preferred. AC-55541 and AC-264613 agonists both contain a bromo-benzyl group. Higher agonist potency is due to substitution in the meta position, substitution in the para or ortho position shows a reduction in activity (Seitzberg *et al*., 2008, Gardell *et al*., 2008).

All of the three agonists outlined lack drug-like properties and this needs to be developed, one technique is the formulation of non-peptidic PAR2 agonists. This approach is based on substitution at the C or N-terminal serine within the hexapeptide structure (Barry *et al*., 2010, Barry *et al*., 2007). This has proved successful, the agonist GB110 activates PAR2 mediating the release of intracellular Ca^{2+} in various cell types. GB110 also has the same potency compared to most synthetic peptide agonists and has shown to be selective for PAR2 over PAR1 (Barry *et al*., 2006).

1.7.3 PAR2- cellular expression, activation, and functions

Following the identification of PAR2, studies examining PAR2 expression and responses to activation in different cell types and tissues, gave an indication of the role of the receptor in normal physiology and pathological conditions. PAR2 is distributed throughout the body including but not limited to pancreas, kidney, liver, airway, gastrointestinal tract, ovary, joint and prostate. PAR2 is strongly expressed in immune cells including; T cells, macrophages, mast cells, neutrophils, eosinophils and dendritic cells (Shpacovitch *et al*., 2008) as well as cells of epithelial origin and endothelial cells, suggesting a role in immunity and inflammation. Indeed, PAR2 also has an important role in a range of pathological conditions, for example in diseases such as; asthma, colitis, arthritis, skin disorders, inflammatory pain, Alzheimer's, and cardiovascular disease (Ossovskaya and Bunnett, 2004, Adams *et al*., 2011). The role of PAR2 in systems physiology and disease states and the development of therapies directed against PAR2 are outlined in more detail in the following sections.

1.8 PAR2 signalling

Upon activation PAR2 undergoes a conformational change and couples to second messenger systems to initiate downstream intracellular signalling pathways which drive a variety of physiological outcomes. As with PAR1, specific heterotrimic G-proteins, such as $G\alpha_s$, $G\alpha_q$, $G\alpha_i$ and $G\alpha_{12/13}$ couple to PAR2 upon activation and mediate different downstream signalling pathways (Adams *et al*., 2011, Hirota *et al*., 2012). PAR2 can also signal independently of G-proteins by coupling to β-arrestins 1 or 2, this pathway is known as the G-protein independent pathway and whilst usually associated with receptor desensitisation (see section 1.7.2) is relevant in MAP kinase signalling (DeFea *et al*., 2000, Ge *et al*., 2003, Soh *et al*., 2010). The coupling of G-protein or arrestins to PAR2 depends on the cell type and the stimulus used perhaps reflecting differences in expression patterns of signalling intermediates.

1.8.1 PAR2 canonical G-protein signalling

PAR2 is predominantly linked to the $G\alpha_{q/11}$/PLC pathway resulting in the generation of the second messengers diacylglycerol (Schaffhauser *et al.*) and inositol 1,4,5-triphosphate (IP_3). This leads to protein kinase C (PKC) activation and Ca^{2+} mobilisation from the endoplasmic reticulum, as illustrated in figure 1.3. This is evidenced usually through the production of intracellular Ca^{2+}, demonstrated in a range of cell lines including intestinal epithelial and kidney cells (Bohm *et al.*, 1996, Molino *et al.*, 1997b). PAR2 mobilises intracellular calcium in hippocampal neurones and astrocytes which was blocked by a PLC inhibitor (Bushell *et al.*, 2006). PAR2 has been shown to be linked to IP_3 formation in COS-7-PAR2 cells, which in turn leads to calcium mobilisation (McCoy *et al.*, 2010). Furthermore, mobilisation of intracellular Ca^{2+} mediated by PAR2 was shown to be inhibited by the $G\alpha_{q/11}$ inhibitor GP2A (Ramachandran *et al.*, 2009). Finally, the $G\alpha_{q/11}$ inhibitor YM254890 has been shown to inhibit PAR2 mediated inhibition of cytokine stimulated JNK activation (McIntosh *et al.*, 2010).

PAR2 also has the potential to interact with other G-proteins depending on the context. SLIGRL-NH_2 activates PAR2 to increase cAMP, and PKA levels suggesting a link to $G\alpha_s$ (Amadesi *et al.*, 2006). In addition, coupling to $G\alpha_i$ leads to inhibition of adenylyl cyclase (Myatt and Hill, 2005) and reduction in cAMP production (Adams *et al.*, 2011, Hirota *et al.*, 2012) suggesting a divergence in coupling mechanisms. In another study, PAR2 couples to $G\alpha_{12/13,}$ which is associated with Rho-dependent phagocytosis (Scott *et al.*, 2003) an effect abrogated by a $G\alpha_{12/13}$ inhibitor (McCoy *et al.*, 2010). However, this mode of coupling is not a widespread phenomenon and is more recognised for PAR1 signalling.

There are also a number of key signalling pathways downstream of PAR2 activation. A well-recognised cascade involves the mitogen-activated protein kinases (MAPKs) in particular, ERK. Activation of this cascade via PAR2 has been demonstrated in various cell types including endothelial cells and dermal fibroblasts (Belham *et al.*, 1996, Dery *et al.*, 1998, Wang *et al.*, 2006a). SLIGRL-NH_2 mediated stimulation of PAR2 activates ERK in HT29 and epithelial cells resulting in the production of IL-8

(Wang *et al*., 2010). A further study has also demonstrated that PAR2-induced ERK signalling mediates the proliferation of human prostate stromal cells (HPSCs), which is dependent upon PKC but insensitive to pertussis toxin (PTX) suggesting preferred coupling to $G\alpha_{q/11}$ in this model (Myatt and Hill, 2005).

Similar to PAR1, PAR2 can also, via a G-protein dependent mechanism, trans-activate the EGFR in intestinal epithelial cells to drive ERK activation and increase epithelial permeability (Tripathi *et al*., 2009). PAR2 has also been shown to couple to β-arrestins to mediate ERK signalling in a manner independent of G-proteins. An original breakthrough study demonstrated that whilst the PAR2-arrestin complex was internalised as part of receptor desensitisation this also mediated ERK activation downstream of Ras within the cytosol and promoted nuclear translocation (DeFea *et al*., 2000). The expression of PAR2 mediated the activation of ERK via coupling to β-arrestins has been approved by Ge *et al,* 2004. For example transfection of breast cancer cells (MDA MB-231) with a fragment of arrestin-1 (ARR^{319}-^{418}GFP), acting as a dominant negative mutant, or siRNA to knockdown arrestin expression, results in a marked inhibition of PAR2 induced ERK activation and migration (Ge *et al*., 2003, Ge *et al*., 2004). In addition, β-arrestin dependent ERK activation leads to cofilin-mediated chemotaxis following PAR2 stimulation, this response was abolished in cells from arrestin KO mice (Zoudilova *et al*., 2007, Zoudilova *et al*., 2010). The PAR2-arrestin complex also induces Raf to stimulate ERK1/2 at the sites of membrane ruffling and filopodia formation (Stalheim *et al*., 2005). This permits permeability of epithelial cells through the redistribution of narrow junction proteins (Nagumo *et al*., 2008).

A number of further studies have demonstrated that both G-protein dependent and independent pathways can contribute to ERK activation and this is temporally linked, the implication being that early activation is G-protein dependent whilst later activation is β-arrestin dependent. Lau and co-workers have demonstrated the biphasic activation of ERK in apical cells, rapid activation at 5 minutes, diminishing at 30 minutes, and returning to a second peak at 60 minutes. In contrast, the activation of ERK is prolonged for up to 60 minutes in basolateral cells and is

prevented by PLC inhibition, calcium chelation and dominant negative arrestin depending on the time of stimulation (Lau *et al*., 2011). This phenomenon has been shown in Kirsten murine sarcoma virus–transformed rat kidney epithelial cells (KNRK) and transfected with PAR2 (KNRK-PAR2), the later activation of ERK at 90 minutes occurs through an internalised PAR2-β-arrestin-raf-1-activated ERK complex, whereas the rapid activation of ERK between 0-5 minutes is $G\alpha_q$ dependant and still apparent in arrestin-deficient cells (DeFea *et al*., 2000, Defea, 2008, Ge *et al*., 2003, Stalheim *et al*., 2005). Prolonged ERK activation via β-arrestin mediates the sustained increase in intestinal paracellular permeability (Jacob *et al*., 2005).

PAR2 has also been shown to activate other signalling cascades. PAR2 activation of the IKK/NFκB has been demonstrated in PAR2 transfected cells (Kanke *et al*., 2001). This effect has been shown to be mediated by $G\alpha_{q/11}$ and PKC dependent pathways (Goon Goh *et al*., 2008). PAR2 also activates the NFκB pathway in coronary smooth muscle cells, primary nasal epithelial cells and human umbilical vein endothelial cells (Kanke *et al*., 2001, Bretschneider *et al*., 1999). In the latter two cell types, this is linked to increased production of the chemokines, CXCL1 and CXCL8 (Rudack *et al*., 2007, Niu *et al*., 2008). Trypsin and SLIGRL-NH$_2$ also activate the NFκB pathway through PAR2 leading to the secretion and expression of both IL-8 and the chemokine CXCL1 in human nasal mucosal cells and intestinal epithelial cells (Wang *et al*., 2010, Rudack *et al*., 2007).

PAR2 coupling to NFκB is cell type specific suggesting a unique mode of interaction. Indeed, PAR2 has been shown to couple to Toll-Like Receptor 4 (TLR4) in human embryonic kidney (HEK293) cells and this leads to the production of IL-8 via NFκB-signalling (Rallabhandi *et al*., 2008). Similar to the study above, PAR2 mediated NFκB signalling can be mediated by cross talk with TLR3 and TLR2 in mouse macrophages (Nhu *et al*., 2010). Whether this is a consistent physiologically relevant interaction is open to question as no other studies have confirmed this phenomenon.
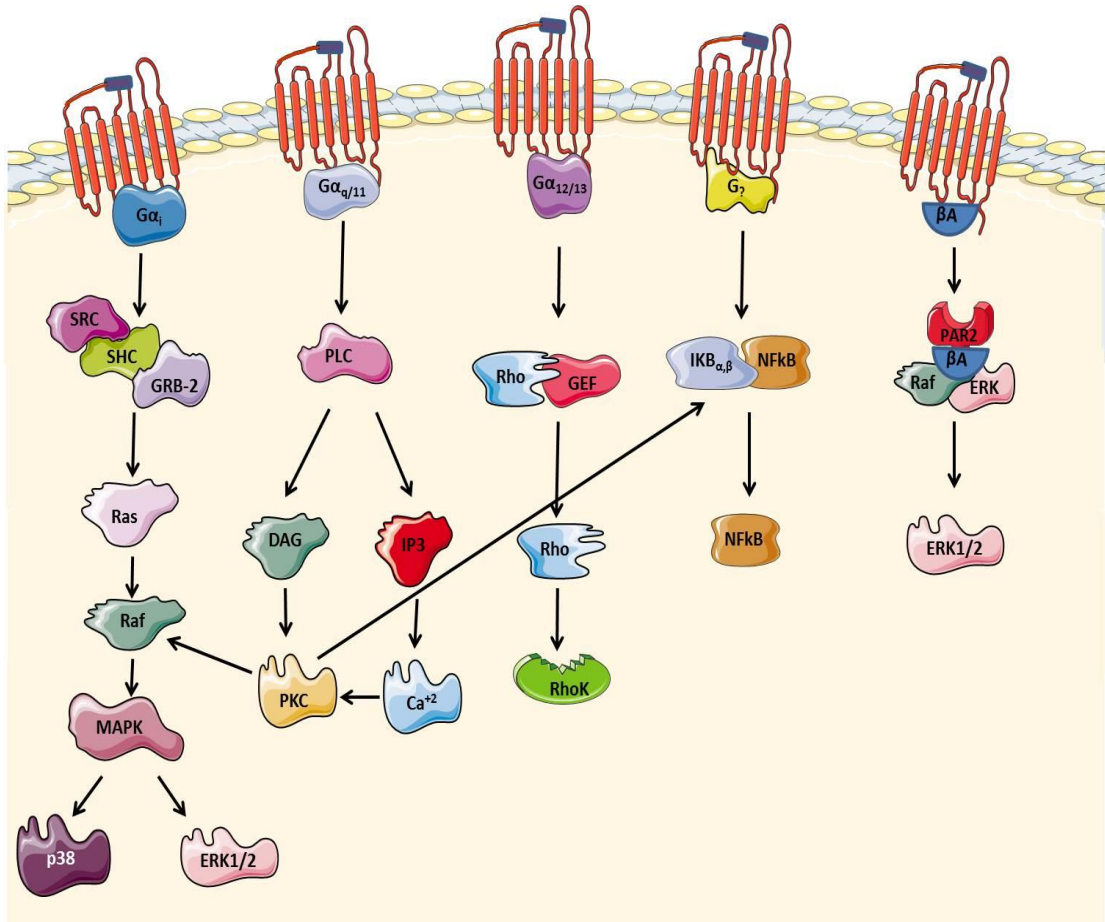
Adapted from (Rothmeier and Ruf, 2012).

Figure 1. 3 PAR2 downstream signalling

G-protein-dependent signalling occurs when PAR2 couples to G-proteins: $G\alpha_i$ induces Ras-Raf-ERK1/2 signalling through SRC-SHC-GRB-2 complex, $G\alpha_{q/11}$ induces PLC leading to Ca^{2+}/PKC signalling, and $G\alpha_{12/13}$ induces Rho kinase. ERK1/2 MAPK also activates through PAR2 couples to $G\alpha_{q/11}$ and induces PLC leading to Ca^{2+}/PKC/Raf/ERK1/2 signalling. β-arrestin-dependent signalling occurs when PAR2 couples to β-arrestin and negatively regulates G-protein signalling leading to mediate the internalisation of PAR2 into early endosomes resulting to activate Raf and ERK1/2.

1.8.2 PAR2 desensitisation

PAR2 mediated signalling must be regulated and in effect, switched off as uncontrolled receptor activation could lead to detrimental effects. As with other GPCRs, PAR2 is therefore effectively desensitized and/or down-regulated (Cottrell *et al*., 2003), as depicted in figure 1.4 . Binding of PAR2 to β-arrestin is initiated by the phosphorylation of the cytoplasmic domain of PAR2, (DeFea *et al*., 2000, Ricks and Trejo, 2009). G-protein coupled receptor kinase (GRK) rapidly phosphorylates PAR2 in the C-terminal and third TM domain as well as uncoupling the receptor from G proteins. The phosphorylated receptor binds to the functional cofactor β-arrestin and this disrupts the interaction between G-proteins and PAR2. PAR2 is then internalised into clarthin coated pits and stored in the early endosomes, this is followed by PAR2 redistribution to the lysosomes where it is degraded (Dery *et al*., 1999). The GTPase Rab5a mediates the translocation of the PAR2-β-arrestin complex to early endosomes, a β-arrestin scaffolded endosomal multi-protein signalling complex forms, followed by PAR2 degradation (Roosterman *et al*., 2003).

Studies have illustrated that cytoplasmic stores of newly synthesised PAR2 exist in the golgi apparatus. Activation of PAR2 revealed redistribution of GTPase rab11a that co-localises with PAR2. Rab11a redistributes to vesicles containing PAR2, followed by PAR2 migration to the cell surface (Roosterman *et al*., 2003). The same studies demonstrated that the receptor was endocytosed into early endosomes that contain the small GTPase rab5a. Rab5a then remains in the early endosomes whilst PAR2 localises to lysosomes (Roosterman *et al*., 2003).
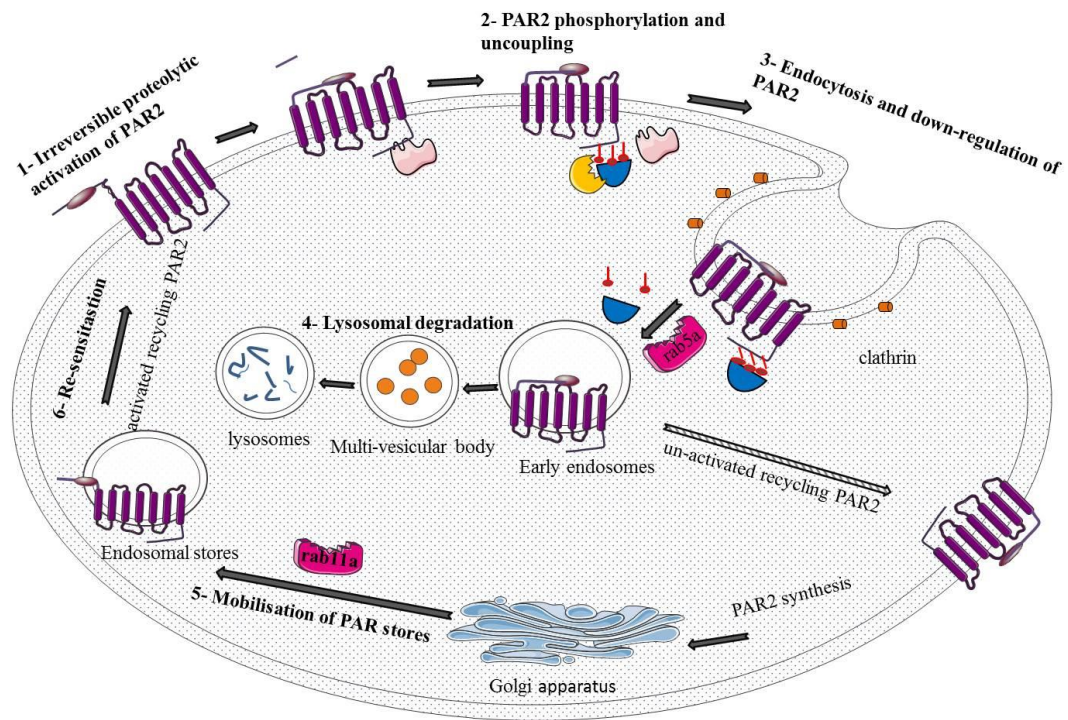
Adapted from (Ossovskaya and Bunnett, 2004).

Figure 1. 4 The mechanism of PAR2 desensitisation and down-regulation.

Desensitisation of PAR2 occurs in many steps: 1-PAR2 cleavage and activation; PAR2 couples to G-proteins. 2- GRK phosphorylates PAR2 in the C-terminus and the third TM domain; phosphorylated PAR2 binds to β-arrestin leading to PAR2 uncoupling from G-proteins. 3- Desensitisation; by clathrin coated pits; PAR2 is stored in the early endosomes, PAR2 is endocytosed and downregulated into early endosomes; trafficking by small GTPase rab5a. 4- The internalised PAR2 is targeted for lysosomal degradation. 5- Newly synthesised PAR2 trans-locates to the cell membrane by redistribution of GTPase rab11a which co-localises with PAR2. 6- PAR2 is then mobilised to the cell surface (re-sensitisation).

1.9 The physiological and pathological roles of PAR2

1.9.1 PAR2 and inflammation

It is well accepted that PAR2 has a crucial role in the cardinal responses of inflammation such as pain, redness, and swelling through a diverse series of cellular effects. It is generally accepted however that under normal conditions PAR2 is protective for example, several studies show trypsin and peptide mediated relaxation in vascular preparations via the release of NO from endothelial cells (Cirino *et al*., 1996, al-Ani *et al*., 1995). This effect can also be a contributor to enhanced blood flow during inflammation. In acute inflammation mast cell tryptase has been shown to activate PAR2 by regulating mast cell infiltration and degranulation within vascular tissues and the GI tract (Corvera *et al*., 1997, Molino *et al*., 1997a).

Furthermore, the level of PAR2 mRNA expression in endothelial cells is enhanced by TNFα for up to 4 days (Hamilton *et al*., 2001a, Nystedt *et al*., 1996) and this is linked to increased functional responses (Ritchie *et al*., 2007), suggesting a link to more chronic inflammation through dynamic receptor upregulation. Arachidonic acid formation and release of prostaglandin E_2 (PGE_2), are also induced by PAR2 activation via coupling to cyclooxygenases 1, 2 and phospholipase A_2 (Syeda *et al*., 2006, Kong *et al*., 1997), again relevant in the context of both acute and chronic inflammation. PAR2 also induces the pro-inflammatory cytokines and leukocyte adhesion molecules such as ICAM-1 (Buddenkotte *et al*., 2005). Another study has shown that ERK MAPK and PI-3 kinase/AKT signalling pathways mediated through activation of PAR2 in gut epithelial cells causes IL-8 release (Tanaka *et al*., 2008). Interestingly, IL-8 is stimulated in response to microbial challenge within the gut and this involves PAR2. PAR2 mediates macrophage activation in the acute inflammatory phase, which in turn modulates the smooth muscle, epithelium, and nerves cells throughout the intestine.

A significant area of study has been in the area of joint inflammation, arthritis, and pain. These studies have been aided by the development of KO mice models. Diminished inflammation has been evidenced in the joints and airways of PAR2

deficient mice compared to WT counterparts (Ferrell *et al*., 2003, Schmidlin *et al*., 2002). Knecht and colleagues have illustrated that thermal hyperalgesia and pain are increased when PAR2 is stimulated with trypsin (Knecht *et al*., 2007). In addition, nociception arising from hyperalgesia, cancer, and chemical agents are all decreased in PAR2 knock-out mice (Lam and Schmidt, 2010, Alier *et al*., 2008). Interestingly, one group has have shown that PAR2-mediated inflammation in a murine oedema model can be reduced by the addition of insulin. This was highlighted by a marked reduction in leukocyte trafficking in mouse intestinal venules and reduced calcium mobilisation mediated by PAR2 in endothelial and cultured dorsal root ganglion neurons cells (Hyun *et al*., 2010).

Several other studies have demonstrated that chronic inflammatory diseases such as arthritis are influenced by activation of PAR2. For example, intra-articular injection of carrageenan (causes inflammation) into mice induces joint oedema and swelling via PAR2, when PAR2 is inhibited by using either antibodies that block PAR2 activation or the antagonist ENMD-1068 (Kelso *et al*., 2006) this arthritic response was markedly reduced. Increased expression of PAR2 has also been observed in synovial biopsies from rheumatoid arthritis patients (Busso *et al*., 2007). In addition, deletion of PAR2 in mice resulted in diminished osteoarthritis (OA) indices, for example; cartilage degradation and raised subchondral bone formation. The osteoarthritis induced by the sectioning of the medial meniscotibial ligament (MMTL) was markedly reduced in PAR2 KO mice. The same study has shown that the progress of osteoarthritis could be inhibited by using the blocking antibody SAM11 (Ferrell *et al*., 2010).

PAR mediated bone damage has also been found to be a feature of OA. Osteophytes were more highly expressed in WT PAR2 mice compared to KO PAR2 mice. Osteosclerosis also presented in WT PAR2 within 14 days following destabilisation of the joint medial meniscus (DMM), while no osteosclerosis was observed in KO PAR2 even after day 28 (Huesa *et al*., 2016). Taken together, these studies suggest the potential of PAR2 inhibition as a promising therapeutic route for the treatment of joint inflammation and pain (McCulloch *et al*., 2018).

1.9.2 PAR2 and Respiratory responses

Unsurprisingly, PAR2 has an important role in allergic inflammation and the immune response in epithelium and myocytes of the airway. Activation of PAR2 increases levels of IgE in response to the airway allergen ovalbumin (OVA), leading to infiltration of leukocytes into BALF and increased methacholine-mediated airway hyper-reactivity. This response is not observed in PAR2 deficient mice (Schmidlin *et al*., 2002). Further use of the PAR2 knockout mouse model, has shown a reduction in both eosinophil infiltration and activation of the chemoattractant eotaxin, resulting in reduced airway inflammation (Takizawa *et al*., 2005).

There is also an important role for PAR2 in response to respiratory bacterial infections. In response to Pseudomonas aeruginosa inflammation, PAR2 KO mice showed enhanced inflammation, which is demonstrated by increased bronchoalveolar lavage fluid, neutrophil, and TNFα levels. In contrast, levels of IFN-γ are decreased and bacterial phagocytosis efficiency in macrophages and neutrophils is diminished in KO PAR2. Based on these observations PAR2 blockade could enhance acute lung injury, chronic obstructive pulmonary disease, adult respiratory distress syndrome and cystic fibrosis (Moraes *et al*., 2008). This suggests a protective role for PAR2 in this situation contrasting with pro-inflammatory roles outlined above.

1.9.3 PAR2 and gastrointestinal system (colitis, stoma, intestinal)

Given that the pancreas is a major source of trypsin and PAR2 is expressed in many intestinal cell types, it is not surprising to find a relationship between increased protease activity and inflammatory disease within the gastrointestinal tract (GI). Indeed, expression of PAR2 is found in various cell types of the GI tract such as enterocytes, smooth muscle cells, and intestinal glands and a direct correlation has been established between the distribution of PAR2 in the intestine and disease (Zannoni *et al*., 2014). However, PAR2 expression is found in other digestive tract

organs such as the pancreas and is activated by secreted trypsin from acinar cells of the pancreas and a role in normal physiology is also apparent (Demaude *et al*., 2009).

Activation of PAR2 via tryptase occurs in gastrointestinal smooth muscle and results in contraction aiding peristalsis (Kandulski *et al*., 2011). Trypsin secretion from the pancreas also aids food digestion and is regulated via PAR2 signalling. Acinar and duct cells are types of exocrine cells which also express PAR2 (Demaude *et al*., 2009), calcium mobilisation and amylase released from isolated pancreatic acini can be induced by trypsin or agonist peptides (Sharma *et al*., 2005b). Trypsin also activates apical PAR2 to induce cell signalling in enterocytes (Lau *et al*., 2011). Actin remodelling and redistribution of tight junction proteins in these cells is mediated by the activation of PAR2 via β-arrestin-dependent activation of ERK (Jacob *et al*., 2005). PAR2, possibly via activation through EGFR, triggers chloride secretion in SCBN cells, mediated through ERK activation and the formation of prostaglandin E_2 acting on EP2 and EP4 receptors (van der Merwe *et al*., 2008).

The main function of epithelial cells in the colon, which express PAR2, is in controlling the colonic barrier as an immune protective barrier, which hinders the translocation of bacteria to submucosal tissues, as well as controlling the trans-epithelial migration of infected cells to the lumen of the gastrointestinal tract (Kong *et al*., 1997). Colonic inflammation has been shown to be mediated by PAR2 activation and is characterised by tissue damage, granulocyte infiltration, increased wall-thickness, and bacterial translocation into peritoneal organs (Hyun *et al*., 2008, Cenac *et al*., 2002). This is linked to high constitutive PAR2 expression in the intestine and high quantities of tryptase and trypsin in the intestinal fluids of patients with inflammatory bowel diseases (Cenac *et al*., 2007).

PAR2 is also expressed in duct and acinar cells of the pancreas and can be activated via secreted trypsin when pancreatic dysfunction occurs. Electrolyte secretion (Nguyen *et al*., 1999) and amylase release are mediated by PAR2 activation which is dependent on intracellular calcium release in pancreatic duct epithelial cells (Kawabata *et al*., 2000). Interestingly in PAR2 KO mice, inflammatory effects within

the pancreas are exacerbated, there is protection from inflammation in wild-type PAR2 mice when the receptor is pre-treated with activating peptides (Singh *et al*., 2007, Sharma *et al*., 2005a). This suggests that high levels of PAR2 in the intestine may not be always linked to disease and PAR2 under some instances may be protective.

1.9.4 PAR2 and the cardiovascular system

Many studies have demonstrated the importance of PAR2 in the cardiovascular system, original work showed a widespread distribution within vascular tissues (Nystedt *et al*., 1994). Hamilton and colleagues initially demonstrated PAR2 regulation of vascular tone using synthetic peptides, endothelium-dependent relaxation occurs via PAR2 activation in rat aorta (Hamilton *et al*., 2001a). Other studies have shown a similar PAR2 endothelium-dependent relaxation in human umbilical vein (Saifeddine *et al*., 1998) and rat pulmonary artery (Hamilton *et al*., 2001b). In these and later studies for example in rat mesenteric arteries, the effect is blocked by pre-treatment with an Nitric Oxide (NO) inhibitor (Maruyama *et al*., 2015). More recently, these effects have been shown to be prevented by pre-treatment with the putative PAR2 antagonists ENMD1068 and GB83 (Roviezzo *et al*., 2014).

The role of PAR2 has been demonstrated in ischemia/reperfusion injury-induced inflammation, myocardial infraction, and heart remodelling, investigated using PAR2 KO mouse models (Antoniak *et al*., 2010). Regulation of blood pressure by PAR2 has been examined in hypertension by measuring the salt-sensitivity parameters, hypertension is mediated by PAR2 through the formation of angiotensin II (McGuire *et al*., 2008). PAR2 expression is enhanced by the pro-inflammatory cytokine TNF-α which increases responsiveness in mammary and coronary arteries (Ballerio *et al*., 2007). However, it is unclear if this mediates vascular inflammation or is protective against it. Indeed, many studies have reported that cardio-protection can be mediated through PAR2. For example, in a mouse model of ischemia-reperfusion injury, there

was a significant decrease in infarct size in WT PAR2 but not in KO PAR2 mice (Lim *et al*., 2009). The studies outlined above demonstrate that increased expression of PAR2 has an influence on acute cardiovascular actions.

PAR2 has also important cardiovascular action in particular at the endothelial cell level; this cell type plays a critical role in the coagulation cascade (D'Andrea *et al*., 1998). Tissue factor (TF) initiates the extrinsic coagulation cascade, which is considered as an integral membrane protein that links with factor VIIa and converts factor X to factor Xa. The complex TF-VIIa is a serine protease complex that has the ability to cleave PAR2 (Camerer *et al*., 2000). The cleavage of PAR2 on endothelial cells by the TF-VIIa complex is facilitated via integrin activation (Dorfleutner *et al*., 2004). Thus, PAR may have an important role in the regulation of coagulation during systemic inflammation. Activation of PAR2 via TF-VIIa also leads to hypoxia-induced angiogenesis through the deletion of cytoplasmic TF domain (Uusitalo-Jarvinen *et al*., 2007) enhancing capillary regrowth following tissue damage.

1.9.5 PAR2 and the Central Nervous System

Several studies have reported that PAR2 is widely expressed in the central and peripheral nervous systems and an increasing body of evidence points to a role in CNS conditions (Bushell *et al*., 2016). Activation of PAR2 has been reported to protect hippocampal neurons from neurotoxicity that is mediated by the cell death agent kainate; this is due to an effect on astrocyte activation, the CXCR2 receptor and the metabotropic glutamate receptors (Greenwood and Bushell, 2010). PAR2 has also been shown to sensitise neurones to extracellular acidosis via activation of the acid-sensing ion channel 3 (ASIC3) (Wu *et al*., 2017). The differentiation and survival of CNS glial and neurons can also be mediated by PAR2 induced ERK activation and protein kinase B (AKT) (Nikolakopoulou *et al*., 2016, Vandell *et al*., 2008). In neurons, PAR2 prevents β-amyloid toxicity, which is neurodegenerative in AD, whereas in some conditions PAR2 mediated expression of pro-inflammatory

cytokines and chemokines are increased in glial cells and linked to pathology through mediating neuronal cell death (Afkhami-Goli *et al.*, 2007).

1.9.6 PAR2 and cancer

As outlined above PAR2 had been shown to be linked to a number of key signalling pathways including MAP kinases (Belham *et al.*, 1996, Yu *et al.*, 1997) and others linked to proliferation, giving rise to a potential role in cancer. This has been examined to some extent at the cellular level but definitive evidence is lacking from xenograft and other mice models of cancer as well as good clinical biomarker data. In colon cancer cells (SW620) PAR2 activation by TV/FVIIa stimulates cell proliferation and migration (Hu *et al.*, 2013). PAR2 activation also promotes cell survival and leads to a decrease in cytokine-induced apoptosis in HT29 cells through the activation of MEK1/2 (Iablokov *et al.*, 2014). In addition, PAR2 mediated activation of ERK induced by TGF-β1 results in cell migration in Panc1 cells (Ungefroren *et al.*, 2017). Recently, stimulation of PAR2 results in an increase in the release of cytokine granulocyte colony-stimulating factor (G-CSF) in metastatic 4T1 and MDA-MB-231 breast cancer cells, which in turn aids tumour formation. The secretion of G-CSF was diminished following KO PAR2 knockdown in 4T1 cells (Carvalho *et al.*, 2018). In contrast, other groups have demonstrated the potential of anti-proliferative effects; activation of PAR2 has been shown to decrease proliferation in keratinocytes (Schepis *et al.*, 2018), whilst in some tumor cell lines, synthetic PAR2 peptides acting via PAR2 inhibit colony formation (Bohm *et al.*, 1996).

A role for PAR2 in cancer progression has been demonstrated more recently. For example, PAR2 has been shown to regulate cancer progression in cells from the colon and stomach through increased levels of FV11a leading to up-regulation of MMP-9 and down-regulation of caspase-3 (the apoptosis activator) (Wu *et al.*, 2013). In the human gastric carcinoma cell line (MKN-1), the methylation ratio (MR), which is an indication of tumour progression, is decreased through PAR2 and linked to cases of stomach carcinogenesis. Interestingly in chronic inflammation MR is

increased suggesting an interesting dual role for PAR2 in both inflammation and cancers of the GI tract (Arisawa *et al*., 2007). In one of very few *in vivo* studies, Versteeg and colleagues have shown that in the absence of PAR2, metastasis is diminished and tumor progression delayed in a mouse mammary tumour virus-polyoma middle T (MMTV-PyMT) model. In addition, the proliferation of the aggressive human breast cancer cell line (MDA-MB-231s) is inhibited in a xenograft model when TF-FVIIa-PAR2 signalling is decreased (Versteeg *et al*., 2008). Finally, PAR2 via its effects upon inflammation may also play a role within the tumour microenvironment and whilst no studies have examined this in detail PAR2 synthetic peptides and TF-VIIa can stimulate cytokine release in MDA-MB-231 cells (Albrektsen *et al*., 2007).

1.10 Targeting PARs for the development of new medicines

Given the role of PARs in disease it is not surprising that there has been a considerable focus on the development of inhibitors and modulators of each receptor. However, this has been a very difficult problem to solve and progress has been slow. The major reason is that the interaction with the tethered ligand with ECL2 of the receptor is difficult to model and until recently, no crystal structures were available. This section focusses on the development of PAR1 antagonists as an exemplar, PAR4 and more recently PAR2.
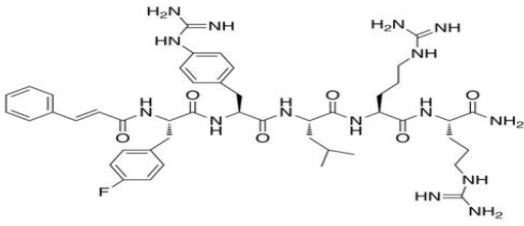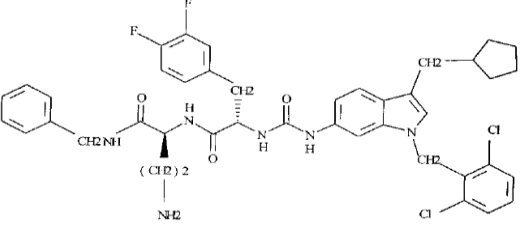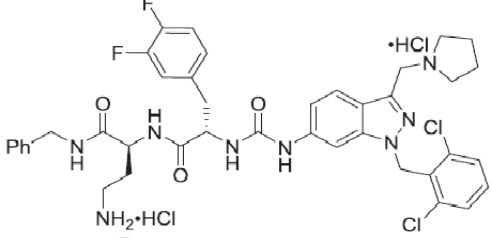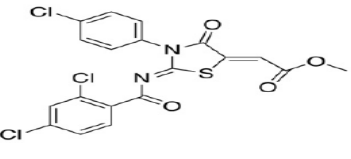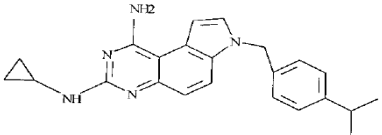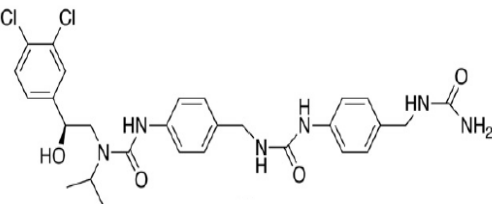
1.10.1 The development of PAR1 antagonists

The first described peptide antagonists for PAR1 were RWJ-56110, RWJ-58259 and SCH530348; all were reported to be potent compounds with good therapeutic properties (Maryanoff *et al*., 2003, Andrade-Gordon *et al*., 1999). The three crucial functional groups in each of these antagonists were found to be the N-terminus amino group, the guanidino group of R^5 and the centre of the benzene ring of the second residue (see table 1-2). These groups were part of a three-point pharmacophore model, where 6-aminoindole is the rigid scaffold attached to the three groups. The antagonist RWJ-56110 was shown to have good potency and selectivity for PAR1 and was able to inhibit both thrombin and SFLLRN-NH$_2$ mediated platelet aggregation. The weakness in this compound however is that it caused hypotensive responses in guinea pigs, the possible reason was thought to be due to the substitution in position 2 of the 6-aminoindole. Replacement of the indole group with indazole resulted in RWJ-58259. This compound displayed high affinity for PAR1, and had the same potency and selectivity compared to RWJ-56110 in the inhibition of platelet aggregation, however RWJ-58259 was found to have no side effects in guinea pigs (Zhang *et al*., 2001).

The PAR1 antagonist atopaxar (E5555) has been used in patients with coronary artery disease and acute coronary syndrome (Cirino and Severino, 2010, Serebruany *et al*., 2009). Reduced platelet aggregation and the platelet-monocyte aggregates are the main mechanism of its action (Serebruany *et al*., 2009). The Tricyclic 3-phenylpyridine (SCH530348), later on known as vorapaxar; has also been described as a PAR1 antagonist in platelets (Chackalamannil *et al*., 2008). The compound has also been used in other atherosclerosis linked conditions (Morrow *et al*., 2009). In clinical studies, vorapaxar caused a decrease in major adverse coronary events (MACE) and excess bleeding in patients with non-ST-segment elevation acute coronary syndrome (Goto *et al*., 2010). Most recently, the anti-platelet drug PAR1 antagonist vorapaxar has been used in acute coronary artery syndrome and in cases of atherothrombosis. It is also used for antiplatelet therapy especially in intracranial haemorrhage with stroke patients (Tricoci *et al*., 2012, Morrow *et al*., 2012). This

PAR1 antagonist was approved in the USA to prevent thrombosis in patients that have a history of peripheral artery disease or myocardial infraction (French *et al*., 2015). However, unfortunately, Vorapaxar is now used for limited cohorts only due to severe bleeding side effects witnessed with its use. A full list of PAR1 non-peptide antagonists can be found in table (1-2).

Another novel approach to inhibit PAR1 has been to utilise pepducins, these are N-palmitoylated peptides, which block the coupling of the receptor to the relevant G-protein. This includes P1pal-12 (pal-RCLSSSAVANRS-NH$_2$) which has been shown to be selective for PAR1 over the other PARs (Covic *et al*., 2002a). P1pal-12 has been shown to prevent PAR1 mediated lung vascular damage, disseminated intravascular coagulation and sepsis lethality (Kaneider *et al*., 2007). Another PAR1 pepducin P1pal-7 (pal-KKSRALF-NH$_2$) has been demonstrated to prevent lung metastasis and induces cellular apoptosis in tumour xenografts, through inhibition of PAR1 induced MMP-1 and blockage of the Akt survival pathway (Yang *et al*., 2009). A more recent study demonstrated that the pepducin PZ-128 is a potent antiplatelet agent through inhibiting PAR1 (Gurbel *et al*., 2016). Nevertheless, despite these promising results these compounds are unlikely to reach the clinic in the immediate future.

Structure and symbol	role	Reference
BMS-197525	Inhibits platelet aggregation	(Bernatowicz *et al.*, 1996)
RWJ-56110	Inhibition platelet aggregation and smooth muscle Ca^{2+} mobilization	(Andrade-Gordon *et al.*, 1999)
RWJ-58259	Anti-platelet agent	(Gandhi *et al.*, 2018)
FR171113	inhibited thrombin-induced platelet aggregation	(Kato *et al.*, 1999)
SCH79797	inhibits human platelet aggregation	(Ahn *et al.*, 2000)
	inhibits thrombin receptor stimulated aggregation of platelets and secretion	(Barrow *et al.*, 2001)
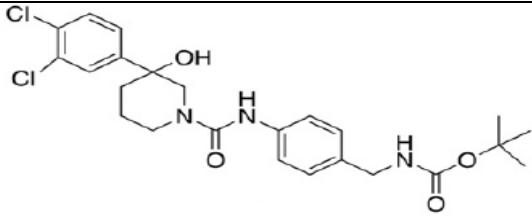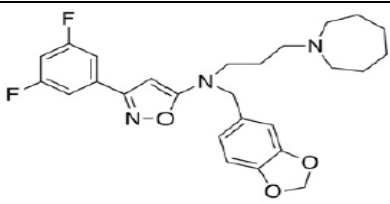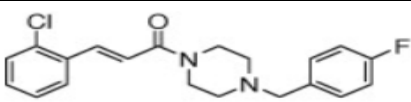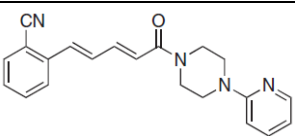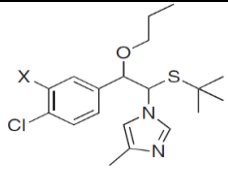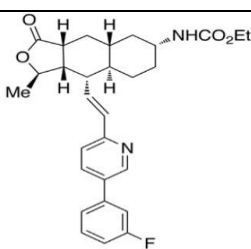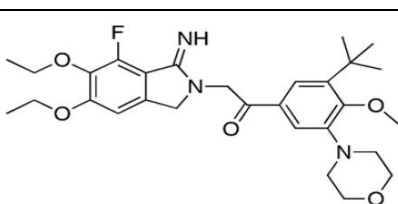
	inhibits thrombin receptor stimulated aggregation of platelets and secretion	(Barrow *et al.*, 2001)
	inhibits platelet activation, blocks platelet aggregation	(Nantermet *et al.*, 2002)
 F16357	High potency to antithrombotic in rat model	(Perez *et al.*, 2009)
 F16618	High potency to antithrombotic in rat model	(Perez *et al.*, 2009)
	Inhibit Ca^{2+} in CHO cells, antithrombotic response in rat	(Planty *et al.*, 2010)
 SCH530348 (Vorapaxar)	Inhibits PAR1 on platelets	(Chackalamannil *et al.*, 2008, French *et al.*, 2015)
 E5555 (Atopaxar)	Inhibits PAR1, inhibits platelet function	(Serebruany *et al.*, 2009)

Table 1. 2 PAR1 antagonists

1.10.2 PAR4 drugs developed to date

There are only a few PAR4 antagonists described to date, as this has proven a more difficult drug target compared to PAR1. An early study utilised the peptide Trans-cinnamoyl-YPGKF (tc-YGPKF) derived from the tethered ligand sequence of PAR4 and found inhibition of platelet aggregation (Hollenberg and Saifeddine, 2001). Another PAR4 antagonist found to block thrombin-activated platelet aggregation in mice is YD-3 [1- benzyl-3 (ethoxycarbonylphenyl)-indazole] (Wu *et al*., 2002). The use of pepducins as a strategy to inhibit PAR4 has also been investigated. For example, the PAR4 pepducin P4pal10 (pal-SGRRYGHALR-NH$_2$) inhibits human platelet aggregation induced through thrombin, prolongs bleeding time and prevents systemic platelet activation in mice (Covic *et al*., 2002b). Recently, BMS-986120 was developed as a PAR4 antagonist and acts as an antiplatelet agent with the potential to treat cardiovascular diseases, the drug reduces the bleeding risk and atherothrombosis mediated by PAR4 in a cynomolgus monkey arterial thrombosis model (Wong *et al*., 2017).

1.11 Challenges in PAR2 drug design PAR2 as a therapeutic target

The challenge in developing PAR2 directed therapies is the same as with all new small molecule drugs. In addition, to ensuring good pharmacodynamics i.e a strong interaction with the target receptor with high potency and selectivity, any drug needs to meet certain criteria linked to toxicity, pharmacokinetics, bioavailability, and delivery. The percentage of new drugs which go forward and make it to the clinic currently is only 0.01% (Milardi and Pappalardo, 2015).

For the PAR1 compounds developed thus far a number have shown off-target effects, lack of potency in particular disease settings or unexpected side effects. The antagonist BMS-197525 while inhibiting PAR1 also behaves as a partial agonist for PAR2 in HEK293 cells. This off-target behaviour is likely due to the high sequence similarity between PAR1 and PAR2 (Kawabata *et al*., 1999). Therefore, designing a new drug which is selective for one PAR over another is difficult. One of the main problems in PAR2 drug discovery is the potency; some initially discovered

compounds although selective have a very low potency. For example, ENMD-1068 is a PAR2 antagonist but displays weak potency *in vitro* (Kelso *et al*., 2006). Some natural compounds have been shown to disarm the activation of PAR2 via inhibition of the NFκB pathway such as triptolide but they show toxic properties with oral administration in rats (Shao *et al*., 2007).

However, PAR2 is still viewed as a highly promising target for the treatment of a number of diseases with small molecules, both agonists and antagonists, antibodies and gene therapy all being considered as strategies for development (Kanke *et al*., 2005). This is based upon expression and function in relevant cell types as outlined above; it links to certain functional outcomes such as inflammation, and its upregulation during inflammatory challenge (Ossovskaya and Bunnett, 2004, Adams *et al*., 2011).

1.12 PAR2 drugs developed to date

Similar to PAR1, the initial research on developing PAR2 antagonists was simple structure activity relationship studies (SAR) using the initial human and rodent tethered ligand sequences. One of the first studies utilising a PAR2 inhibitor was by Al-Ani, in 2002. They demonstrated that the peptides, FSLLRY-NH_2 and LSIGRL-NH_2 prevented trypsin-mediated cleavage of PAR2 and inhibited activation by synthetic peptides (Al-Ani *et al*., 2002). Another study identified the small molecule ENMD-1068 (N1-3- methylbutyryl-N4-6-aminohexanoyl-piperazine) as the first non-peptidic antagonist for PAR2 with the ability to decrease acute inflammation in mice (Kelso *et al*., 2006). However, the apparent affinity for PAR2 was in the high micromolar range. Our laboratory discovered the peptide antagonist K-14585 (N-[1-(2,6-dichlorophenyl)methyl]-3-(1-pyrrolidinylmethyl)-1H-indol-5-yl] aminocarbonyl]-glycinyl-L-lysinyl-L-phenylalanyl-N-benzhydrylamide). This compound inhibited the phosphorylation of p65 NFκB and DNA binding in addition to decreasing the release of intracellular Ca^{2+} mediated by PAR2; however, ERK signalling was not affected by K-14585 suggesting the potential of a bias agonist action, which was identified more recently. Significantly, K-14585 only inhibits

PAR2 signalling activated by synthetic peptides (Goh *et al*., 2009), and was therefore not considered useful therapeutically.

Another compound Nordihydroguaiaretic acid (NDGA) was also identified as a PAR2 antagonist through inhibition of calcium release and a decrease in IL-8 production in HaCat keratinocytes. NDGA negatively affects anti-inflammatory cytokines and inhibits oxazolone-induced chronic dermatitis symptoms in a hairless mice model (Kim *et al*., 2012). Triptolide extracts from *Tripterygium wilfordii Hook F* used in Chinese medicine were also found to inhibit the activity of NFκB induced by 2f-LIGRLO-NH$_2$ in A549/NF-κB-luc cells. Although triptolide was proposed for the treatment of lung inflammation (Hoyle *et al*., 2010), it displayed significant toxicity when taken orally in rats (Shao *et al*., 2007).

1.12.1 PAR2 pepducins

Due to the very slow development of PAR2 antagonist drugs, peducins were also developed. As outlined above pepducins are highly stable sequences of short lipidated peptides that are derived from different intracellular loop domains of GPCRs. The cell-penetratable pepducin is a N-palmitoylated peptide derived from the third intracellular helix within the C-terminal of the cognate PAR2. Pepducins were originally developed as blockers of receptor activation but both activators and inhibitors have been developed as structure/function relationships are better explored. Therefore, some pepducins show biphasic agonist and antagonist activity on GPCR signalling and can be considered as allosteric modulators (Covic *et al*., 2002a).

Selective PAR2 pepducin agonists or antagonists are designed from the key residues (M274, R284, and K287) in the ICL3-TM6 domain. The composition of the competitive inhibitor pepducin for PAR2 is often derived from ICL3 or the C-terminal of PAR2 and designed in a manner similar to other GPCRs (O'Callaghan *et al*., 2012). Some PAR2 ICL3 pepducins actually bind to a small eighth helix within the C-terminal to disrupt receptor/G-protein interactions (Sevigny *et al*., 2011). The

third intracellular loop (ICL3) pepducin antagonist has been shown to inhibit PAR2-mediated inflammation in paw oedema via blockade of agonist-induced inositol phosphate hydrolysis, leukocyte chemotaxis and Ca^{2+} mobilisation, resulting in the attenuation of inflammation in mast cells (Sevigny *et al*., 2011). In addition, the pepducin P1pal-13 inhibits the barrier-protective effects mediated by PAR1 but via trans-activation of PAR2 signalling (Kaneider *et al*., 2007).

Some PAR2 pepducins act as allosteric modulators and have a role in directing PAR2 functions. Modifying the pepducin P2pal-21 at residues R267 to K287 gives rise to a partial PAR2 activator but only following activation by an endogenous peptide (Sevigny *et al*., 2011). In addition, P2pal-21 shows biphasic activity over a limited concentration range acting as a partial agonist at low concentrations in PLC-β-dependent IP_3 production and an antagonist at higher concentrations (Covic *et al*., 2002a). The full agonist pepducin, derived from P2pal-21 is P2pal-21F as outlined above, whilst another moiety P21pal-18Q shows partial PAR2 blocking activity, P2pal-18S behaves as a full antagonist of PAR2 as tested by calcium flux. Interestingly structure activity relationships are clearly being developed for pepducins in a manner similar to small molecules, for example, removal of the first residues from the N-terminal reduces agonist like activity to antagonist activity (Sevigny *et al*., 2011). Despite the potential of these types of molecule, there are a number of major challenges in defining potency, specificity, off-target effects, bioavailability, and delivery. However, current developments are promising.

1.12.2 PAR2 antibodies

Given the role of PAR2 in inflammation and immune conditions the development of specific humanised antibodies has the potential as a treatment. However, even the utilisation of commercially available antibodies has resulted in considerable difficulties in reliable detection and specificity making the potential to develop therapeutics antibodies a very difficult one (Adams *et al*., 2011). The PAR2 antibody most routinely utilised to observe the expression of PAR2 on cell surfaces is SAM11 and whilst the specificity of this antibody is still questionable, it has been show to

block PAR2 mediated responses *in vitro* and inhibit collagen-induced arthritis in mice (Crilly *et al*., 2012). Moreover, SAM11 has been found to inhibit migration during cancer metastasis induced by 2f-LIGRLO-NH$_2$ in human breast cancer cells (MDA-MB-231) (Yau *et al*., 2016b).   Most recently, a series of humanised antibodies have been developed paving the way for extensive *in vivo* studies and evaluation in humans. They have a good binding affinity for PAR2 and have been shown to inhibit intracellular Ca^{2+} release and prevent cytokine secretion mediated by PAR2, as well as inflammatory oedema *in vivo* (Giblin *et al*., 2011). However, it remains to be determined if anti-PAR2 antibodies have a potential clinical use but conditions such as rheumatoid arthritis (RA) would be a viable target.

1.12.3 PAR2 Non-peptides antagonists

A major breakthrough in the development of antagonists for PAR2 have been in the last 8 years which involves the development of non-peptide antagonists. These were derived from non-peptide PAR2 agonists such as GB110 using standard medicinal chemistry approaches and SAR. Modification of the C-terminus gave rise to the compounds GB83 and GB88 (Barry *et al*., 2010, Suen *et al*., 2012) and the potential of GB88 as a possible viable molecule has been strongly scrutinised.

1.12.3.1 GB88

A series of papers have identified and characterised a PAR2 antagonist, named GB88, which is a spiroindenepiperidine compound derived from the agonist GB110. Significantly, GB88 has been shown to inhibit PAR2 activation in not only response to synthetic peptides such as peptide 2f-LIGRLO-NH$_2$ but also the endogenous protease trypsin, as well as synthetic and non-peptidic agonists such as GB110. In a number of cell lines GB88 has found to be a surmountable and competitive antagonist for PAR2 in response to 2f-LIGRLO-NH$_2$, while behaving as an insurmountable antagonist with trypsin and GB110 as the activators (Suen *et al*., 2012). Nevertheless, GB88 showed selectivity over other PARs, good stability in

serum and reasonable bioavailability following oral administration in rodents (Suen *et al*., 2012, Lohman *et al*., 2012b, Lohman *et al*., 2012a).

More recent work has challenged the definition of GB88 as an antagonist. In one study, GB88 has been shown to inhibit intracellular Ca^{2+} release, PKC phosphorylation and pro-inflammatory cytokine release (such as IL-6, IL-8, and TNFα) mediated by PAR2 whilst at the same time stimulating ERK and cAMP suggesting the compound has bias antagonist properties (Suen *et al*., 2014). These properties may be beneficial or detrimental in regarding its possible use clinically.

A very recent major breakthrough has been in the resolution of the crystal structure of PAR2 structure by Cheng *et al* in 2017, and this was achieved through stabilisation of PAR2 with two distinct antagonists and a blocking antibody, as listed in table 1.3. They demonstrated that the antagonist AZ8838 binds in a fully occluded pocket near the extracellular surface. Further investigation of AZ8838 using functional and binding studies showed the antagonist to display slow binding kinetics which is an appealing trait for a PAR2 antagonist competing against a tethered ligand. The other antagonist described, AZ3451, was shown to bind to a remote allosteric site outside of the helical bundle. A blocking antibody antigen-binding fragment was also explored in this study and shown to bind to the extracellular surface of PAR2, thereby preventing access of the tethered ligand to the peptide-binding site on extracellular loop 2 (Cheng *et al*., 2017).

With the discovery of the PAR2 crystal structure and these new antagonists, this paves the way for the development of further selective and potent antagonists of PAR2, which can be of therapeutic benefit.
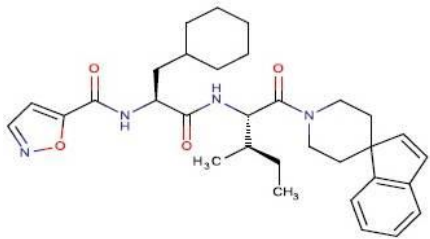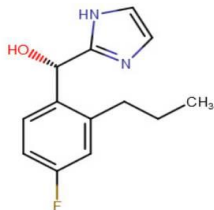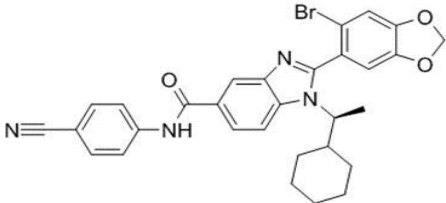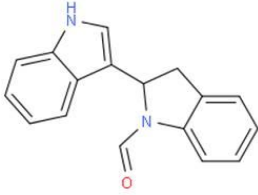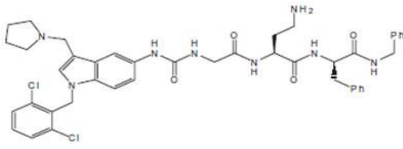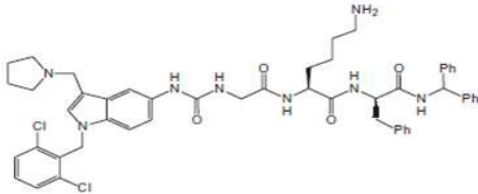
Compound	Chemical structure	reference
GB88		(Suen *et al*., 2012)
AZ8838		
AZ3451		(Cheng *et al*., 2017)
AZ7188		
K-12940		
K-14585		(Kanke *et al*., 2009)

Table 1. 3 PAR2 antagonists

1.13 Aims and Objectives

The studies outlined in this chapter demonstrate the coupling of PAR2 to cellular outcomes, which are linked to a number of functional outcomes relevant to disease. The development of PAR2-KO mice models have confirmed roles in GI tract disorders, RA and OA. Inhibition of PAR2 could therefore be a promising approach to the treatment of these and other diseases. However, there have been challenges in developing appropriate small molecule antagonists for PAR2 due to its mode of activation. However, recently a number of putative antagonists have been developed including GB88 and more recently, AZ8838. These drugs have not been fully characterised in a number of systems and warrant further characterisation and analysis. Establishing the utility of these drugs as potential preclinical drugs requires considerable study. Therefore in this thesis, the following objectives will be addressed in two major results chapters. Firstly, identification and characterisation of derivatives of GB88 as new PAR2 antagonists. It was hypothesised that GB88 acts as a biased antagonist. Secondly, the assessment of the novel recently described AZ8838 compound as a lead molecule for study in cellular systems. It was hypothesised that AZ8838 behaves as an allosteric modulator. Each chapter has these objects:

i)   To examine the effect of compounds on NFκB-transcriptional activity mediated by PAR2 in NFκB-Reporter cells.

ii)   Assess the effect of compounds on ERK activation mediated by PAR2 in HEK293 cells.

iii) Examine the effect of PAR2 induced calcium mobilisation in HEK293 cells.

Chapter Two

Materials and Methods

2.1 Materials

2.1.1 General Reagents

All materials and reagents used were of the highest commercial grade available and purchased from Sigma-Aldrich Chemical Company Ltd. (Dorset, U.K.) unless otherwise stated.

Pre-stained SDS-PAGE molecular weight markers: Bio-Rad Laboratories (Hertfordshire, UK)

Methanol: VWR International Ltd. (Leicestershire, UK)

FLUO-4 AM: Fisher Scientific Ltd (Leicestershire, UK)

Nitrocellulose Blotting Membrane (Protram): Fisher Scientific Ltd (Leicestershire, UK)

TNF-α: Insight Biotechnology Ltd (Wembley, UK)

4',6-diamidino-2-phenylindole (DAPI): Fisher Scientific Ltd (Leicestershire, UK)

3MM blotting paper: VWR International Ltd. (Leicestershire, UK)

Mowiol: Merck-Calbiochem (Nottingham, UK)

Luciferase Assay Substrate: (Promega, USA)

Fetal Bovine Serum (FBS): Fisher Scientific Ltd (Leicestershire, UK)

Hank's Balanced Salt Solution (HBSS) 1X (w/o Ca^{2+} and Mg^{2+}): Fisher Scientific Ltd (Leicestershire, UK)

PAR2 agonists:

2f-LIGRLO-NH$_2$: Peptide protein research (PPR Ltd.), (Fareham, UK). It is selected as a synthetic PAR2 agonist.

Trypsin: Sigma-Aldrich Chemical Company Ltd. (Dorset, U.K.). It is selected   as a protease activator for PAR2.

2.1.2 Reagents for cell culture

Corning B.V. (Buckinghamshire, UK)

All Cell Culture plastic ware including; flasks, falcon tubes, and graduated pipettes.

Thermo Fisher Scientific UK Ltd (Leicestershire, UK)

96 well Black with Clear Flat Bottom, and 12 well plates

Minimum Essential Medium (Khedr *et al.*) (10X): Gibco (Life Technologies, Paisley, UK)

L-glutamine: Gibco (Life Technologies, Paisley, UK)

Penicillin-Streptomycin: Gibco (Life Technologies, Paisley, UK)

Geneticin (G148): Gibco (Life Technologies, Paisley, UK)

Blasticidin: Gibco (Life Technologies, Paisley, UK)

2.1.3 Antibodies

Table 2. 1 Antibodies.

Information on primary antibodies used including the conditions for concentrations and temperature of the incubation.

Name	Company	Dilution-Incubation
Anti-p-ERK Mouse	Santa Cruz Biotechnology	1:7500 - RT
Anti-ERK Rabbit	Santa Cruz Biotechnology	1:15000 - RT
Anti-p-p38 MAPK Rabbit (T180/Y180)	Cell Signalling	$1:2000 - 4^0C$
Anti-P38 MAPK Rabbit	Cell Signalling	1:10000 - RT
Anti-p-NF-Kappa B p65 Rabbit	Cell Signalling	$1:3000 - 4^0C$
Anti-NF-Kappa B p65 Rabbit	Cell Signalling	1:15000 - RT
Anti-IKB-alpha Rabbit	Cell Signalling	1:10000 - RT
Anti-GAPDH Rabbit	Cell Signalling Technology	1:30000 - RT

2.1.4 Equipment:

luminometer Wallac MicroBeta TriLux 1450-024 Counter (Wallac Oy, Finland)

FlexStation 3 (FLIPR): Molecular Devices UK Ltd, (Wokingham, UK)

2.1.5 Compounds Preparation

2.1.5.1 GB88 was synthesised in house by the department of Pure and Applied Chemistry in collaboration with Dr C. Jamison. The chemical structures were confirmed by mass spectrometry and nuclear magnetic resonance. The purity of compounds ($\geq$ 95%) was determined by high-performance liquid chromatography-mass spectrophotometry (HPLC-MS) and proton nuclear magnetic resonance (1H NMR) analysis. The water-insoluble molecule was dissolved in 100% DMSO to obtain a stock concentration of 10 mM, which was stored at -20^0C. Due to lack of water solubility, a minimum 1:50 dilution into water was required for a 200μM intermediate preparation. This was then further diluted when added to the cell media for stimulations. Treatment of cells with an equivalent volume of DMSO (0.2%) was used as a vehicle control.

GB88 derivative compounds DM/7/34, DM/8/45, DM/8/53, JAMI1026A, and JAMI1028A were synthesised as described for GB88 (Yau *et al*., 2016a), figure 2.1.

rac-AZ8838 was purchased from YProTech Ltd, (Cheshire, UK)

YPT-1 & YPT-2 were purchased from Reach Separations (Nottingham, UK)

rac-AZ8838, YPT-1 and YPT-2 were prepare with 10 mM as stock concentrations in
DMSO and diluted them the same way to GB88 solution.
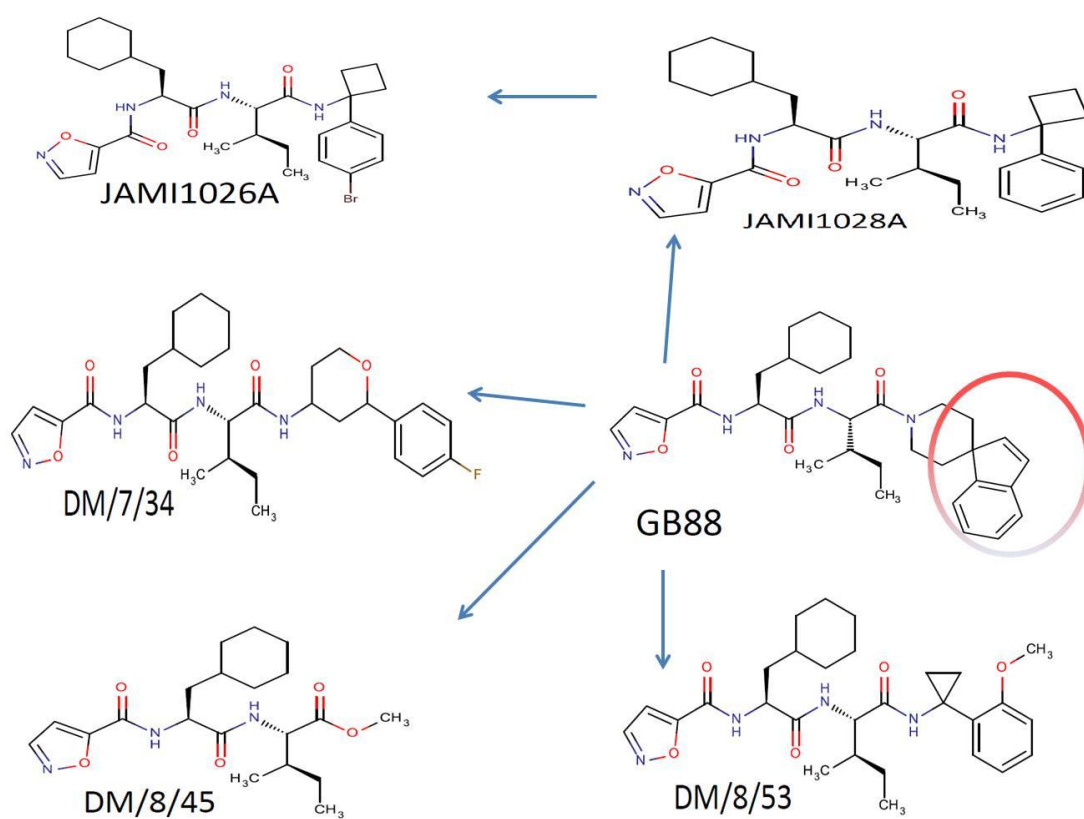
Figure 2. 1 GB88 and its derivatives compounds

2.2 Cell Culture

All cell culture work was performed in class II laminar flow cell culture fume hood, under sterile conditions. Two cell lines were used in this thesis; human embryonic kidney and NFκB-Reporter cells and the expression to PAR2 is explained in table 2.2.

Table 2. 2 The lines of cells

Cell type	
Human Embryonic Kidney cells (HEK)	Endogenous expression for PAR2
NFκB-Reporter cells (overexpression to PAR2)	Its originally epithelial skin cells (NCTC), is not expressed to PAR2, transcript with PAR2 and NFκB-Luc (p65) x 3 construct.
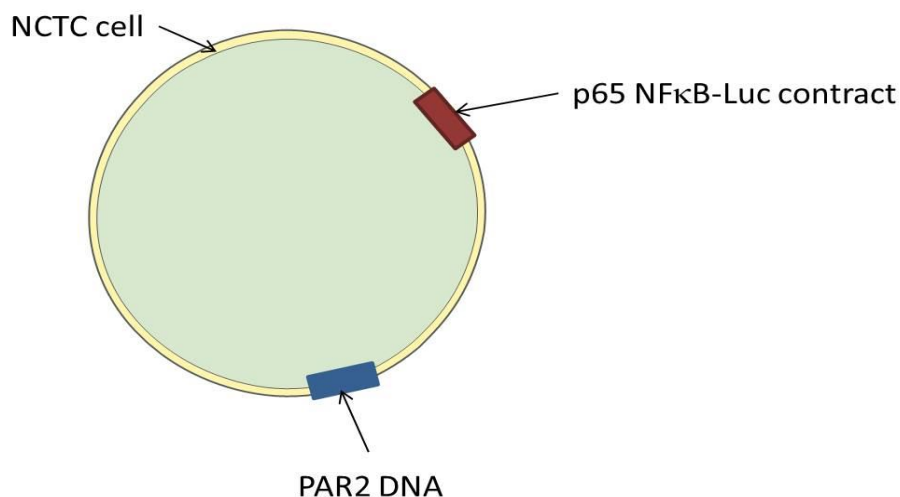
Figure 2. 2 The transcription of NCTC cell with PAR2 and NFκB-Luc constructs.

2.2.1 NFκB-Reporter cells

NFκB-Reporter cells were maintained in medium 199 supplemented with 10% FBS, L-glutamine (1%), and penicillin/streptomycin (1%). Cells were incubated at 37^{0}C in a humidified environment (5 % CO_2). NFκB-Reporter cells stably expressing a human PAR2 (Clone G) and an NFκB-luciferase reporter plasmid were grown in media 199 supplemented with (400 µg/ml) from the antibiotic Geneticin to survive the cells introduced gene and (5 g/ml) from the antibiotic Blasticidin to maintain PAR2-DNA in cells. Once the cells had reached 90-100% confluency the media was removed via aspiration and the cells washed once in 1.5 ml Versene (0.2% EDTA/PBS) (0.53 mM) EDTA in phosphate-buffered saline (PBS)) [PBS (154 mM sodium chloride, 5.36 mM potassium chloride, 1.46 mM potassium hydrogen orthophosphate, 8 mM di-sodium hydrogen orthophosphate anhydrous) pH 7.4]. The purpose of using Versene to passage cells is to avoid trypsin exposure and therefore activation of PAR2. The Versene was aspirated off and replaced with a further 2 ml and the cells incubated at 37^{0}C. Once some of the cells had started to lift off the culture flask the Versene was removed and the cells washed off the culture flask with 10 ml Medium 199. The cells were diluted as required in Medium 199 and seeded into new T75 cm2 cell culture flasks to maintain stock flask, or into 96 black well plates for luciferase assay or 12 well plates for other experiments. Cells were quiesced in serum-free media for 18 hours prior to stimulation.

2.2.2 Human embryonic kidney (HEK 293) cells

HEK293 cells were maintained in modified eagle's medium (Khedr *et al.*) supplemented with 10% (v/v) foetal bovine serum, penicillin/streptomycin (1%), L-glutamine (1%), 0.375% (v/v) sodium bicarbonate. Cells were then incubated at 37^0C in a humidified atmosphere with 5% CO_2 and the medium was replaced every two days. Cells were passaged using 1x sodium citrate solution (SSC) [1.5 mM NaCl and 0.54 mM sodium acetate dissolved in 100ml of distilled water, then adjusted to pH 7.0] again to avoid using trypsin. The cells were diluted as required in MEM medium and seeded into 96 black well plates for calcium assay or 12 well plates for other experiments. Otherwise, the cells were seeded into new T75 cm^2 cell culture flask to maintain stock flasks. HEKs were quiesced in 2% serum for 24 hours prior to stimulation.

2.3 NFκB-Luciferase reporter gene activity assay

NFκB-Reporter cells stably expressing both PAR2 and the NFκB reporter plasmid were seeded in 96- black well plates and incubated until 90-100% confluence. Then, the cells were rendered quiescent in serum-free media for 18 hours. Cells were treated with the PAR2 agonists trypsin and 2f-LIGRLO-NH$_2$ or GB88 and derivative compounds for 6 hours at 37^0C. The GB88 test compounds were also used in pre-treatment experiments added 1 hour prior to PAR2 agonists for a further 4 hours. Reactions were terminated by rapid aspiration and washing steps, before addition of lysis buffer containing the luciferin substrate (luciferin substrate (0.2 mM), 1 mM ATP, 1 mM DTT, and 1% (v/v) BSA added to lysis buffer [25 mM Tris- Base, 8 mM

MgCl$_2$, 1% (v/v) Triton X-100, 15% (v/v) Glycerol]), for 5 minutes at room-emperature. The relative light units were measured on the Wallac MicroBeta TriLux 1450 luminometer (Wallac Oy, Finland), using a bottom read at 450nm for 1 sec per well.

2.4 Western Blotting

Detection and analysis of specific cellular protein expression were achieved using western blotting.

2.4.1 Preparation of samples for SDS-PAGE

Cells were grown to 90-100% confluency in 12-well plates and quiesced for 18 hours on prior to stimulation. Reactions were terminated by rapid aspiration of media followed by PBS wash steps, cells were then solubilised by the addition of hot (~85^{0}C) Laemmli SDS sample buffer (63 mM Tris/ HCl, 2 mM Na$_4$P$_2$O$_7$, 5 mM EDTA, 50 mM DTT, 10% v/v Glycerol, 2% w/v SDS and 0.007% bromophenol blue, pH 6.8). Cells were harvested via scraping on ice and lysates drawn repeatedly through a syringe to shear chromosomal DNA. Samples were transferred to Eppendorf tubes, and boiled at 95^{0}C for 5 min to denature proteins then stored at -20^{0}C until further use.

2.4.2 SDS-polyacrylamide Gel Electrophoresis and western immunoblotting

The SDS-PAGE was prepared using the Bio-Rad miniPROTEAN-3 assembly unit. Resolving gel was prepared using 10% of polyacrylamide: [0.27% N, N'-methylene-bis-acrylamide, 0.375 M Tris-base (pH 8.8), 0.1% (w/v) SDS and 0.05% (w/v) ammonium persulphate. The polymerisation of the resolving gel was initiated by the addition of 0.05% (v/v) N, N, N', N'-tetramethylethylenediamine (TEMED). The gel solution was poured into 1mm glass plates and allowed to polymerise. A thin layer of 0.1% SDS solution was added to the gel, to prevent drying and to disperse bubbles. Once the gel was set, the 0.1% SDS was discarded and the appropriate Teflon welled combs slotted into the glass plates, the stacking gel solution [5% (w/v) acrylamide, 125 mM Tris-base (pH 6.8), 0.1% (w/v) ammonium persulphate, 0.1% (v/v) TEMED] was then added on top of resolving gel. The gel was allowed to polymerise for 15 min before comb was removed. Gels were placed in the specified western blot tank and this was filled with running buffer [25 mM Tris-base, 192 mM glycine, and 3.5 mM SDS], samples were loaded into the appropriate wells. Proteins were separated using Sodium Dodecyl Sulphate Polyacrylamide Gel Electrophoresis (SDS-PAGE) with a pre-stained SDS protein marker of known molecular weights at 125 V for approx. 115 minutes.

2.4.3 Transfer to nitrocellulose membrane

The resolved proteins on the gel were then transferred onto nitrocellulose membranes. The gel was placed on top of the nitrocellulose membrane and sandwiched between two Whatmann 3MM papers and two fibrous blotting pads (Bio-Rad). The cassette(s) were then placed in a Bio-rad mini trans-blot electrophoresis tank along with an ice pack. The tank was then filled with transfer buffer [20mM Tris-base, 192 mM glycine, and 20% (v/v) methanol] and was left to run for 1 hour and 45 minutes at a constant current of 290 mA.

2.4.4 Membrane blocking and immunoblotting

After transfer of proteins the membrane was trimmed to the size of the gel, and then blocked in a 3% BSA/NATT [150 mM NaCl, 50 mM Tris-base (pH 7.4), 0.2% (v/v) Tween 20] solution for 2 hours at room temperature, orbital shaking at 46 r.p.m. The membrane was immunoblotted with a primary antibody overnight of choice at an appropriate concentration in 0.3% BSA/NATT solution. The following morning, the membrane was washed with NATT buffer (6 x 15 minutes washes), then the membrane was incubated with the appropriate horseradish peroxidase-conjugated polyclonal secondary antibody diluted in 0.3% BSA/NATT for 2 hours at room temperature, orbital shaking at 46 r.p.m. The membrane was then subjected to a further 6 x 15 min NATT washes.

2.4.5 ECL detection

For detection of proteins, membranes were incubated with enhanced chemiluminescent (Busso *et al.*) reagents ECL 1 [0.1 M Tris-HCl (pH 8.5), 25 M luminol and 25 M coumaric acid] and ECL 2 [0.1 M tric-HCL (pH 8.5) and 6.27 mM H2O2] for three mins. Membranes were then transferred to an exposure cassette and exposed to X-ray film (Kodak LS X-OMAT) under red light for the required time. The X-ray film was developed and fixed using a JP-33 processor. Protein expression was quantified by densitometry (background pixel intensity subtracted from corresponding band pixel intensity) using Scion Image software.

2.4.6 Nitrocellulose membrane stripping and re-probing

Membranes were stripped and re-probed to ensure total protein levels across samples. The membrane was incubated with stripping buffer [0.05 M Tris-HCl, 2% SDS, pH 6.7 and 0.1 M β-mercaptoethanol] for 1 hour at 60^0C, orbital shaking at 70 r.p.m to strip previously bound antibodies. The membrane was repeatedly washed (3 x 10 minutes) with NATT solution then incubated with a total primary antibody overnight. The membrane was probed with secondary antibody and visualised as described in section 2.4.5.

2.4.7 Scanning and densitometry

Western blots were scanned on an Epson Perfection 1640SU scanner using Adobe Photoshop 5.0.2 software. The scanned images when then normalised to an unstimulated control and quantified using ScionImage (Scion Corp., Maryland U.S.A).

2.5 Intracellular calcium release assay

PAR2 agonist-stimulated intracellular calcium mobilisation was assessed in HEK293 cells by the modified fluorescence technique. Black, clear-bottom 96-well plates were coated with poly-L-lysine prior to the addition of HEK293 cells. Plates were incubated at 37^0C 5% CO_2 until confluent. Prior to the experiment, the medium was removed and the cells washed once with Hank's balanced salt solution (HBSS) containing 1 mM calcium chloride and 1 mM magnesium chloride. 50 µl of HBSS containing Fluo-4 AM dye (3 µM, 0.03 % pluronic acid) was added to the wells. The plate was wrapped in foil to keep it dark and incubated for 45 minutes at 37^oC. Then, the dye loading buffer was removed and the cells washed once with HBSS. The cells were stimulated with various concentrations of agonists prepared in HBSS. Alternatively, after 45 minutes incubation with dye loading buffer, cells were incubated with different concentrations of test compounds for various times. The plate was then examined via fluorescence using the FlexStation 3 machine using SoftMax Pro 5.4.5 software for the concentration-dependent effects of the activity of agonists in the presence of different concentration of antagonist. The fluorescence change was monitored at 37^oC (excitation wavelength 458 nm; and emission wavelength 525 nm, and auto-off wavelength 515 nm), the runtime for each well is 120 second and the interval is every 3 seconds. Agonist-induced Ca^{2+} peak signals are expressed as the percentage of the reference unstimulated Ca^{2+} response. Change in fluorescence (% response) were plotted against log [compound]. The half-maximal effective concentration values (EC50) were assessed from the concentration-response curve.

The data generated was exported into Microsoft Excel for analysis. The relative fluorescent units (RFU) for each trace were displayed in a table. Stimulations were performed in triplicate in each plate and independent experiments conducted. A baseline fluorescent measure was chosen between the 10-20 sec initial count, averaged across replicates and subtracted from the peak signal across each condition. The peak fluorescent value was determined by finding the average of three highest values across the replicates, this tended to be between 29-34 secs before rapidly tailing off. The averages were then analysed and graphed using GraphPad Prism v5.0 software.

2.6 Statistical analysis

All values shown were expressed as a mean ± standard error of the mean (s.e.m) and were representative of one of at least three independent experiments. Data gathered was analysed using GraphPad Prism v.5.0 analytical software. Statistically significant differences between groups were performed by using one-way analysis of variance (Stoyanov *et al*.) (three or more group comparisons) with Dunnet's post-test (control vs. non-control group). Differences were considered significant at $P<0.05$. Concentration-response curves were generated by fitting a non-linear regression curve (sigmoidal dose-response curve with variable slope). Where indicated in the figure legend, constraints were applied (i.e. bottom of the curve constrained to 1 for data represented as fold control and top constraint set at 100 for viability experiments where data depicted as % control). A separate curve was formed for each individual experiment (3 experiments analysed) and the EC50/IC50 value attained from each curve compiled to find the mean ± s.e.m.

Chapter Three

Characterisation of Derivatives of GB88 as new PAR2 antagonists

3.1 Introduction

Activation of PAR2 as discussed previously is related to many physiological and pathological outcomes, including but not limited to respiratory, cardiovascular, gastrointestinal, skin, as well as inflammatory diseases and pain (Adams *et al*., 2011, Kanke *et al*., 2005, Lieu *et al*., 2016, Sekiguchi, 2005, Ferrell *et al*., 2003, Cocks *et al*., 1999). Previous studies have investigated the role of PAR2 in various settings with an emphasis on its pathological role, particularly in inflammation. Until recently examining the role of PAR2 in disease has been through the use of KO animal models and receptor deletion experiments, only a few papers have focused on PAR2 antagonists as a method to inhibit PAR2. This has in part been due to the tethered ligand nature of receptor activation and resolution of the crystal structure which was only achieved last year (Cheng *et al*., 2017). There are potential therapeutic uses for treating many diseases through disarming the signalling pathways of PAR2.

In 2006, new compounds were discovered that behave as PAR2 inhibitors. Both K-14585 and ENMD1068 were identified as low potent antagonists able to inhibit NFκB-transcriptional activity mediated by PAR2 activation. ENMD1068 has antagonist properties *in vivo* as well *in vitro* and was shown to attenuate joint inflammation induced by carrageenan/kaolin (C/K) in mice models (Kanke *et al*., 2009, Kelso *et al*., 2006). More recently, the small molecules GB88 and GB83 have been found to inhibit activation of PAR2 as measured through the release of intracellular Ca^{2+}. They inhibited PAR2 activation by both trypsin and peptide agonists, 2f-LIGRLO-NH_2 and GB110 in various human cell types (Barry *et al*., 2010, Suen *et al*., 2012). Another group have shown that the molecule C391 has the ability to inhibit intracellular Ca^{2+} and MAP kinase pathways are mediated via PAR2 (Boitano *et al*., 2015).

Different studies have demonstrated GB88 as a new potential PAR2 inhibitor *in vivo* and *in vitro* (Lohman *et al*., 2012a, Suen *et al*., 2012, Lohman *et al*., 2012b). However, more studies are needed to confirm the characteristics of this compound. Therefore, the aim of this chapter is to characterise further the

pharmacological properties of GB88 and derivative compounds synthesised in-house in different functional assays. It was hypotheses that GB88 and its derivatives behave as biased antagonists. This would allow SAR to be developed around the GB88 scaffold to find more effective compounds.

3.2 The effect of synthetic compounds on PAR2 dependent NFκB activity

NFκB-luciferase reporter assays were utilized to measure NFκB mediated gene transcription activated via PAR2 agonists (Macfarlane *et al*., 2005). An NCTC2544 stable clone co-expressing hPAR2 and NFκB-Luciferase (previously generated in-house) was utilised for these experiments. Cells were pre-incubated with PAR2 compounds prior to receptor activation with trypsin or 2f-LIGRLO-NH$_2$.

3.2.1 PAR2 mediated NFκB transcriptional activity stimulated by trypsin & 2f-LIGRLO-NH$_2$

The kinetics of PAR2 mediated NFκB transcriptional activity was measured over a period of 6 hours as shown in figure 3.1. Both trypsin and 2f-LIGRLO-NH$_2$ stimulated a time-dependent increase in NFκB-driven gene transcription, reaching a maximum by 4 hours. Trypsin stimulated a 3.5-4 fold response over basal values (3.38 $\pm$ 0.30, n=3) as shown in figure 3.1.a, whereas 2f-LIGRLO-NH$_2$ stimulated an approximate 12 fold over basal control (11.934 $\pm$ 0.437, n=5) as shown in figure 3.1.b. Measured over 4 hours, trypsin and 2f-LIGRLO-NH$_2$ both gave a concentration-dependent increase in NFκB-driven gene transcription with EC$_{50}$ values of 40 nM and 3 μM, respectively.

a)
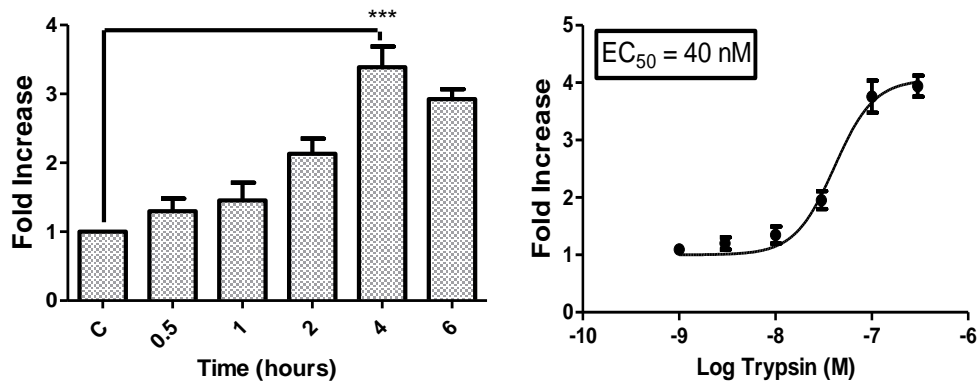
b)
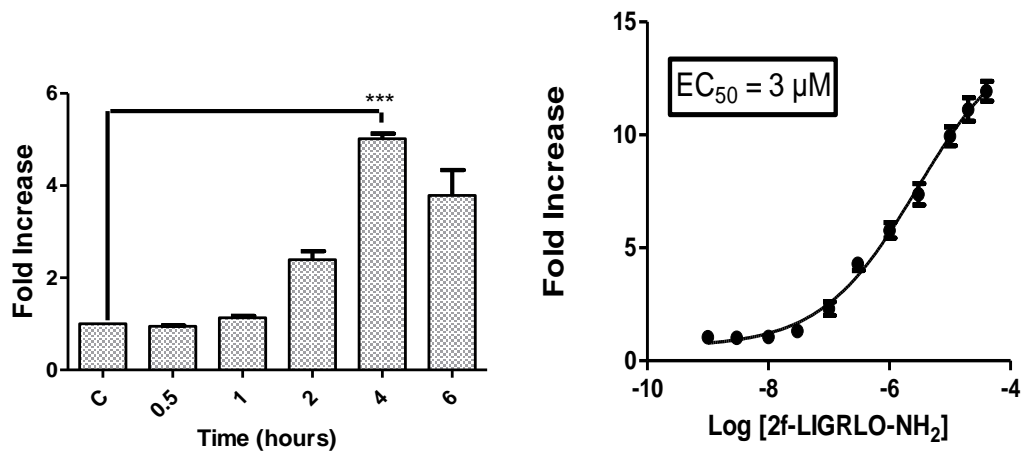
Figure 3. 1 The effect of trypsin and 2f-LIGRLO-NH$_2$ on NFκB-driven transcription activity in NFκB-Reporter cells

NFκB-Reporter cells were grown to confluency in 96 black well plates and rendered quiescent for 18 hours prior to stimulation with (a) Trypsin (100 nM) and (b) 2f-LIGRLO-NH$_2$ (10 μM) for time points up to 6 hours (left panel) and with increasing concentrations at 4 hours (right panel). Whole cell lysates were measured for luciferase activity as previously described (section 2.3). Data shown are expressed as fold stimulation over unstimulated basal values. For trypsin, n=3 and 2f-LIGRLO-NH$_2$, n=5.

3.2.2 Characterisation of PAR2 modulators on NFκB transcriptional activity

The effect of six synthesised PAR2 antagonist compounds comprising of; GB88, DM/7/34, DM/8/45, DM/8/53, JAMI1026A and JAMI1028A were examined as shown in figure 3.2. Initially these compounds were tested on the assumption they would be antagonists and not be active. However, single time point studies surprisingly showed activity. Thus, cells were treated with each compound over 4 hours and NFκB transcriptional activity assessed with varying concentrations as described in the methods section. Responses were concentration-dependent, effective in the low to mid micromolar range. Relative to 2f-LIGRLO-NH$_2$, the response was smaller by approximately 50% as shown in figures 3.2 for a number of compounds suggesting the potential of partial agonist activity. The EC$_{50}$ value of each compound is shown in panels a, b, and c (See table 3.1 for the EC$_{50}$ values).

a)
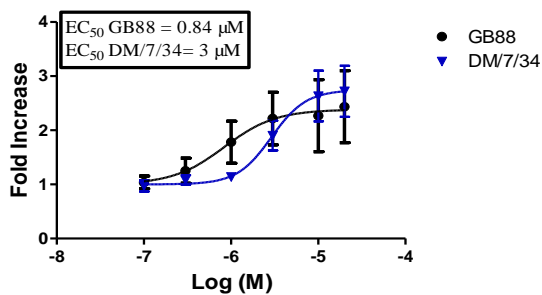
b)
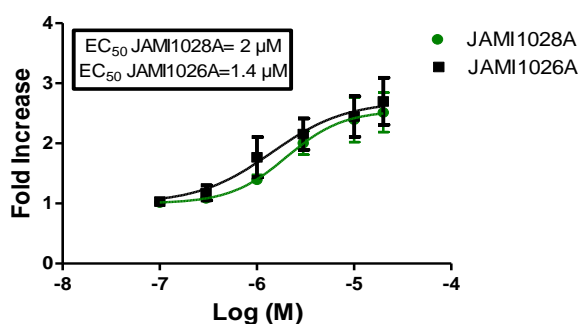
c)
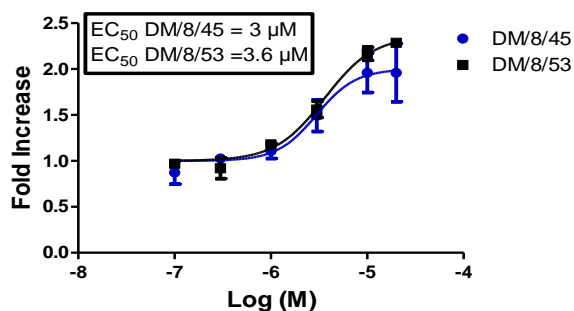
Figure 3.2   Effect of GB88 derivatives on PAR2-mediated transcriptional activity in NFκB-Reporter cells

NFκB-Reporter cells stably expressing both hPAR2 and an NFκB-luciferase reporter plasmid were grown to confluence in black 96 well plates and rendered quiescent for 18 hours prior to addition of increasing concentrations of each compound for another 4 hours. Cell lysates were measured for luciferase activity as previously described (section 2.3). The data shown are expressed as fold stimulation relative to controls and each value represents n=3.

Compound	EC$_{50}$ (μM)
GB88	0.84
DM/7/34	3
DM/8/45	3
DM/8/53	3.6
JAMI1026A	1.4
JAMI1028A	2

Table 3. 1   EC$_{50}$ values of each compound in the NFκB luciferase reporter assay

3.2.3 Effect of derivative GB88 compounds on 2f-LIGRLO-NH$_2$ stimulated gene transcription in NFκB-Reporter cells

The effect of pre-treatment with GB88 prior to the addition of a sub-maximal concentration of 2f-LIGRLO-NH$_2$ on PAR2 mediated NFκB-driven gene transcription is shown in figure 3.3. As a control, stimulation with 2f-LIGRLO-NH$_2$ plus DMSO gave an approximate 8 fold increase of reporter gene activity (8.390 $\pm$ 0.812) when compared to basal values. Lower concentrations of GB88, which were not active, gave a very small inhibition of agonist stimulation, which was not statistically significant. However, as the concentration of GB88 increased and the effect of GB88 became apparent there is a small reduction in the simulation by 2f-LIGRLO-NH$_2$ although this was not significant. Overall, it can be observed that over the 3 - 20 μM concentration range for GB88 the responses were not additive with 2f-LIGRLO-NH$_2$. For example, the fold increase for 3 μM GB88+2f-LIGRLO-NH$_2$ was approximately 7 fold (6.720 $\pm$ 0.391) marginally reduced than that for 2f-LIGRLO-NH$_2$/DMSO alone. The concentration dependent effect of GB88 was consistent with that observed in previous experiments.

This outcome was repeated for a number of the other agents. Pre-treatment of cells with increasing concentrations of DM/7/34 followed by incubation with 0.3 μM 2f-LIGRLO-NH$_2$ for 4 hours is shown in figure 3.4. There was a strong, 11.5 fold stimulation for DMSO + 2f-LIGRLO-NH$_2$ (11.457 $\pm$ 2.119) relative to basal values. Figure 3.4 clearly shows the lack of additivity in the stimulation with increasing concentrations of DM/7/34. These fold stimulations are 10.140 $\pm$ 1.584, 9.787 $\pm$ 2.437 and 10.777$\pm$ 3.002 for 1, 10 and 20μM respectively. In the same figure, it was observed that there was a concentration-dependent increase in NFκB-transcriptional activity when the cells were treated with increasing concentrations of DM/7/34 alone.

Figures 3.5-3.8 demonstrate a similar phenomenon to those experiments outlined above for DM/8/45, DM/8/53, JAMI1026A and JAMI1028A. There is a consistent lack of inhibition with the agonist peptide response using low concentrations of the compound and as the concentration of the compound increases there is no additivity with 2f-LIGRLO-NH$_2$.

Taken together, these results show that GB88 and derivative compounds are acting as weak PAR2 agonists by mediating NFκB-transcriptional activity, and show little to no inhibitory properties. However, it should be noted the NFκB-Reporter cells over-express human PAR2, and this may have a bearing of the effects observed.

DMSO	-	-	+	+	-	-	-	-	-	-	-	-	-	-	-
GB88 (µM)	-	-	-	-	0.1	0.1	0.3	0.3	1	1	3	3	10	10	20	20
2F-LIGRLO-NH$_2$ (0.3 µM)	-	+	-	+	-	+	-	+	-	+	-	+	-	+	-	+

Figure 3. 3 Effect of GB88 on 2f-LIGRLO-NH$_2$ -mediated transcription activity in NFκB-reporter cells

Cells were grown to confluency and rendered quiescent for 18 hours prior to pre-treatment with various concentrations of GB88 for 1 hour. The cells were then stimulated with 0.3 µM 2f-LIGRLO-NH$_2$ for a further 4 hours. Cell lysates were measured for luciferase activity as previously described (section 2.3). The data shown are expressed as fold stimulation over DMSO control and each value represents n=3. Statistical analysis was performed using one way ANOVA, with Dunnett's post-test comparison. ***p<0.001.

DMSO	-	-	+	+	-	-	-	-	-	-	-	-	-	-	-
DM/7/34 (µM)	-	-	-	-	0.1	0.1	0.3	0.3	1	1	3	3	10	10	20	20
2F-LIGRLO-NH$_2$ (0.3 µM)	-	+	-	+	-	+	-	+	-	+	-	+	-	+	-	+

Figure 3. 4 The effect of DM/7/34 on 2f-LIGRLO-NH$_2$ -mediated transcription activity in NFκB-reporter cells

Cells were grown to confluence and rendered quiescent for 18 hours prior to pre-treatment with various concentrations of DM/7/34 for 1 hour. The cells were then stimulated with 0.3 µM 2f-LIGRLO-NH$_2$ for a further 4 hours. Cell lysates were then measured for luciferase activity as previously described (section 2.3). The data shown are expressed as fold over DMSO control and each value represented n=3. Statistical analysis was performed via one way ANOVA, with Dunnett's post-test comparison. ***p<0.001.

DMSO	-	-	+	+	-	-	-	-	-	-	-	-	-	-	-	-
DM/8/45 (μM)	-	-	-	-	0.1	0.1	0.3	0.3	1	1	3	3	10	10	20	20
2F-LIGRLO-NH₂ (0.3 μM)	-	+	-	+	-	+	-	+	-	+	-	+	-	+	-	+

Figure 3. 5 The effect of DM/8/45 on 2f-LIGRLO-NH$_2$ -mediated transcription activity in NFκB-reporter cells

The cells were grown to confluence and rendered quiescent for 18 hours prior to pre-treatment with various concentrations of DM/8/45 for 1 hour. The cells were then stimulated with 0.3 μM 2f-LIGRLO-NH$_2$ for a further 4 hours. Cell lysates were then measured for luciferase activity as previously described (section 2.3). The data shown are expressed as fold stimulation over DMSO control and each value represents n=3. Statistical analysis was performed via one way ANOVA, with Dunnett's post-test comparison. ***p<0.001.

DMSO	-	-	+	+	-	-	-	-	-	-	-	-	-	-	-	-
DM/8/53 (μM)	-	-	-	-	0.1	0.1	0.3	0.3	1	1	3	3	10	10	20	20
2F-LIGRLO-NH₂ (0.3 μM)	-	+	-	+	-	+	-	+	-	+	-	+	-	+	-	+

Figure 3. 6 The effect of DM/8/53 on 2f-LIGRLO-NH$_2$ -mediated transcription activity in NFκB-reporter cells

Cells were grown to confluency and rendered quiescent for 18 hours prior to pre-treatment with increasing concentrations of DM/8/53 for 1 hour. The cells were then stimulated with 0.3 μM 2f-LIGRLO-NH$_2$ for a further 4 hours. Cell lysates were then measured for luciferase activity as previously described (section 2.3). The data shown are expressed as fold over DMSO control and each value represented n=3. Statistical analysis was performed via one way ANOVA, with Dunnett's post-test comparison. ***p<0.001.
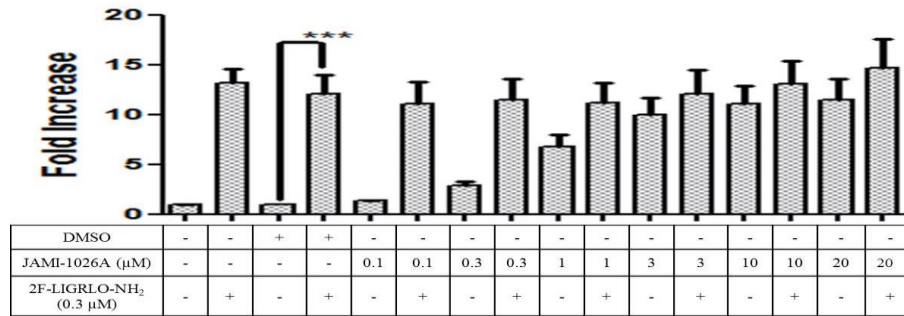
Figure 3. 7 The effect of JAMI1026A on 2f-LIGRLO-NH₂ -mediated transcription activity in NFκB-reporter cells

Cells were grown to confluence and rendered quiescent for 18 hours prior to pre-treatment with increasing concentrations of JAMI1026A for 1 hour. Cells were then stimulated with 0.3 μM 2f-LIGRLO-NH₂ for a further 4 hours. Cell lysates were then measured for luciferase activity as previously described (section 2.3). The data shown are expressed as fold stimulation over DMSO control and each value represented n=3. Statistical analysis was performed via one way ANOVA, with Dunnett's post-test comparison. ***p<0.001
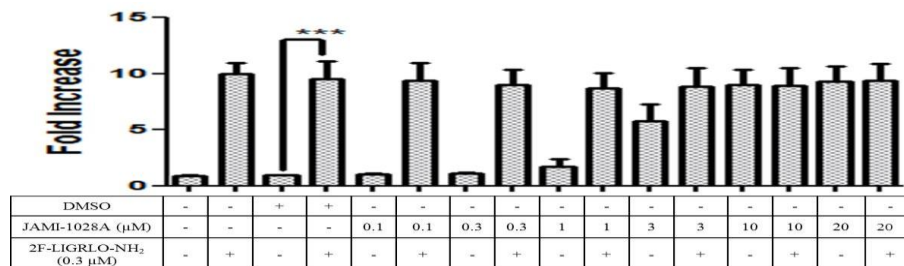
Figure 3. 8 The effect of JAMI1028A on 2f-LIGRLO-NH₂ -mediated transcription activity in NFκB-reporter cells

Cells were grown to confluency and rendered quiescent for 18 hours prior to pre-treatment with increasing concentrations of JAMI1028A for 1 hour. The cells were then stimulated with 0.3 μM 2f-LIGRLO-NH₂ for another 4 hours. Cell lysates were then measured for luciferase activity as previously described (section 2.3). The data shown are expressed as fold over DMSO control and each value represented n=3. Statistical analysis was performed via one way ANOVA, with Dunnett's post-test comparison. ***p<0.001.

3.2.4 Effect of GB88 compounds on trypsin stimulated NFκB-driven gene transcription

In this section, the effect of pre-treatment with GB88 and its derivative compounds on trypsin-mediated NFκB transcriptional activity was investigated. Figure 3.9 shows pre-treatment of NFκB-Reporter cells for 1 hour with increasing concentrations of GB88 (0.1-20 μM) and then addition of 30 nM trypsin for 4 hours. The increase for NFκB transcriptional activity for trypsin was approximately 9 fold (8.867 ± 1.272) compared to DMSO alone. Pre-treatment with low concentrations of GB88 (0.1 and 0.3 μM) did not significantly increase the response to trypsin. A small additive effect was noticed following pre-treatment with 1 μM GB88 with approximately 10 fold (10.233 ± 0.991), however this was not significant. Also, GB88 (10 and 20 μM) alone once again induced a strong increase in activity which reached approximately the same value as cells pre-treated with GB88 (10 and 20 μM) prior to the addition of trypsin. The fold stimulation was approximately 13 fold (13.370 ± 0.728) for cells pre-treated with 20 μM GB88 prior to trypsin, significantly greater than cells stimulated with trypsin alone, but comparable to GB88 (20 μM) alone.

Figure 3.10 shows the results for pre-treatment of cells with increasing concentrations (0.1 − 20 μM) of DM/7/34 for 1 hour prior to the addition of 30 nM trypsin for 4 hours. The fold increase on addition of trypsin was approximately 8 fold (8.057 ± 0.986) compared to DMSO alone. There was no statistically significant inhibitory effect for the low concentrations of DM/7/34; 0.1-3 μM. A significant increase in NFκB activity was observed using higher concentrations of DM/7/34 for pre-treatment with 10 and 20 μM giving approximately 12 fold (11.937 ± 0.717) and 14 fold (14.170 ± 0.894) respectively but values were less than additive for the compounds.

Figures 3.11-14 demonstrate a similar phenomenon to those experiments outlined above. There is a lack of consistent inhibition of the trypsin response with low concentrations of the compound and as the concentration of the compounds, DM/8/45, DM/8/53, JAMI1026A, JAMI1028A increases there is no additivity with trypsin.

From the previous results, it was concluded that GB88 and its derivative compounds alone showed increased effects on PAR2-mediated NFκB transcriptional activity and this increasing is a concentration-dependent manner. GB88 compounds showed no inhibitory properties on NFκB transcriptional activity mediated by PAR2 when NFκB-Reporter cells are pre-incubated with GB88 and derivative compounds then added trypsin. Conversely in some instances higher concentrations of compounds appeared to cause an additive effect with trypsin to PAR2 activation in NFκB-Reporter cells overexpress human PAR2. However, it could then concluded that GB88 and its compounds act as weak agonists.

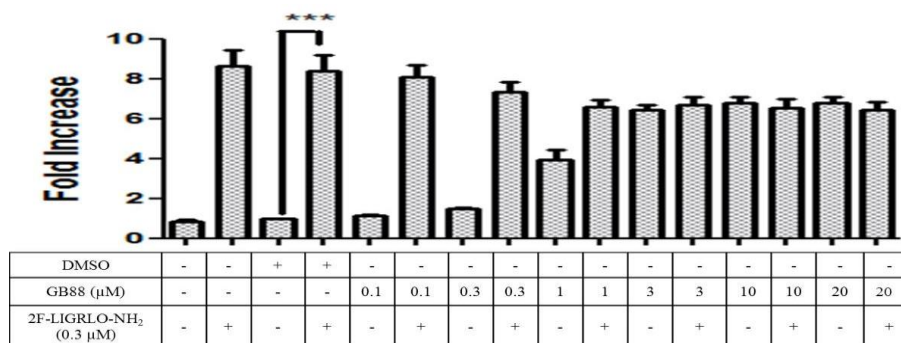| DMSO | - | - | + | + | - | - | - | - | - | - | - | - | - | - | - | - |
| GB88 (µM) | - | - | - | - | 0.1 | 0.1 | 0.3 | 0.3 | 1 | 1 | 3 | 3 | 10 | 10 | 20 | 20 |
| Trypsin (30 nM) | - | + | - | + | - | + | - | + | - | + | - | + | - | + | - | + |
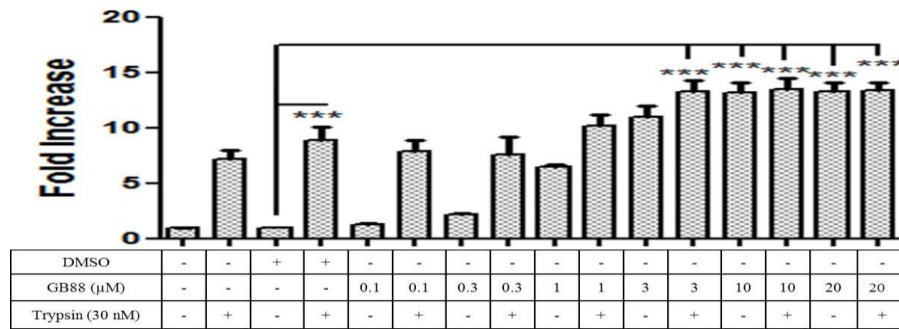
Figure 3. 9 The effect of GB88 on trypsin mediated transcription activity in NFκB-reporter cells

Cells were grown to confluence and rendered quiescent for 18 hours prior to pre-treatment with increasing concentrations of GB88 for 1 hour. The cells were then stimulated with 30 nM trypsin for 4 hours. Cell lysates were then measured for luciferase activity as previously described (section 2.3). The data shown are expressed as fold stimulation over DMSO alone and each value represents n=3. Statistical analysis was performed via one way ANOVA, with Dunnett's post-test comparison. ***p<0.001

DMSO	-	-	+	+	-	-	-	-	-	-	-	-	-	-	-	-
DM/7/34 (µM)	-	-	-	-	0.1	0.1	0.3	0.3	1	1	3	3	10	10	20	20
Trypsin (30 nM)	-	+	-	+	-	+	-	+	-	+	-	+	-	+	-	+
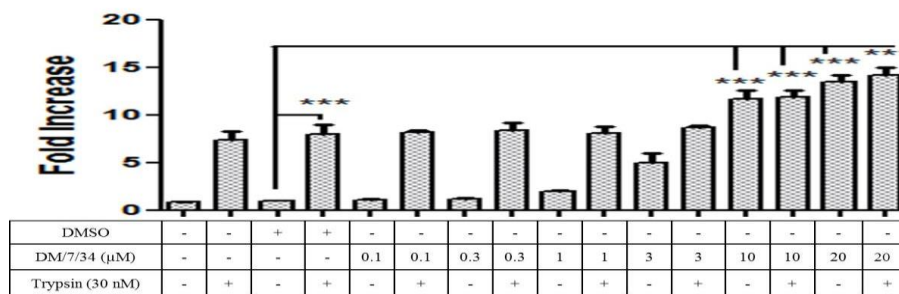
Figure 3. 10 The effect of DM/7/34 on trypsin-mediated transcription activity in NFκB-reporter cells

Cells were grown to confluence and rendered quiescent for 18 hours prior to pre-treatment with increasing concentrations of DM/7/34 for 1 hour. The cells were then stimulated with 30 nM trypsin for 4 hours. Cell lysates were then measured for luciferase activity as previously described (section 2.3). The data shown are expressed as fold stimulation over DMSO alone and each value represents n=3. Statistical analysis was performed via one way ANOVA, with Dunnett's post-test comparison. ***p<0.001.
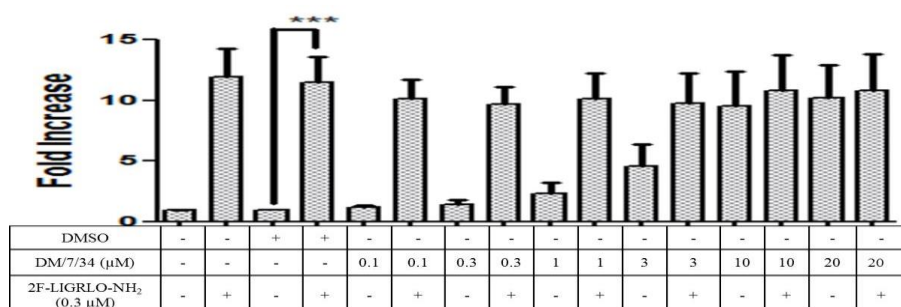
DMSO	-	-	+	+	-	-	-	-	-	-	-	-	-	-	-	-
DM/8/45 (µM)	-	-	-	-	0.1	0.1	0.3	0.3	1	1	3	3	10	10	20	20
Trypsin (30 nM)	-	+	-	+	-	+	-	+	-	+	-	+	-	+	-	+
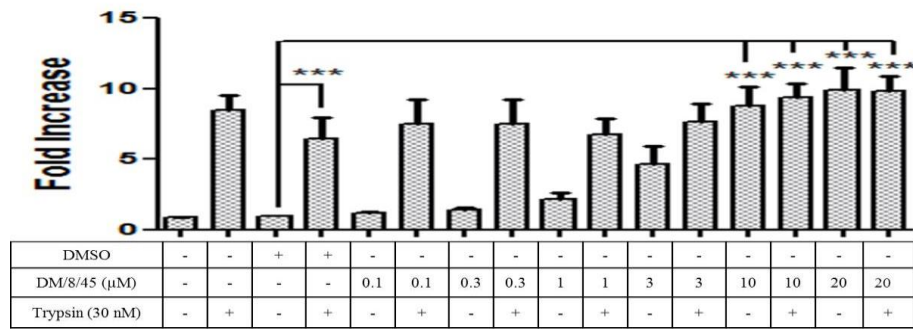
Figure 3. 11 The effect of DM/8/45 on trypsin-mediated transcription activity in NFκB-reporter cells

The cells were grown to confluence and rendered quiescent for 18 hours prior to pre-treatment with various concentrations of DM/8/45 for 1 hour. The cells were then stimulated with 30 nM trypsin for 4 hours. Cell lysates were then measured for luciferase activity as previously described (section 2.3). The data shown are expressed as fold stimulation over DMSO alone and each value represents n=3. Statistical analysis was performed via one way ANOVA, with Dunnett's post-test comparison. ***p<0.001.
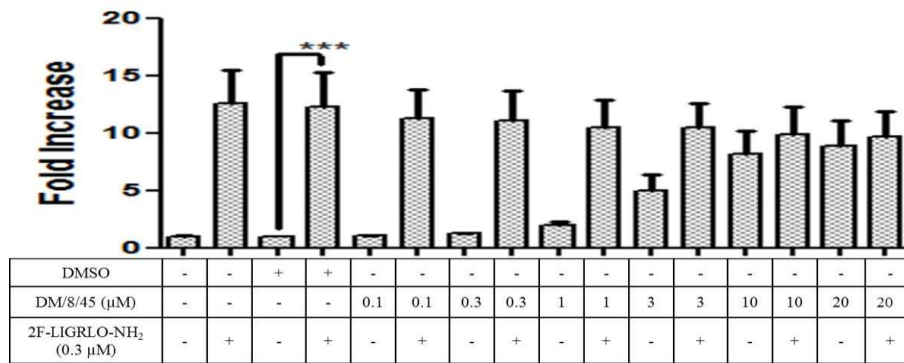

DMSO	-	-	+	+	-	-	-	-	-	-	-	-	-	-	-	-
DM/8/53 (µM)	-	-	-	-	0.1	0.1	0.3	0.3	1	1	3	3	10	10	20	20
Trypsin (30 nM)	-	+	-	+	-	+	-	+	-	+	-	+	-	+	-	+
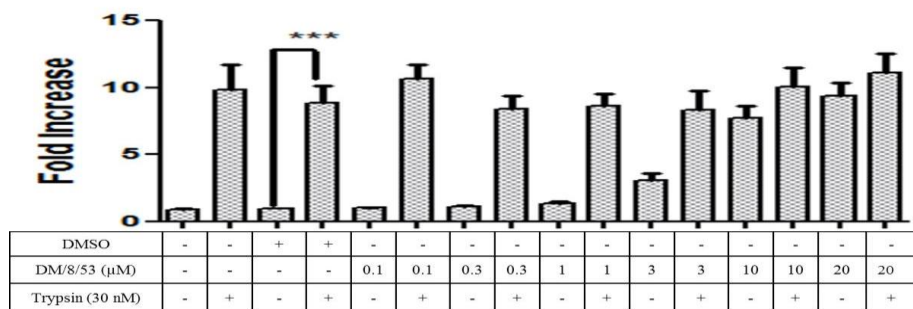
Figure 3. 12 The effect of DM/8/53 on trypsin-mediated transcription activity in NFκB-reporter cells

Cells were grown to confluency and rendered quiescent for 18 hours prior to pre-treatment with increasing concentrations of DM/8/53 for 1 hour. The cells were then stimulated with 30 nM trypsin for 4 hours. Cell lysates were then measured for luciferase activity as previously described (section 2.3). The data shown are expressed as fold stimulation over DMSO alone and each value represents n=3. Statistical analysis was performed via one way ANOVA, with Dunnett's post-test comparison. ***p<0.001.
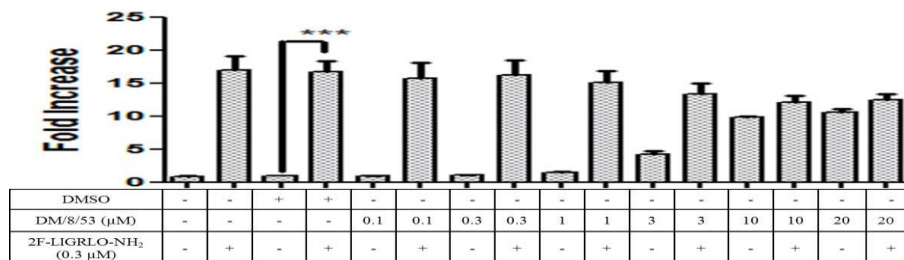
DMSO	-	-	+	+	-	-	-	-	-	-	-	-	-	-	-	-
JAMI-1026A (µM)	-	-	-	-	0.1	0.1	0.3	0.3	1	1	3	3	10	10	20	20
Trypsin (30 nM)	-	+	-	+	-	+	-	+	-	+	-	+	-	+	-	+
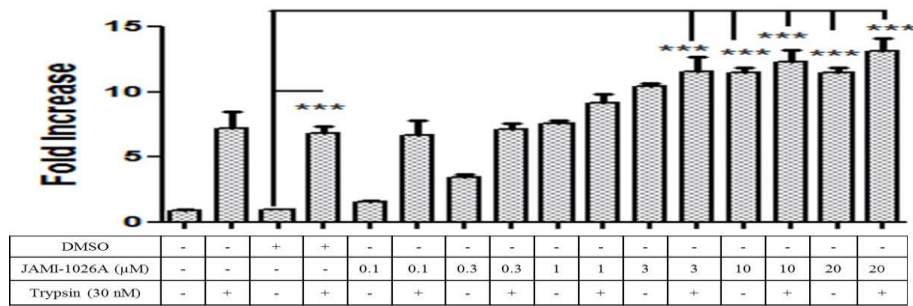
Figure 3. 13 The effect of JAMI1026A on trypsin-mediated NFκB transcription activity in NFκB-reporter cells

Cells were grown to confluency and rendered quiescent for 18 hours prior to pre-treatment with increasing concentrations of JAMI1026A for 1 hour. Cells were then stimulated with 30 nM trypsin for 4 hours. Cell lysates were then measured for luciferase activity as previously described (section 2.3). The data shown are expressed as fold stimulation over DMSO alone and each value represents n=3. Statistical analysis was performed via one way ANOVA, with Dunnett's post-test comparison. ***p<0.001.


DMSO	-	-	+	+	-	-	-	-	-	-	-	-	-	-	-	-
JAMI-1028A (µM)	-	-	-	-	0.1	0.1	0.3	0.3	1	1	3	3	10	10	20	20
Trypsin (30 nM)	-	+	-	+	-	+	-	+	-	+	-	+	-	+	-	+
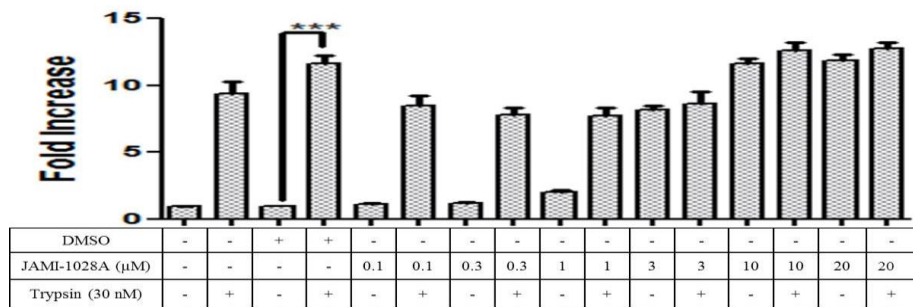
Figure 3. 14 The effect of JAMI1028A on trypsin -mediated transcriptional activity in NFκB-reporter cells

Cells were grown to confluency and rendered quiescent for 18 hours prior to pre-treatment with increasing concentrations of JAMI1028A for 1 hour. Cells were then stimulated with 30 nM trypsin for 4 hours. Cell lysates were then measured for luciferase activity as previously described (section 2.3). The data shown are expressed as fold stimulation over DMSO alone and each value represents n=3. Statistical analysis was performed via using one way ANOVA, with Dunnett's post-test comparison. ***p<0.001.

3.3 PAR2-mediated phosphorylation of extracellular signal-related kinase (ERK) in HEK293 cells

The studies in PAR2 overexpressing cells strongly suggested that GB88 rather than being an antagonist is more likely to have agonist properties. However, it is recognised that there are limitations in using receptor-overexpressing cells. In addition, there is the potential for antagonist properties to be manifest at the level of different signalling pathways a phenomenon called agonist directed signalling (see chapter 1). Therefore, the effect of the compounds on PAR2 mediated ERK signalling in HEK293 cells, a line that expresses PAR2 endogenously, was examined. Initially the kinetics of trypsin-mediated phosphorylation of p42/44, extracellular signal-related kinase 1/2 (ERK1/2) was examined in figure 3.15 (a). Over a number of experiments it was found that trypsin induced ERK1/2 phosphorylation increased rapidly with maximum activation observed between 2 and 5 minutes at approximately 6 fold (5.643 ± 0.715 and 5.163 ± 0.676 fold of control, respectively) before gradually decreasing at 15 minutes to approximately 2 fold of basal values (1.537 ± 0.269 fold). Therefore, 5 minutes was used in the next set of experiments as the incubation time for PAR2 activation via trypsin. Using increasing concentrations of trypsin, starting from 1 to 1000 nM as shown in figure 3.15 (b), a concentration-dependent increase in ERK1/2 phosphorylation was demonstrated with a maximal response between 300-1000 nM of trypsin, over a 5 minute period. Table 3.2 shows the determination of EC_{50} values.

Figure 3.15 (c) illustrates the effect of 2f-LIGRLO-NH_2-mediated PAR2 activation on the phosphorylation of ERK1/2. The kinetics of ERK phosphorylation was measured over a 90 minute time period. 2f-LIGRLO-NH_2 induced ERK1/2, giving a maximum response at 5 minutes at approximately 13 fold (12.770 ± 1.075 fold of basal control) before gradually decreasing at 15 minutes to approximately 6 fold (5.623 ± 1.354 fold of basal control). Using increasing concentrations of 2f-LIGRLO-NH_2, starting from 0.01 μM up to 10 μM a concentration-dependent increase in ERK1/2 phosphorylation was constructed with a maximal response obtained between 1-10μM of 2f-LIGRLO-NH_2, over a 5 minutes period, figure 3.15 (d).
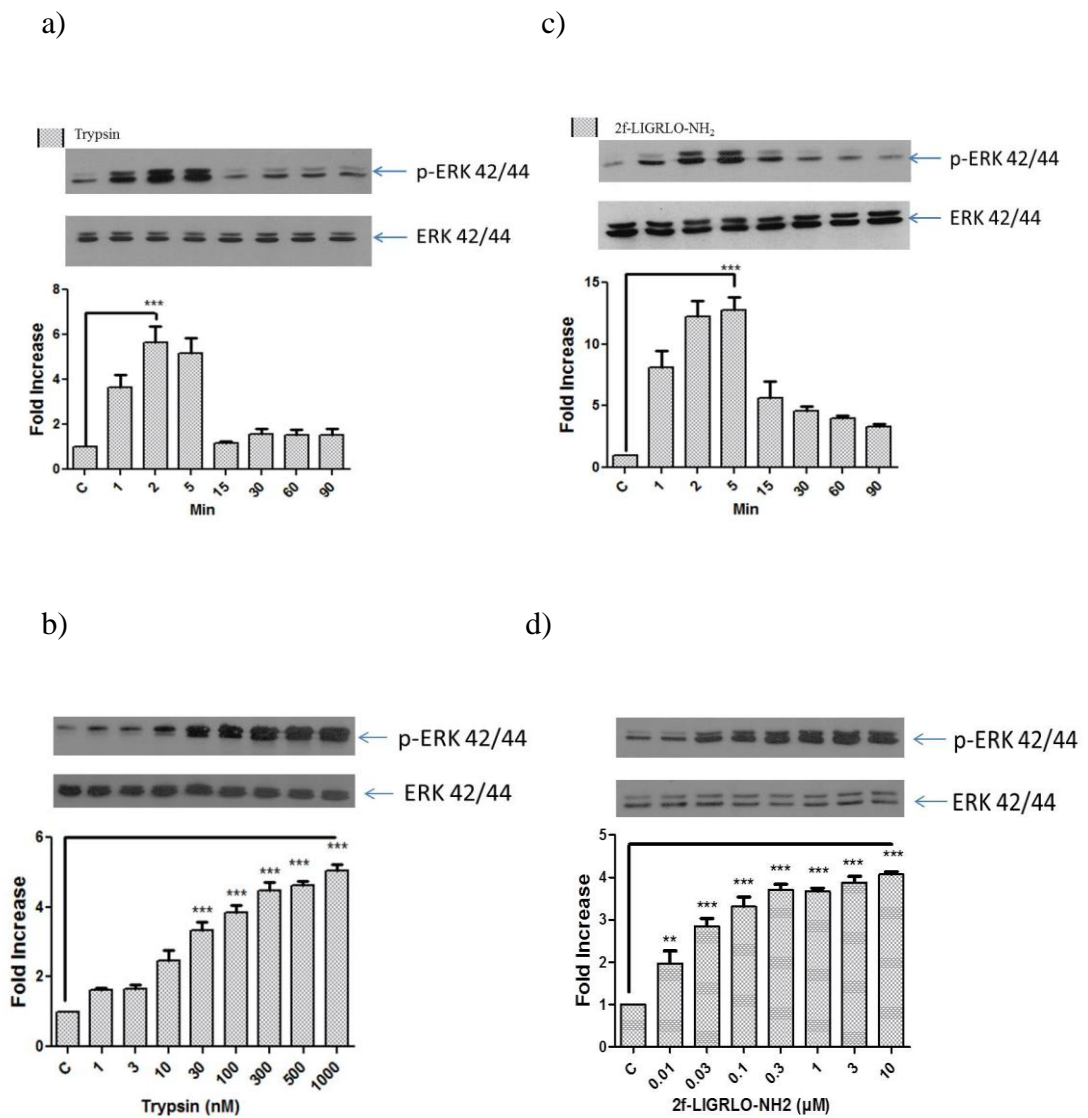
Figure 3. 15 Trypsin and 2f-LIGRLO-NH$_2$ stimulated phosphorylation of ERK in HEK293 cells

HEK293 cells were incubated in 2% media for 24 hours prior to stimulation with (a) 100 nM trypsin (c) 1µM 2f-LIGRLO-NH$_2$ for the times indicated or (b) with increasing concentrations of trypsin or (d) 2f-LIGRLO-NH$_2$ for 5 minutes. Whole cell lysates were prepared as previously described (section 2.41) and resolved by Western blotting (section 2.4.2). Blot is representative of n=3, quantified by densitometry and expressed as mean ± s.e.m (fold stimulation). ***p<0.001 versus controls.

The effect of GB88-mediated phosphorylation of ER1/2 is demonstrated in figure 3.16 (a). The kinetics of the activation of ERK was measured over a 90 minute time period. GB88-mediated phosphorylation of ERK1/2 was rapid, peaking at 5 minutes at approximately 3.5 fold (3.443 ± 0.503 fold of DMSO basal) before rapidly decreasing at 15 minutes to approximately 2 fold (2.183 ± 0.256 fold). Using increasing concentrations of GB88, starting from 0.1 µM up to 20 µM a concentration-dependent increase in ERK1/2 phosphorylation was observed with a maximal response using 20 µM of GB88, over a 5 minutes period, figure 3.16 (b). Generally, the levels of stimulation was lower than that observed for 2f-LIGRLO-NH_2, although the concentration response curve did not plateau out at the maximum concentration employed.

The effect of compound DM/7/34 on PAR2-mediated phosphorylation of ERK MAP kinase was demonstrated in figure 3.16 (c & d). Initially the kinetics of ERK phosphorylation was measured over a 90 minute time period using DM/7/34 alone. Treatment with DM/7/34 increased phosphorylation of ERK1/2 with a peak at 5 minutes at approximately 7 fold (7.147 ± 0.777) increase over basal, before gradually decreasing at 90 minutes to approximately 3 fold (3.333 ± 0.007 fold). Using increasing concentrations of DM/7/34, a concentration-dependent increase in ERK1/2 phosphorylation was observed with a maximal response using 20 µM of DM/7/34, over a 5 minutes period, figure 3.16 (d). Again, the concentration response curve did not reach a plateau at the maximum concentration employed.
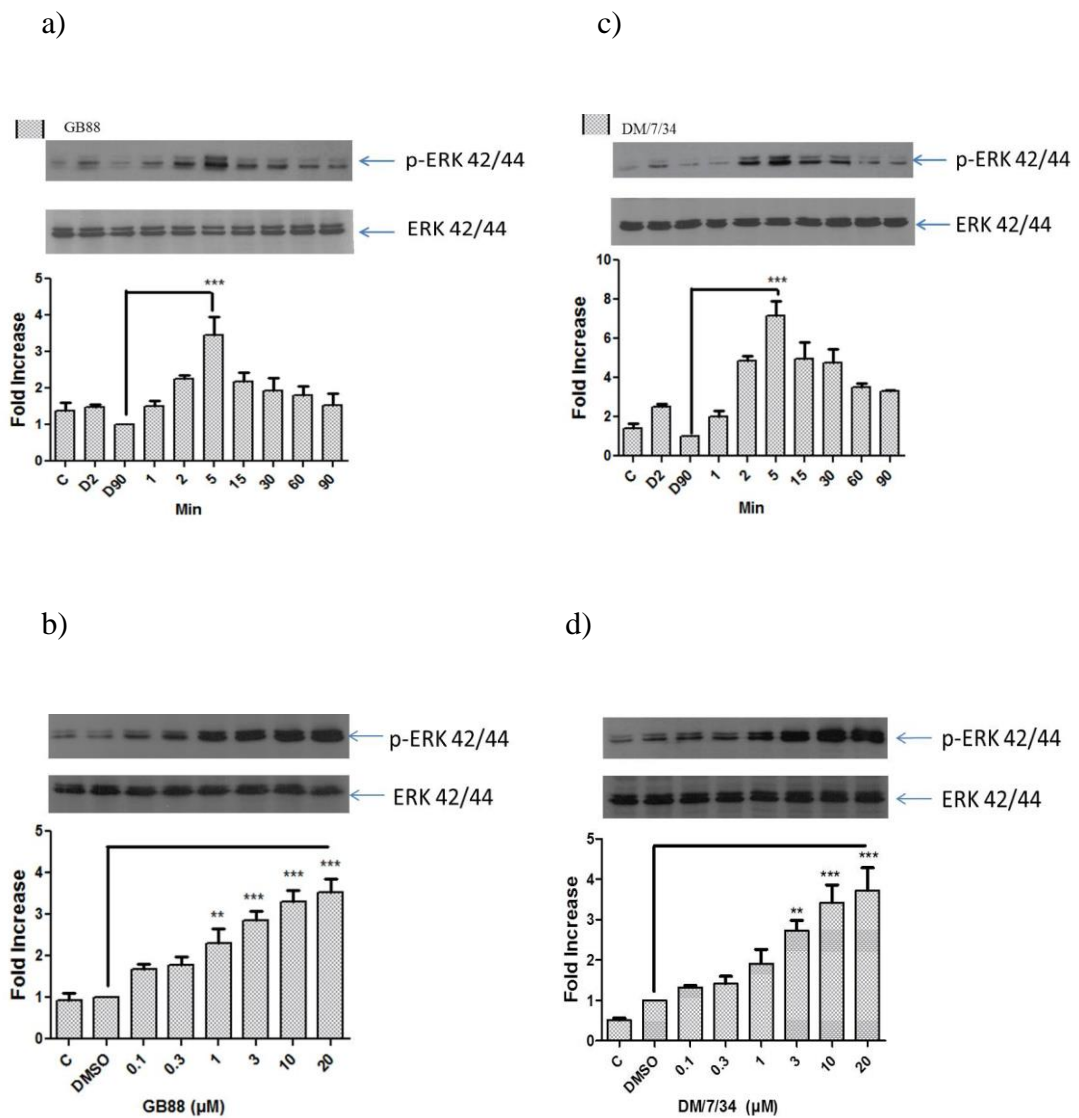
Figure 3.16 Phosphorylation of ERK stimulated by GB88 and DM/7/34 in HEK293 cells

HEK293 cells were incubated in 2% media for 24 hours prior to stimulation with (a) 10 μM GB88 (c) 10 μM DM/7/34 for the times indicated or (b) with increasing concentrations of GB88 (d) DM/7/34 for 5 minutes. Whole cell lysates were prepared as previously described (section 2.4.1), and resolved by Western blotting (section 2.4.2). Blot is representative of n=3 and they were quantified by densitometry and expressed as mean ± s.e.m (fold stimulation). ***p<0.001 versus controls.

The effect of DM/8/45 on PAR2-mediated phosphorylation of ERK is illustrated in figure 3.17 (a). ERK phosphorylation was induced with DM/8/45 (10 μM) with maximum activation seen at 5 minutes with approximately 4 fold (4.130 ± 0.800) increase over basal before quickly decreasing at 15 minutes to approximately 1 fold (1.343 ± 0.133 fold). Again a concentration-dependent increase in ERK1/2 phosphorylation was observed with a maximal response using 20 μM of DM/8/45, over a 5 minutes time period, figure 3.17 (b). Another compound DM/8/53 induced ERK phosphorylation with maximum activation at 5 minutes with approximately 6 fold (5.827 ± 0.536 fold of DMSO basal) before quickly decreasing to DMSO basal levels of approximately 2 fold at 15 minutes (2.223 ± 0.199 fold). A concentration-dependent increase in ERK phosphorylation was observed with a maximal response recorded using 20 μM of DM/8/53, over a 5 minutes period, figure 3.17 (d).

The effect of JAMI1026A on PAR2-mediated phosphorylation of ERK is illustrated in figure 3.18 (a). ERK1/2 phosphorylation was measured over a 90 minute time period for JAMI1026A (10 μM). The kinetics were slightly different compared to other agonists; whilst phosphorylation of ERK peaked at 5 minutes at approximately 5 fold (4.520 ± 0.280) over basal, the decrease towards basal values was relatively slow giving a 2 fold response at 90 min (2.107 ± 0.049 fold). A concentration-dependent increase in ERK1/2 phosphorylation was observed with a maximal response using 20 μM of JAMI1026A, over a 5 minutes period, figure 3.18 (b). Figure 3.18 (c) shows that the effect of JAMI1028A on PAR2-mediated phosphorylation of ERK1/2 was similar to JAMI1026A. Maximum ERK1/2 phosphorylation was observed at 5 minutes with an approximate 4 fold (4.103 ± 0.267) increase over basal. The response was decreasing gradually but then plateaued and by 90 minutes was approximately 2 fold (1.980 ± 0.205 fold). A similar concentration response curve was generated over a 5 minutes period, figure 3.18 (d).

Figure 3. 17 Phosphorylation of ERK by DM/8/45 and DM/8/53 in HEK293 cells

HEK293 cells were incubated in 2% media for 24 hours prior to stimulation with (a) 10 µM DM/8/45 (c) 10 µM DM/8/53 for the times indicated or (b) with increasing concentrations of DM/8/45 (d) DM/8/53 at 5 minutes. Whole cell lysates were prepared as previously described (section 2.4.1), and resolved by Western blotting (section 2.4.2). Blot is representative of n=3 and they were quantified by densitometry and expressed as mean ± s.e.m (fold stimulation). ***p<0.001 versus control.
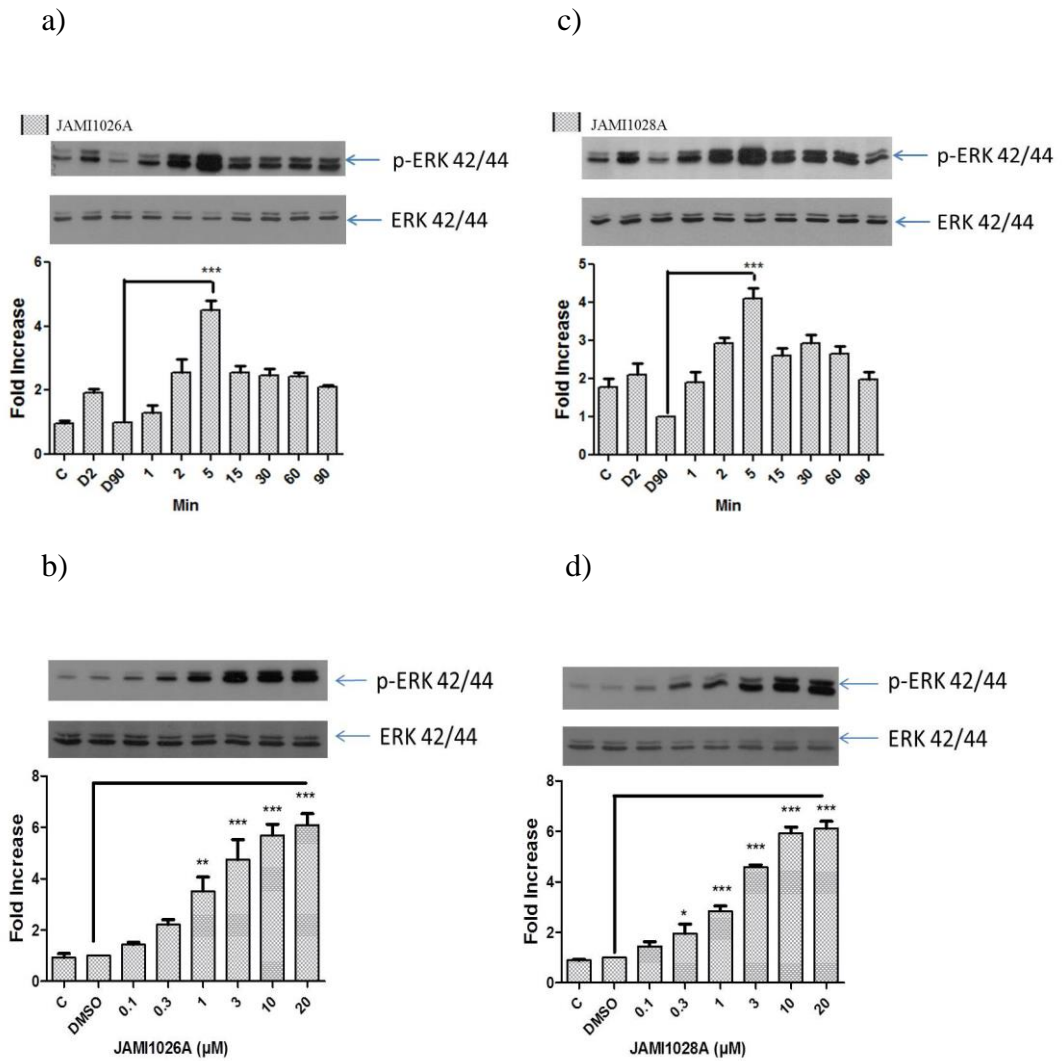
Figure 3. 18 Phosphorylation of ERK by JAMI1026A and JAMI1028A in HEK293 cells

HEK293 cells were incubated in 2% media for 24 hours prior to stimulation with (a) 10 μM JAMI1026A (c) 10 μM JAMI1028A for the times indicated or (b) with increasing concentrations of JAMI1026A (d) JAMI1028A for 5 minutes. Whole cell lysates were prepared as previously described (section 2.4.1), and resolved by Western blotting (section 2.4.2). Blot is representative of n=3 and they were quantified by densitometry and expressed as mean ± s.e.m (fold stimulation). ***$p < 0.001$ versus control.

From the previous experiments, it was observed that the optimum time for ERK1/2 phosphorylation using either PAR2 agonists or the six compounds was at 5 minutes where a peak signal was observed; therefore, this time was used in the next experiments. Cells were treated for 5 minutes with increasing concentrations of trypsin from 1 nM up to 1000 nM, 2f-LIGRLO-NH$_2$ from 0.01 up to 10 µM and all GB88 compounds from 0.1 up to 20 µM. A concentration-dependent increase in ERK1/2 phosphorylation was observed, across all compounds used. Figure 3.19 shows concentration responses curves and in table 3.2, the EC$_{50}$ values for each compound. It should be noted that the potency of trypsin and 2f-LIGRLO-NH$_2$ is considerably higher for ERK activation than that observed for activation of reporter activity. EC$_{50}$ values for 2f-LIGRLO-NH$_2$ and trypsin are lower than that recorded for GB88 compounds as expected, but the size of the responses for GB88 and related compounds were generally lower again suggesting partial agonist activity. However, the EC$_{50}$ values for GB88 and other compounds are approximately similar to note for stimulation of reporter activity.
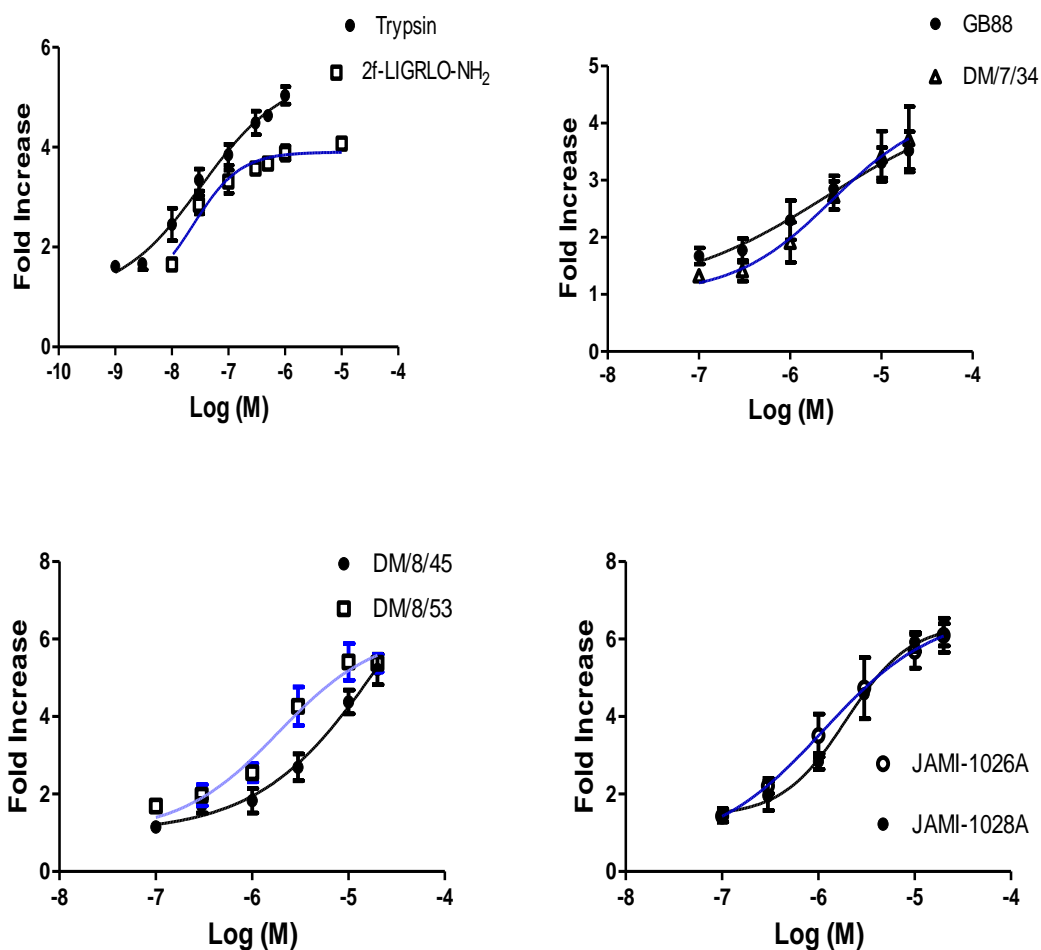
Figure 3. 19 Concentration response curves for PAR2 agonists and GB88 compounds on ERK phosphorylation in HEK 293 cells

HEK293s were incubated in 2% media for 24 hours prior to stimulation with increasing concentrations with each agonist (Trypsin and 2f-LIGRLO-NH$_2$) and each compound (GB88, DM/7/34, DM/8/45, DM/8/53, JAMI1028A and JAMI1026A) for 5 minutes. Whole cell lysates were prepared as previously described (section 2.4.2), and resolved by Western blotting (section 2.4.1). All data are representative of n=3, and were quantified by densitometry and expressed as mean ± s.e.m (fold stimulation).

Compound	EC$_{50}$ (µM)
Trypsin	0.033
2f-LIGRLO-NH$_2$	0.02
GB88	2.6
DM/7/34	3
DM/8/45	2.3
DM/8/53	2
JAMI1026A	1.1
JAMI1028A	2

Table 3. 2 EC$_{50}$ values for PAR2 agonists and test compounds on ERK1/2 phosphorylation in HEK293 cells. N=3

3.4 PAR2-mediated phosphorylation of p38 MAPK in HEK293 cells

Having established that GB88 and associated compounds were able to couple to the ERK pathway it was decided to determine if these compounds had antagonist activity on other pathways so p38 MAPK was examined. This approach would help to establish if GB88 and related compounds behaved as agonists and could preferentially activate other pathways. In a number of studies, it has been shown that PAR2 can couple to ERK but coupling to p38 MAP kinase may be dependent on receptor expression. Overall, it was found that relative to ERK, p38 MAPK was found to be weakly phosphorylated as a result of PAR2 activation as demonstrated in figure 3.20., with a significant variation in the level of response across experiments. For trypsin the stimulation was poor, a maximum activation of p38 MAP kinase was observed at 5 minutes at 1.5 fold basal values (1.370 ± 0.075 fold n=3). The weak response mediated by trypsin decreased and returned to near basal level by 90 minutes. Using the 5 minutes time point, a concentration-dependent increase in p38 MAPK phosphorylation was observed with a maximal and significant response using 1000 nM trypsin (4.510 ± 0.718 fold basal) as shown in figure 3.20 (b). The EC_{50} value was lower than that observed for ERK signalling.

The effect of PAR2 activation by 2f-LIGRLO-NH$_2$ on the phosphorylation of p38 MAP kinase was illustrated in figure 3.20 (c). 2f-LIGRLO-NH$_2$ induced p38 MAPK phosphorylation but with different kinetics to trypsin, maximal activation was at 15 minutes at approximately 3 fold (2.777 ± 0.363, n=3) before gradually decreasing by 30 minutes to 2 fold (2.013 ± 0.424 fold) and by 90 minutes dropping to near basal levels. Using the 15 minute time point for stimulation a concentration-dependent increase in p38 MAPK phosphorylation was observed with a maximal response recorded at 10 µM 2f-LIGRLO-NH$_2$ (5.637 ± 0.561 fold basal) as shown in figure 3.20 (d).
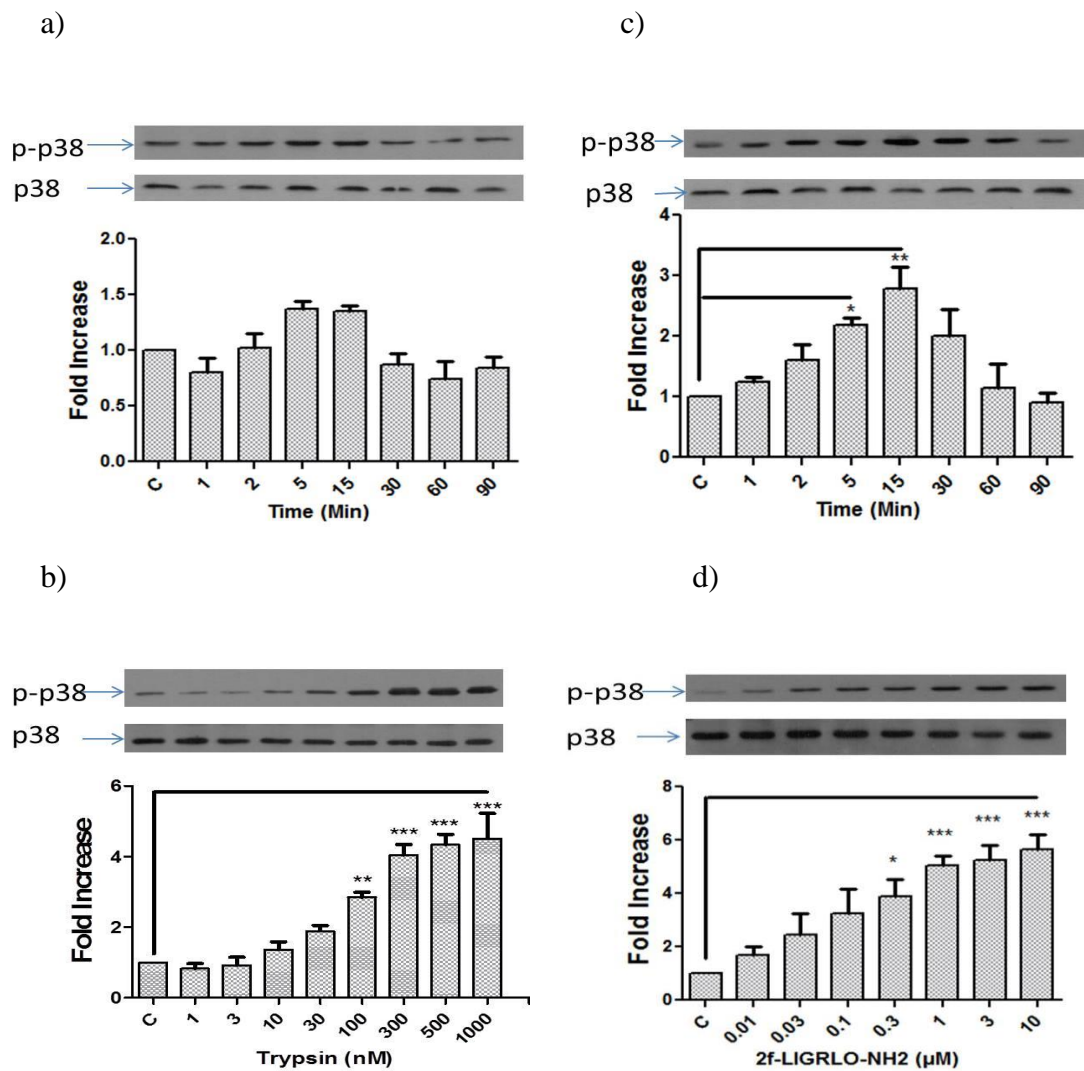
Figure 3. 20 PAR2-mediated phosphorylation of p38 by trypsin and 2f-LIGRLO-NH$_2$ in HEK293 cells

HEK293 cells were incubated in 2% media for 24 hours prior to stimulation with (a) 100 nM trypsin (c) 1 μM 2f-LIGRLO-NH$_2$ for the times indicated or (b) with increasing concentrations of trypsin (d) 2f-LIGRLO-NH$_2$ at 15 minutes. Whole cell lysates were prepared as previously described (section 2.4.1) and resolved by Western blotting (section 2.4.2). Each blot is representative of n=3, quantified by densitometry and expressed as mean ± s.e.m (fold stimulation), ***P<0.001 versus control.

Figure 3.21 (a) illustrated the effect of PAR2 stimulation by GB88 on the phosphorylation of p38 MAP kinase. GB88 (10 μM) induced p38 MAP kinase with maximal activation between 2 to 15 minutes with approximately 2.5 fold (2.467 ± 0.194 fold of DMSO control). The response mediated by GB88 gradually decreased by 60 minutes to 1 fold (1.280 ± 0.099) or basal. Using increasing concentrations of GB88, starting from 0.1 up to 20 μM, a concentration-dependent increase in p38 MAPK phosphorylation was observed at the 5 minute time point with a maximal response using 20 μM GB88 (3.910 ± 0.222 fold basal) as shown in figure 3.21 (b). This was largely consistent with that observed for ERK activation.

The effect of DM/7/34 on phosphorylation of p38 MAP kinase was demonstrated in figure 3.21 (c). The kinetics of p38 MAPK phosphorylation was measured over a 90 minute time period for DM/7/34 (10 μM). DM/7/34 induced p38 MAPK with a maximal activation at 5 minutes at approximately 2.5 fold (2.447 ± 0.263 fold of DMSO control) before gradually decreasing by 15 minutes to 2 fold (2.173 ± 0.324 fold) and by 90 minutes returning to basal values (0.873 ± 0.158 fold). Therefore, 5 minutes were used as the typical time for PAR2 activation by DM/7/34. Using increasing concentrations of DM/7/34, from 0.1 up to 20 μM, a concentration-dependent increase in p38 MAPK phosphorylation was observed with a maximal response using 20 μM DM/7/34 (4.677 ± 0.156 fold basal) as shown in figure 3.21 (d).
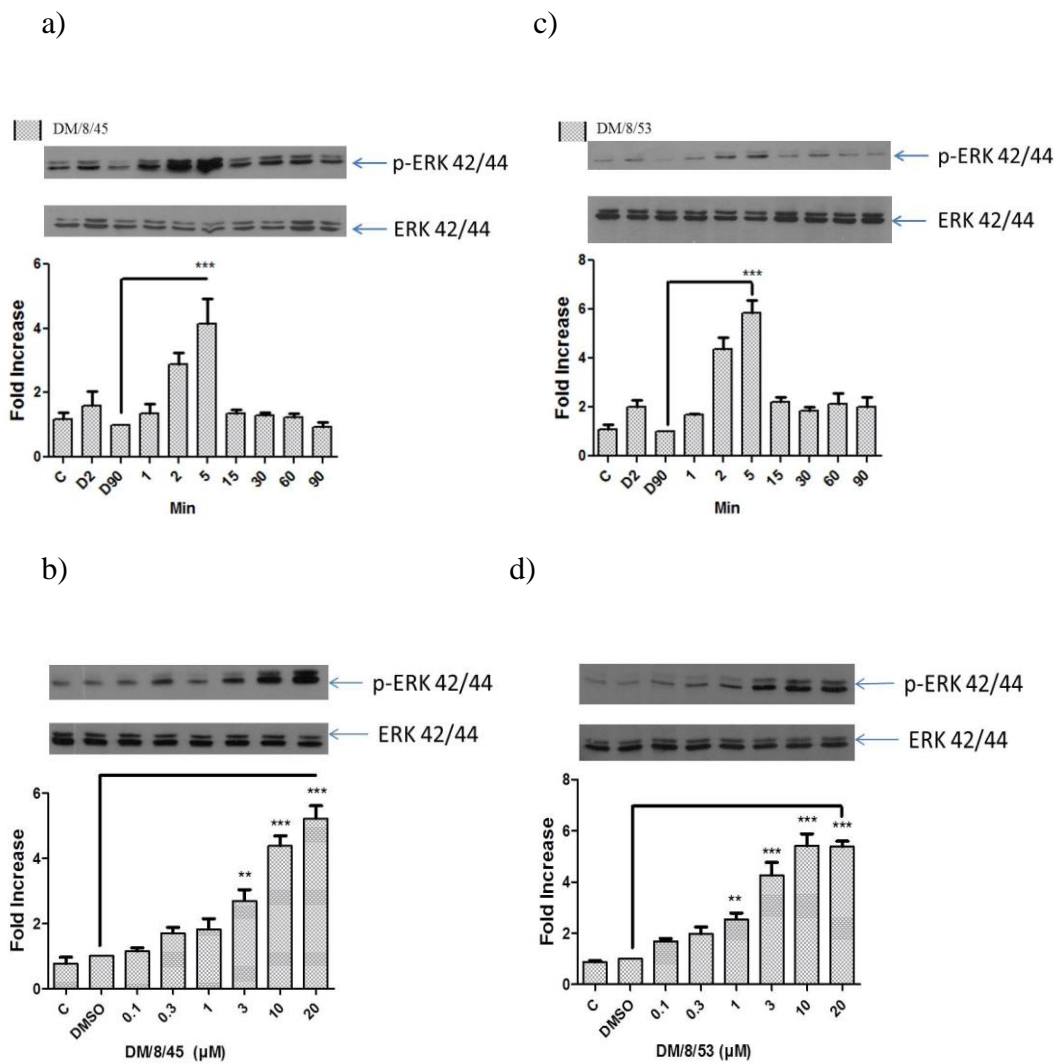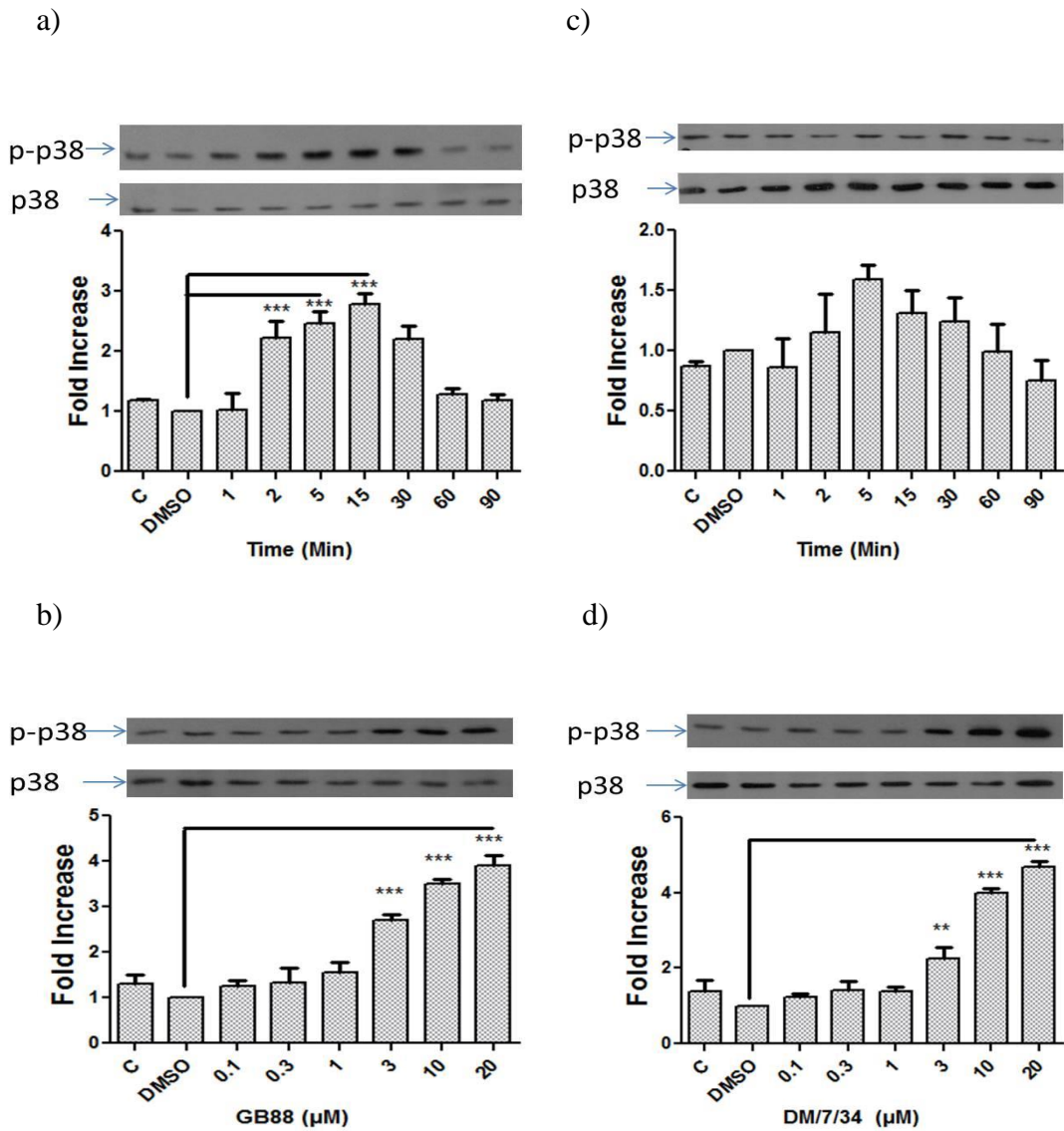
Figure 3. 21 PAR2-mediated phosphorylation of p38 by GB88 and DM/7/34 in HEK293 cells

HEK293 cells were incubated in 2% media for 24 hours prior to stimulation with (a) 10 μM GB88 (c) 10 μM DM/7/34 for the time indicated or (b) with increasing concentrations of GB88 (d) DM/7/34 at 15 minutes. Whole cell lysates were prepared as previously described (section 2.4.1), and resolved by Western blotting (section 2.4.2). Blot is representative of n=3 and they were quantified by densitometry and expressed as mean ± s.e.m (fold stimulation). ***$P<0.001$ versus control.

Figure 3.22 and 3.23 (a) shows the effect of PAR2 activation on the phosphorylation of p38 MAPK by the remaining compounds; DM/8/45, DM/8/53, JAMI1026A and JAMI102A. Panels a and c for each figure show comparative time courses for each compounds, whilst b and d panels show the concentration response curves. Consistently, the responses were weak giving only 2-3 fold maximum stimulation at higher agonist concentrations (10μM). For some of the agonists the maximum stimulation was later or with a slightly more sustained response for example, JAMI1026A and 1028A. All agonists were moderately potent in this assay, response curves were not completed at the maximum concentration of agonist employed. This is better illustrated in Figure 3.24. Determination of EC_{50} values were difficult due to the potential error in reiterative curve fitting procedure to a single site sigmoid curve, nevertheless the approximate EC_{50} value for each compound is listed in Table 3.3.
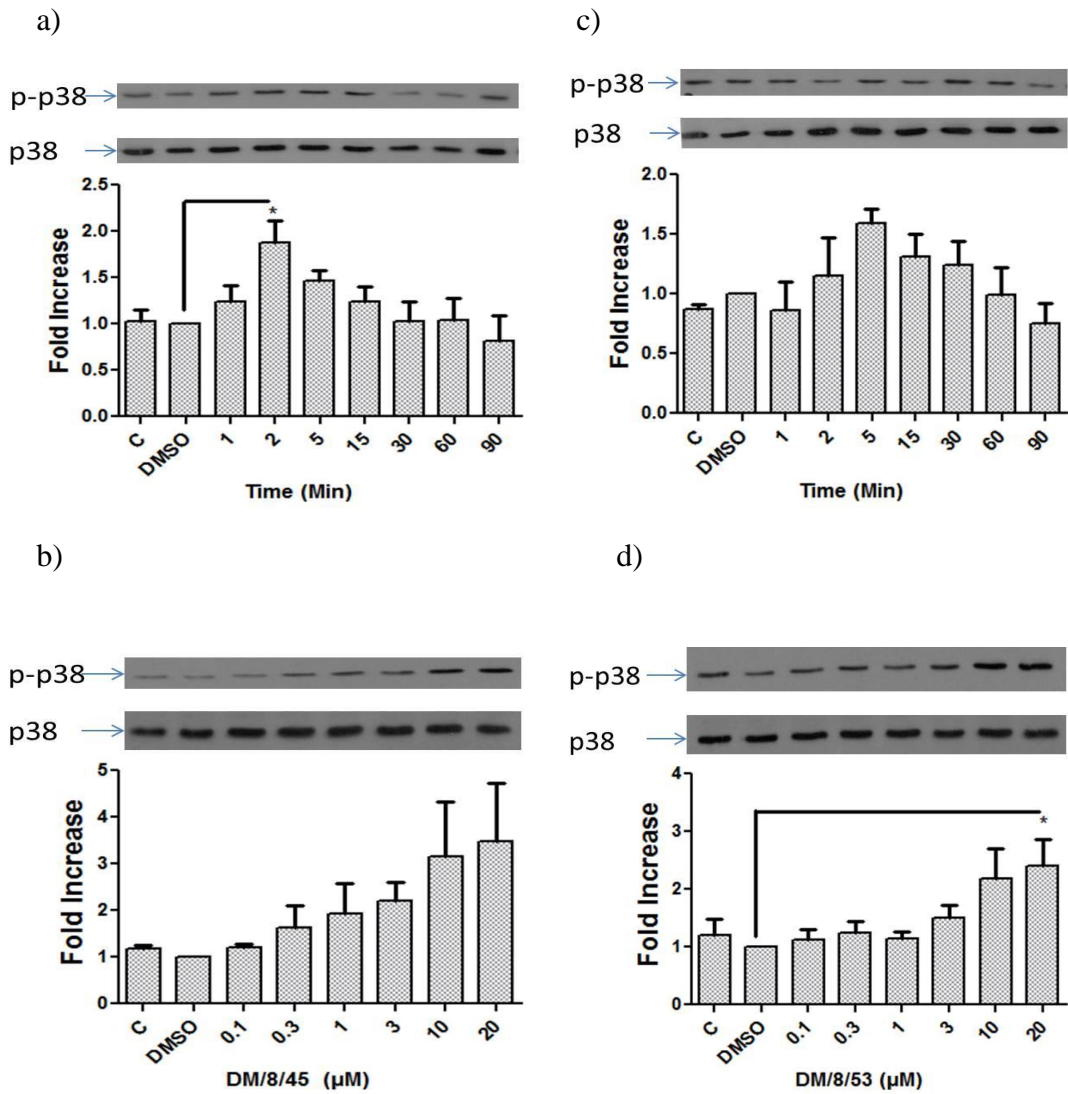
Figure 3. 22 PAR2-mediated phosphorylation of p38 by DM/8/45 and DM/8/53 in HEK293 cells

HEK293 cells were incubated in 2% media for 24 hours prior to stimulation with (a) 10 µM DM/8/45 (c) 10 µM DM/8/53 for the time indicated or (b) with increasing concentrations of DM/8/45 (d) DM/8/53 at 5 minutes. Whole cell lysates were prepared as previously described (section 2.4.1), and resolved by Western blotting (section 2.4.2). Each blot is representative of n=3, quantified by densitometry and expressed as mean ± s.e.m (fold stimulation), *P>0.05 versus control.
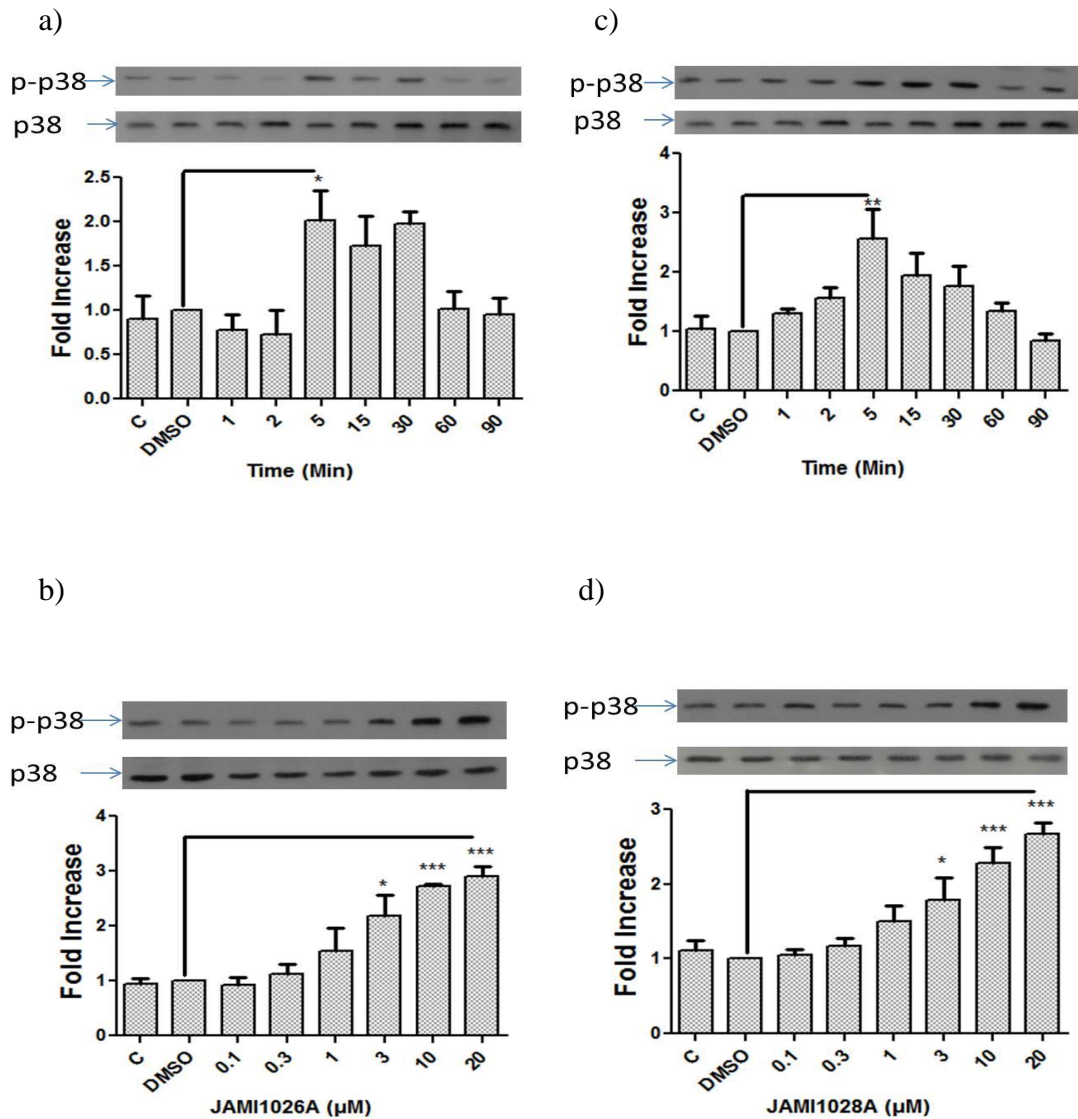
Figure 3. 23 PAR2-mediated phosphorylation of p38 by JAMI1026A and JAMI1028A in HEK293 cells

HEK293 cells were incubated in 2% media for 24 hours prior to stimulation with (a) 10 μM JAMI1026A (c) 10 μM JAMI028A for the time indicated or (b) with increasing concentrations of JAMI1026A (d) JAMI1028A at 15 minutes. Whole cell lysates were prepared as previously described (section 2.4.1), and resolved by Western blotting (section 2.4.2). Each blot is representative of n=3, quantified by densitometry and expressed as mean ± s.e.m (fold stimulation), ***P<0.001 versus control.
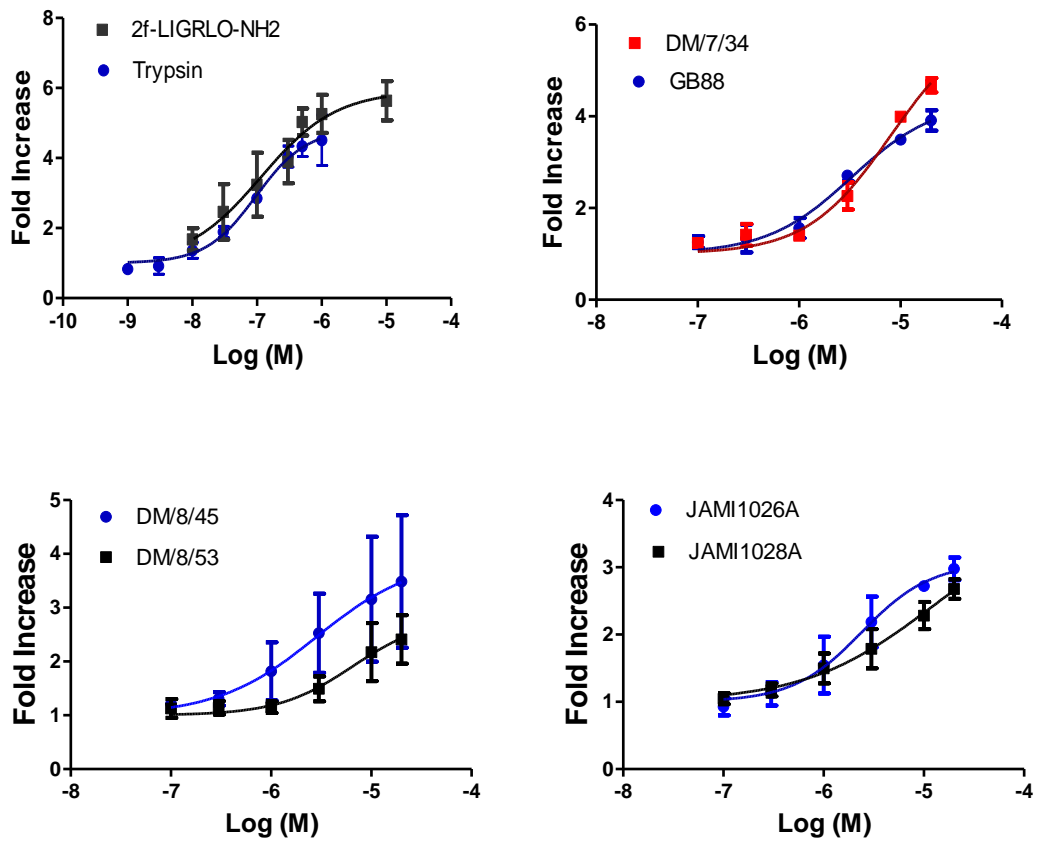
Figure 3. 24 The effect of different concentrations of GB88 compounds on PAR2 mediated p38 phosphorylation.

HEK293 cells were incubated in 2% media for 24 hours prior to stimulation with increasing concentrations with each agonist (Trypsin and 2f-LIGRLO-NH$_2$) and each compound (GB88, DM/7/34, DM/8/45, DM/8/53, JAMI1026A and JAMI1028A) for 5 minutes. Whole cell lysates were prepared as previously described (section 2.4.2), and separated by SDS.PAGE (section 2.4.1). All data are representative of n=3, quantified by densitometry and expressed as mean ± s.e.m (fold stimulation).

Compound	EC$_{50}$ (µM)
Trypsin	0.1
2f-LIGRLO-NH$_2$	0.12
GB88	3.3
DM/7/34	8
DM/8/45	3
DM/8/53	6.5
JAMI1026A	2.5
JAMI1028A	11

Table 3. 3 EC$_{50}$ values for p38 MAPK phosphorylation (N=3)

3.5 PAR2-mediated phosphorylation of p65 NFκB in HEK293 cells

Having established the patterns of activation by the GB88 compounds on the MAPK pathway the activation of p65 NFκB was examined. PAR2-mediated NFκB reporter activity was investigated earlier in this chapter but it was decided to look at activation of the pathway in HEK293 cells which express endogenous levels of PAR2. This helps again to determine if GB88 and associated compounds have any unusual characteristics and link to this pathway at more physiological levels of receptor expression. The phosphorylation and transcription of p65 NFκB is a key marker for activation of the pathway; in the absence of a cell line expressing the NFκB luciferase reporter it was decided to use this as an assay readout. In PAR2 expressing reporter cells the activation of p65 NFκB by PAR2 is via a Ca^{2+}-dependent PKC pathway, with receptor coupling to $G\alpha_{q/11}$ (Goon Goh *et al.*, 2008).

However, over a number of experiments it was shown that in HEK293s stimulated with trypsin no p65 phosphorylation was observed, in comparison to the TNFα positive control as shown in figure 3.25. This was also true when using 2f-LIGRLO-NH_2 or any of the GB88 compounds (see figures 3.25 and 3.26). Reasons for this are likely due to the cell type chosen, HEK293s having low levels of endogenous PAR2. In inflammatory disease, PAR2 has been shown across many cell types to be upregulated, with high levels of receptor expression. Therefore, in retrospect using the PAR2 overexpressing cell line may have been a better cell line. However, the experiments presented here demonstrate a lack of coupling to the NFκB pathway at the physiological level.
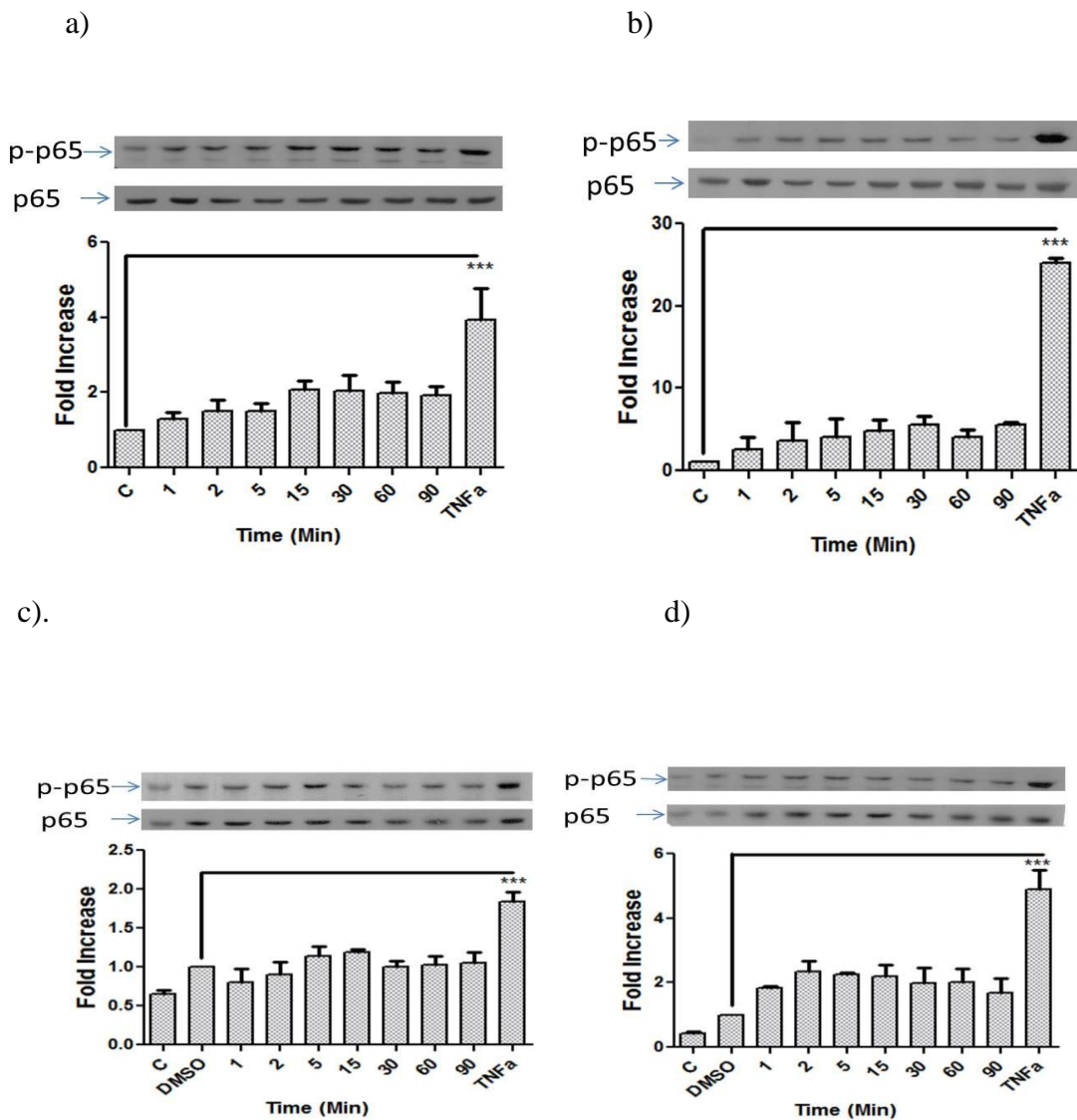
Figure 3. 25 Effect of trypsin, 2f-LIGRLO-NH₂, GB88, and DM/7/34 on phosphorylation of p65 NFκB in HEK293 cells

HEK293 cells were incubated in 2% media for 24 hours prior to stimulation with (a) 100 nM trypsin (b) 1 µM 2f-LIGRLO-NH₂ (c) 10 µM GB88 (d) 10 µM DM/7/34for the times indicated. The whole cell lysates were prepared as previously described (section 2.41), and analysed by Western blotting (section 2.4.2). Each blot is representative of n=3 and semi-quantified by densitometry. Values are expressed as mean ± s.e.m (fold stimulation).
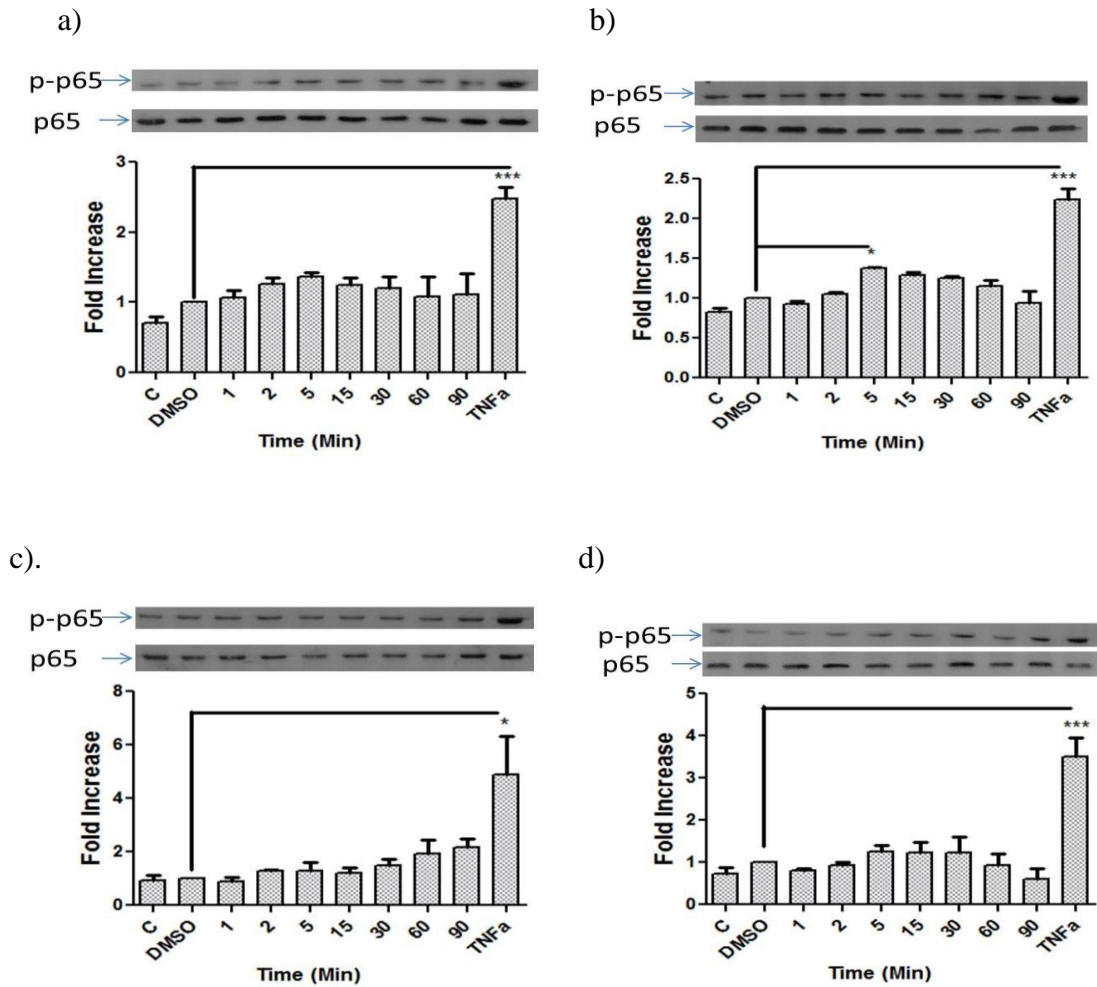
Figure 3. 26 Effect of DM/8/45, DM/8/53, JAMI1026A, and JAMI1028A on phosphorylation of p65 NFκB in HEK293 cells

HEK293 cells were incubated in 2% media for 24 hours prior to stimulation with (a) 10 μM DM/8/45 (b) 10 μM DM/8/53 (c) 10 μM JAMI1026A (d) 10 μM JAMI1028A for the time indicated. Whole cell lysates were prepared as previously described (section 2.41), and analysed by Western blotting (section 2.4.2). Each blot is representative of n=3 and quantified by densitometry. Values are expressed as mean ± s.e.m (fold stimulation).

3.6 PAR2-mediated calcium mobilisation in HEK293 cells

PAR2 mediates intracellular calcium release in normal human keratinocytes (Kawabata *et al*., 2004). Here, HEK239 cells were used to screen intracellular calcium release using the GB88 compounds compared to both agonist trypsin and 2f-LIGRLO-NH$_2$. Barry *et al* discovered that GB88 was a PAR2 antagonist with the ability to inhibit PAR2-induced intracellular calcium mobilization in different cell types treated with protease, peptide or non-peptide agonists of PAR2 (Barry *et al*., 2010, Suen *et al*., 2012). The expectation was that these compounds would have inhibitory actions in this assay.

Initially, it was observed that activation of PAR2 by either endogenous agonist trypsin or synthetic peptide 2f-LIGRLO-NH$_2$ stimulated an increase in intracellular calcium which peaked within 30 seconds and returned to baseline after 2 minutes. Concentration response curves were established for each compound over a number of experiments giving EC$_{50}$ values of 0.15 μM for trypsin and for 2f-LIGRLO-NH$_2$ 0.26 μM as shown in figure 3.27. In the same figure, intracellular Ca^{2+} mobilisation was analysed when HEK293 cells where treated with GB88 and derivative compounds. GB88 compounds yielded weaker calcium signalling mediated by PAR2. In particular, DM/8/53 and JAM1026A had low efficacy relative to both GB88 and 2f-LIGRLO-NH$_2$. In terms of Ca^{2+} release, GB88 and other compounds were considerably less potent and efficacious compared to 2f-LIGRLO-NH$_2$ in inducing PAR2. The responses were between 15-50 fold less potent, as shown by the EC$_{50}$ values in table 3.4. In fact, a full concentration response curve could not be established for JAM1026A. Therefore, GB88 compounds appear to be weak partial PAR2 agonists compared to the full agonists trypsin and 2f-LIGRLO-NH$_2$.
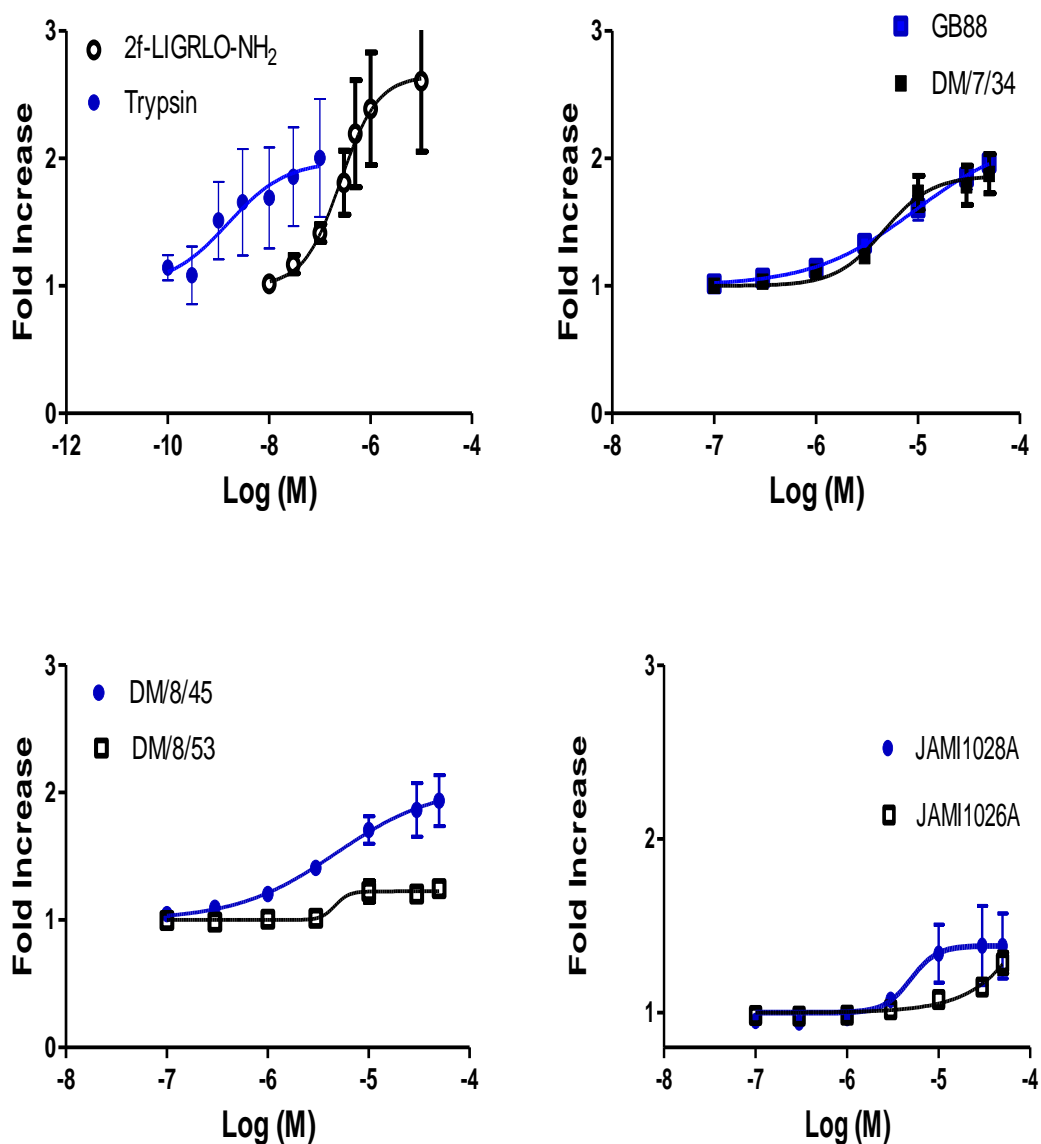
Figure 3. 27 The effect of different concentrations of compounds on PAR2 mediated calcium mobilisation

HEK293 cells were seeded in 96-well black, clear-bottomed plates until confluent then stimulated with increasing concentrations of each agonist (Trypsin or 2f-LIGRLO-NH$_2$) and each compound (GB88, DM/7/34, DM/8/45, DM/8/53, JAMI1028A and JAMI1026A). Concentration-dependent curves for $_i$Ca^{2+} mobilisation by PAR2 agonists were generated. All data are representative of n=3 and expressed as mean ± s.e.m (fold stimulation).

Compound	EC$_{50}$ (µM)
Trypsin	0.15
2f-LIGRLO-NH$_2$	0.26
GB88	15
DM/7/34	4.2
DM/8/45	5.6
DM/8/53	5.5
JAMI1026A	ND
JAMI1028A	7.4

Table 3. 4 EC$_{50}$ values for all compounds tested against PAR2-mediated calcium mobilisation.

(N=3). ND is not determined.

In the next set of experiments, the compounds were tested for antagonist activity as outlined in figures 3.28-30. Cells were pre-incubated with GB88 and related compounds for 15 minutes prior to addition of 3 concentrations of 2f-LIGRLO-NH$_2$ and Ca^{2+} responses measured at 2 minutes. For GB88 there was a slight inhibitory effect of the agonist response at concentrations which had little or no stimulation, however, this effect was not significant. This suggested the potential of a minor level of antagonist activity. However, as the concentration of GB88 increased and the stimulation became apparent this in turn mediated a decrease in subsequent agonist activation. This pattern was replicated with the other compounds with the most pronounced effect with JAMI1026A. These data confirm that all GB88-derivatives compounds activate PAR2 and show little to no inhibitory properties in this assay and others examined. Also by mediating PAR2-induced calcium mobilisation it is probable that GB88 and derivatives are activating PAR2 leading to coupling to G$\alpha_{q/11}$ to mediate calcium responses, similar to 2f-LIGRLO-NH$_2$. This is contradictory to the research published by Barry *et al*, who described GB88 as an antagonist within the G$\alpha_{q/11}$ pathway (Barry *et al*., 2010).
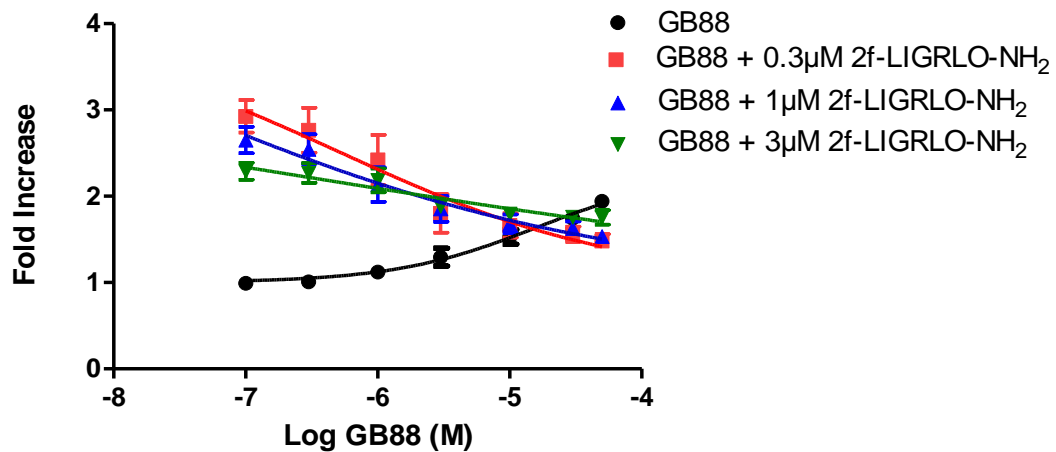
Figure 3. 28 The effect of GB88 on 2f-LIGRLO-NH$_2$ stimulated calcium mobilization in HEK293 cells

HEK293 cells were seeded in 96-well black clear-bottomed plates until confluent then pre-treated with increasing concentrations of GB88 for 15 minutes. Different concentrations of 2f-LIGRLO-NH$_2$ were used to activate PAR2-mediated calcium mobilization as indicated. All data are representative of n=5 and expressed as mean ± s.e.m (Ca^{2+} mobilisation).

a)

b)

c)
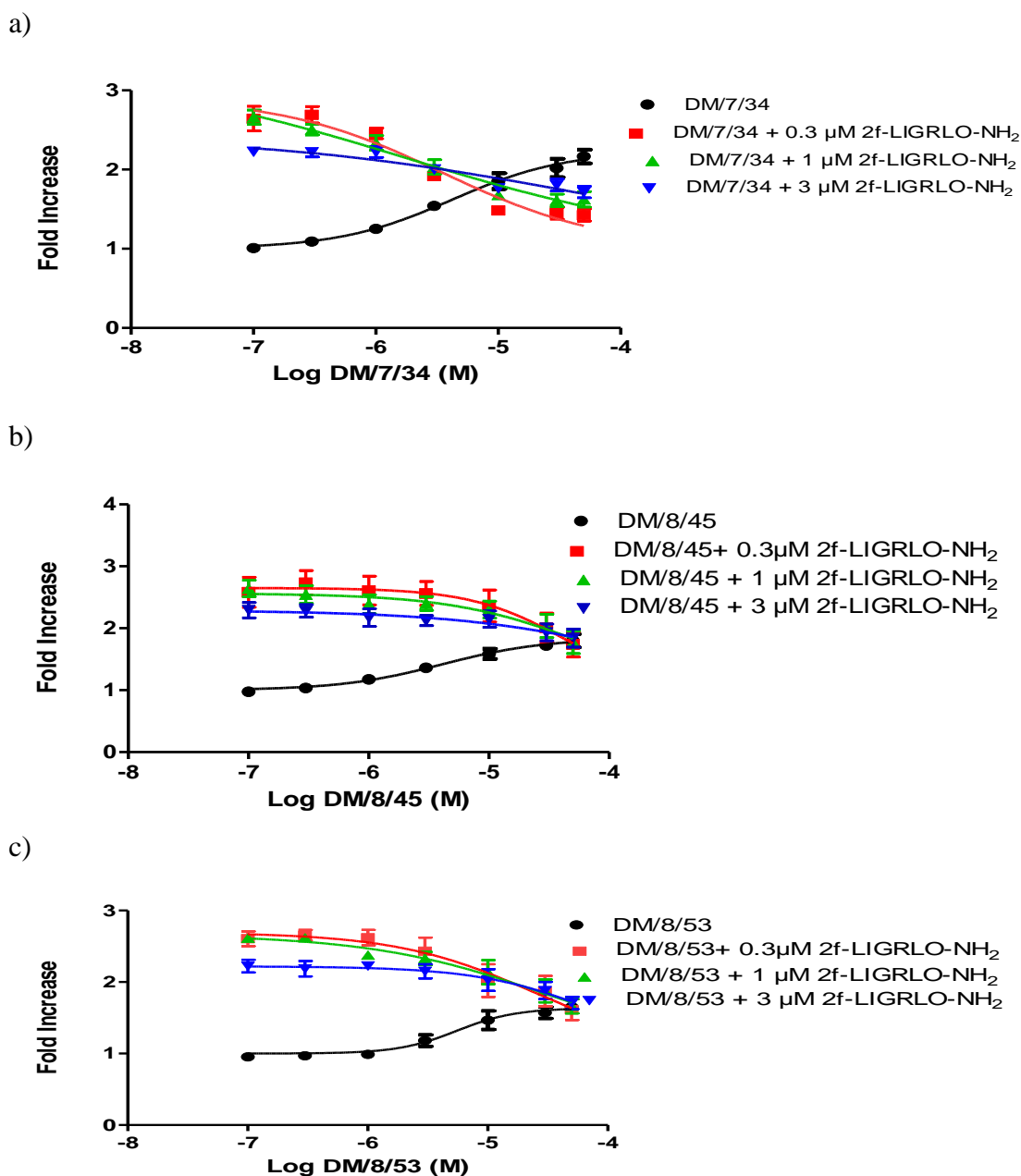
Figure 3. 29 The effect of DM/7/34, DM/8/45, and DM/8/53 on 2f-LIGRLO-NH$_2$-induced calcium mobilisation in HEK293 cells

HEK293 cells were seeded in 96-black wall plate until confluent then pre-treated with increasing concentrations of each agonist (a) DM/7/34 (b) DM/8/45 (c) DM/8/53 for 15 minutes. A different concentration of 2f-LIGRLO-NH$_2$ was used to activate PAR2-mediated calcium mobilization as indicated. All data are representative of n=5 and expressed as mean ± s.e.m (Ca^{2+} mobilisation).

a)

b)
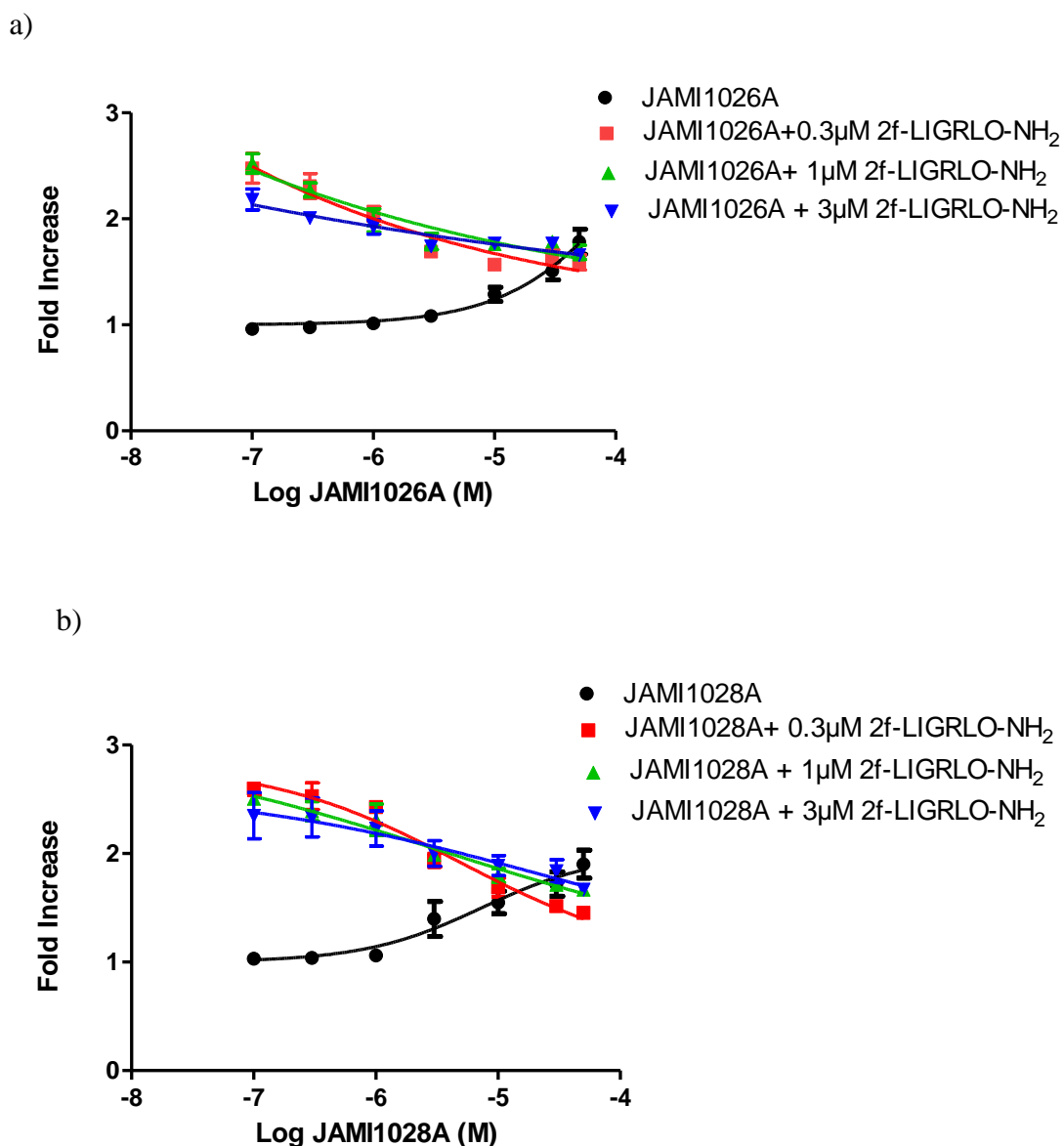
Figure 3. 30 The effect JAMI1026A and JAMI1028A on 2f-LIGRLO-NH₂-induced calcium mobilization in HEK293 cells

HEK293 cells were seeded in 96-black wall plate until confluent then pre-treated with increasing concentrations of each agonist (a) JAMI1026A (b) JAMI1028A for 15 minutes. A different concentration of 2f-LIGRLO-NH$_2$ was used to activate PAR2-mediated calcium mobilization as indicated. All data are representative of n=5 and expressed as mean ± s.e.m (Ca^{2+} mobilisation).

3.7 The role of $G\alpha_{q/11}$ in the calcium mobilisation mediated by PAR2

Having established that GB88 and other agonists can activate Ca^{2+} mobilisation, it was useful to confirm that this effect did involve coupling to the $G\alpha_{q/11}$ pathway. Previously, a number of groups including our own have investigated PAR2 coupling to downstream signalling pathways using the novel $G\alpha_{q/11}$ inhibitor YM-254890 (Goon Goh *et al*., 2008, Goh *et al*., 2009). We utilised this particular compound and examined its effect upon Ca^{2+} mobilisation. As shown in figure 3.31, 100 nM YM254890 inhibited intracellular Ca^{2+} induced by 2f-LIGRLO-NH$_2$ by approximately 70%. In other experiments, as shown in figure 3.32, YM-254890 caused a substantial inhibition of Ca^{2+} mobilization stimulated with GB88, the response was almost completely abolished. This strongly suggests that the activation of Ca^{2+} mobilisation through GB88 is dependent upon the $G\alpha_{q/11}$ pathway.
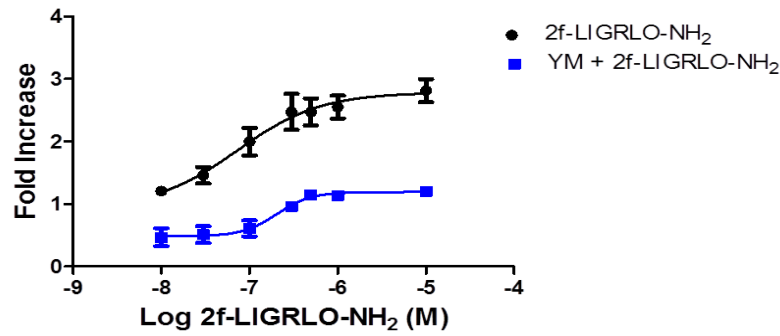
Figure 3. 31 Effect of YM-254890 on 2f-LIGRLO-NH$_2$ stimulated Ca^{2+} mobilisation in HEK293 cells

HEK293 cells were seeded in 96-black wall plates until confluent then pre-incubated with 100 nM of YM-254890 for 15 minutes, and then intracellular Ca^{2+} mobilization was measured after stimulation with increasing concentrations of 2f-LIGRLO-NH$_2$. Concentration-dependent curves for intracellular Ca^{2+} mobilisation induced by the PAR2 agonist were generated. All data are representative of n=5 and expressed as mean ± s.e.m (fold stimulation).
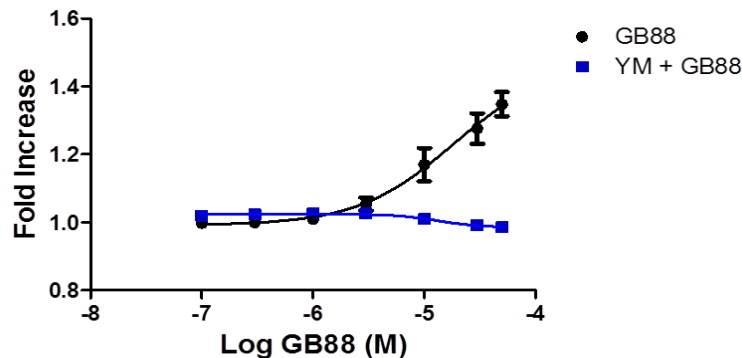
Figure 3. 32 Effect of YM-254890 on Ca^{2+} mobilisation mediated by PAR2 induced by GB88 in HEK293 cells.

HEK293 cells were seeded in 96-black wall plate until confluent then pre-incubated with 100 nM YM-254890 for 15 minutes, and then intracellular Ca^{2+} mobilization measured after stimulation with increasing concentrations of GB88. Concentration-dependent curves for intracellular Ca^{2+} mobilisation by PAR2 agonists were generated. All data are representative of n=5 and expressed as mean ± s.e.m (fold stimulation).

3.8 The role of $G\alpha_{q/11}$ in PAR2-mediated activation of ERK MAP kinase

Having established that GB88 increased Ca^{2+} mobilisation, we sought to examine if the activation of Ca^{2+} signalling via $G\alpha_{q/11}$ had any influence on PAR2-mediated phosphorylation of ERK MAP kinase. This is important because activation of PAR2 by trypsin and activating peptide is thought to be solely dependent on β-arrestin as evidenced by DeFea *et al* (DeFea *et al*., 2000).

The effect of pre-incubation with YM-254890 on the phosphorylation of ERK MAP kinase-activated via trypsin was demonstrated in figure 3.33 (a). Similar to previous experiments trypsin-induced ERK phosphorylation which peaked at 5 minutes with approximately 4 fold of the phosphorylated ERK (3.693 ± 0.190 fold of basal control). Pre-incubation with 30 or 100 nM YM-254890 alone caused a small but non-significant reduction (% inhibition = 28 %) in the phosphorylation of ERK, however with 300 nM of YM-254890 a greater and significant level of inhibition was seen (fold stimulation = 2.653 ± 0.089 fold compared to trypsin alone, *P>0.05). Figure 3.33 (b) shows a similar effect following stimulation via 2f-LIGRLO-NH$_2$. Alone 2f-LIGRLO-NH$_2$ induced the phosphorylation of ERK at 5 minutes at approximately 9 fold (9.073 ± 1.207 fold of basal control). Again, there was partial inhibition, approximately one third in the phosphorylation of ERK following incubation with 300 nM YM-254890 reducing the activation to approximately 6 fold (6.083 ± 0.670 fold for 2f-LIGRLO-NH$_2$).

a)
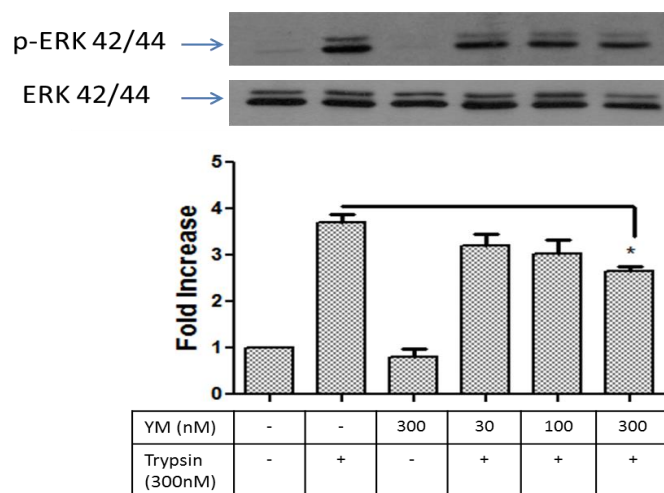
b)
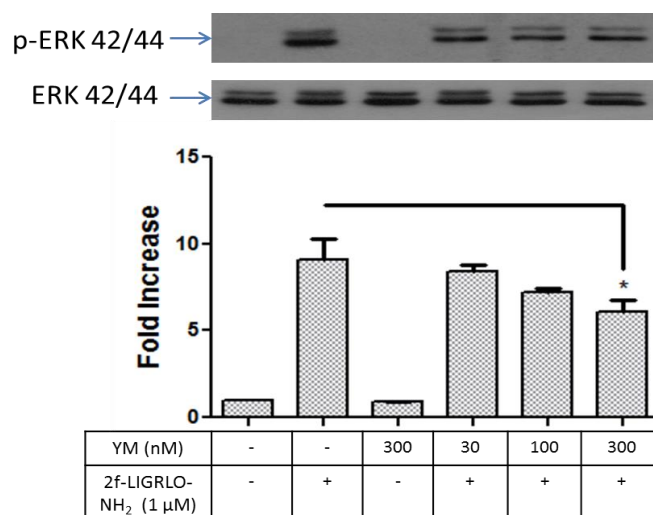
Figure 3. 33 The effect of YM-254890 on trypsin and 2f-LIGRLO-NH$_2$ stimulated ERK phosphorylation in HEK293 cells

HEK293 cells were incubated with 2% media for 24 hours prior to pre-treatment with increasing concentrations of YM-254890 (Rohatgi *et al*.) for 30 minutes and stimulated with (a) 300 nM trypsin (b) 1µM 2f-LIGRLO-NH$_2$ for an additional 5 minutes. Whole cell lysates were prepared as previously described (section 2.41) and analysed by Western blotting (section 2.4.2). Each Blot is representative of n=3, quantified by densitometry and expressed as mean ± s.e.m (fold stimulation). *P>0.05 versus control.

The effect of pre-incubation with YM-254890 on the phosphorylation of ERK activated via GB88 was illustrated in figure 3.34 (a). It was shown that GB88 induced the phosphorylation of ERK at 5 minutes at approximately 7 fold (7.380 ± 0.850 fold of DMSO basal). There was no effect following pre-incubation with 30 nM YM-254890 alone but there was a moderate inhibition with 100 nM YM-254890 reducing phosphorylation to under 5 fold (4.583 ± 0.583 fold) and also significant inhibition (approximately 50%) following pre-incubation using 300 nM YM-254890 (3.740 ± 0.422 fold compare to GB88 stimulation).

A similar pattern was identified when the other GB88 related compounds were utilised. This is shown in figures 3.34.(b), 3.35 and 3.36. It is of interest to note that whilst for some of the compounds inhibition was only observed at the very maximal concentration of 300nM, for other compounds in particularly DM/8/53 and JAMI1026A there was significant inhibition approximately 50% at the 100nM concentration.

a)
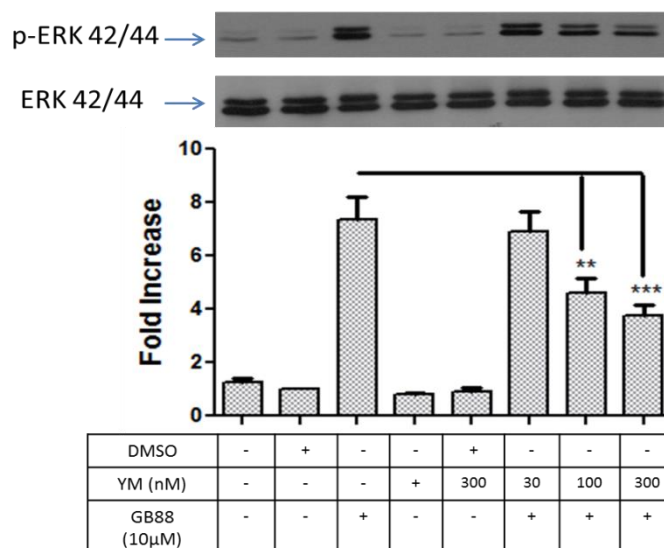
b)
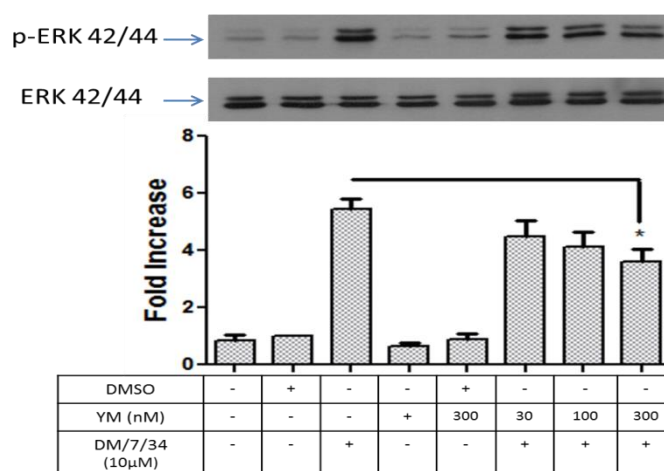
Figure 3. 34 Effect of YM-254890 on GB88 and DM/7/34 stimulated phosphorylation of ERK MAP kinase in HEK293 cells

HEK293 cells were incubated with 2% media for 24 hours prior to pre-treatment with increasing concentrations of YM-254890 (Rohatgi *et al*.) for 30 minutes and stimulated with (a) 10 μM GB88 (b) 10 μM DM/7/34 for an additional 5 minutes. Whole cell lysates were prepared as previously described (section 2.41) and analysed by Western blotting (section 2.4.2). Each blot is representative of n=3, quantified by densitometry and expressed as mean ± s.e.m (fold stimulation). **P<0.01 ***P<0.001 or *P>0.05 versus stimulated control.

a)
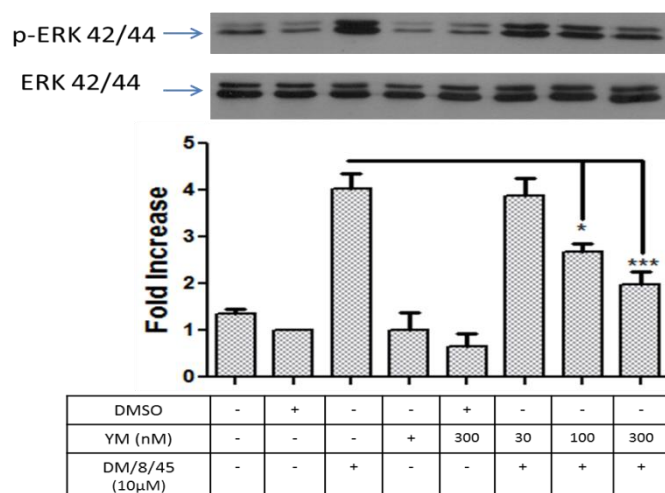
b)
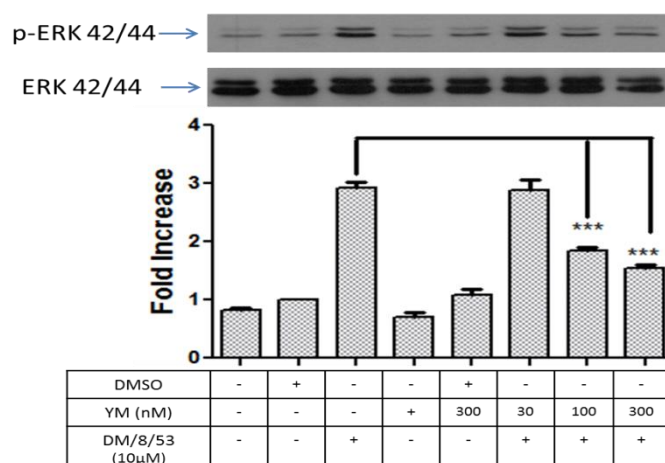
Figure 3. 35 Effect of YM-254890 on DM/8/45 and DM/8/53 stimulated ERK phosphorylation in HEK293 cells

HEK293 cells were incubated with 2% media for 24 hours prior to pre-treatment with increasing concentrations of YM-254890 (Rohatgi *et al*.) for 30 minutes and stimulated with (a) 10 μM DM/8/45 (b) 10 μM DM/8/53 for an additional 5 minutes. Whole cell lysates were prepared as previously described (section 2.41) and analysed by Western blotting (section 2.4.2). Each blot is representative of n=3, quantified by densitometry and expressed as mean ± s.e.m (fold stimulation). *P<0.05 ***P<0.001 compared to stimulated control.

a)
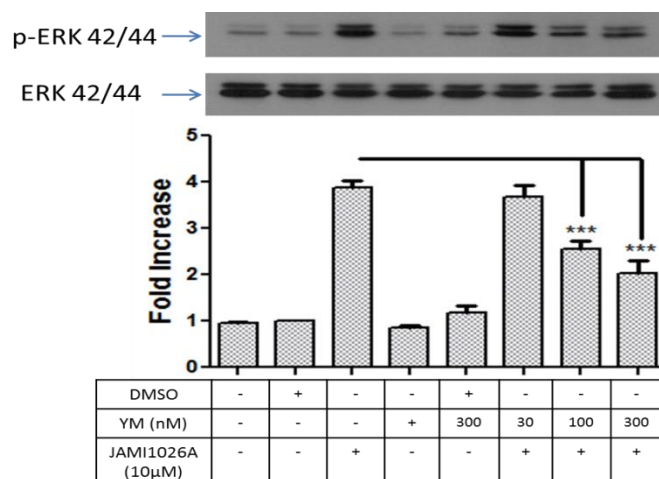
b)
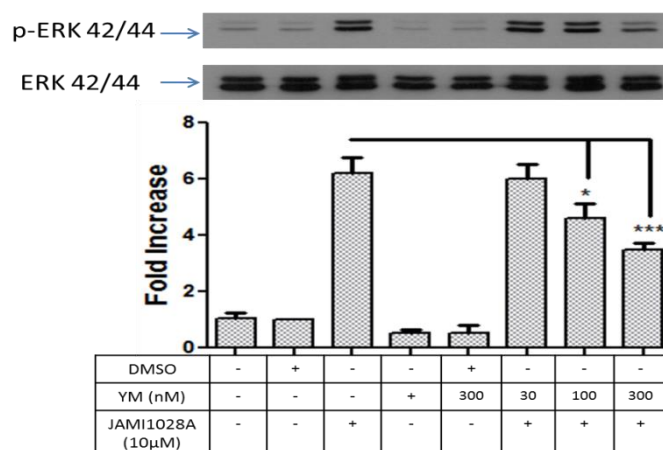
Figure 3. 36 The effect of YM-254890 on JAMI1026A and JAMI1028A stimulated ERK phosphorylation in HEK293 cells

HEK293 cells were incubated with 2% media for 24 hours prior to pre-treatment with increasing concentrations of YM-254890 (Rohatgi *et al*.) for 30 minutes and stimulated with (a) 10 μM JAMI1026A (b) 10 μM JAMI1028A for an additional 5 minutes. Whole cell lysates were prepared as previously described (section 2.41), and separated by SDS.PAGE (section 2.4.2). Blot is representative of n=3, quantified by densitometry and expressed as mean ± s.e.m (fold stimulation). *P<0.05 ***P<0.001 versus agonist stimulated control.

3.9 Discussion

Initially, this chapter assessed the actions of trypsin and 2f-LIGRO-NH$_2$, which activate PAR2 and the effects of the non-peptide compound GB88 and other derivatives generated in house. The investigation has been achieved by utilising three key distinct signalling pathways that are relevant to PAR2 signalling, for example: down-stream NFκB transcriptional activity, the mid-stream ERK MAP kinase and the up-stream calcium mobilisation. In order to do this, the keratinocyte line NCTC2544 cells overexpressing both hPAR2 (Clone G) and an NFκB-Luc plasmid (NFκB-Reporter cells) are used. In addition, HEK293 cells have been utilised, as a cell line displaying endogenous expression of PAR2.

Initially, the effect of the five compounds based on the structure of GB88 was tested on PAR2-mediated transcriptional activation of NFκB. At the start of this study GB88 and other compounds had been identified as novel antagonists (Barry *et al*., 2010) and an improvement on ENMD-1068, K-12940, and K-14585 compounds (Kelso *et al*., 2006, Kanke *et al*., 2009). The PAR2 compound, GB88 is a non-peptide compound; it has the ability to disarm both endogenous and synthetic peptide agonists (Barry *et al*., 2010). In this study, the structure of GB88 compounds was used as a basis to develop additional C-terminal derivatives. These derivatives (DM/7/34, DM/8/45, DM/8/53, JAMI1026A, and JAMI1028A) have similar structures to GB88, with slight modifications made in the C-terminal whereas the N-terminal was unaltered. It was predicted that these compounds might have enhanced potency.

Activation of the receptor has the potential to link to a number of intracellular signalling pathways. One is NFκB mediated through the activation of isoforms of inhibitory kappa B (IKK1 and IKK2) (Kanke *et al*., 2001). This also involves partial coupling of PAR2 to Ca^{2+} and G$\alpha_{q/11}$ which partially regulates the pathway (Goon Goh *et al*., 2008). The activation of NFκB in response to PAR2 activation can be assessed in several ways in normal cells for example NFκB-DNA binding or p65 NFκB phosphorylation (Macfarlane *et al*., 2005). However, these assays are time-

critical. The cell line generated for this study overexpressed PAR2 and a luciferase reporter construct expressing 6 NFκB binding sites within the promoter making it an ideal cell line for multiple compound analysis (Kanke *et al*., 2001). It was found out that GB88 and related compounds were able to activate reporter activity rather than inhibit it. In addition, the novel compounds, many of which had comparable efficacy to GB88 although some do not reach a maximum activation relative to 2f-LIGRO-NH$_2$. These above findings showed the first implication that such compounds were not antagonists but may have other properties.

The potential of inhibition was also studied by pre-incubating reporter cells with compound. Using this approach there was no evidence for any antagonist effects. GB88, DM/7/34, DM/8/45, DM/8/53, JAMI1026A, and JAMI1028A did not inhibit peptide or trypsin induced reporter activity at lower concentrations. However, as the concentration of the compounds increased there was some inhibition of the peptide or trypsin response or at least there was additive effect. This might again support the idea that the compounds are partial agonists; they are able to compete with 2f-LIGRLO-NH$_2$ for binding to the receptor however as they occupy the receptor more they are not able to active the receptor as strongly, thus actually reducing the response. However, if as mentioned above the cells overexpressed the receptor and coupled to a strong reporter system the responses to a weak partial agonist looks greater as is the case here.

However, other PAR2 inhibitors have been identified using this readout suggesting that an inhibitory activity can be identified (Goh *et al*., 2009). Both peptide-mimetic compounds K-12940 and K-14585, mediated a concentration-dependent inhibition of luciferase activity stimulated by SLIGKV-OH up to 80% and about 25% in PAR2 activated by trypsin (Kanke *et al*., 2009). Other research also confirms these antagonist properties and relative effects of K-12940 and K-14585 against trypsin and peptide using *in vivo* models (Kanke *et al*., 2001).

Other studies have found that incubation of these cells with the cell permeable chelator BAPTA-AM leads to a notable inhibition of trypsin-stimulated PAR2

activity and this inhibition is almost complete (Macfarlane *et al.*, 2005). This suggests the potential to link PAR2 to luciferase via $G\alpha_{q/11}$. Whilst this has not been directly demonstrated, Goh *et al* (Goon Goh *et al.*, 2008) utilised the $G\alpha_{q/11}$ inhibitor YM-254890 and showed approximately 50% inhibition of the peptide mediated response. Thus, any inhibition of the pathway by GB88 and other antagonists in this pathway should have been observed in the reporter assay.

Measuring PAR2 mediated phosphorylation of ERK was utilised next as an approach to characterise the pharmacological properties of GB88 and its derivative compounds. This was done in HEK293 cells, which are recognised to express a moderate level of PAR2. As indicated in the introduction, previous research has demonstrated phosphorylation of ERK mediated by PAR2 (Zhang *et al.*, 2012a) which is linked to a number of downstream responses (DeFea *et al.*, 2000, Kramer *et al.*, 1995). Previous research from our lab demonstrated that ERK, p38 and JNK MAPK are mediated by PAR2 activation but again this is in a system where PAR2 is overexpressed (Macfarlane *et al.*, 2005).

The ERK1/2 signaling pathway is initiated via receptor coupling to several types of G proteins, such as $G\alpha_s$, $G\alpha_{q/11}$ and $G\alpha_{i/o}$ (DeFea *et al.*, 2000, Ramachandran *et al.*, 2009) and also β-arrestin. The activation of ERK particularly at early time points is in some instances, PKC-dependent as shown in KNRK cells transfected with hPAR2 (Ramachandran *et al.*, 2009, DeFea *et al.*, 2000). Indeed Early ERK activation in HSP cells by SLIGKV-NH$_2$ occurs between at 3-5 minutes and is PKC-dependent due to PAR2 coupling to $G\alpha_{q/11}$ (Myatt and Hill, 2005). Thus, 5 minutes was identified as the time point for study of the inhibitors.

Once again, GB88 and its relative compounds display robust increases in ERK activation although they were far less efficacious than 2f-LIGRLNH$_2$ stimulation suggesting again partial agonist activity. These results to some extent agree with the most recent studies. GB88 was re-classified as a biased antagonist by Suen and colleagues. They demonstrated, at least in HT29 and CHO-hPAR2 cells, that GB88 could inhibit $G\alpha_{q/11}$ mediated PAR2-signalling while activating $G\alpha_{i/o}$ driven pathways

which couple to ERK. Thus, in their study GB88 activated ERK through PAR2 coupling to $G\alpha_{i/o}$ and inhibited PAR2-mediated $G\alpha_{q/11}$- Ca^{2+}-PKC pathway (Suen *et al.*, 2014). A bias agonist is also found in response of the signalling of PAR2. Ramachandran and colleagues found that both trypsin and SLIGRL have an ability to activate ERK MAP kinase and intracellular calcium pathways in PAR2-KNRK cells, while it was also noticed that SLAAAA-NH$_2$ behaves as a biased agonist, SLAAAA-NH$_2$ did not activate intracellular calcium but activated p42/44 MAPK in the same cell line (Ramachandran *et al.*, 2009). Elastin and related enzymes also have biased properties by promoting PAR2 coupling to $G\alpha_s$, and activating PKA and adenylyl cyclase-mediated by TRPV4 (Steinhoff *et al.*, 2000, Zhao *et al.*, 2014, Zhao *et al.*, 2015). This allows an influx of calcium ions from the extracellular fluid via PKA, while the canonical peptide agonist only promotes coupling of PAR2 to $G\alpha_{q/11}$ to promote intracellular Ca^{2+} mobilisation (Zhao *et al.*, 2015, Zhao *et al.*, 2014).

Work from other groups have identified coupling of PAR2 to β-arrestin as a common mechanism by which ERK is activated through biased agonist activity. For example, PAR2 activates cofflin via β-arrestin and ERK activation independently of $G\alpha_{q/11}$ (Wang and DeFea, 2006, Zoudilova *et al.*, 2007). A study from Ge and co-workers has also demonstrated that the prolonged activation of ERK-induced by PAR2 is dependent on binding with β-arrestin, co-immunoprecipitation identified an active receptor/arrestin complex for up to 90 minutes (Ge *et al.*, 2003). This mode of coupling has also been observed for G-protein coupled receptors, such as; angiotensin AT$_1$ (Wei *et al.*, 2003) and vasopressin V$_2$ receptors (Charest *et al.*, 2007).

Interestingly, this work is also similar to results from the Plevin laboratory in which the peptide antagonist K-14585 was found to activate ERK and p38 MAP kinase in the same cells where inhibition of NFκB luciferase was recorded (Goh *et al.*, 2009). In HEK293 cells, there was no activation of p38 MAPK nor phosphorylation of p65 NFκB presumably due to the lower expression of the receptor and the less likelihood of aberrant coupling so this possibility could not be tested. Other studies, for example (Sethi *et al.*, 2005) have demonstrated PAR2 activation of p38 MAP kinase which in

turn stimulates IL-1β and IL-8 release from intestinal epithelial cells, were it is assumed receptor expression is also moderate (Fyfe *et al.*, 2005), suggesting differences in coupling efficiencies in different cells. Other studies also point to the potential of dual functions and thus bias antagonist activity for example, PAR2 activates PI3 kinase via the $G\alpha_{q/11}$ pathway, but also ERK via β-arrestin-mediated binding which can also negatively modulate PI3 kinase (Wang *et al.*, 2007a). Thus, overall, our compounds have the potential to be bias ligands if due to using overexpressing cells the antagonist function of GB88 and other compounds are manifest as partial agonists due to the high levels of receptor and extremely efficient coupling to the NFκB readout.

To further address the question regarding PAR2 mediated antagonism in HEK293 cells, a fluorescence-based Ca^{2+} imaging was used and allowed GB88 and associated compounds to be assessed for calcium mobilisation in HEKs. Multiple studies link PAR2 to rapid intracellular Ca^{2+} mobilisation (Myatt and Hill, 2005, Lieu *et al.*, 2016). Intracellular calcium mobilisation activated by furoylated peptides has been measured in NCTC2544-PAR2 and human colon adenocarcinoma cells (HCT-15) using similar systems (Kawabata *et al.*, 2004). Bushell and colleagues have demonstrated calcium mobilisation in various cell types and illustrated that PAR2 binds to $G\alpha_{q/11}$ leading to IP_3 release and subsequent intracellular Ca^{2+} (Bushell *et al.*, 2006). Ca^{2+} mobilisation is the standard approach to test new agonist and antagonist drugs in a variety of cells expressing endogenous receptor (McGuire *et al.*, 2004, Hollenberg *et al.*, 2008) and in transfected cells (Hela-PAR2) (Boitano *et al.*, 2011).

Disappointingly, our studies did not indicate significant inhibition for NFκB transcriptional activity, the phosphorylated of ERK and calcium internalisation by GB88 and related compounds. PAR2 activation in these cells is $G\alpha_{q/11}$ dependent as the Ca^{2+} response was blocked by YM-254890 a compound which directly inhibits $G\alpha_{q/11}$. These findings are at odds with a number of recent studies and cannot be readily explained. It is noted that pre-incubation times in a number of these studies is

up to 60 min, this may result in desensitisation of the receptor though internalisation thus reducing the subsequent stimulation.

Nevertheless, Lohman *et al*. 2012, have shown that GB88 is the first PAR2 antagonist which can inhibit both protease and peptide activation *in vivo* and *in vitro* (Lohman *et al*., 2012a). This finding is consistent with a study from Suen *et al*. 2012, which illustrated that GB88 was able to reduce PAR2-induced calcium mobilisation mediated by three different PAR2 agonists (trypsin, 2f-LIGRLO-NH$_2$, and GB110). This finding was shown in various types of human cells for example; Panc-1, HT29, HUVEC, MKN45, MKN1, and MDA-MB-231 cell lines, which have a vast variation in PAR2 expression (Suen *et al*., 2012, Barry *et al*., 2010).

Elements of these papers demonstrate inhibitory effects in human monocyte-derived macrophages (HMDMs) as well as rat paw oedema (Lohman *et al*., 2012a, Suen *et al*., 2012). GB88 also inhibits trypsin, elastase and cathepsin-s induced Ca^{2+} responses in dorsal root ganglion (DRG) neurons (Lieu *et al*., 2016, Zhao *et al*., 2015, Zhao *et al*., 2014). Other studies noted that GB88 is effective in reducing protease- and peptide- mediated pain and inflammation in rats including mast cell degranulation, macrophage infiltration and collagen-induced arthritis (Barry *et al*., 2010, Suen *et al*., 2012, Lohman *et al*., 2012a, Lieu *et al*., 2016).

Recently, Yau's colleagues have found that three of the N-terminal derivatives of GB88 (isoxazole, cyclohexylalanine, and isoleucine) bind to distinct sites on PAR2 regulating selectivity and affinity, whereas the C-terminal residue spiro[indene-1,4'-piperidine] determines dual function. One of the GB88 derivatives, AY117 behaves as a PAR2 biased antagonist; it decreases internalisation of calcium responses mediated by PAR2 and acts as an agonist to phosphorylate of ERK MAPK in HT29 cells. The selective PAR2 antagonist AY117 inhibits secretion of the pro-inflammatory cytokines TNFα and IL-6 in human tubule epithelial cells (HTEC). It also reduces rat paw oedema. This study demonstrated that the isoxazole in GB88 has a crucial role in showing the antagonist properties through the nitrogen/oxygen atoms (Yau *et al*., 2016a). This finding does not conform to the present study as the

results presented here show GB88 and its derivatives to be agonists via $G\alpha_{q/11}$ across several pathways in spite of containing the aforementioned isoxazole ring.

GB88 may also have an additional benefit as a bias antagonist in terms of drug design being able to disarm a specific PAR2 mediated signaling pathway linked to a disease with no effect on another signalling event linked to normal physiology (Suen *et al*., 2014). The low affinity PAR2 antagonist ENMD-1068 has been found to inhibit PAR2-mediated calcium mobilisation activated via SLIGKV-NH$_2$ in Lewis lung carcinoma cells (LLC) as well as attenuated murine joint inflammation (Kelso *et al*., 2006). The anti-osteoarthritic compound ENMD-520 has been reported as a PAR2 antagonist in mice, however it required very high concentrations to elicit inhibitory effects, ruling it unsuitable for the next stages of testing (Ferrell *et al*., 2010). If a better more potent bioavailable drug such as GB88 can be made available, it has the potential to be used clinically in this condition.

The main finding in this chapter was that GB88 and its derivatives behaved as PAR2 partial agonists compared to trypsin and 2f-LIGRLO-NH$_2$. This was evidenced through the measurement of a series of outputs; and NFκB activation, ERK MAP kinase phosphorylation and $G\alpha_{q/11}$ dependent calcium mobilisation. This finding is in contradiction to that reported by Barry *et al* in 2010 who described GB88 as a PAR2 antagonist in terms of inhibiting calcium mobilisation in HT29 cells (Barry *et al*., 2010). Others have also concluded that GB88 is a PAR2 antagonist in terms of inhibiting $_iCa^{2+}$ in different cell types and has the ability to reduce rat paw oedema (Suen *et al*., 2012, Lohman *et al*., 2012a). However, following these studies, GB88 was re-classified as a biased antagonist by Suen and colleagues. They demonstrated GB88 could inhibit $G\alpha_{q/11}$ mediated PAR2-signalling, while activating $G\alpha_{i/o}$ driven pathways (Suen *et al*., 2014).

Chapter Four

Characterisation of the novel PAR2 modulator

compound AZ8838

4.1 Introduction

The previous chapter evaluated the pharmacological properties of GB88 and derivative compounds designed around its parent structure, as potential PAR2 antagonists. The conclusions drawn from these studies were that GB88 and its derivatives all behaved as partial agonists for PAR2 in terms of activation of multiple downstream signalling pathways. Unpublished research from our laboratory have also demonstrated that GB88 has the ability to internalise PAR2 at low micromolar concentrations (not shown) again supporting the idea that GB88 has agonist properties.

So far, there have been limited PAR2 antagonists developed to date and none have been successfully utilised clinically. For PAR1 there has been more success; Vorapaxar was the first drug marketed as a PAR1 antagonist to reduce thrombosis (Chackalamannil *et al*., 2008). However, due to side effects, including uncontrolled bleeding, Vorapaxar is now used in only a limited cohort of patients (no history of stroke) and its use is currently being revaluated. Recently, together with the resolution of the PAR2 crystal structure, the PAR2 antagonist AZ3451 has been discovered and reported to bind to the allosteric site of PAR2. Studies suggest that AZ3451 binds to the receptor, hindering structural rearrangement, thereby preventing PAR2 activation and signalling. Another antagonist, AZ8838, has also been generated via the information from the PAR2 crystal structure; this compound inhibits PAR2 mediated calcium mobilisation. Both AZ3451 and AZ8838 are competitive antagonists, competing with the agonist to prevent receptor activation and signalling (Cheng *et al*., 2017).

The focus of this chapter was to evaluate the pharmacological properties of the PAR2 antagonist AZ8838 and its component structures based on the stereoisomers of the molecule, named YPT-1 (R-AZ8838) and YPT-2 (S-AZ8838). These structures are pure structures compared to ra-AZ8838, which is a racemic mixture. The hypothesis presented in this chapter is that YPT-1 (R-AZ8838) is not active as an antagonist while YPT-2 (S-AZ8838) and ra-AZ8838 are antagonists in terms of blocking PAR2 mediated NFκB-Reporter gene transcription and the phosphorylation of ERK MAP

kinase. It has been show in the studies by Cheng that R-AZ8838 does not inhibit PAR2 (Cheng *et al.*, 2017).

4.2 The effect of AZ8838 compounds on PAR2 dependent NFκB activity

4.2.1 Effect of AZ8838 compounds on NFκB reporter activity stimulated by 2f-LIGRLO-NH$_2$

The effect of pre-treatment with YPT-1 for an hour before the addition of 2f-LIGRLO-NH$_2$ for a further 4 hours on NFκB-driven gene transcription in NFκB-Reporter cells is shown in figure 4.1.a. As shown previously, 2f-LIGRLO-NH$_2$ stimulated a significant increase in luciferase activity as expected, with approximately 4.5 fold of basal values and this was not significantly affected by the presence of DMSO (2f-LIGRLO-NH$_2$ = 4.71 ± 0.55, DMSO plus 2f-LIGRLO-NH$_2$ = 4.96 ± 0.57, n=4). No effect was observed on NFκB gene transcription when the cells were pre-incubated with YPT-1 prior to the addition of 2f-LIGRO-NH$_2$ even at the highest concentration tested.

The effect of pre-treatment with YPT-2 for 1 hour prior to the addition of 2f-LIGRLO-NH$_2$ for 4 hours on NFκB-driven gene transcription in NFκB-Reporter cells is shown in figure 4.1.b. Alone, YPT-2 had no effect on the levels of NFκB gene transcription when compared to the untreated control. Furthermore, 2f-LIGRLO-NH$_2$ stimulated a significant increase in luciferase activity as expected of around 2.8 fold and this was not significantly affected by DMSO (Fold stimulation: 2f-LIGRLO-NH$_2$ = 2.793 ± 0.35, DMSO & 2f-LIGRLO-NH$_2$ = 3.05 ± 0.28, n=4). However, following incubation with increasing concentrations of YPT-2, a decrease in NFκB gene transcription was observed. There was complete inhibition at 20 μM,

the maximum concentration tested (% stim = 20 μM YPT-2&2FLIG = -2.425 ± 2.00, vs 2FLIG&DMSO = 100% n=4), dropping values to below basal levels.

The effect of the racemic mixture ra-AZ8838 on PAR2 mediated NFκB-driven gene transcription is shown in figure 4.1.c. The compound ra-AZ8838 had no effect on the levels of luciferase activity when compared to untreated controls. Furthermore, 2f-LIGRLO-NH$_2$ stimulated a significant increase in NFκB gene transcription as expected, in this case 2.8 fold. The maximum response was not affected by the presence of DMSO, if anything there was a minor increase (Fold stimulation: 2f-LIGRLO-NH$_2$ = 2.79 ± 0.35, vs. DMSO & 2f-LIGRLO-NH$_2$ = 3.05 ± 0.28, n=4). However, following incubation with increasing concentrations of ra-AZ8838, a corresponding concentration-dependent decrease in NFκB gene transcription was observed between 0.3-20 μM, with approximately 99% inhibition using 20 μM (% stimulation using 20 μM AZ & 2FLIG = 1.368 ± 3.707, vs. DMSO&2FLIG = 100 n=4).

IC$_{50}$ values for YPT-1, YPT-2 and ra-AZ8838 were then calculated using a sigmoidal non-linear regression curve using GraphPad Prism software (see figure 4.2). Both YPT-2 and ra-AZ8838 generated a concentration-dependent inhibition of 2f-LIGRLO-NH$_2$ driven NFκB-transcriptional activity with IC$_{50}$ values of 0.5 and 1.2 μM respectively, n=4. In contrast, YPT-1 had no inhibitory effect upon 2f-LIGRLO-NH$_2$ induced NFκB-transcriptional activity and no IC$_{50}$ could be calculated.

a)

DMSO	-	-	+	+	-	-	-	-	-	-
YPT-1 (µM)	-	-	-	-	0.1	0.3	1	3	10	20
2f-LIGRLO-NH2 (0.3 µM)	-	+	-	+	+	+	+	+	+	+

b)

DMSO	-	-	+	+	-	-	-	-	-	-	-	-	-	-
YPT-2 (µM)	-	-	-	-	20	0.003	0.01	0.03	0.1	0.3	1	3	10	20
2f-LIGRLO-NH2 (0.3 µM)	-	+	-	+	-	+	+	+	+	+	+	+	+	+

c)
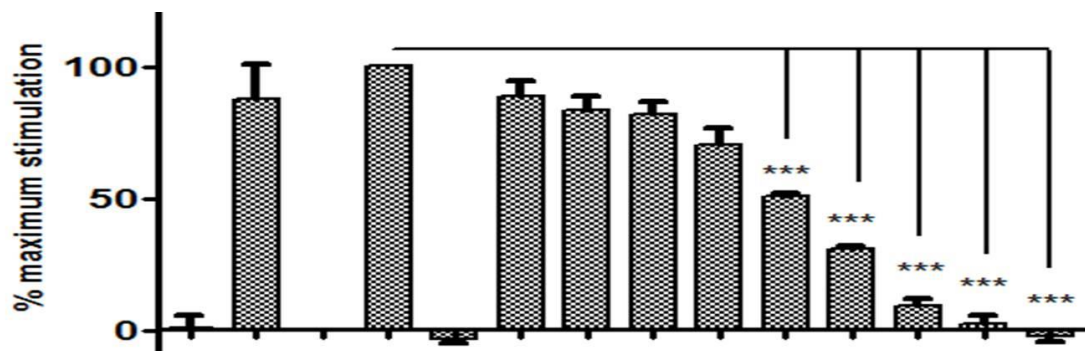
DMSO	-	-	+	+	-	-	-	-	-	-	-	-	-	-
ra-AZ8838 (μM)	-	-	-	-	20	0.003	0.01	0.03	0.1	0.3	1	3	10	20
2f-LIGRLO-NH2 (0.3 μM)	-	+	-	+	-	+	+	+	+	+	+	+	+	+

Figure 4. 1 The effect of YPT-1, YPT-2 and ra-AZ8838 on 2f-LIGRLO-NH$_2$ – stimulated NFκB transcriptional activity.

NFκB-reporter cells were grown to confluence and rendered quiescent for 18 hours prior to pre-treatment with increasing concentrations of a) YPT-1, b) YPT-2, and c) ra-AZ8838 for 1 hour. Cells were then stimulated with 0.3 μM 2f-LIGRLO-NH$_2$ for a further 4 hours. Cell lysates were then measured for luciferase activity as previously described (section 2.3). The data shown are expressed as % maximum stimulation and each value represented n=4 except YPT-1 =3. Statistical analysis was via one-way ANOVA, with Dunnett's post-test comparison ***p<0.0001 compared to DMSO + 2f-LIGRLO-NH$_2$ stimulation.
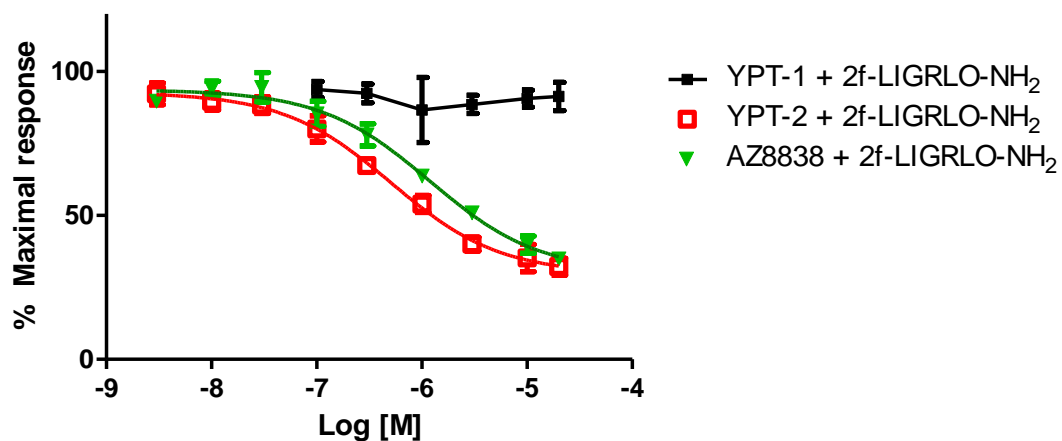
Figure 4. 2 IC_{50} values for AZ compounds against the transcriptional activity stimulated by 2f-LIGRLO-NH₂ in NFκB-Reporter cells

IC_{50} curves from, YPT-1, YPT-2, and ra-AZ8838 were generated by fitting data to a Sigmoidal non-linear regression curve (variable slope). Each value represents the mean ± SEM of four independent experiments.

4.2.2 Effect of AZ8838 and YPTs compounds on trypsin -mediated NFκB-driven gene transcription in NFκB-Reporter cells

The effect of pre-treatment with YPT-1 for 1 hour prior to stimulation by trypsin for a further 4 hours on PAR2 mediated NFκB-driven gene transcription is shown in figure 4.3 (a). Trypsin stimulated a significant increase in NFκB gene transcription, which was approximately 4.7 fold and this was not significantly affected by the presence of DMSO (Fold stimulation; trypsin = 4.69 ± 0.90, DMSO & trypsin = 5.06 ± 0.58, n=3). No additional effect was observed in NFκB gene transcription when the cells were pre-incubated with increasing concentrations of YPT-1 even at the highest concentration used of 20 μM.

Figure 4.3.b illustrates the effect of pre-treatment with YPT-2 on trypsin stimulated NFκB-driven gene transcription. The compound had a small effect on basal activity, compared with the untreated control, however this was not significant (% stimulation: YPT-2 = -0.766 ± 0.461, vs. DMSO control = 0, n=5). Furthermore, trypsin stimulated a significant increase in reporter activity as expected, approximately 16.6 fold, this response was not affected by the addition of DMSO (Fold stimulation: trypsin = 16.58 ± 2.81, DMSO & trypsin = 16.760 ± 2.55, n=5). However, following incubation with YPT-2, a significant, concentration-dependent inhibition of NFκB gene transcription was observed between 1-20 μM, with approximately 85% inhibition observed at 20 μM (% stimulation at 20 μM = 15.816 ± 1.670, vs. trypsin & DMSO control = 100 n=5).

The effect of pre-treatment with ra-AZ8838 for 1 hour prior to the addition of trypsin for 4 hours on PAR2 mediated NFκB-driven gene transcription is shown in figure 4.3.c. The compound ra-AZ8838 had a small effect on the basal levels of luciferase activity, which was not significantly different when compared with the untreated control (%stimulation: ra-AZ8838 = -0.658 ± 0.620, vs. DMSO control = 0, n=5). Furthermore, as expected, trypsin stimulated a significant increase in luciferase activity, approximately 16.6 fold, this response was not affected by the presence of

DMSO (Fold stimulation: trypsin = 16.58 ± 2.81, DMSO & trypsin = 16.760 ± 2.55, n=5). However, following incubation with ra-AZ8838, a significant concentration-dependent inhibition of NFκB gene transcription was observed between 3-20 μM, with approximately 82% inhibition observed using 20 μM, the maximum concentration of compound employed (% stimulation at 20 μM AZ & trypsin = 17.404 ± 2.2446, vs. trypsin & DMSO control = 100, n=5).

Again, IC$_{50}$ values for YPT-2 and ra-AZ8838 were calculated using a sigmoidal non-linear regression curve and shown in Figure 4.4. Both YPT-2 and ra-AZ8838 exhibited a concentration-dependent inhibition of NFκB-transcriptional activity when cells were stimulated with trypsin and gave IC$_{50}$ values of 0.54 and 1 μM respectively, n=5. YPT-1 had no inhibitory effect upon the trypsin response and an IC$_{50}$ value could not be calculated.

a)

DMSO	-	-	+	+	-	-	-	-	-	-
YPT-1 (µM)	-	-	-	-	0.1	0.3	1	3	10	20
Trypsin (100 nM)	-	+	-	+	+	+	+	+	+	+

b)

DMSO	-	-	+	+	-	-	-	-	-	-	-	-	-	-
YPT-2 (µM)	-	-	-	-	20	0.003	0.01	0.03	0.1	0.3	1	3	10	20
Trypsin (100 nM)	-	+	-	+	-	+	+	+	+	+	+	+	+	+

c)

DMSO	-	-	+	+	-	-	-	-	-	-	-	-	-	-
ra-AZ8838 (µM)	-	-	-	-	20	0.003	0.01	0.03	0.1	0.3	1	3	10	20
Trypsin (100 nM)	-	+	-	+	-	+	+	+	+	+	+	+	+	+
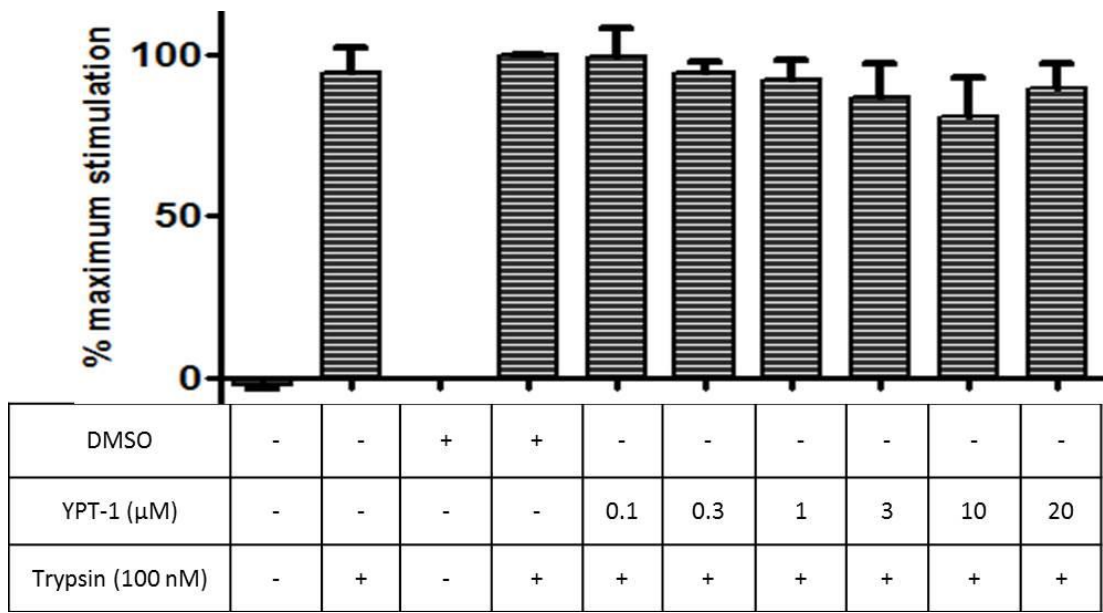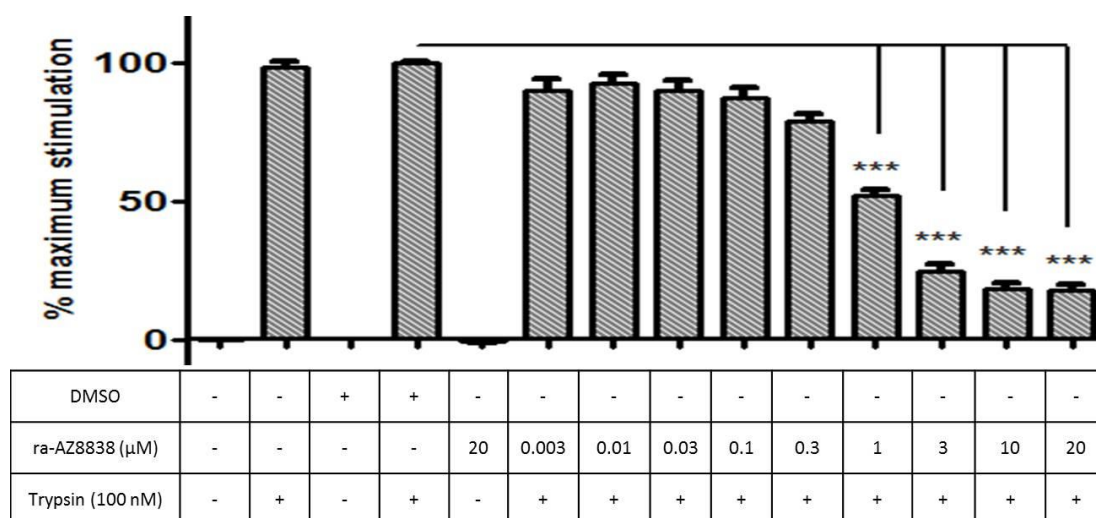
Figure 4. 3 The effect of YPT-1, YPT-2 and ra-AZ8838 on trypsin-stimulated NFκB transcriptional activity

NFκB-reporter cells were grown to confluency and rendered quiescent for 18 hours prior to pre-incubated with various concentrations of a) YPT-1, b) YPT-2 and c) ra-AZ8838 for 1 hour. The cells were then stimulated with 100 nM trypsin for a further 4 hours. Cell lysates were assayed for luciferase activity as previously described (section 2.3). The data shown are expressed as % maximum stimulation and each value represents n=5 except YPT-1 =4. Statistical analysis was performed using one way ANOVA, with Dunnett's post-test comparison. ***p<0.0001 compared to DMSO plus trypsin.
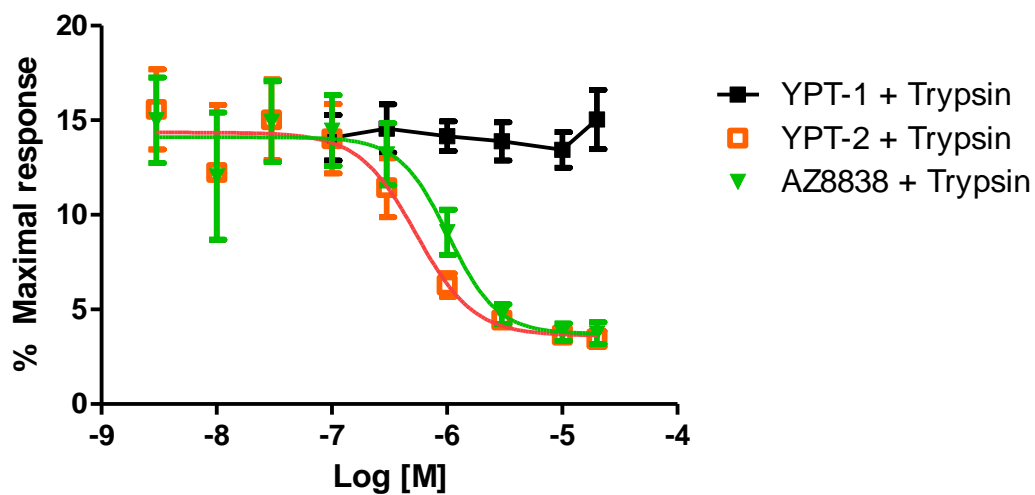
Figure 4. 4 IC$_{50}$ values for AZ compounds against trypsin-stimulated NFκB transcriptional activity in NFκB reporter cells

IC$_{50}$ curves from ra-AZ8838, YPT-1 and YPT-2 were generated by fitting data to a Sigmoidal non-linear regression curve (variable slope). Each value represents the mean ± SEM of five independent experiments for YPT-2 and ra-AZ8838 and three independent experiments for YPT-1.

4.2.3 Effect of AZ8838 compounds on GB88 stimulated gene transcription in NFκB-Reporter cells

Having established in the previous chapter that GB88 has partial agonist properties, the effect of the AZ compounds on stimulation by GB88 was examined. The effect of pre-treatment with YPT-1 prior to stimulation with GB88 on PAR2 mediated NFκB-driven gene transcription is shown in figure 4.5.a. Again, GB88 stimulated a significant increase in luciferase activity which was approximately 4 fold similar to that routinely observed for 2f-LIGRLO-NH$_2$. This response was not significantly affected by the presence of DMSO (Fold stimulation of GB88 = 3.92 ± 0.56 vs. GB88 & DMSO = 4.13 ± 0.50, n=4). Furthermore, no effect was observed on the response to GB88 even at the highest concentration of YPT-1 used.

The effect of pre-treatment with YPT-2 on GB88-stimulated NFκB-driven gene transcription is shown in figure 4.5.b. As before, YPT-2 had a small effect on basal NFκB gene transcription, which was not significant compared to the untreated control wells (% maximum stimulation: YPT-2 = -4.548 ± 1.60, DMSO= 0). Furthermore, GB88 stimulated a significant increase in luciferase activity as expected, with approximately 2.5 fold over basal, and this response was not affected by the presence of DMSO (Fold stimulation: GB88 = 2.46 ± 0.14, vs. DMSO & GB88 = 2.78 ± 0.24, n=4). However, following incubation with increasing concentrations of YPT-2, a significant inhibition of NFκB dependent gene transcription was observed between 1-20 µM, with full inhibition at 20 µM (% stimulation = -6.257 ± 4.493, n=4).

The effect of pre-treatment with ra-AZ8838 on GB88 stimulated luciferase activity was further examined in figure 4.5.c. Again, GB88 stimulated a significant increase in NFκB dependent gene transcription, with approximately 2.5 fold over basal, this response was not affected by the presence of DMSO (Fold stimulation: GB88 = 2.46 ± 0.14, vs. DMSO & GB88 = 2.78 ± 0.24, n=4). However, following incubation with increasing concentrations of ra-AZ8838, a corresponding concentration-dependent

reduction of NFκB gene transcription was observed between 0.3-20 μM, with approximately 99% inhibition at 20 μM (% stimulation = 0.939 ± 4.939, n=4).

IC$_{50}$ values for both YPT-2 and ra-AZ8838 were calculated as described previously and shown in (Figure 4.6). The IC$_{50}$ values for YPT-2 and ra-AZ8838 were 0.38 and 0.76 μM respectively, n=4. The compound YPT-1 had no effect on NFκB-driven gene transcription induced via GB88 even at the high concentrations employed and value was generated.

a)
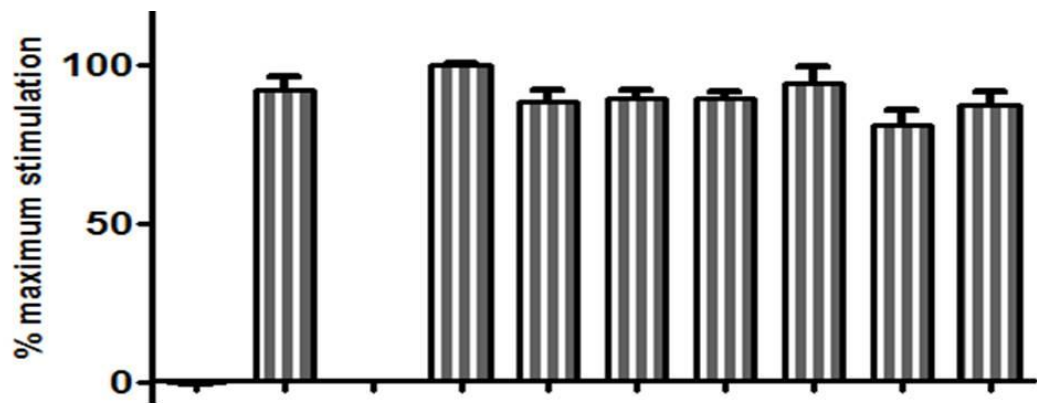
DMSO	-	-	+	+	-	-	-	-	-	-
YPT-1 (µM)	-	-	-	-	0.1	0.3	1	3	10	20
GB88 (20 µM)	-	+	-	+	+	+	+	+	+	+

b)

DMSO	-	-	+	+	-	-	-	-	-	-	-	-	-	-
YPT-2 (µM)	-	-	-	-	20	0.003	0.01	0.03	0.1	0.3	1	3	10	20
GB88 (20 µM)	-	+	-	+	-	+	+	+	+	+	+	+	+	+

c)
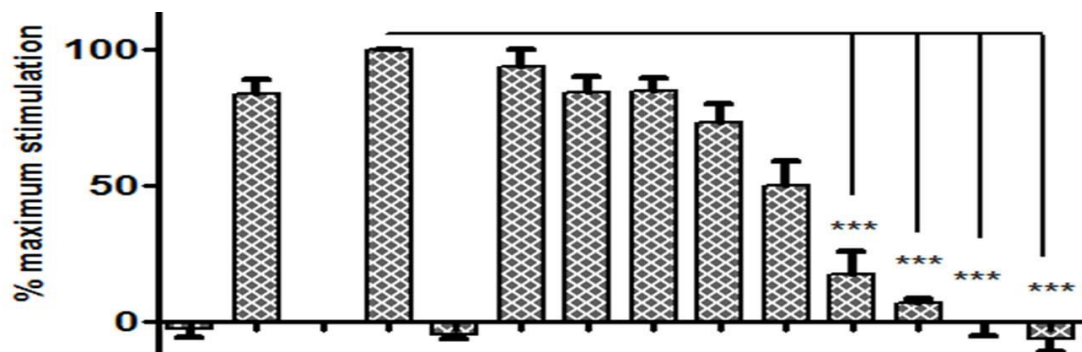
DMSO	-	-	+	+	-	-	-	-	-	-	-	-	-	-
ra-AZ8838 (µM)	-	-	-	-	20	0.003	0.01	0.03	0.1	0.3	1	3	10	20
GB88 (20 µM)	-	+	-	+	-	+	+	+	+	+	+	+	+	+
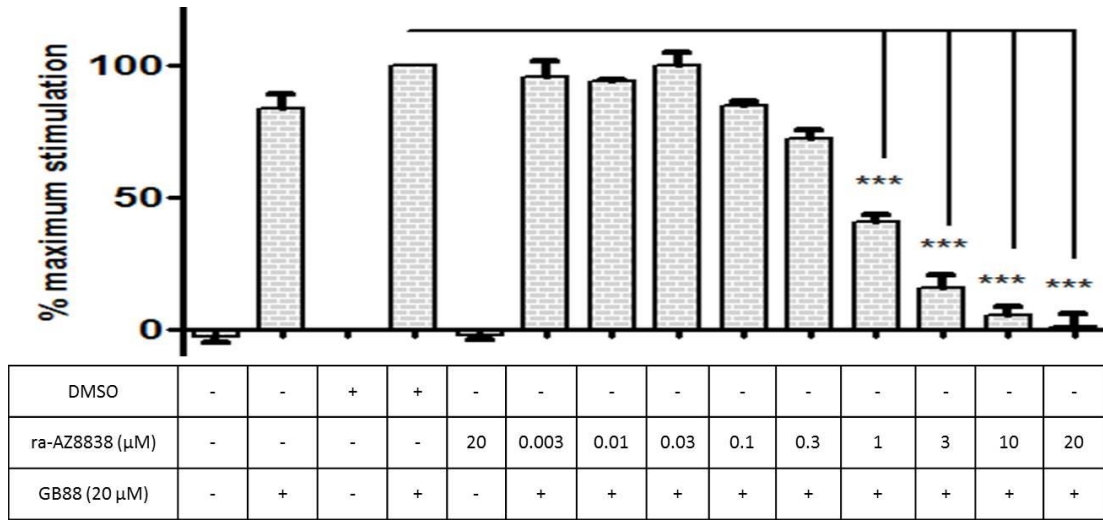
Figure 4. 5 The effect of YPT-1, YPT-2 and ra-AZ8838 on PAR2-mediated NFκB transcriptional activity stimulated by GB88

NFκB-reporter cells were grown to confluency and rendered quiescent for 18 hours prior to pre-treatment with various concentrations of a) YPT-1 b) YPT-2 and c) ra-AZ8838 for an hour. Cells were then stimulated with 20 µM GB88 for a further 4 hours. Cell lysates were measured for luciferase activity as previously described (section 2.3). The data shown are expressed as % maximum stimulation and each value represents n=4. Statistical analysis was performed using one way ANOVA, with Dunnett's post-test comparison. ***$p<0.0001$ compared to DMSO + GB88 stimulation.
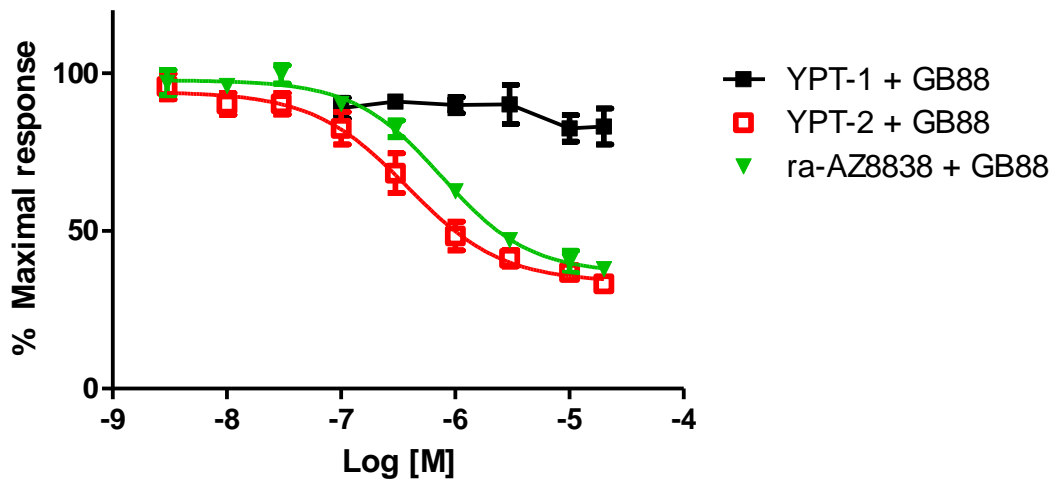
Figure 4. 6 IC$_{50}$ curves for AZ compounds against GB88 mediated NFκB dependent transcriptional activity

IC$_{50}$ curves for ra-AZ8838, YPT-1 and YPT-2 were generated by fitting data to a Sigmoidal non-linear regression curve (variable slope). Each value represents the mean ± SEM of four independent experiments.

4.3 Lack of effect of AZ compounds on TNFα -mediated NFκB transcriptional activity

In order to establish specificity in the inhibitory effect of the AZ compounds on PAR2 mediated NFκB transcriptional activity, these were tested against the response to TNFα. Initially a time course for TNFα stimulation was measured over a period of 8 hours in NFκB-Reporter cells as shown in figure 4.7. TNFα stimulates a time-dependent increase in luciferase activity, reaching a peak by 6 hours at approximately 5 fold over basal values (fold increase; 4.543 ± 0.817, n=4) as shown in figure 4.7 (a). NFκB-driven gene transcription was further evaluated using increasing concentrations of TNFα for a 6 hour stimulation period. TNFα gave a concentration-dependent increase in luciferase activity with maximal activation observed at 30 ng/ml (fold increase; 7.557 ± 2.073) as shown in figure 4.7 (b). A concentration of 10 ng/ml TNFα gave a moderate, mid-range stimulation of NFκB-transcriptional activity; therefore, it was decided to use this concentration for the next set of experiments.
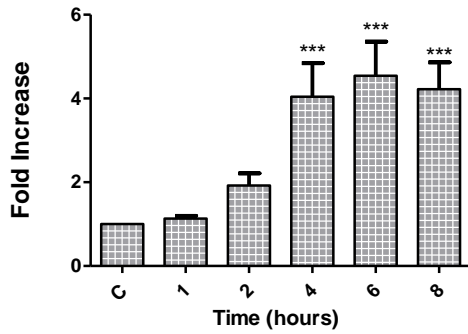
a)   b)
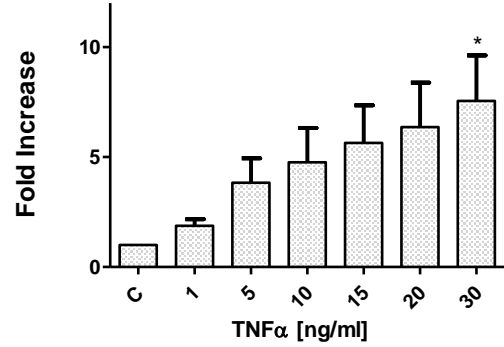
Figure 4. 7 The effect of TNFα on NFκB-driven transcriptional activation in NFκB-Reporter cells

NFκB-reporter cells were grown to confluency in 96-well black clear bottomed plates and cells rendered quiescent for 18 hours prior to (a) stimulation with TNFα for up to 8 hours and (b) increasing concentrations of TNFα from 1 to 30 ng/ml. Whole cell lysates were measured for luciferase activity as previously described (section 2.3). The data shown are expressed as fold increase and each value represents n=3. ***$p < 0.0001$ or *$p < 0.05$ compared to unstimulated cells.

4.3.1 The effect of AZ compounds on TNFα -mediated NFκB transcriptional activity

The effect of YPT-2 on TNFα stimulated luciferase activity in NFκB-reporter cells was shown in figure 4.8 (a). The compound YPT-2 alone had no effect on basal activity compared with untreated control (0.868 ± 0.035, n=4). Furthermore, as expected TNFα stimulated a significant increase in NFκB gene transcription, approximately 1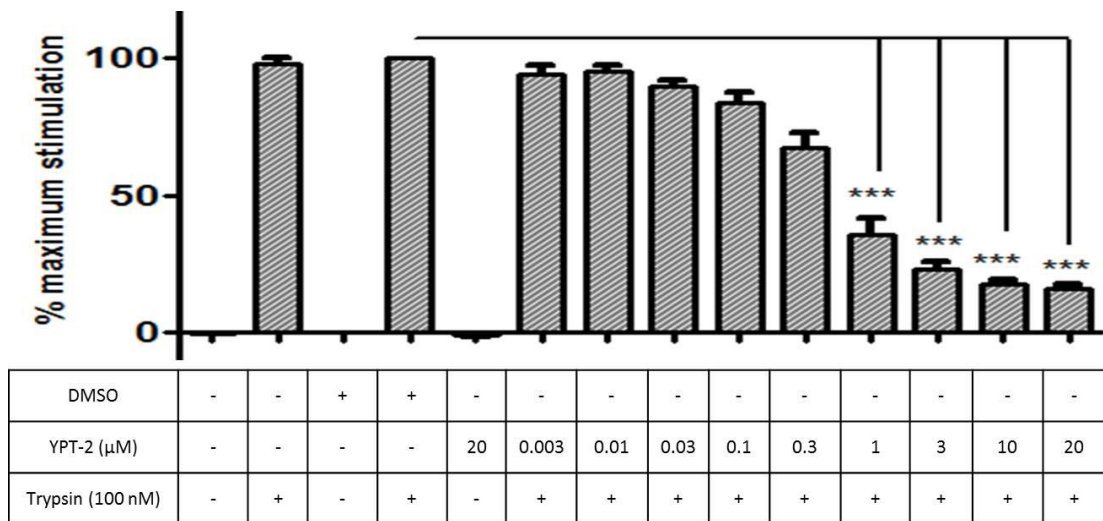2 fold, and this response was not affected by the presence of DMSO (fold response: TNFα = 11.377 ± 1.289, DMSO plus TNFα = 11.068 ± 0.840, n=4). Pre-treatment with high concentrations of YPT-2 (3, 10, 20 μM), prior to the addition of TNFα had a slight but non-significant effect on luciferase reporter activity (Fold increase = YPT-2 & TNFα = 9.783 ± 0.576, DMSO plus TNFα = 11.068 ± 0.840, n=4). By contrast, YPT-2 substantially inhibited 2f-LIGRLO-NH$_2$ and trypsin stimulated activity as outlined previously with substantial and significant inhibition at 10 and 20 μM. This result highlights the specificity of YPT-2 for PAR2 driven NFκB transcriptional activity.

Figure 4.8.(b) shows the effect of ra-AZ8838 on TNFα -mediated NFκB-driven gene transcription in NFκB-Reporter cells. The compound ra-AZ8838 had no effect on the basal response of NFκB gene transcription compared with the untreated control (0.825 ± 0.065, n=4). Furthermore, as observed previously TNFα stimulated a significant increase in NFκB gene transcription, and this response was not affected by the addition of DMSO (fold response: TNFα = 11.377 ± 1.289, DMSO & TNFα = 11.068 ± 0.840, n=4). Pre-treatment with higher concentrations of ra-AZ8838 (3, 10, 20 μM) prior to TNFα treatment had no effect on NFκB transcription activity (Fold stim: AZ8838 20 μM & TNFα = 10.195 ± 0.581, DMSO & TNFα = 11.068 ± 0.840, n=4). By contrast, ra-AZ8838 substantially inhibited 2f-LIGRLO-NH$_2$ and trypsin stimulated activity as outlined previously with substantial and significant inhibition at 10 and 20 μM of the compound. This confirms the specificity of AZ8838, even as a racemic mixture, for PAR2 driven NFκB transcriptional activity.

a)

DMSO	-	+	-	-	+	-	-	-	-	+	-	-		+	-	-
YPT-2 (µM)	-	-	20	-	-	3	10	20	-	-	10	20	-	-	10	20
TNFα (10 ng/ml)	-	-	-	+	+	+	+	+	-	-	-	-	-	-	-	-
2f-LIGRLO-NH$_2$ (0.3 µM)	-	-	-	-	-	-	-	-	+	+	+	+	-	-	-	-
Trypsin (100 nM)	-	-	-	-	-	-	-	-	-	-	-	-	+	+	+	+

b)

DMSO	-	+	-	-	+	-	-	-	-	+	-	-		+	-	-
ra-AZ8838 (µM)	-	-	20	-	-	3	10	20	-	-	10	20	-	-	10	20
TNFα (10 ng/ml)	-	-	-	+	+	+	+	+	-	-	-	-	-	-	-	-
2f-LIGRLO-NH$_2$ (0.3 µM)	-	-	-	-	-	-	-	-	+	+	+	+	-	-	-	-
Trypsin (100 nM)	-	-	-	-	-	-	-	-	-	-	-	-	+	+	+	+
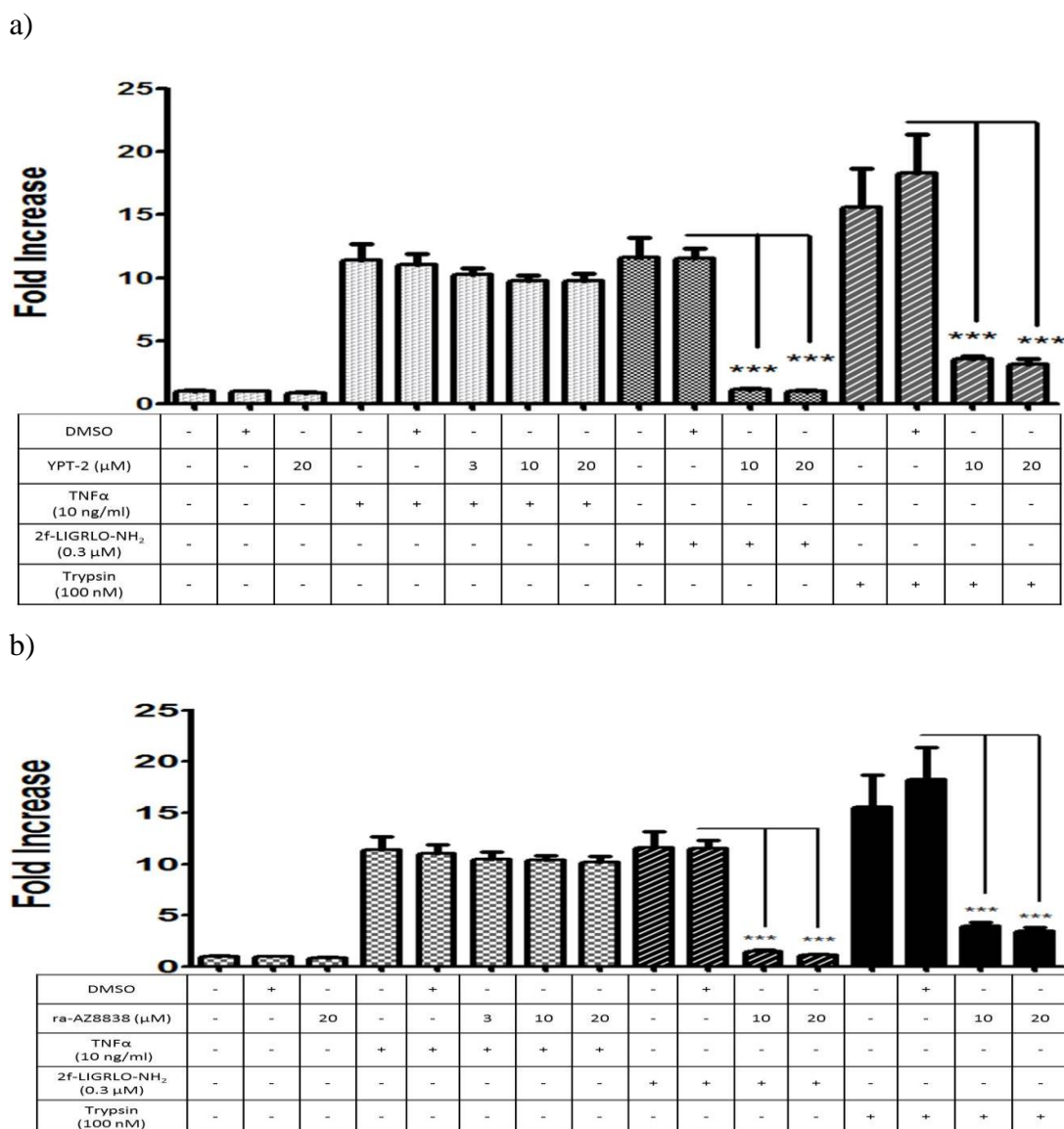
Figure 4. 8 The effect of YPT-2 and ra-AZ8838 on TNFα-stimulated transcriptional activity in NFκB-Reporter cells

NFκB-reporter cells were grown to confluency and rendered quiescent for 18 hours prior to pre-treatment with various concentrations of a) YPT-2 and b) ra-AZ8838 for 1 hour. The cells were then stimulated with 10 ng/ml TNFα for a further 6 hours, 0.3µM 2f-LIGRLO-NH$_2$, or 100 nM trypsin for 4 hours. Cell lysates were measured for luciferase activity as previously described (section 2.3). The data shown are expressed as fold over unstimulated basal and each value represents n=4. Statistical analysis was performed using one way ANOVA, with Dunnett's post-test comparison. ***$p < 0.0001$ compared to compounds plus 2f-LIGRLO-NH$_2$ or trypsin.

4.4 The effect of AZ compounds on PAR2 mediated phosphorylation of ERK in NFκB-Reporter cells

Having established a clear inhibition of PAR2 mediated reporter activity in NFκB-Reporter cells by YPT-2 and ra-AZ8838, the effects of the compounds on ERK phosphorylation was examined in the same cell line. Initially, the effect of the PAR2 agonist 2f-LIGRLO-NH$_2$ on the phosphorylation of ERK1/2 was characterised for the kinetics of activation and concentration -dependent responses (Figure 4.9). A time course is illustrated in figure 4.9 (a). 2f-LIGRLO-NH$_2$ induced ERK phosphorylation which peaked by 5 minutes at approximately 8 fold over basal (7.780 ± 0.518 fold of basal control) before gradually decreasing at 15 minutes to approximately 3 fold (3.290 ± 1.010). Using increasing concentrations of 2f-LIGRLO-NH$_2$, from 0.01 μM to 10 μM, a concentration-dependent increase in ERK phosphorylation was established with a maximal response obtained at 3 μM (figure 4.9 (b).

The time course of trypsin stimulated phosphorylation of ERK1/2 is illustrated in figure 4.9 (c). The response peaked at 5 minutes with an approximate 2.5 fold increase over basal (fold increase = 2.310 ± 0.189) before gradually decreasing between 15-90 minutes towards basal levels (1.073 ± 0.222 fold), shown in figure 4.9 (c). Using increasing concentrations of trypsin, from 1 nM up to 1000 nM, a concentration-dependent increase in ERK1/2 phosphorylation was observed with a maximal response obtained at 500 nM of trypsin, over a 5 minutes period, figure 4.9 (d).

Similarly, phosphorylation of ERK was observed using 10 μM of GB88 again peaking at 5 minutes at approximately 3 fold over basal control (2.623 ± 0.534 fold of DMSO level). This then gradually decreased at 15 minutes, reaching basal levels by 90 minutes (1.177 ± 0.110 fold of DMSO level), figure 4.9 (e). Using increasing concentrations of GB88, from 0.1 μM up to 20 μM a concentration-dependent increase in ERK1/2 phosphorylation was observed with a maximal response using 3-20μM of GB88, over a 5 minute time period, figure 4.9 (f).

Figure 4. 9 PAR2-mediated phosphorylation of ERK by different agonists in NFκB-Reporter cells

Cells were rendered quiescent for 18 hours prior to stimulation with (a) 10 μM 2f-LIGRLO-NH$_2$, (c) 100 nM Trypsin, and (e) 10 μM GB88 for the times indicated or with increasing concentrations of (b) 2f-LIGRLO-NH$_2$ (d) Trypsin and (f) GB88 for 5 minutes. Whole cell lysates were prepared as previously described (section 2.41), and assessed by Western blotting (section 2.4.2). Each blot is representative of n=3 for 2f-LIGRLO-NH$_2$ & trypsin, and n=1 for GB88 and quantified by densitometry and expressed as mean ± s.e.m (fold stimulation). ***$p < 0.001$ compared to control (untreated cells).

4.4.1 The effect of AZ compounds on 2f-LIGRLO-NH$_2$ mediated phosphorylation of ERK in NFκB-Reporter cells

The effect of pre-treatment with YPT-2 on 2f-LIGRLO-NH$_2$-stimulated ERK1/2 phosphorylation in NFκB-Reporter cells is shown in figure 4.10 (a). The compound YPT-2 had no effect on basal levels of ERK when compared to control (fold stimulation: DMSO & YPT-2 = 0.967 ± 0.293, n=3). Furthermore, 2f-LIGRLO-NH$_2$ stimulated a significant increase in phosphorylation of ERK, this response was not affected by the presence of DMSO (fold stimulation: 2f-LIGRLO-NH$_2$ = 3.560 ± 0.201, DMSO plus 2f-LIGRLO-NH$_2$ = 3.317 ± 0.439, n=3). However, following incubation with increasing concentrations of YPT-2, a corresponding concentration-dependent inhibition was observed with a significant effect recorded at 10 and 20 µM (fold stimulation at 20 µM = 1.097 ± 0.147, n=3).

The effect of ra-AZ8838 for 1 hour prior to stimulation with 2f-LIGRLO-NH$_2$ on ERK1/2 phosphorylation in NFκB-Reporter cells is shown in figure 4.10 (b). Similarly to YPT-2, AZ8838 had no effect on the basal level of ERK when compared to unstimulated controls (fold stim: DMSO + AZ = 0.860 ± 0.125, n=3). Furthermore, 2f-LIGRLO-NH$_2$ stimulated a significant increase in the phosphorylation of ERK1/2, and this was only slightly affected by DMSO (fold stim: 2f-LIGRLO-NH$_2$ = 4.220 ± 0.357, DMSO & 2f-LIGRLO-NH$_2$ = 3.797 ± 0.510, n=3). However, following incubation with increasing concentrations of ra-AZ8838, a marked inhibition of ERK1/2 phosphorylation was observed with significant inhibition using 10 and 20 µM of the compound (fold stim: AZ, 20 µM = 1.563 ± 0.381, n=3).

a)

b)
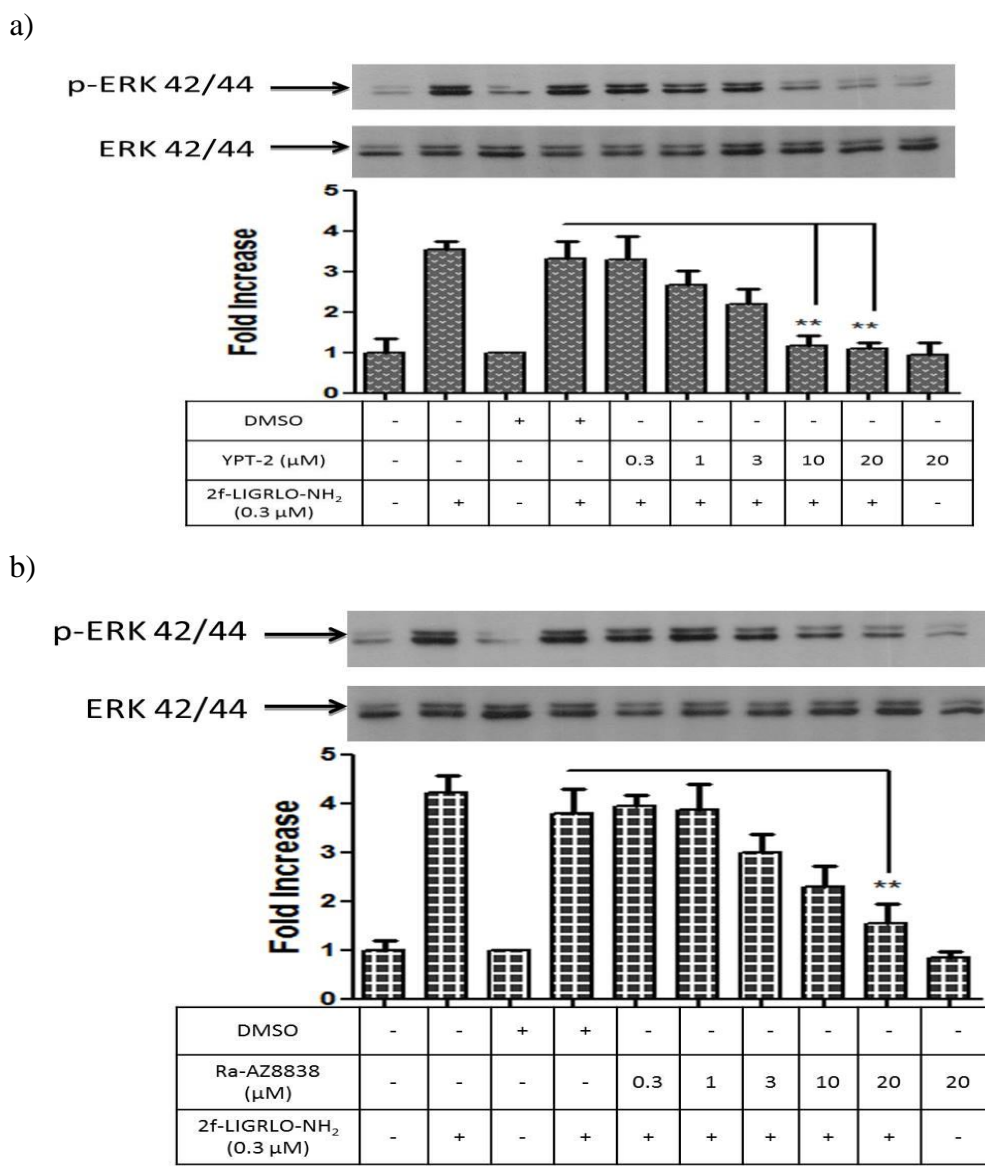
Figure 4. 10 The effect of YPT-2 and ra-AZ8838 on 2f-LIGRLO-NH$_2$ mediated ERK phosphorylation in NFκB-Reporter cells

NFκB-Reporter cells were rendered quiescent for 18 hours prior to pre-treatment with increasing concentrations of (a) YPT-2 and (b) ra-AZ8838 for 1 hour. Cells were then stimulated with 0.3 μM 2f-LIGRLO-NH$_2$ for 5 minutes. Whole cell lysates were prepared as previously described (section 2.41), and assessed by Western blotting (section 2.4.2). Each value represents the mean ± S.E.M of three independent experiments. Statistical analysis was performed using one way ANOVA, with Dunnett's post-test comparison. **p<0.01 compared to 2f-LIGRLO-NH$_2$ plus DMSO.

As an additional control, cells were pre-treated with YPT-1 for 1 hour prior to the addition of different agonists; 2f-LIGRLO-NH$_2$, trypsin, and GB88, for 5 minutes as shown in figure 4.11. The compound YPT-1 had no effect on basal levels of ERK when compared with untreated cells. Each agonist 2f-LIGRLO-NH$_2$, trypsin, and GB88 increased ERK phosphorylation, and this response was unaffected by DMSO or high concentrations of YPT-1 (20 μM) as observed in figure 4.11.

IC$_{50}$ values for both YPT-2 and ra-AZ8838 on the phosphorylation of ERK MAPK were calculated as described previously and shown in Figure 4.12. The IC$_{50}$ values for YPT-2 and ra-AZ8838 were 3 and 12 μM respectively, n=3.

DMSO	-	+	-	-	+	-	-	+		-	+	-
YPT-1 (20 µM)	-	-	+	-	-	+	-	-	+	-	-	+
2f-LIGRLO-NH$_2$ (0.3 µM)	-	-	-	+	+	+	-	-	-	-	-	-
Trypsin (30 nM)	-	-	-	-	-	-	+	+	+	-	-	-
GB88 (10 µM)	-	-	-	-	-	-	-	-	-	+	+	+
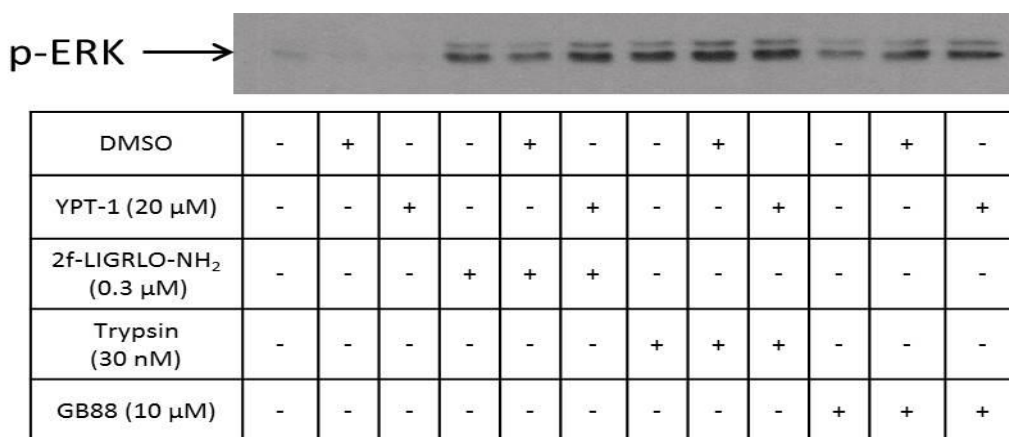
Figure 4. 11 Lack of effect of YPT-1 on PAR2 mediated ERK phosphorylation in NFκB-Reporter cells

Cells were rendered quiescent for 18 hours prior to pre-treatment with YPT-1 for 1 hour, followed by stimulation with the agonists; 2f-LIGRLO-NH$_2$, trypsin, or GB88 for 5 minutes. Whole cell lysates were prepared as previously described (section 2.41), and by SDS.PAGE (section 2.4.2). n=1
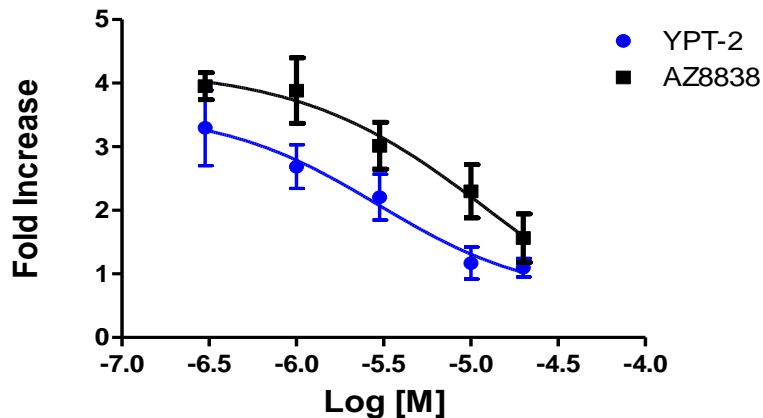
Figure 4. 12 IC$_{50}$ values for YPT-2 and ra-AZ8838 compounds against 2f-LIGRLO-NH$_2$ stimulated ERK phosphorylation in NFκB-Reporter cells

IC$_{50}$ curves from AZ8838 and YPT-2 were generated by fitting data to a Sigmoidal non-linear regression curve (variable slope). Each value represents the mean ± SEM of four independent experiments for YPT-2 and ra-AZ8838.

4.5 PAR2-mediated phosphorylation of stress-activated protein kinase p38 (p38 MAPK) in NFκB-Reporter cells

Having established the effects of the AZ compound on ERK activation, p38 MAPK was also examined. This was possible because the relatively higher expression of PAR2 in the reporter cells allowed p38 MAPK to be activated as demonstrated in figure 4.13. Initially the phosphorylation of p38 MAPK was measured over a 90 minute time period for 2f-LIGRLO-NH$_2$. 2f-LIGRLO-NH$_2$-induced p38 MAPK phosphorylation peaking between 15 and 30 minutes with approximately 8 fold stimulation at 30 minutes (8.590 ± 2.179 fold of control basal, n=3) figure 4.13 (a). This response decreased towards basal levels by 90 minutes. Therefore, the 30 minute time point was used in the next set of experiments as shown in figure 4.13 (b). Using increasing concentrations of 2f-LIGRLO-NH$_2$ from 0.01 to 10 μM, a concentration-dependent increase in p38 MAPK phosphorylation was observed with a maximal response achieved using 10μM of 2f-LIGRLO-NH$_2$ (8.900 ± 0.437 fold basal, n=3).

Figure 4.13 (c) illustrates trypsin stimulated PAR2 activation of p38 MAPK. Trypsin stimulated an increase in p38 MAP kinase phosphorylation which peaked between 15 and 30 minutes with an approximate 4.5 fold increase (4.323 ± 0.887 fold over basal control, n=3) figure 4.13 (c). Using increasing concentrations of trypsin from 1 to 1000 nM over 30 minutes, a concentration-dependent increase in p38 MAPK phosphorylation was observed with a maximal response at 300 nM (6.983 ± 0.638 fold basal, n=3) as shown in figure 4.13 (d).

The effect of GB88 on p38 MAPK phosphorylation is demonstrated in figure 4.13 (e). GB88 induced p38 MAP kinase phosphorylation with a maximum response observed at 30 minutes giving a 4 fold increase (4.493 ± 0.619 fold of DMSO level, n=3) (figure 4.13 (e)). This response decreased towards basal levels by 90 minutes. Therefore, 30 minutes was used in the next set of experiments. Using increasing concentrations of GB88 from 0.1 to 20 μM, a concentration-dependent increase in p38 MAPK phosphorylation was observed with a maximal response achieved using 20 μM 2f-LIGRLO-NH$_2$ (2.210 ± 0.110 fold basal, n=3), as shown in figure 4.13 (f).
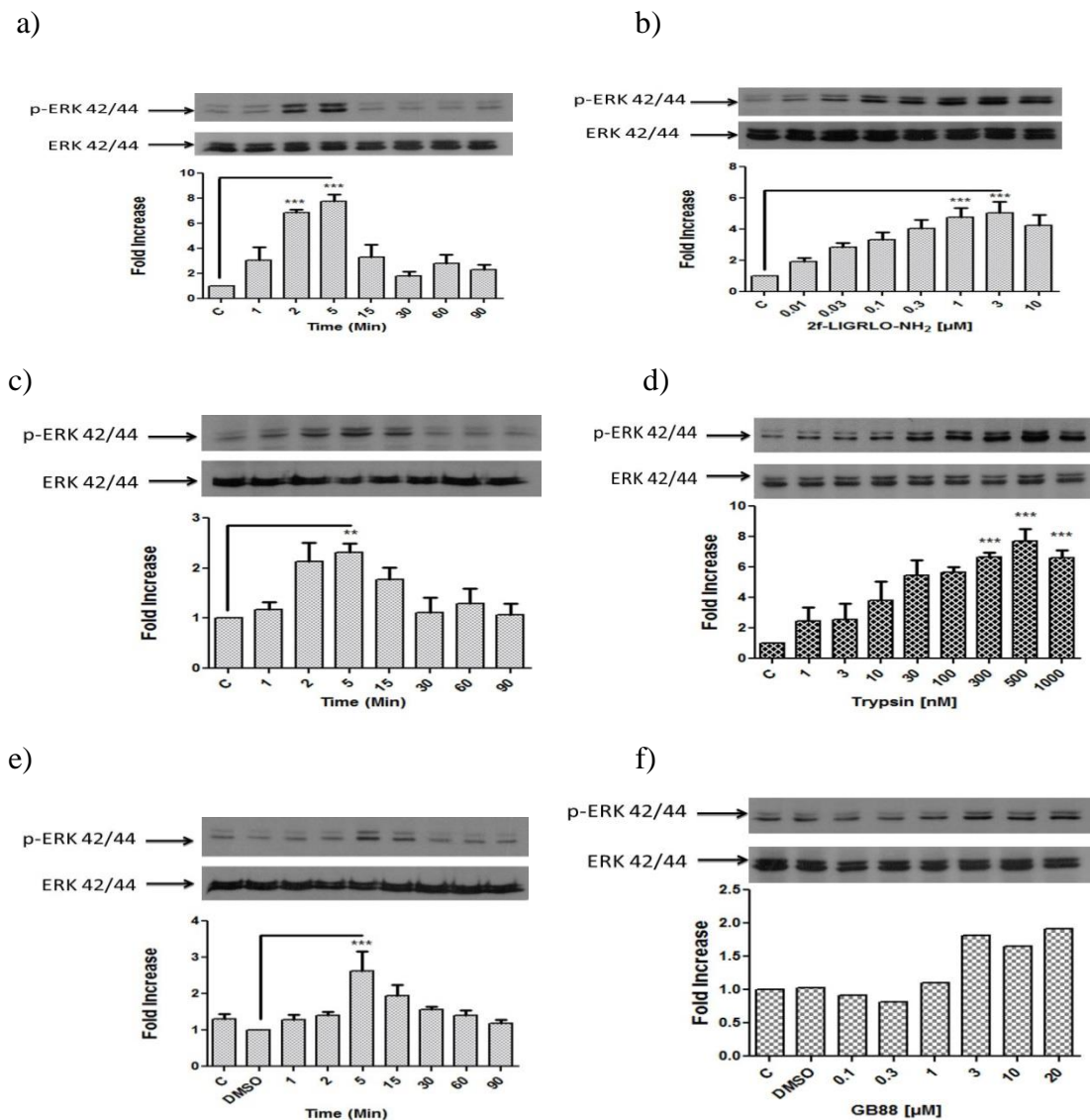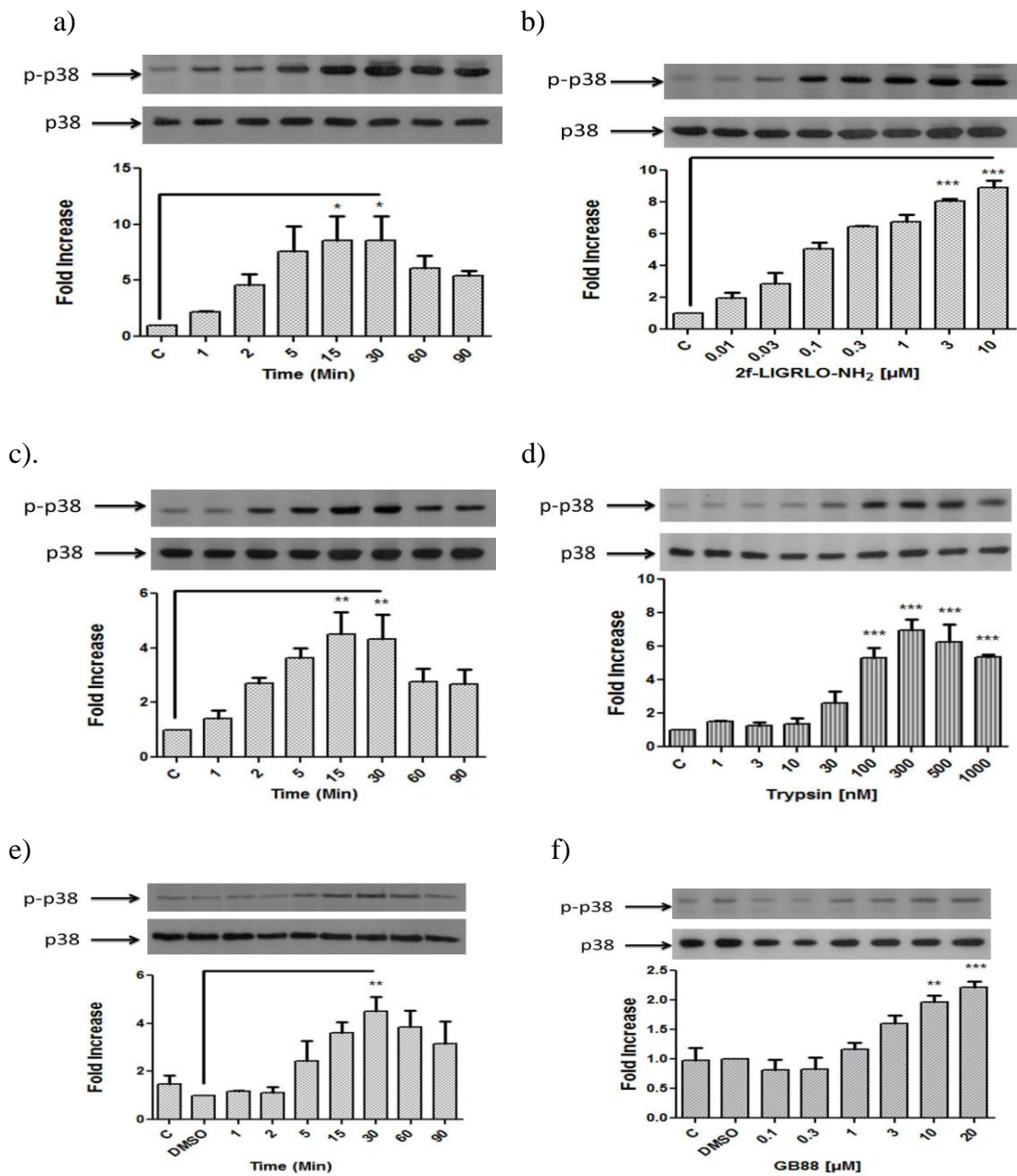
Figure 4. 13 PAR2-mediated phosphorylation of p38 MAPK in NFκB-Reporter cells

Cells were rendered quiescent for 18 hours prior to stimulation with (a) 1 μM 2f-LIGRLO-NH$_2$ (c) 100 nM trypsin (e) 10 μM GB88 for the times indicated or with increasing concentrations of (b) 2f-LIGRLO-NH$_2$ (d) trypsin (f) GB88 for 30 minutes. Whole cell lysates were prepared as previously described (section 2.41), and assessed by Western blotting (section 2.4.2). Each Blot is representative of n=3, quantified by densitometry and expressed as mean ± s.e.m (fold stimulation).

4.5.1 The effect of AZ-compounds on 2f-LIGRLO-NH$_2$ mediated phosphorylation of p38 MAPK in NFκB-Reporter cells

The effect of pre-treatment with YPT-2 for 1 hour prior to the addition of 2f-LIGRLO-NH$_2$ on ERK phosphorylation in NFκB-Reporter cells is shown in figure 4.14 (a). The compound YPT-2 had a slight but not significant effect on the basal levels of phosphorylated p38 MAPK when compared with the untreated control (fold stimulation = 0.543 ± 0.164, vs. DMSO control n=3). Furthermore, 2f-LIGRLO-NH$_2$ stimulated a significant increase in phosphorylation of p38 MAPK, this response was not affected by the presence of DMSO (fold stimulation: 2f-LIGRLO-NH$_2$ = 3.503 ± 0.456, DMSO plus 2f-LIGRLO-NH$_2$ = 3.217 ± 0.312, n=3). However, following incubation with increasing concentrations of YPT-2, a corresponding concentration-dependent decrease in the phosphorylation of p38 MAPK was observed between 1-20 μM (fold stimulation at 20 μM = 1.190 ± 0.154, n=3).

The effect of ra-AZ8838 on 2f-LIGRLO-NH$_2$ stimulation of p38 MAP kinase phosphorylation in NFκB-Reporter cells is shown in figure 4.14 (b). Again, ra-AZ8838 had no effect on the basal levels of p38 MAPK when compared with untreated control (fold stimulation relative to DMSO level 0.547 ± 0.163, n=3). 2f-LIGRLO-NH$_2$ also stimulated a significant increase in phosphorylation of p38 MAPK of approximately 2 fold (fold stimulation: 2f-LIGRLO-NH$_2$ = 2.003 ± 0.128, n=3). However, following incubation with ra-AZ8838, a concentration-dependent decrease in the phosphorylation of p38 MAPK was observed between 1-20 μM with significant inhibition at 20 μM (fold stimulation at 20 μM = 0.670 ± 0.091, n=3).
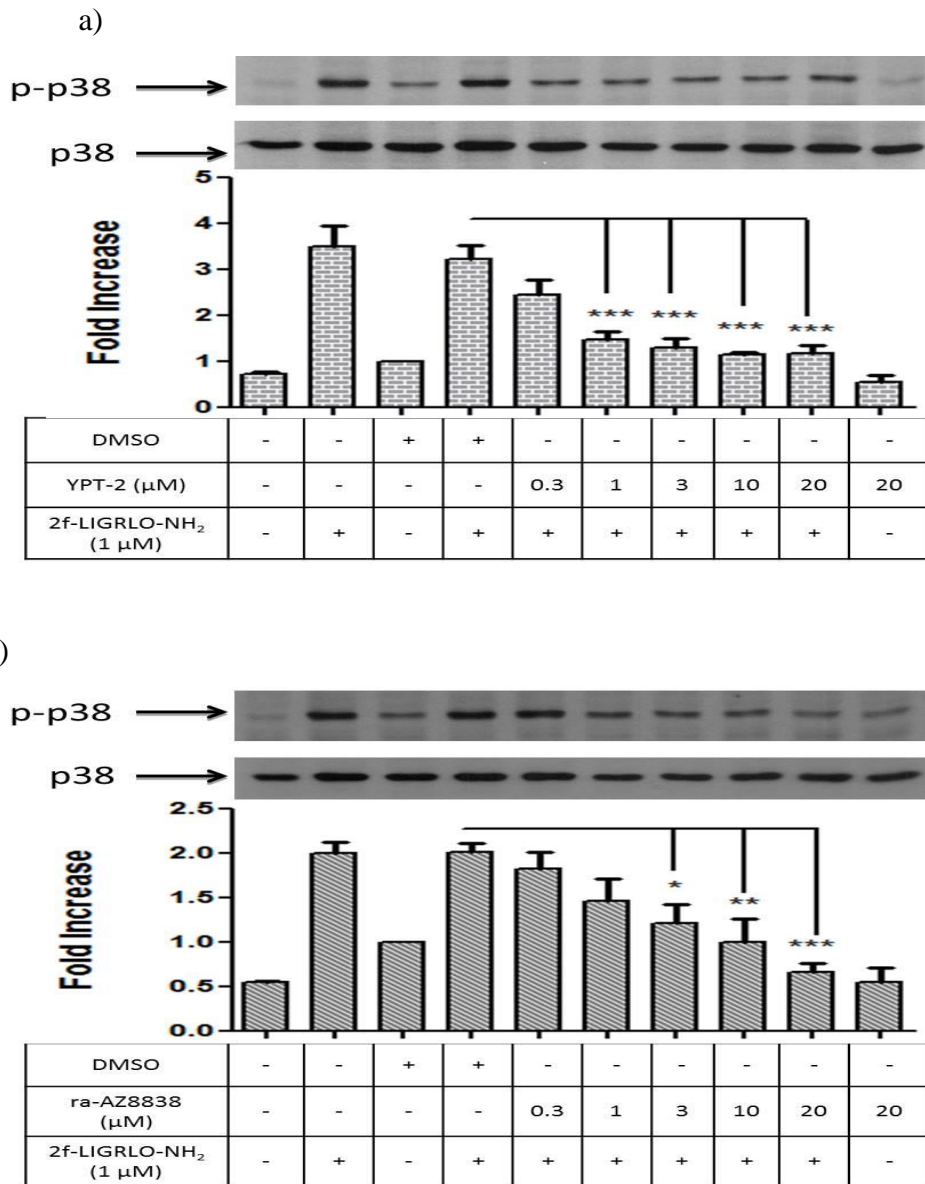
Figure 4. 14 The effect of YPT-2 and ra-AZ8838 on p38 MAPK phosphorylation stimulated by 2f-LIGRLO-NH₂ in NFκB-Reporter cells

Cells were rendered quiescent for 18 hours prior to pre-incubation with increasing concentrations of (a) YPT-2 (b) ra-AZ8838 for 1 hour. The cells were then stimulated with 1 μM 2f-LIGRLO-NH₂ for a further 30 minutes. Whole cell lysates were prepared as previously described (section 2.41), and assessed by Western blotting (section 2.4.2). Each value represents the mean ± S.E.M of three independent experiments. Statistical analysis employed one way ANOVA, with Dunnett's post-test comparison. ***p<0.0001 compared to DMSO + 2f-LIGRLO-NH₂ stimulation.

4.6 TNFα stimulated NFκB pathway activation in NFκB-Reporter cells

Next, the activation of the classical IKKβ -mediated NFκB pathway was investigated upstream of reporter output. This was achieved by measuring the phosphorylation of p65 NFκB and the degradation of IκBα in NFκB-Reporter cells as shown in figure 4.15 (a). Initially, in order to characterise the system, cells were stimulated with TNFα over a 90 minute time course and cellular IκBα degradation was observed, starting at 5 minutes and reaching a maximum after 30 minutes (0.203 ± 0.035 of basal expression) compared with untreated cells. Levels gradually returned towards basal levels by 90 minutes, figure 4.15 (c). Furthermore, as shown in figure 4.15 (b), the phosphorylation of p65 NFκB was also stimulated in response to TNFα, this activation was apparent at 5 minutes and reached a maximum between $15 - 30$ minutes (4.035 ± 1.082 of basal control).

In figure 4.16 TNFα demonstrated a concentration-dependent increase in the phosphorylation of p65 and degradation of IκBα with a maximum response achieved at 30 ng/ml (8.995 ± 0.055 fold basal and 0.320 ± 0.160 of fold expression), as shown in figure 4.16 (b-c). From these data 10 ng/ml of TNFα was used as an effective concentration for further experiments.

a)

| TNFa (10ng/ml) | - | + | + | + | + | + | + | + |
| Time (min) | - | 1 | 2 | 5 | 15 | 30 | 60 | 90 |

b)

| TNFa (10ng/ml) | - | + | + | + | + | + | + | + |
| Time (min) | - | 1 | 2 | 5 | 15 | 30 | 60 | 90 |

c)

| TNFa (10ng/ml) | - | + | + | + | + | + | + | + |
| Time (min) | - | 1 | 2 | 5 | 15 | 30 | 60 | 90 |
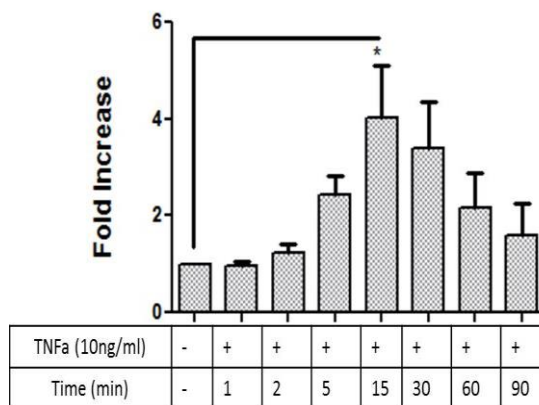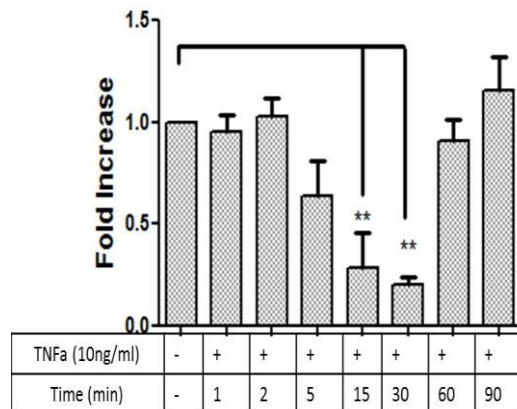
Figure 4. 15 TNFα induced phosphorylation of p65 and IκBα degradation in NFκB-Reporter cells

Cells were rendered quiescent for 18 hours prior to stimulation with 10 ng/ml of TNFα for the times indicated. (a) The blots for p-p65 NFκB (65kDa) and IKBα losing (37 kDa) and GAPDH (37 kDa) was used as a loading control for the times indicated. (b) Blots were assessed by semi-quantitative densitometry and results expressed as fold stimulation relative for p-p65 and (c) for IκBα degradation. Whole cell lysates were prepared as previously described (section 2.41), and assessed by Western blotting (section 2.4.2). Each Blot is representative of n=3, expressed as mean ± s.e.m (fold stimulation).
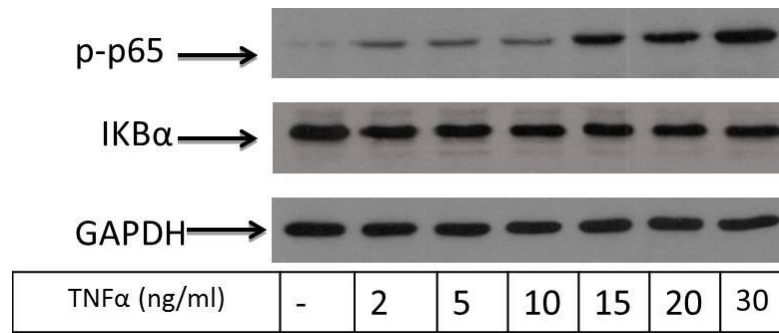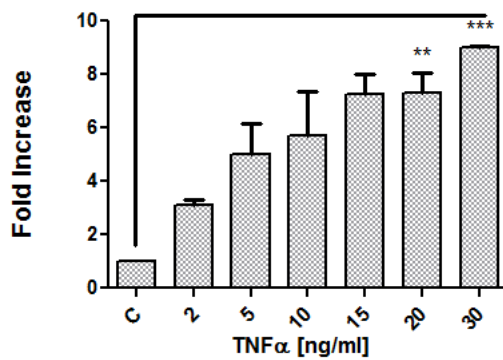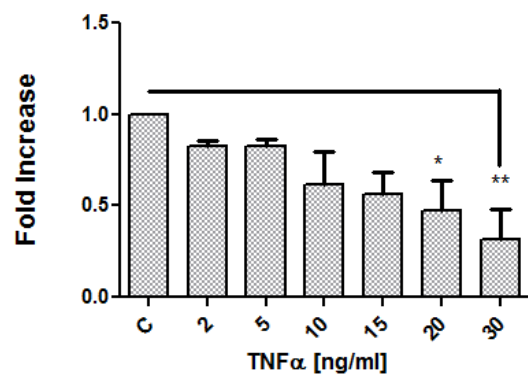
a)

| TNFα (ng/ml) | - | 2 | 5 | 10 | 15 | 20 | 30 |

b)   c)

Figure 4. 16 TNFα-mediated phosphorylation of p65 NFκB and degradation of IκBα in NFκB-Reporter cells

Cells were rendered quiescent for 18 hours prior to the addition of different concentrations of TNFα for 30 minutes. (a) The blots for p-p65 NFκB (65kDa) and IκBα degradation (37 kDa) and GAPDH (37 kDa) was used as a loading control at pointed time. (b) Blots were assessed by semi-quantitative densitometry and results expressed as fold stimulation relative for p-p65 and (c) IκBα loss. Whole cell lysates were prepared as previously described (section 2.41), and separated by SDS.PAGE (section 2.4.2). Each blot is representative of n=3 and quantified by densitometry and expressed as mean ± s.e.m (fold stimulation).

Figure 4.17 shows the effect of 2f-LIGRLO-NH$_2$ on the phosphorylation of p65 NFκB and degradation of IκBα in NFκB-Reporter cells. 2f-LIGRLO-NH$_2$ stimulated a time dependent increase in p65 phosphorylation, which peaked at 15 minutes at approximately 4 fold of basal values (4.100 ± 0.476 of basal control), and remained at this level for the rest of the time course, figure 4.17 (b). In contrast, the peptide produced a minor decrease in cellular IκBα degradation, which was maximal by 30 minutes (0.450 ± 0.046 of basal expression) compared to untreated cells. Levels gradually returned to basal levels by 90 minutes, figure 4.17 (c).

The effect of ra-AZ8838 on PAR2 mediated phosphorylation of p65 NFκB in NFκB-Reporter cells is shown in figure 4.18. As expected, the compound ra-AZ8838 had no effect on the basal levels when compared with untreated control. 2f-LIGRLO-NH$_2$ stimulated a marked increase in phosphorylation of p65; this response was not affected by the presence of DMSO. Following incubation with increasing concentrations of ra-AZ8838, a corresponding concentration-dependent decrease in the phosphorylation of p65 was observed between 3-20 μM. In contrast, there was no effect upon TNFα stimulation. YPT-2 was not examined due to time-constraints.

a)

2f-LIGRLO-NH$_2$ (1µM)	-	+	+	+	+	+	+	+
Time (min)	-	1	2	5	15	30	60	90

b)   c)

2f-LIGRLO-NH$_2$ (1µM)	-	+	+	+	+	+	+	+
Time (min)	-	1	2	5	15	30	60	90

2f-LIGRLO-NH$_2$ (1µM)	-	+	+	+	+	+	+	+
Time (min)	-	1	2	5	15	30	60	90
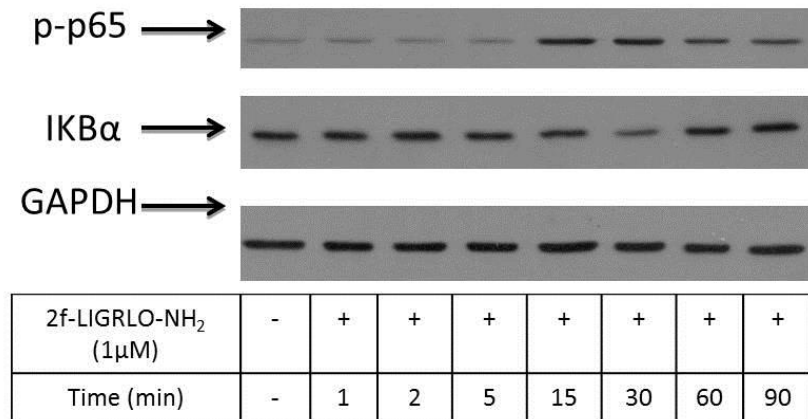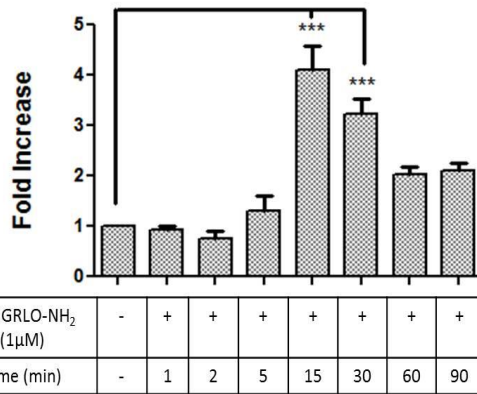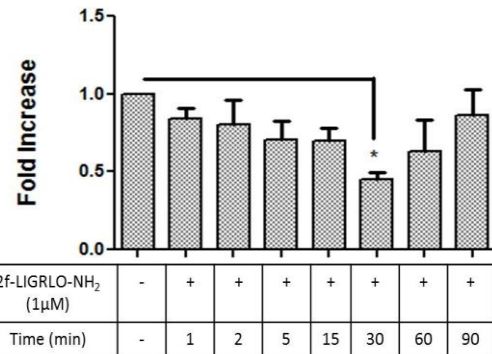
Figure 4. 17 2f-LIGRLO-NH$_2$ induced phosphorylation of p65 and IκBα degradation in NFκB-Reporter cells

Cells were quiescent for 18 hours prior to stimulation with 1µM of 2f-LIGRLO-NH$_2$ for the times indicated. (a) Samples were blotted for p-p65 NFκB (65kDa) and IKBα degradation (37 kDa) and GAPDH (37 kDa) was used as a loading control. (b) Blots were assessed by semi-quantitative densitometry and results expressed as fold stimulation. Whole cell lysates were prepared as previously described (section 2.41), and assessed by Western blotting. Each Blot is representative of n=3 and semi-quantified by densitometry and expressed as mean ± s.e.m (fold stimulation).

p-p65 →													
DMSO	-	+	-	-	+	-	-	-	-	+	-	-	-
ra-AZ8838 (µM)	-	-	20	-	-	3	10	20	-	-	3	10	20
2f-LIGRLO-NH₂ (0.3 µM)	-	-	-	+	+	+	+	+	-	-	-	-	-
TNFα (10 ng/ml)	-	-	-	-	-	-	-	-	+	+	+	+	+
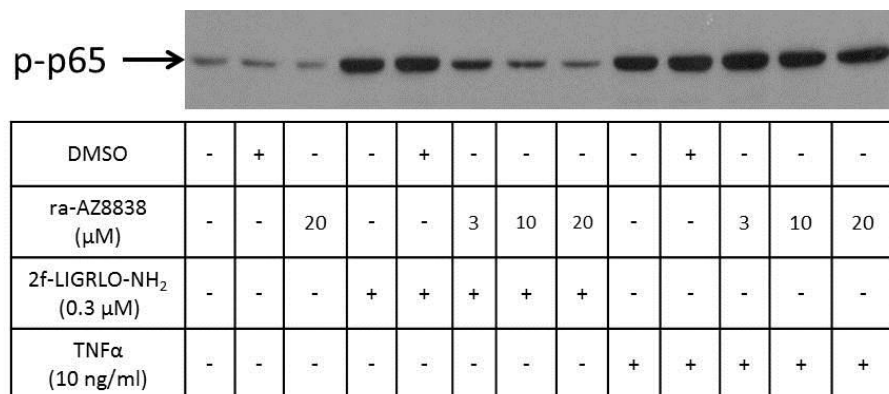
Figure 4. 18 The effect of ra-AZ8838 on 2f-LIGRLO-NH$_2$ stimulated phosphorylation of p65 in NFκB-Reporter cells
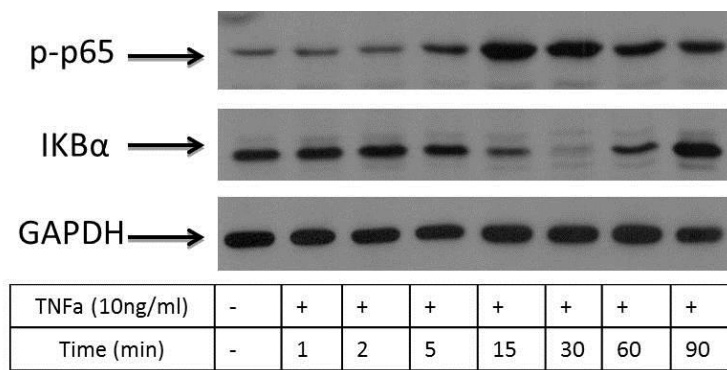
Cells were rendered quiescent for 18 hours prior to pre-incubation with increasing concentrations of ra-AZ8838 for 1 hour. The cells were then stimulated with 0.3 µM 2f-LIGRLO-NH$_2$ or 10 ng/ml TNFα for 30 minutes. Whole cell lysates were prepared as previously described (section 2.41), and assessed by Western blotting (section 2.4.2). The result represents N=2.

4.7 The effect of AZ compounds on PAR2 mediated phosphorylation of ERK in HEK293 cells

The next set of experiments then tested the effect of the AZ compounds on ERK activation in HEK293 cells used in the previous chapter where receptor expression is more moderate. The effect of pre-treatment with YPT-2 prior to the addition of 2f-LIGRLO-NH$_2$ is shown in figure 4.19 (a). The compound YPT-2 had no effect on the basal level of ERK when compared with the untreated control (fold stimulation relative to DMSO level 0.850 ± 0.157, n=3). Furthermore, 2f-LIGRLO-NH$_2$ stimulated a significant increase in phosphorylation of ERK as expected, this response was not affected by the presence of DMSO (fold stimulation: 2f-LIGRLO-NH$_2$ = 9.487 ± 1.277, DMSO plus 2f-LIGRLO-NH$_2$ = 8.993 ± 1.277, n=3). However, following incubation with increasing concentration of YPT-2, a marked inhibition of ERK phosphorylation was observed with significance at 10 and 20μM (fold stimulation at 20 μM = 1.930 ± 0.261, n=3).

The effect of pre-treatment with ra-AZ8838 on PAR2 mediated ERK phosphorylation is shown in figure 4.19 (b). As expected, 2f-LIGRLO-NH$_2$ stimulated a significant increase in phosphorylation of ERK, this response was not affected by the presence of DMSO (fold stimulation: 2f-LIGRLO-NH$_2$ = 7.280 ± 0.601, DMSO plus 2f-LIGRLO-NH$_2$ = 7.027 ± 0.368, n=3). However, following incubation with increasing concentrations of ra-AZ8883, a significant concentration-dependent decrease in the phosphorylation of ERK was observed becoming significant at 10 and 20 μM of the compound (fold stimulation at 20 μM = 1.463 ± 0.408, n=3).

a)

b)
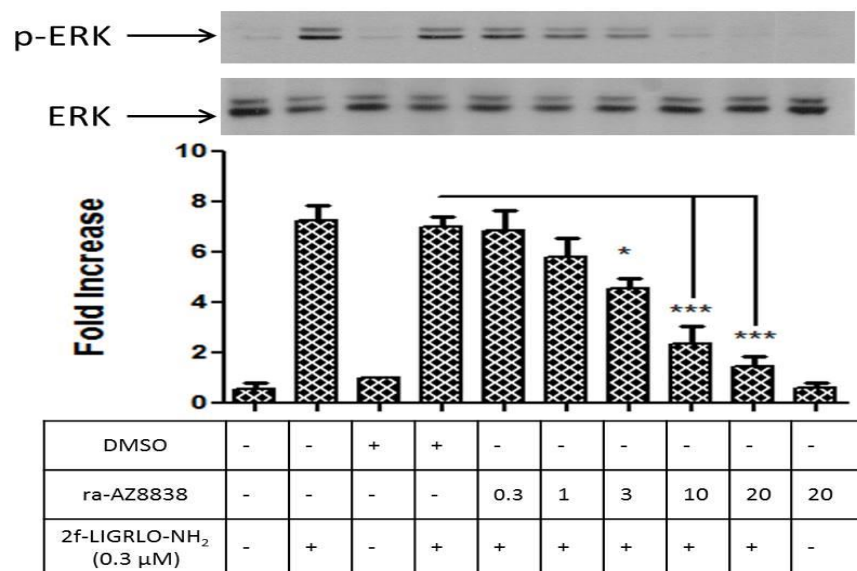
Figure 4. 19 The effect of YPT-2 and ra-AZ8838 on 2f-LIGRLO-NH₂ stimulated ERK phosphorylation in HEK293 cells

Cells were rendered quiescent for 24 hours prior to pre-incubation with various concentrations of (a) YPT-2 (b) ra-AZ8838 for 1 hour, then stimulated with 0.3 μM 2f-LIGRLO-NH₂ for 5 minutes. Whole cell lysates were prepared as previously described (section 2.41), and assessed by Western blotting (section 2.4.2). Each value represents the mean ± S.E.M of three independent experiments. Statistical analysis was applied using one way ANOVA, with Dunnett's post-test comparison. ***p<0.0001 compared to DMSO + 2f-LIGRLO-NH₂.

The effect of pre-treatment with YPT-2 on trypsin stimulated ERK phosphorylation is shown in figure 4.20 (a). Trypsin stimulated a significant increase in phosphorylation of ERK, this response was not affected by the presence of DMSO (fold stimulation: trypsin = 8.940 ± 0.397, DMSO plus trypsin = 8.610 ± 1.037, n=3). However, following incubation with increasing concentrations of YPT-2, an observed but not significant concentration-dependent decrease in the phosphorylation of ERK was observed for 10 and 20 μM (fold stimulation at 20 μM = 4.037 ± 0.681, n=3).

The effect of pre-treatment with ra-AZ8838 on the trypsin mediated ERK response is shown in figure 4.20 (b). Trypsin stimulated a significant increase in phosphorylation of ERK, this response was not affected by the presence of DMSO (fold stimulation: trypsin = 5.870 ± 0.432, DMSO plus trypsin = 5.573 ± 0.544, n=3). However, following incubation with increasing concentrations of ra-AZ8838, a concentration-dependent decrease in the phosphorylation of ERK was observed (fold stimulation at 20 μM = 2.803 ± 0.303, n=3). However, this effect did not reach significance except for the 20 μM concentration point.

a)

DMSO	-	-	+	+	-	-	-	-	-	-
YPT-2	-	-	-	-	0.3	1	3	10	20	20
Trypsin (30 nM)	-	+	-	+	+	+	+	+	+	-

b)

DMSO	-	-	+	+	-	-	-	-	-	-
ra-AZ8838	-	-	-	-	0.3	1	3	10	20	20
Trypsin (30 μM)	-	+	-	+	+	+	+	+	+	-
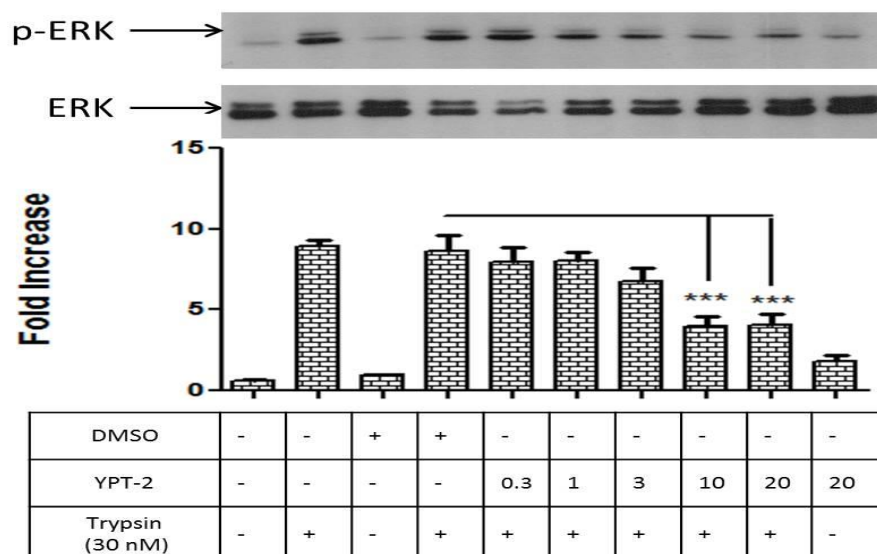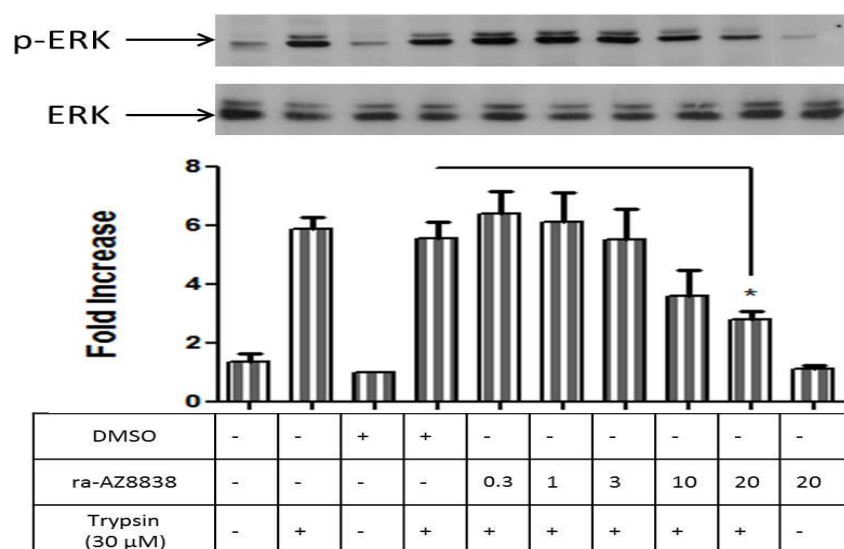
Figure 4. 20 The effect of YPT-2 and ra-AZ8838 on trypsin mediated ERK phosphorylation in HEK293 cells

Cells were rendered quiescent for 24 hours prior to pre-incubation with various concentrations of (a) YPT-2 (b) ra-AZ8838 for 1 hour. The cells were then stimulated with 30 nM trypsin for 5 minutes. Whole cell lysates were prepared as previously described (section 2.41), and assessed by Western blotting (section 2.4.2). Each value represents the mean $\pm$ S.E.M of three independent experiments. Statistical analysis was applied using one way ANOVA, with Dunnett's post-test comparison. ***$p < 0.0001$ compared to DMSO + trypsin stimulation.

The effect of the compounds on GB88 is shown in Figure 4.21. Panel (a) shows the effect of YPT-2 for 1 hour prior to the addition of GB88 for 5 minutes on PAR2 mediated ERK MAP kinase in HEK293 cells. Again, GB88 stimulated a significant increase in the phosphorylation of ERK, this response was not affected by the presence of DMSO (fold stimulation: GB88 = 4.507 ± 0.294, DMSO plus GB88 = 4.610 ± 0.684, n=3). However, following incubation with increasing concentrations of YPT-2, a significant concentration-dependent decrease in the phosphorylation of ERK was observed for 10 and 20 μM (fold stimulation at 20 μM = 0.853 ± 0.128, n=3).

Figure 4.21 (b) shows the effect ra-AZ8838 on GB88 -mediated ERK phosphorylation in HEK293 cells. GB88 stimulated a significant increase in phosphorylation of ERK, this response was not affected by the presence of DMSO (fold stimulation: GB88 = 4.277 ± 0.575, DMSO plus GB88 = 4.210 ± 0.195, n=3). However, following incubation with increasing concentration of ra-AZ8838, a significant concentration-dependent decrease in the phosphorylation of ERK was observed for 10 and 20μM (fold stimulation at 20 μM = 0.947 ± 0.105, n=3).

a)

DMSO	-	-	+	+	-	-	-	-	-	-
YPT-2	-	-	-	-	0.3	1	3	10	20	20
GB88 (10 µM)	-	+	-	+	+	+	+	+	+	-

b)

DMSO	-	-	+	+	-	-	-	-	-	-
ra-AZ8838	-	-	-	-	0.3	1	3	10	20	20
GB88 (10 µM)	-	+	-	+	+	+	+	+	+	-
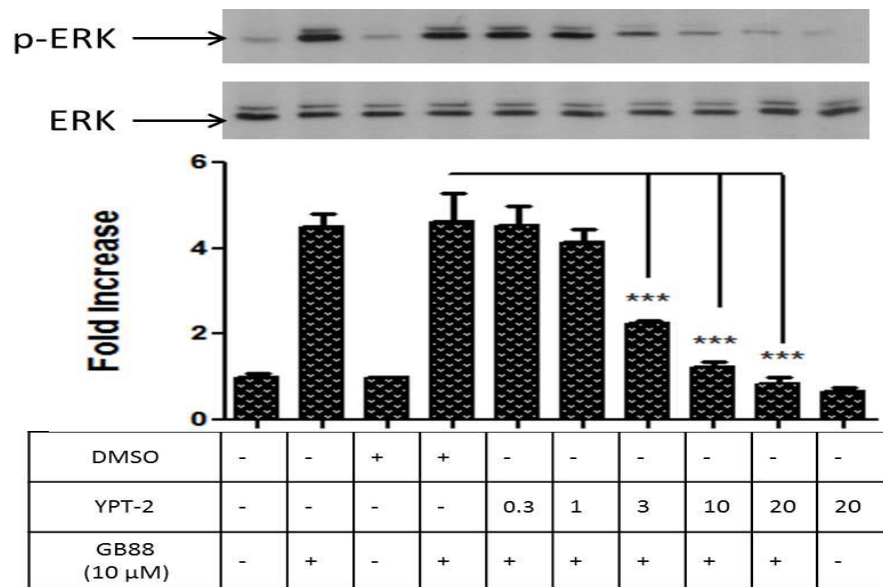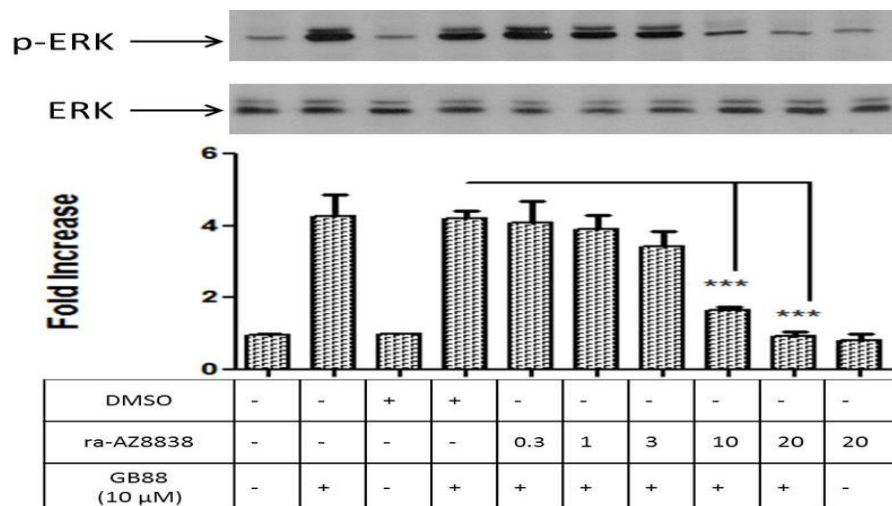
Figure 4. 21 The effect of YPT-2 and ra-AZ8838 on GB88-mediated ERK phosphorylation in HEK293 cells
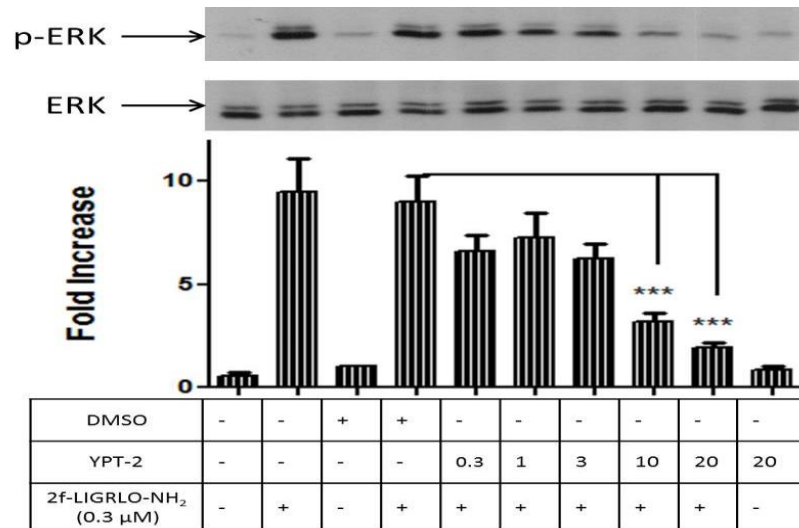
Cells were rendered quiescent for 18 hours prior to pre-incubation with increasing concentrations of (a) YPT-2 (b) ra-AZ8838 for 1 hour. The cells were then stimulated with 10 µM GB88 for 5 minutes. Whole cell lysates were prepared as previously described (section 2.41), and assessed by Western blotting (section 2.4.2). Each value represents the mean ± S.E.M of three independent experiments. A statistical analysis has been applied via using one way ANOVA, with Dunnett's post-test comparison. ***$p < 0.0001$ compared to DMSO + GB88 stimulation.

4.8 Effect of AZ compounds on PAR2 mediated intracellular Ca^{2+} mobilisation in HEK293 cells.

Initially, it was reported that 2f-LIGRLO-NH$_2$ could induce PAR2-dependent calcium mobilisation in HEKs with an EC$_{50}$ of 0.3 µM, as demonstrated in chapter 3. The recent paper by Cheng and co-workers identified that incubation time may be of importance in the potency of AZ8838 (Cheng *et al*., 2017). Therefore, the effect of different pre-incubation times on 2f-LIGRLO-NH$_2$ induced Ca^{2+} mobilisation was examined in figure 4.22.

Initially concentration response curves were established for 2f-LIGRLO-NH$_2$ as indicated in panel A and values recorded as expected for this assay. Figure 4.22 (b) shows the effect of YPT-1 on intracellular calcium induced by 2f-LIGRLO-NH$_2$. The results are inconsistent possibly due to the fairly low level of response but overall there was no effect of the compound at any of the times tested.

Figure 4.22 (c) shows the effect of different pre-incubation times on the ability of YPT-2 to inhibit 2f-LIGRLO-NH$_2$ induced Ca^{2+} mobilisation in HEKs. It was found that the inhibitory effect of YPT-2 was dependent to some extent on the time of pre-incubation. With 15 minutes pre-incubation, a decrease in the response occurred but the curve was flat and the inhibition incomplete making it impossible to generate an IC$_{50}$ value? By contrast, following either 30 or 60 minute pre-incubation, YPT-2 gave consistent inhibition curves with IC$_{50}$ values of approximately 8 and 10 µM, respectively. These values are however shifted to the right in terms of potency relative to other parameters measured previously in the chapter such as ERK activation.

Figure 4.22 (d) shows the effect of increasing pre-incubation times on the ability of ra-AZ8838 to prevent 2f-LIGRLO-NH$_2$ induced Ca^{2+} mobilisation in HEKs. Again, the effect was found to be dependent to some extent on the time of pre-incubation.

Clear inhibition was only observed following pre-incubation for 30 or 60 minutes with ra-AZ8838. With IC_{50} values of 10 and 11 µM respectively again suggesting a far lower potency than previously recorded.

Finally, a single set of experiments utilised SLIGKV-OH as a PAR2 activating peptide to assess the effect of YPT-1 and 2 on induced Ca^{2+} mobilisation in HEKs. The results confirmed that YPT-1 has no antagonist properties but YPT-2 is more effective as an antagonist when the compound is incubated for longer periods of time, as shown in figure 4.23. In this instance, inhibition curves were more suggestive of potency in the range of those observed for other measurements earlier in the chapter.
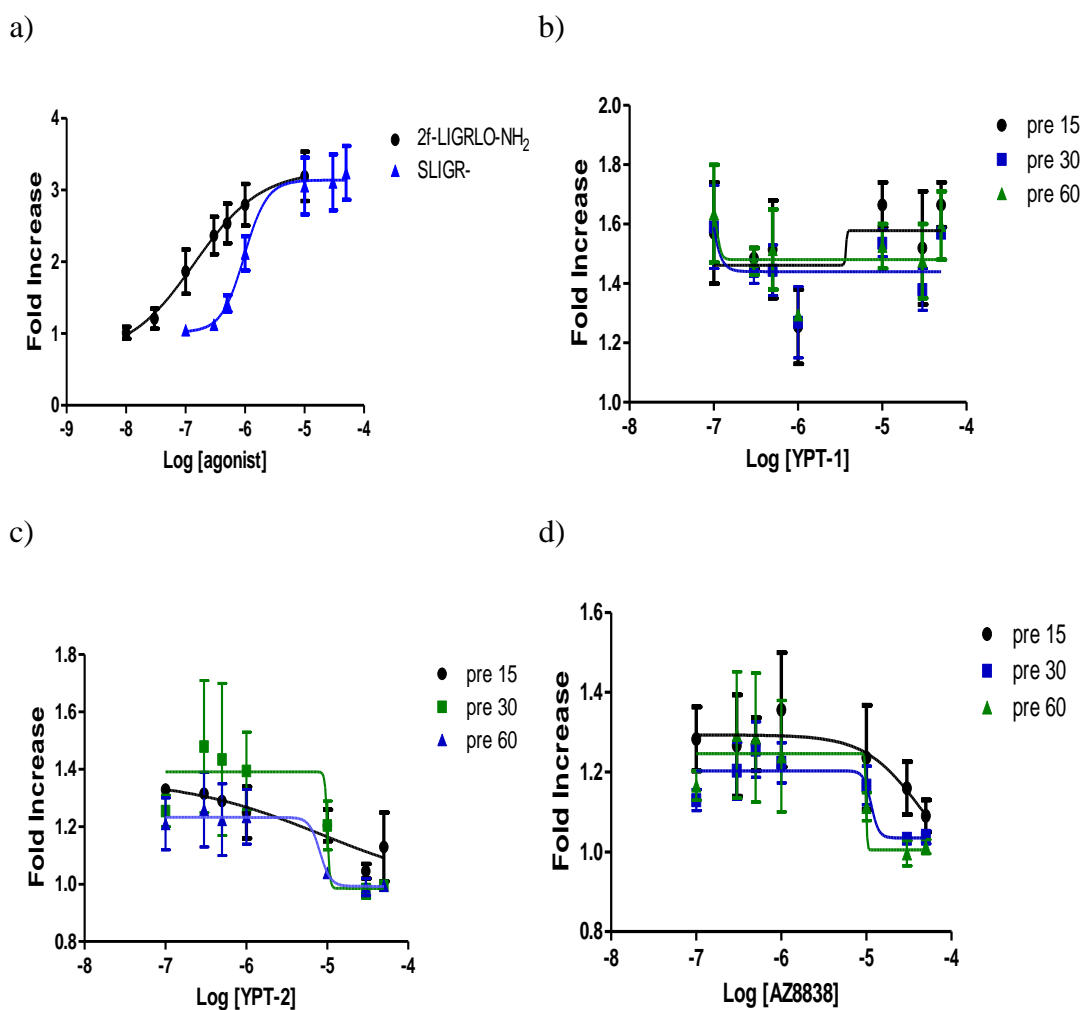
Figure 4. 22 The effect of YPT-1, YPT-2, and ra-AZ8838 on 2f-LIGRLO-NH$_2$-induced Ca^{2+} mobilisation in HEKs.

HEK293 cells were seeded in 96-black well plates until confluent (a) cells were stimulated with increasing concentrations of 2f-LIGRLO-NH$_2$ and SLIGRL-NH$_2$, or pre-incubated with increasing concentrations of (b) YPT-1, (c) YPT-2, (d) ra-AZ8838 for different times (15, 30, 60 minutes). An EC$_{80}$ of 2f-LIGRLO-NH$_2$ (1 µM) was used to activate PAR2-mediated calcium mobilisation. Data represents n=2 for YPT-1 and YPT-2 and n=3 for ra-AZ8838.
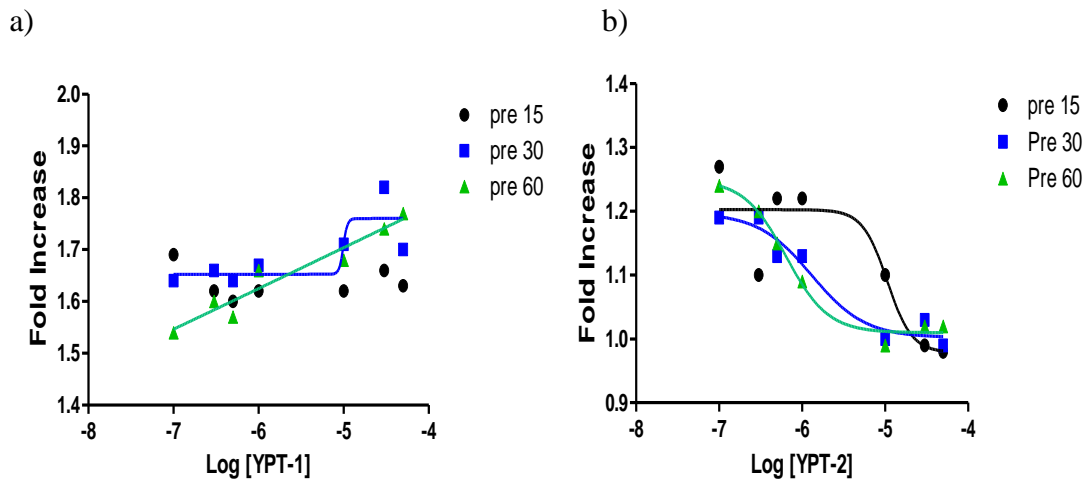
Figure 4. 23 The effect of YPT-1 and YPT-2 on SLIGRL-NH$_2$-induced Ca^{2+} mobilisation in HEKs.

HEK293 cells were seeded in 96-black well plates until confluent and then pre-incubated with increasing concentrations of (a) YPT-1 (b) YPT-2 for different times (15, 30, 60 minutes). An EC$_{80}$ of SLIGRL-NH$_2$ (1.5 µM) was used to activate PAR2-mediated calcium mobilisation.

3.9 Discussion

This chapter investigated the effect of the novel compounds YPT-1, YPT-2, and ra-AZ8838 in multiple signalling pathways mediated by PAR2. The investigation was achieved by utilising the three assays outlined in chapter 3. The compound was initially synthesised as a racemic mixture, ra-AZ8838, and then the enantiomers separated by a commercial company to give YPT-1 and YPT-2. AZ8838 has two structure-stereoisomers; (S) stereoisomer that is the active isomer and (R) stereoisomer that is inactive. These compounds have strong similarity in chemical structure the only difference between them is in the configuration at the hydroxyl group. The (S)-AZ8838 is designated YPT-2, and (R)-AZ8838 is designed YPT-1 in this chapter.

The resolution of the crystal structure of PAR2 have been resolved by Cheng and colleagues in 2017 and gives an important insight into the interaction with the AZ compounds. Two hydrogen bonds are made between the imidazole ring of (S)-AZ8838 and Asp228^{ECL2}, and Tyr82$^{1.39}$ of PAR2. The π-stacking interaction occurs between the fluorophenyl ring of (S)-AZ8838 and His227^{ECL2}. The crucial element which seems to give rise to an active AZ8838 is the hydrogen bond which connects between the hydroxyl group of (S)-AZ8838 and the side chain of His135$^{2.64}$. In the case of (R)-AZ8838, which is an inactive isomer, the hydroxyl group diverts away from His135$^{2.64}$ of PAR2. The hydrogen bond linked between (S)-AZ8838 and the carboxylate of ASP228^{ECL2} has a role in preventing agonist binding to the receptor (Cheng *et al*., 2017).

Initial testing of the compounds again utilised the NFκB reporter cell system as this was able to generate reproducible results. Pre-treatment with YTP-1 was without effect, whist pre-incubation with YPT-2 or ra-AZ8838 was effective against all PAR2 agonists; trypsin, 2f-LIGRLO-NH$_2$, or GB88. The effects were specific for PAR2 with no effect on TNFα mediated activity. Ultimately, it found that the inhibitory effect was concentration-dependent and from the IC$_{50}$ values YPT-2 is more potent than the compound ra-AZ8838, by approximately two fold, which would be expected. These values are consistent with those observed by Cheng *et al*, 2017,

who recorded values for AZ8838 in intracellular calcium mobilisation assays of 2.3 μM and 4.2 μM for SLIGRL and trypsin respectively. Similar to the studies conducted here this was in a cell line (1321N1) over expressing human PAR2 (Cheng *et al*., 2017).

The compounds YPT-2 and ra-AZ8838 also compare well with others as putative antagonists. For example, the IC_{50} values for K-12940 and K-14585 are 3 and 1 μM, respectively for inhibition of luciferase reporter activity (Kanke *et al*., 2009).

Interestingly, the compounds were also effective against the putative antagonist GB88. This might indicate that the two compounds compete for exactly the same site on the receptor, however a recent study has revealed how GB88 binds to PAR2 and suggests some differences (Cheng *et al*., 2017). The isoxazole ring of GB88 is positioned close to TM1 and TM, the binding between them through a hydrogen bond via $Tyr82^{1.39}$ and nitrogen of isoxazole. Cyclohexylalanine of GB88 positions near to $Phe155^{3.32}$ between TM2 and 3. Isoleucine sits to $Tyr156^{3.33}$ and $Leu307^{6.55}$, the last binding is spiro-piperidine of GB88 binds to $Tyr326^{7.35}$ (Xu *et al*., 2015).

It was also found that the compounds were not as effective against trypsin mediated NFκB reporter activity, in that full inhibition was not observed with the maximum concentrations of the compound. This might be as expected as it is difficult to compete as effectively with the tethered ligand for the orthosteric site than with PAR2 activating peptides. However, it is possible that the tethered ligand is able to activate the receptor via several sites including one that allosteric modulation cannot influence. This may be of significance in future drug design.

The opportunity was then taken to asses ERK phosphorylation in the NFκB-Reporter cells as well as HEK293 cells as indicated in figures 4.10 - 4.12. The results were the same, compared to reporter activity; YPT-1 had no effect on the response whilst YPT-2 or ra-AZ8838 caused inhibition of ERK phosphorylation in either cell type. The IC_{50} values of 0.12 and 3 μM were consistent with those obtained for NFκB reporter activity. This again suggests that if ERK is activated through coupling to a G-protein other than $G\alpha_{q/11}$, for example $G\alpha_o$ or $G\alpha_i$ (Defea, 2008, Ramachandran *et al*., 2009, DeFea *et al*., 2000) or indeed via beta arrestin (DeFea *et al*., 2000), modulation at the allosteric site is still effective against receptor activation and

coupling to these pathways. In addition, the ERK pathway is downstream in the cascade thus inhibition will often require higher concentrations of antagonist due to pathway amplification.

The compounds were also found to be effective against both p38 MAP kinase activation and the phosphorylation of p65 NFκB. As indicated in chapter 3, often under normal levels of receptor expression PAR2 does not readily couple up to these pathways, the response is usually weak or non-existent. However, the higher levels of PAR2 expression allow these parameters to be examined. The coupling of PAR2 to the NFκB pathway is unusual. Whilst it has been shown in these cells that PAR2 activation results in an increase in IKK activity, the upstream regulator of the pathway, and associated NFκB reporter activity (Kanke *et al*., 2001), the loss in IκBα is very minimal and inconsistent (Macfarlane *et al*., 2005, Goh *et al*., 2009), and in contrast to that observed with TNFα. This shows a different mechanism of activation at this point in the pathway. In contrast, phosphorylation of p65 NFκB is strong following PAR2 activation and consistent with what might be expected for the activation of this pathway.

Irrespective of the nature of PAR2 coupling to p38 and NFκB pathways in the PAR2 over expressing cells, the results nevertheless suggest the potential to use the compounds in conditions were PAR2 is linked to these pathways for example in arthritis (Ferrell *et al*., 2010). Studies have shown PAR2 coupling to p38 MAP kinase in epithelial cells (Fyfe *et al*., 2005), whilst another study has demonstrated that pre-treatment with TNFα can up-regulate PAR2 and induce p38 MAPK in bovine aortic endothelial (Sethi *et al*., 2005). Thus future studies should examine the effects of AZ8838 in a range of cells and tissues where PAR2 is expressed at varying levels.

The study by Cheng *et al* indicated that the effect of AZ8838 was time dependent (Cheng *et al*., 2017). As a precaution, long pre-incubation times were used in examining the effects of the compounds on NFκB reporter activity and ERK and p38 MAPK activation. However, utilising the multi-well Ca^{2+} reporter system allowed the examination of the phenomenon in more detail using 15, 30 and 60 minute pre-incubation times to construct concentration curves. The results whilst not optimal in

terms of effect were very clear; the minimum time for effective inhibition is approximately 30 minutes. This data agreed with the Cheng's study which demonstrated slow kinetics for binding between PAR2 and AZ8838 in 1321N1-hPAR2 cells assessed by surface plasmon resonance (SPR) on immobilised detergent-solubilised PAR2-StaR.

The slower binding kinetics may have a beneficial aspect leading effective competition with the agonist (Cheng *et al*., 2017). Given the relatively high Ki, the off rate for AZ8838 is likely to be very slow. However, the slow on rate could also limit the use of the antagonist in clinical studies for example, it is unclear if the compound is able to work on cells post PAR2 activation or that the activation of a disease mediated by PAR2 would be already well established prior to treatment for example, arthritis. Other recent studies have identified other putative antagonists with different kinetics of binding. The peptidomimetic PAR2 antagonist C391 was effective in 16HBE14o- cells following pre-incubation for 2 minutes prior to the addition of agonist peptide and this was sufficient to suppress PAR2 mediated mast cell degranulation and thermal hyperalgesia in mice (Boitano *et al*., 2015). A recent study by Gandhi and co-workers has discovered that the specific PAR2 antagonist TJF5 inhibits the internalisation of calcium activated by SLIGKV-NH$_2$ in EA.hy926 endothelial cell line (Gandhi *et al*., 2018). This suggests different modes of binding relative to the AZ compounds.

Overall, in this chapter the effectiveness of the novel PAR2 antagonist, AZ8838, has been illustrated in different techniques and it was found that the antagonist inhibits calcium mobilisation, NFκB transcriptional activity, and ERK MAP kinase mediated by PAR2. From this perspective, the compound is a promising new candidate for the treatment of a number of diseases. AZ8838 has not been tested *in vitro* or *in vivo* and would have to be comparable or better than GB88, K-14585, or K-12940. The compound could be compared with ENMD for example (Kelso *et al*., 2006), as a treatment for osteoarthritis (Ferrell *et al*., 2010). Kanke *et al* have also illustrated that K-12940 and K-14585 have the ability to inhibit paw oedema; comparative studies could also be conducted in this system.

Chapter Five

General Discussion

5.1 General discussion and future works

Receptors mediate and co-ordinate a vast number of extracellular stimuli into a coordinated physiological response via the coupling to a number of key second messenger and kinase signalling pathways. They include tyrosine kinase receptors, nuclear receptors and receptors for a vast array of cytokines. However, the most abundant is the class of G-protein coupled receptors, so called because of the coupling to heterotrimeric G-proteins of different subtypes. Their activation and regulation is one of the most intensely studied fields in pharmacology.

Historically GPCRs have been key targets for the development of new medicines. For example, beta blockers for CV disease and, H1 antagonists used as treatment for hay fever feature H2 antagonists for stomach ulcers and acid conditions. GPCRs remain the major target for the development of new drugs and approximately one third of all medicines are based on interacting with this class of receptor. Whilst previous drugs were identified by structure activity relationships (SAR) using isolated organ preparations or more recently ligand binding and other high throughput screening assays, modern drug discovery is more dependent on a deep structural knowledge of GPCRs (Overington *et al*., 2006). To date thirty crystal structures of GPCRs have been resolved, spanning the main classes A, B, C, and F. The first structure characterised by X-ray crystallography was the light receptor rhodopsin which was identified by Palczewski *et al* in 2000 (Palczewski *et al*., 2000). However whilst this was of major interest analysis of agonist binding was impossible because of the lack of a cognate ligand. It was only through the elucidation of the structure of the β_2-adrenergic receptor by Brain Kobilka and colleagues, which has allowed a host of GPCRs to be resolved (Rasmussen *et al*., 2007). It is likely that numerous other GPCRs will be resolved particularly of class B, C, and F GPCRs as fewer of these have been crystallised thus far.

The resolution of crystal structures helped to confirm basic ideas regarding drug interactions with GPCRs. For example a ligand is now recognised to bind to the

orthosteric binding site. This site lays in the extracellular half helices close to ECL2 and composes from III, VI, and VII. Many receptors have the orthosteric ligand binding pocket such as the β_2-adrenergic (Warne and Tate, 2013) and sphingosine-1-phospate (S1P) receptors (Hanson *et al*., 2012).

Another realisation was that drugs can bind to a second site to modulate the binding of a ligand at the orthosteric site. An allosteric modulator is thought to work via two methods; enhancing binding of the orthosteric ligand which give rise to positive allosteric modulators (PAM), or alternatively compounds can obstruct the binding of the orthosteric ligand and are classified as negative allosteric modulators (NAM). In some instances a single one modulator could behave as PAM or NAM such as indocarbazole staurosporine depending on the agonist which is binding to the orthosteric site. In the case of the Muscarinic M1 receptor N-methylscopolamine alone acts as a PAM, while competing for the same receptor as the endogenous agonist, while acetylcholine acts as a NAM (Lazareno *et al*., 2000). It seems that the nature of the allosteric modulator depends on the presence of the endogenous agonist. Given these properties, allosteric modulators are increasingly considered to be primarily a new class of drug from which medicines can be discovered because their effect is negligible except when the receptor is endogenously activated. Furthermore, because of the inherent saturability of allosteric modulators, their actions lead to other moderate potentiation of an agonist response or a limited inhibitory effect. This prevents more extreme acute effects of the drug and results in a moderate but manageable clinical effect.

These definitions build upon other properties of known drugs acting at GPCRs. For example a number of "antagonists" are known to further inhibit the function of resting receptor bringing basal activity down even further and are defined as inverse agonists. Furthermore, a number of drugs can engage in biased signalling, mediating an inhibition of receptor coupling to one pathway but at the same time activating another. This doesn't just include standard "agonist" compounds but synthetic allosteric as well as bitopic modulators which bind directly to G-proteins or arrestin

by passing the receptor and resulting in bias downstream signalling pathways (Reiter *et al*., 2012).

The experiments of this thesis were used two type cell lines, NFκB-Reporter cells; are parentally NCTC epithelial skin cells. These cells are not expressed to PAR2 but it could be PAR2 over-expressed when the mother cells are transfected with both PAR2 and NFκB-Luc constructs. It was utilised NFκB-Reporter cells with NFκB-transcriptional activity assay to evaluate the compounds. The later assay is simple and cheap and could be giving an idea that the specific compound act as an agonist or antagonist behaviour. Another cell line is HEKs; the endogenous expression of PAR2. HEKs are utilised with both ERK MAP kinase and calcium mobilisation assays that mediated by PAR2 and activated via trypsin and 2f-LIGRLO-NH$_2$. However, HEKs are giving a veritable expression of PAR2. In addition, it was selected two agonists; trypsin and 2f-LIGRLO-NH$_2$ to compare between them for PAR2 activation. Trypsin is a protease agonist for PAR2 that have been used early times to activate PAR2. It gives a moderate potency at PAR2. Another agonist is 2f-LIGRLO-NH$_2$; is a synthetic PAR2 agonist; and used to give a significant potency to activate PAR2 compared to trypsin.

The current thesis examined PAR2 drugs based on both standard SAR techniques but also through analysis of the crystal structure of PAR2. Of the two compounds, the drug AZ8838 was found to be the most effective compound, identified clearly as an allosteric modulator. Interesting properties included a very slow on rate, which given the potency of the drug also means a relatively long off rate. It would be very interesting to track the binding of AZ8838 to PAR2 to determine the off rate as this may be a property of the drug which would enhance its clinical effectiveness. A slow off rate helps prolong the time the drug is in contact with the receptor and may help ensure lack of removal from the local cellular environment. In this study, AZ8838 functioned as an antagonist/allosteric modulator (NAM) under any conditions of study suggesting it to be a drug with major clinical potential.

In contrast GB88 functioned as a partial agonist although the evidence in the literature does suggest that it is an antagonist. However, it should be noted that the drug was reclassified as a bias antagonist suggesting that in some cells were coupling of PAR2 to $G\alpha_{q/11}$ is small the compound could display agonist activity as identified in this study. It also remains to be determined if inhibition of $G\alpha_{q/11}$ directed signalling is the best outcome in terms of its profile as a new drug with clinical potential. Whilst GB88 was shown to inhibit some forms of inflammatory challenge, activation of ERK signalling is likely to have profound effects on cell function in particular in relation to proliferation. Thus the drug may have long term positive effects on tumour growth or for example tumour migration. This might be against the anti-inflammatory effect of GB88 which might be of relevance in maintaining the tumour microenvironment.

However one major advantage of GB88 over AZ8838 is the more advanced characterisation as a drug molecule. The safety and effectiveness of new compounds are associated with a number of elements; absorption, distribution, metabolism, excretion and toxicity (ADMET). Lipinski's rules must be obeyed to design new drugs to prevent the high risk of ADMET during investigation, the antagonist should have a small molecular weight and low lipophilicity to decrease the toxicity and get successful clinical usage (Lipinski *et al*., 2001). The investigation of the drug cannot be limited to studies *in vitro*, it is important to investigate the selected drug *in vivo* systems. A key study has shown that GB88 can be given orally, has a good kinetic profile and remains in the plasma 24 hours after administration (Lohman *et al*., 2012a). Therefore, if this drug is able to pass important toxicity tests it may be used more quickly in Phase I and II clinical trials. However, it is unclear if the moderate potency of the drug is sufficient to ensure good clinical efficacy in a series of tests in appropriate mouse models. Further studies are required to investigate the plasma stability after administration with AZ8838, in addition, the safety and effectiveness could be investigated for AZ8838. Whilst some progress has been made *in vitro,* there has been no discovery of clinical trial are required.

Previous studies have characterised the inflammatory responses and pain induced by PAR2 activation, both *in vivo* and *in vitro*. It is therefore important to evaluate, in future research, PAR2 antagonists as a therapy to treat different types of inflammatory disease. There is a considerable list including; asthma, neurogenic pain, rheumatoid arthritis, and allergic dermatitis. It will be interesting to correlate effects at the cellular level with effects in tissues and *in vivo* studies. It will also be of interest to determine if AZ8388 modulates the action of the large array of endogenous PAR2 activators such as tryptase, outlined in chapter 3, all in the same way as modulation may be ligand independent. Some caution is also required as PAR2 does have a protective role in the body so long term studies on cardiovascular markers would be required. Further studies are required to investigate the effect of the new compound AZ8838 in a particular disease such as arthritis, osteoarthritis, or paw oedema in rodent.

However, despite the exciting findings in relation to GB88 and AZ8388 experience with PAR1 shows that the development of a clinically effective drug is not easy. The only marketed drug to date is vorapaxar, commercially known as Zontivity the first PAR1 antagonist. Zhang and colleagues resolved the crystal structure of PAR1-vorapaxar and identified the binding sites between vorapaxar and PAR1 (Zhang *et al*., 2012b). Vorapaxar acts as an antiplatelet drug and could be used clinically in the acute coronary syndrome (Tricoci *et al*., 2012). Vorapaxar is different to other GPCR members within deep binding pockets, it has hydrophobic properties that leads to high affinity of binding of vorapaxar to the extracellular surface of PAR1 (Zhang *et al*., 2012b). Many PAR1 antagonists have been successfully developed through understanding this structure (Chackalamannil *et al*., 2008), however caution should be noted as a number of these drugs have unwanted side effects. No successful drugs have been developed for the other thrombin-stimulated receptors, PARs 3 and 4.

Given the role for PAR2 in aspects of inflammation, another type of treatment which could be developed is a humanised antibody which may be more clinically efficacious and could be developed more rapidly. Studies were also conducted recently examining antibody binding to PAR2 (Cheng *et al*., 2017). The antibody

Mab3949 has a high binding affinity to PAR2 and binds to the extracellular part of the receptor. Mab3949 targets Arg36[17] which is the site of proteolytic cleavage. Competition was found between Mab3949 and trysin or exogenous activating peptide, and the antagonist activity of Mab3949 appears to be through binding to ECL2. Given the success with a host of therapeutic antibodies targeting cytokines such as Inflixmab it is easy to envisage an equivalent anti-PAR2 antibody for use in rheumatoid arthritis and other immune pathologies. These types of molecule may be preferred to the longer development profile for small molecules.

Future studies in the PAR2 field, could involve utilising the modern technique of CRISPR. Where PAR2 could be knocked-down and its expression blocked. This could be used as a comparative tool for drug design.

In conclusion, this current thesis has shown two main findings. Firstly and surprisingly, GB88 and relative compounds are found to act as PAR2 partial agonists with moderate potencies compared to the endogenous activator and synthetic peptide. This finding is not consistent to other studies which concluded that GB88 is an antagonist. Secondly, this thesis has shown that the novel PAR2 allosteric modulator, AZ8838, behaves as an antagonist and inhibits PAR2 induced intracellular signalling at multiple levels. However, considerably future studies are required to confirm that AZ8838 is PAR2 selective over other PARs. Other studies are needed to ensure that the new pharmaceutically useful molecules can be generated from the current work and other studies including animal testing *in vivo* and clinical studies in human. To finally generate a clinically useful PAR2 inhibitor medicine.

Chapter Six

References

ADAM, E., HANSEN, K. K., ASTUDILLO FERNANDEZ, O., COULON, L., BEX, F., DUHANT, X., JAUMOTTE, E., HOLLENBERG, M. D. & JACQUET, A. 2006. The house dust mite allergen Der p 1, unlike Der p 3, stimulates the expression of interleukin-8 in human airway epithelial cells via a proteinase-activated receptor-2-independent mechanism. *J Biol Chem,* 281**,** 6910-23.

ADAMS, M. N., RAMACHANDRAN, R., YAU, M. K., SUEN, J. Y., FAIRLIE, D. P., HOLLENBERG, M. D. & HOOPER, J. D. 2011. Structure, function and pathophysiology of protease activated receptors. *Pharmacol Ther,* 130**,** 248-82.

AFKHAMI-GOLI, A., NOORBAKHSH, F., KELLER, A. J., VERGNOLLE, N., WESTAWAY, D., JHAMANDAS, J. H., ANDRADE-GORDON, P., HOLLENBERG, M. D., ARAB, H., DYCK, R. H. & POWER, C. 2007. Proteinase-activated receptor-2 exerts protective and pathogenic cell type-specific effects in Alzheimer's disease. *J Immunol,* 179**,** 5493-503.

AHN, H. S., FOSTER, C., BOYKOW, G., STAMFORD, A., MANNA, M. & GRAZIANO, M. 2000. Inhibition of cellular action of thrombin by N3-cyclopropyl-7-[[4-(1-methylethyl)phenyl]methyl]-7H-pyrrolo[3, 2-f]quinazoline-1,3-diamine (SCH 79797), a nonpeptide thrombin receptor antagonist. *Biochem Pharmacol,* 60**,** 1425-34.

AKERS, I. A., PARSONS, M., HILL, M. R., HOLLENBERG, M. D., SANJAR, S., LAURENT, G. J. & MCANULTY, R. J. 2000. Mast cell tryptase stimulates human lung fibroblast proliferation via protease-activated receptor-2. *Am J Physiol Lung Cell Mol Physiol,* 278**,** L193-201.

AL-ANI, B., SAIFEDDINE, M. & HOLLENBERG, M. D. 1995. Detection of functional receptors for the proteinase-activated-receptor-2-activating polypeptide, SLIGRL-NH2, in rat vascular and gastric smooth muscle. *Can J Physiol Pharmacol,* 73**,** 1203-7.

AL-ANI, B., SAIFEDDINE, M., WIJESURIYA, S. J. & HOLLENBERG, M. D. 2002. Modified proteinase-activated receptor-1 and -2 derived peptides inhibit proteinase-activated receptor-2 activation by trypsin. *J Pharmacol Exp Ther,* 300**,** 702-8.

ALBERELLI, M. A. & DE CANDIA, E. 2014. Functional role of protease activated receptors in vascular biology. *Vascul Pharmacol,* 62**,** 72-81.

ALBREKTSEN, T., SORENSEN, B. B., HJORTO, G. M., FLECKNER, J., RAO, L. V. & PETERSEN, L. C. 2007. Transcriptional program induced by factor VIIa-tissue factor, PAR1 and PAR2 in MDA-MB-231 cells. *J Thromb Haemost,* 5**,** 1588-97.

ALIER, K. A., ENDICOTT, J. A., STEMKOWSKI, P. L., CENAC, N., CELLARS, L., CHAPMAN, K., ANDRADE-GORDON, P., VERGNOLLE, N. & SMITH, P. A. 2008. Intrathecal administration of proteinase-activated receptor-2 agonists produces hyperalgesia by exciting the cell bodies of primary sensory neurons. *J Pharmacol Exp Ther,* 324**,** 224-33.

AMADESI, S., COTTRELL, G. S., DIVINO, L., CHAPMAN, K., GRADY, E. F., BAUTISTA, F., KARANJIA, R., BARAJAS-LOPEZ, C., VANNER, S., VERGNOLLE, N. & BUNNETT, N. W. 2006. Protease-activated receptor 2 sensitizes TRPV1 by protein kinase Cepsilon- and A-dependent mechanisms in rats and mice. *J Physiol,* 575**,** 555-71.

ANDRADE-GORDON, P., MARYANOFF, B. E., DERIAN, C. K., ZHANG, H. C., ADDO, M. F., DARROW, A. L., ECKARDT, A. J., HOEKSTRA, W. J., MCCOMSEY, D. F., OKSENBERG, D., REYNOLDS, E. E., SANTULLI, R. J., SCARBOROUGH, R. M., SMITH, C. E. & WHITE, K. B. 1999. Design, synthesis, and biological characterization of a peptide-mimetic antagonist for a tethered-ligand receptor. *Proc Natl Acad Sci U S A,* 96**,** 12257-62.

ANISOWICZ, A., SOTIROPOULOU, G., STENMAN, G., MOK, S. C. & SAGER, R. 1996. A novel protease homolog differentially expressed in breast and ovarian cancer. *Mol Med,* 2**,** 624-36.

ANTONACCIO, M. J., NORMANDIN, D., SERAFINO, R. & MORELAND, S. 1993. Effects of thrombin and thrombin receptor activating peptides on rat aortic vascular smooth muscle. *J Pharmacol Exp Ther,* 266**,** 125-32.

ANTONIAK, S., ROJAS, M., SPRING, D., BULLARD, T. A., VERRIER, E. D., BLAXALL, B. C., MACKMAN, N. & PAWLINSKI, R. 2010. Protease-activated receptor 2 deficiency reduces cardiac ischemia/reperfusion injury. *Arterioscler Thromb Vasc Biol,* 30**,** 2136-42.

ARAI, T., MIKLOSSY, J., KLEGERIS, A., GUO, J. P. & MCGEER, P. L. 2006. Thrombin and prothrombin are expressed by neurons and glial cells and accumulate in neurofibrillary tangles in Alzheimer disease brain. *J Neuropathol Exp Neurol,* 65**,** 19-25.

ARCHBOLD, J. K., FLANAGAN, J. U., WATKINS, H. A., GINGELL, J. J. & HAY, D. L. 2011. Structural insights into RAMP modification of secretin family G protein-coupled receptors: implications for drug development. *Trends Pharmacol Sci,* 32**,** 591-600.

ARENA, C. S., QUIRK, S. M., ZHANG, Y. Q. & HENRIKSON, K. P. 1996. Rat uterine stromal cells: thrombin receptor and growth stimulation by thrombin. *Endocrinology,* 137**,** 3744-9.

ARISAWA, T., TAHARA, T., SHIBATA, T., NAGASAKA, M., NAKAMURA, M., KAMIYA, Y., FUJITA, H., TAKAGI, T., HASEGAWA, S., WANG, F. Y., HIRATA, I. & NAKANO, H. 2007. Promoter hypomethylation of protease-activated receptor 2 associated with carcinogenesis in the stomach. *J Gastroenterol Hepatol,* 22**,** 943-8.

ASOKANANTHAN, N., GRAHAM, P. T., STEWART, D. J., BAKKER, A. J., EIDNE, K. A., THOMPSON, P. J. & STEWART, G. A. 2002. House dust mite allergens induce proinflammatory cytokines from respiratory epithelial cells: the cysteine protease allergen, Der p 1, activates protease-activated receptor (PAR)-2 and inactivates PAR-1. *J Immunol,* 169**,** 4572-8.

ATZORI, L., LUCATTELLI, M., SCOTTON, C. J., LAURENT, G. J., BARTALESI, B., DE CUNTO, G., LUNGHI, B., CHAMBERS, R. C. & LUNGARELLA, G. 2009. Absence of proteinase-activated receptor-1 signaling in mice confers protection from fMLP-induced goblet cell metaplasia. *Am J Respir Cell Mol Biol,* 41**,** 680-7.

AUDET, M. & BOUVIER, M. 2012. Restructuring G-protein- coupled receptor activation. *Cell,* 151**,** 14-23.

BALLERIO, R., BRAMBILLA, M., COLNAGO, D., PAROLARI, A., AGRIFOGLIO, M., CAMERA, M., TREMOLI, E. & MUSSONI, L. 2007. Distinct roles for PAR1- and PAR2-mediated vasomotor modulation in human arterial and venous conduits. *J Thromb Haemost,* 5**,** 174-80.

BARROW, J. C., NANTERMET, P. G., SELNICK, H. G., GLASS, K. L., NGO, P. L., YOUNG, M. B., PELLICORE, J. M., BRESLIN, M. J., HUTCHINSON, J. H., FREIDINGER, R. M., CONDRA, C., KARCZEWSKI, J., BEDNAR, R. A., GAUL, S. L., STERN, A., GOULD, R. & CONNOLLY, T. M. 2001. Discovery and initial structure-activity relationships of trisubstituted ureas as thrombin receptor (PAR-1) antagonists. *Bioorg Med Chem Lett,* 11**,** 2691-6.

BARRY, G. D., LE, G. T. & FAIRLIE, D. P. 2006. Agonists and antagonists of protease activated receptors (PARs). *Curr Med Chem,* 13**,** 243-65.

BARRY, G. D., SUEN, J. Y., LE, G. T., COTTERELL, A., REID, R. C. & FAIRLIE, D. P. 2010. Novel agonists and antagonists for human protease activated receptor 2. *J Med Chem,* 53**,** 7428-40.

BARRY, G. D., SUEN, J. Y., LOW, H. B., PFEIFFER, B., FLANAGAN, B., HALILI, M., LE, G. T. & FAIRLIE, D. P. 2007. A refined agonist pharmacophore for protease activated receptor 2. *Bioorg Med Chem Lett,* 17**,** 5552-7.

BEECHER, K. L., ANDERSEN, T. T., FENTON, J. W., 2ND & FESTOFF, B. W. 1994. Thrombin receptor peptides induce shape change in neonatal murine astrocytes in culture. *J Neurosci Res,* 37**,** 108-15.

BEITELSHEES, A. L. & MCLEOD, H. L. 2006. Clopidogrel pharmacogenetics: promising steps towards patient care? *Arterioscler Thromb Vasc Biol,* 26**,** 1681-3.

BELHAM, C. M., TATE, R. J., SCOTT, P. H., PEMBERTON, A. D., MILLER, H. R., WADSWORTH, R. M., GOULD, G. W. & PLEVIN, R. 1996. Trypsin stimulates proteinase-activated receptor-2-dependent and -independent activation of mitogen-activated protein kinases. *Biochem J,* 320 (Pt 3)**,** 939-46.

BENKA, M. L., LEE, M., WANG, G. R., BUCKMAN, S., BURLACU, A., COLE, L., DEPINA, A., DIAS, P., GRANGER, A., GRANT, B. & ET AL. 1995. The thrombin receptor in human platelets is coupled to a GTP binding protein of the G alpha q family. *FEBS Lett,* 363**,** 49-52.

BERNATOWICZ, M. S., KLIMAS, C. E., HARTL, K. S., PELUSO, M., ALLEGRETTO, N. J. & SEILER, S. M. 1996. Development of potent thrombin receptor antagonist peptides. *J Med Chem,* 39**,** 4879-87.

BLENIS, J. 1993. Signal transduction via the MAP kinases: proceed at your own RSK. *Proc Natl Acad Sci U S A,* 90**,** 5889-92.

BOHM, S. K., KONG, W., BROMME, D., SMEEKENS, S. P., ANDERSON, D. C., CONNOLLY, A., KAHN, M., NELKEN, N. A., COUGHLIN, S. R., PAYAN, D. G. & BUNNETT, N. W. 1996. Molecular cloning, expression and potential functions of the human proteinase-activated receptor-2. *Biochem J,* 314 (Pt 3)**,** 1009-16.

BOIRE, A., COVIC, L., AGARWAL, A., JACQUES, S., SHERIFI, S. & KULIOPULOS, A. 2005. PAR1 is a matrix metalloprotease-1 receptor that promotes invasion and tumorigenesis of breast cancer cells. *Cell,* 120**,** 303-13.

BOITANO, S., FLYNN, A. N., SCHULZ, S. M., HOFFMAN, J., PRICE, T. J. & VAGNER, J. 2011. Potent agonists of the protease activated receptor 2 (PAR2). *J Med Chem,* 54**,** 1308-13.

BOITANO, S., HOFFMAN, J., FLYNN, A. N., ASIEDU, M. N., TILLU, D. V., ZHANG, Z., SHERWOOD, C. L., RIVAS, C. M., DEFEA, K. A., VAGNER, J. & PRICE, T. J. 2015. The novel PAR2 ligand C391 blocks multiple PAR2 signalling pathways in vitro and in vivo. *Br J Pharmacol*.

BRADESI, S. 2009. PAR4: a new role in the modulation of visceral nociception. *Neurogastroenterol Motil,* 21**,** 1129-32.

BRETSCHNEIDER, E., KAUFMANN, R., BRAUN, M., WITTPOTH, M., GLUSA, E., NOWAK, G. & SCHROR, K. 1999. Evidence for proteinase-activated receptor-2 (PAR-2)-mediated mitogenesis in coronary artery smooth muscle cells. *Br J Pharmacol,* 126**,** 1735-40.

BRIDGES, T. M. & LINDSLEY, C. W. 2008. G-protein-coupled receptors: from classical modes of modulation to allosteric mechanisms. *ACS Chem Biol,* 3**,** 530-41.

BUDDENKOTTE, J., STROH, C., ENGELS, I. H., MOORMANN, C., SHPACOVITCH, V. M., SEELIGER, S., VERGNOLLE, N., VESTWEBER, D., LUGER, T. A., SCHULZE-OSTHOFF, K. & STEINHOFF, M. 2005. Agonists of proteinase-activated receptor-2 stimulate upregulation of intercellular cell adhesion molecule-1 in primary human keratinocytes via activation of NF-kappa B. *J Invest Dermatol,* 124**,** 38-45.

BURESI, M. C., VERGNOLLE, N., SHARKEY, K. A., KEENAN, C. M., ANDRADE-GORDON, P., CIRINO, G., CIRILLO, D., HOLLENBERG, M. D. & MACNAUGHTON, W. K. 2005. Activation of proteinase-activated receptor-1 inhibits neurally evoked chloride secretion in the mouse colon in vitro. *Am J Physiol Gastrointest Liver Physiol,* 288**,** G337-45.

BUSHELL, T. J., CUNNINGHAM, M. R., MCINTOSH, K. A., MOUDIO, S. & PLEVIN, R. 2016. Protease-Activated Receptor 2: Are Common Functions in Glial and Immune Cells Linked to Inflammation-Related CNS Disorders? *Curr Drug Targets,* 17**,** 1861-1870.

BUSHELL, T. J., PLEVIN, R., COBB, S. & IRVING, A. J. 2006. Characterization of proteinase-activated receptor 2 signalling and expression in rat hippocampal neurons and astrocytes. *Neuropharmacology,* 50**,** 714-25.

BUSSO, N., CHOBAZ-PECLAT, V., HAMILTON, J., SPEE, P., WAGTMANN, N. & SO, A. 2008. Essential role of platelet activation via protease activated receptor 4 in tissue factor-initiated inflammation. *Arthritis Res Ther,* 10**,** R42.

BUSSO, N., FRASNELLI, M., FEIFEL, R., CENNI, B., STEINHOFF, M., HAMILTON, J. & SO, A. 2007. Evaluation of protease-activated receptor 2 in murine models of arthritis. *Arthritis Rheum,* 56**,** 101-7.

CAMERER, E., HUANG, W. & COUGHLIN, S. R. 2000. Tissue factor- and factor X-dependent activation of protease-activated receptor 2 by factor VIIa. *Proc Natl Acad Sci U S A,* 97**,** 5255-60.

CARVALHO, E., HUGO DE ALMEIDA, V., RONDON, A., POSSIK, P. A., VIOLA, J. P. B. & MONTEIRO, R. Q. 2018. Protease-activated receptor 2 (PAR2) upregulates granulocyte colony stimulating factor (G-CSF) expression in breast cancer cells. *Biochem Biophys Res Commun,* 504**,** 270-276.

CATANIA, A., GATTI, S., COLOMBO, G. & LIPTON, J. M. 2004. Targeting melanocortin receptors as a novel strategy to control inflammation. *Pharmacol Rev,* 56**,** 1-29.

CENAC, N., ANDREWS, C. N., HOLZHAUSEN, M., CHAPMAN, K., COTTRELL, G., ANDRADE-GORDON, P., STEINHOFF, M., BARBARA, G., BECK, P., BUNNETT, N. W., SHARKEY, K. A., FERRAZ, J. G., SHAFFER, E. & VERGNOLLE, N. 2007. Role for protease activity in visceral pain in irritable bowel syndrome. *J Clin Invest,* 117**,** 636-47.

CENAC, N., CELLARS, L., STEINHOFF, M., ANDRADE-GORDON, P., HOLLENBERG, M. D., WALLACE, J. L., FIORUCCI, S. & VERGNOLLE, N. 2005. Proteinase-activated receptor-1 is an anti-inflammatory signal for colitis mediated by a type 2 immune response. *Inflamm Bowel Dis,* 11**,** 792-8.

CENAC, N., CHIN, A. C., GARCIA-VILLAR, R., SALVADOR-CARTIER, C., FERRIER, L., VERGNOLLE, N., BURET, A. G., FIORAMONTI, J. & BUENO, L. 2004. PAR2 activation alters colonic paracellular permeability in mice via IFN-gamma-dependent and -independent pathways. *J Physiol,* 558**,** 913-25.

CENAC, N., COELHO, A. M., NGUYEN, C., COMPTON, S., ANDRADE-GORDON, P., MACNAUGHTON, W. K., WALLACE, J. L., HOLLENBERG, M. D., BUNNETT, N. W., GARCIA-VILLAR, R., BUENO, L. & VERGNOLLE, N. 2002. Induction of intestinal inflammation in mouse by activation of proteinase-activated receptor-2. *Am J Pathol,* 161**,** 1903-15.

CHACKALAMANNIL, S., WANG, Y., GREENLEE, W. J., HU, Z., XIA, Y., AHN, H. S., BOYKOW, G., HSIEH, Y., PALAMANDA, J., AGANS-FANTUZZI, J., KUROWSKI, S., GRAZIANO, M. & CHINTALA, M. 2008. Discovery of a novel, orally active himbacine-based thrombin receptor antagonist (SCH 530348) with potent antiplatelet activity. *J Med Chem,* 51**,** 3061-4.

CHAREST, P. G., OLIGNY-LONGPRE, G., BONIN, H., AZZI, M. & BOUVIER, M. 2007. The V2 vasopressin receptor stimulates ERK1/2 activity independently of heterotrimeric G protein signalling. *Cell Signal,* 19**,** 32-41.

CHEN, D., CARPENTER, A., ABRAHAMS, J., CHAMBERS, R. C., LECHLER, R. I., MCVEY, J. H. & DORLING, A. 2008. Protease-activated receptor 1 activation is necessary for monocyte chemoattractant protein 1-dependent leukocyte recruitment in vivo. *J Exp Med,* 205**,** 1739-46.

CHEN, Y., GRALL, D., SALCINI, A. E., PELICCI, P. G., POUYSSEGUR, J. & VAN OBBERGHEN-SCHILLING, E. 1996. Shc adaptor proteins are key transducers of mitogenic signaling mediated by the G protein-coupled thrombin receptor. *Embo j,* 15**,** 1037-44.

CHENG, R. K. Y., FIEZ-VANDAL, C., SCHLENKER, O., EDMAN, K., AGGELER, B., BROWN, D. G., BROWN, G. A., COOKE, R. M., DUMELIN, C. E., DORE, A. S., GESCHWINDNER, S., GREBNER, C., HERMANSSON, N. O., JAZAYERI, A., JOHANSSON, P., LEONG, L., PRIHANDOKO, R., RAPPAS, M., SOUTTER, H., SNIJDER, A., SUNDSTROM, L., TEHAN, B., THORNTON, P., TROAST, D., WIGGIN, G., ZHUKOV, A., MARSHALL, F. H. & DEKKER, N. 2017. Structural insight into allosteric modulation of protease-activated receptor 2. *Nature,* 545**,** 112-115.

CHEUNG, W. M., D'ANDREA, M. R., ANDRADE-GORDON, P. & DAMIANO, B. P. 1999. Altered vascular injury responses in mice deficient in protease-activated receptor-1. *Arterioscler Thromb Vasc Biol,* 19**,** 3014-24.

CHRISTOPOULOS, A., CHANGEUX, J. P., CATTERALL, W. A., FABBRO, D., BURRIS, T. P., CIDLOWSKI, J. A., OLSEN, R. W., PETERS, J. A., NEUBIG, R. R., PIN, J. P., SEXTON, P. M., KENAKIN, T. P., EHLERT, F. J., SPEDDING, M. & LANGMEAD, C. J. 2014. International Union of Basic and Clinical Pharmacology. XC. multisite pharmacology: recommendations for the nomenclature of receptor allosterism and allosteric ligands. *Pharmacol Rev,* 66**,** 918-47.

CIRINO, G., CICALA, C., BUCCI, M. R., SORRENTINO, L., MARAGANORE, J. M. & STONE, S. R. 1996. Thrombin functions as an inflammatory mediator through activation of its receptor. *J Exp Med,* 183**,** 821-7.

CIRINO, G., NAPOLI, C., BUCCI, M. & CICALA, C. 2000. Inflammation-coagulation network: are serine protease receptors the knot? *Trends Pharmacol Sci,* 21**,** 170-2.

CIRINO, G. & SEVERINO, B. 2010. Thrombin receptors and their antagonists: an update on the patent literature. *Expert Opin Ther Pat,* 20**,** 875-84.

CLAPHAM, D. E. & NEER, E. J. 1997. G protein beta gamma subunits. *Annu Rev Pharmacol Toxicol,* 37**,** 167-203.

COCKS, T. M., FONG, B., CHOW, J. M., ANDERSON, G. P., FRAUMAN, A. G., GOLDIE, R. G., HENRY, P. J., CARR, M. J., HAMILTON, J. R. & MOFFATT, J. D. 1999. A protective role for protease-activated receptors in the airways. *Nature,* 398**,** 156-60.

COLOTTA, F., SCIACCA, F. L., SIRONI, M., LUINI, W., RABIET, M. J. & MANTOVANI, A. 1994. Expression of monocyte chemotactic protein-1 by monocytes and endothelial cells exposed to thrombin. *Am J Pathol,* 144**,** 975-85.

CONGREVE, M., LANGMEAD, C. J., MASON, J. S. & MARSHALL, F. H. 2011. Progress in structure based drug design for G protein-coupled receptors. *J Med Chem,* 54**,** 4283-311.

CORVERA, C. U., DERY, O., MCCONALOGUE, K., BOHM, S. K., KHITIN, L. M., CAUGHEY, G. H., PAYAN, D. G. & BUNNETT, N. W. 1997. Mast cell tryptase regulates rat colonic myocytes through proteinase-activated receptor 2. *J Clin Invest,* 100**,** 1383-93.

COTTRELL, G. S., AMADESI, S., GRADY, E. F. & BUNNETT, N. W. 2004. Trypsin IV, a novel agonist of protease-activated receptors 2 and 4. *J Biol Chem,* 279**,** 13532-9.

COTTRELL, G. S., AMADESI, S., SCHMIDLIN, F. & BUNNETT, N. 2003. Protease-activated receptor 2: activation, signalling and function. *Biochem Soc Trans,* 31, 1191-7.

COUGHLIN, S. R. 1998. Sol Sherry lecture in thrombosis: how thrombin 'talks' to cells: molecular mechanisms and roles in vivo. *Arterioscler Thromb Vasc Biol,* 18**,** 514-8.

COUGHLIN, S. R. 2000. Thrombin signalling and protease-activated receptors. *Nature,* 407**,** 258-64.

COVIC, L., GRESSER, A. L., TALAVERA, J., SWIFT, S. & KULIOPULOS, A. 2002a. Activation and inhibition of G protein-coupled receptors by cell-penetrating membrane-tethered peptides. *Proc Natl Acad Sci U S A,* 99**,** 643-8.

COVIC, L., MISRA, M., BADAR, J., SINGH, C. & KULIOPULOS, A. 2002b. Pepducin-based intervention of thrombin-receptor signaling and systemic platelet activation. *Nat Med,* 8**,** 1161-5.

COX, C. D., BRESLIN, M. J., WHITMAN, D. B., SCHREIER, J. D., MCGAUGHEY, G. B., BOGUSKY, M. J., ROECKER, A. J., MERCER, S. P., BEDNAR, R. A., LEMAIRE, W., BRUNO, J. G., REISS, D. R., HARRELL, C. M., MURPHY, K. L., GARSON, S. L., DORAN, S. M., PRUEKSARITANONT, T., ANDERSON, W. B., TANG, C., ROLLER, S., CABALU, T. D., CUI, D., HARTMAN, G. D., YOUNG, S. D., KOBLAN, K. S., WINROW, C. J., RENGER, J. J. & COLEMAN, P. J. 2010. Discovery of the dual orexin receptor antagonist [(7R)-4-(5-chloro-1,3-benzoxazol-2-yl)-7-methyl-1,4-diazepan-1-yl][5-methyl-2-(2H -1,2,3-triazol-2-yl)phenyl]methanone (MK-4305) for the treatment of insomnia. *J Med Chem,* 53**,** 5320-32.

CRILLY, A., PALMER, H., NICKDEL, M. B., DUNNING, L., LOCKHART, J. C., PLEVIN, R., MCINNES, I. B. & FERRELL, W. R. 2012. Immunomodulatory role of proteinase-activated receptor-2. *Ann Rheum Dis,* 71**,** 1559-66.

D'ANDREA, M. R., DERIAN, C. K., LETURCQ, D., BAKER, S. M., BRUNMARK, A., LING, P., DARROW, A. L., SANTULLI, R. J., BRASS, L. F. & ANDRADE-GORDON, P. 1998. Characterization of protease-activated receptor-2 immunoreactivity in normal human tissues. *J Histochem Cytochem,* 46**,** 157-64.

DAMIANO, B. P., CHEUNG, W. M., SANTULLI, R. J., FUNG-LEUNG, W. P., NGO, K., YE, R. D., DARROW, A. L., DERIAN, C. K., DE GARAVILLA, L. & ANDRADE-GORDON, P. 1999. Cardiovascular responses mediated by protease-activated receptor-2 (PAR-2) and thrombin receptor (PAR-1) are distinguished in mice deficient in PAR-2 or PAR-1. *J Pharmacol Exp Ther,* 288**,** 671-8.

DARMOUL, D., GRATIO, V., DEVAUD, H., PEIRETTI, F. & LABURTHE, M. 2004. Activation of proteinase-activated receptor 1 promotes human colon cancer cell proliferation through epidermal growth factor receptor transactivation. *Mol Cancer Res,* 2**,** 514-22.

DAVEY, M. G. & LUSCHER, E. F. 1967. Actions of thrombin and other coagulant and proteolytic enzymes on blood platelets. *Nature,* 216**,** 857-8.

DEFEA, K. 2008. Beta-arrestins and heterotrimeric G-proteins: collaborators and competitors in signal transduction. *Br J Pharmacol,* 153 Suppl 1**,** S298-309.

DEFEA, K. A., ZALEVSKY, J., THOMA, M. S., DERY, O., MULLINS, R. D. & BUNNETT, N. W. 2000. beta-arrestin-dependent endocytosis of proteinase-activated receptor 2 is required for intracellular targeting of activated ERK1/2. *J Cell Biol,* 148**,** 1267-81.

DEMAUDE, J., LEVEQUE, M., CHAUMAZ, G., EUTAMENE, H., FIORAMONTI, J., BUENO, L. & FERRIER, L. 2009. Acute stress increases colonic paracellular permeability in mice through a mast cell-independent mechanism: involvement of pancreatic trypsin. *Life Sci,* 84**,** 847-52.

DERY, O., CORVERA, C. U., STEINHOFF, M. & BUNNETT, N. W. 1998. Proteinase-activated receptors: novel mechanisms of signaling by serine proteases. *Am J Physiol,* 274**,** C1429-52.

DERY, O., THOMA, M. S., WONG, H., GRADY, E. F. & BUNNETT, N. W. 1999. Trafficking of proteinase-activated receptor-2 and beta-arrestin-1 tagged with green fluorescent protein. beta-Arrestin-dependent endocytosis of a proteinase receptor. *J Biol Chem,* 274**,** 18524-35.

DORFLEUTNER, A., HINTERMANN, E., TARUI, T., TAKADA, Y. & RUF, W. 2004. Cross-talk of integrin alpha3beta1 and tissue factor in cell migration. *Mol Biol Cell,* 15**,** 4416-25.

DROR, R. O., PAN, A. C., ARLOW, D. H., BORHANI, D. W., MARAGAKIS, P., SHAN, Y., XU, H. & SHAW, D. E. 2011. Pathway and mechanism of drug binding to G-protein-coupled receptors. *Proc Natl Acad Sci U S A,* 108**,** 13118-23.

EDELSTEIN, L. C., SIMON, L. M., LINDSAY, C. R., KONG, X., TERUEL-MONTOYA, R., TOURDOT, B. E., CHEN, E. S., MA, L., COUGHLIN, S., NIEMAN, M., HOLINSTAT, M., SHAW, C. A. & BRAY, P. F. 2014. Common variants in the human platelet PAR4 thrombin receptor alter platelet function and differ by race. *Blood,* 124**,** 3450-8.

EHRENREICH, H., COSTA, T., CLOUSE, K. A., PLUTA, R. M., OGINO, Y., COLIGAN, J. E. & BURD, P. R. 1993. Thrombin is a regulator of astrocytic endothelin-1. *Brain Res,* 600**,** 201-7.

EMPFIELD, J. R. & LEESON, P. D. 2010. Lessons learned from candidate drug attrition. *IDrugs,* 13**,** 869-73.

EVEN-RAM, S., UZIELY, B., COHEN, P., GRISARU-GRANOVSKY, S., MAOZ, M., GINZBURG, Y., REICH, R., VLODAVSKY, I. & BAR-SHAVIT, R. 1998. Thrombin receptor overexpression in malignant and physiological invasion processes. *Nat Med,* 4**,** 909-14.

FENDER, A. C., RAUCH, B. H., GEISLER, T. & SCHROR, K. 2017. Protease-Activated Receptor PAR-4: An Inducible Switch between Thrombosis and Vascular Inflammation? *Thromb Haemost,* 117**,** 2013-2025.

FERRELL, W. R., KELSO, E. B., LOCKHART, J. C., PLEVIN, R. & MCINNES, I. B. 2010. Protease-activated receptor 2: a novel pathogenic pathway in a murine model of osteoarthritis. *Ann Rheum Dis,* 69**,** 2051-4.

FERRELL, W. R., LOCKHART, J. C., KELSO, E. B., DUNNING, L., PLEVIN, R., MEEK, S. E., SMITH, A. J., HUNTER, G. D., MCLEAN, J. S., MCGARRY, F., RAMAGE, R., JIANG, L., KANKE, T. & KAWAGOE, J. 2003. Essential role for proteinase-activated receptor-2 in arthritis. *J Clin Invest,* 111**,** 35-41.

FREDRIKSSON, R., LAGERSTROM, M. C., LUNDIN, L. G. & SCHIOTH, H. B. 2003. The G-protein-coupled receptors in the human genome form five main families. Phylogenetic analysis, paralogon groups, and fingerprints. *Mol Pharmacol,* 63**,** 1256-72.

FRENCH, S. L., ARTHUR, J. F., TRAN, H. A. & HAMILTON, J. R. 2015. Approval of the first protease-activated receptor antagonist: Rationale, development, significance, and considerations of a novel anti-platelet agent. *Blood Rev,* 29**,** 179-89.

FUKUHARA, S., MURGA, C., ZOHAR, M., IGISHI, T. & GUTKIND, J. S. 1999. A novel PDZ domain containing guanine nucleotide exchange factor links heterotrimeric G proteins to Rho. *J Biol Chem,* 274**,** 5868-79.

FYFE, M., BERGSTROM, M., ASPENGREN, S. & PETERSON, A. 2005. PAR-2 activation in intestinal epithelial cells potentiates interleukin-1beta-induced chemokine secretion via MAP kinase signaling pathways. *Cytokine,* 31**,** 358-67.

GANDHI, D. M., MAJEWSKI, M. W., ROSAS, R., JR., KENTALA, K., FOSTER, T. J., GREVE, E. & DOCKENDORFF, C. 2018. Characterization of Protease-Activated Receptor (PAR) ligands: Parmodulins are reversible allosteric inhibitors of PAR1-driven calcium mobilization in endothelial cells. *Bioorg Med Chem,* 26**,** 2514-2529.

GARDELL, L. R., MA, J. N., SEITZBERG, J. G., KNAPP, A. E., SCHIFFER, H. H., TABATABAEI, A., DAVIS, C. N., OWENS, M., CLEMONS, B., WONG, K. K., LUND, B., NASH, N. R., GAO, Y., LAMEH, J., SCHMELZER, K., OLSSON, R. & BURSTEIN, E. S. 2008. Identification and characterization of novel small-molecule protease-activated receptor 2 agonists. *J Pharmacol Exp Ther,* 327**,** 799-808.

GE, L., LY, Y., HOLLENBERG, M. & DEFEA, K. 2003. A beta-arrestin-dependent scaffold is associated with prolonged MAPK activation in pseudopodia during protease-activated receptor-2-induced chemotaxis. *J Biol Chem,* 278**,** 34418-26.

GE, L., SHENOY, S. K., LEFKOWITZ, R. J. & DEFEA, K. 2004. Constitutive protease-activated receptor-2-mediated migration of MDA MB-231 breast cancer cells requires both beta-arrestin-1 and -2. *J Biol Chem,* 279**,** 55419-24.

GIBLIN, P., BOXHAMMER, R., DESAI, S., KROE-BARRETT, R., HANSEN, G., KSIAZEK, J., PANZENBECK, M., RALPH, K., SCHWARTZ, R., ZIMMITTI, C., PRACHT, C., MILLER, S., MAGRAM, J. & LITZENBURGER, T. 2011. Fully human antibodies against the Protease-Activated Receptor-2 (PAR-2) with anti-inflammatory activity. *Hum Antibodies,* 20**,** 83-94.

GOH, F. G., NG, P. Y., NILSSON, M., KANKE, T. & PLEVIN, R. 2009. Dual effect of the novel peptide antagonist K-14585 on proteinase-activated receptor-2-mediated signalling. *Br J Pharmacol,* 158**,** 1695-704.

GOMIDES, L. F., LIMA, O. C., MATOS, N. A., FREITAS, K. M., FRANCISCHI, J. N., TAVARES, J. C. & KLEIN, A. 2014. Blockade of proteinase-activated receptor 4 inhibits neutrophil recruitment in experimental inflammation in mice. *Inflamm Res,* 63**,** 935-41.

GOON GOH, F., SLOSS, C. M., CUNNINGHAM, M. R., NILSSON, M., CADALBERT, L. & PLEVIN, R. 2008. G-protein-dependent and -independent pathways regulate proteinase-activated receptor-2 mediated p65 NFkappaB serine 536 phosphorylation in human keratinocytes. *Cell Signal,* 20**,** 1267-74.

GOTO, S., YAMAGUCHI, T., IKEDA, Y., KATO, K., YAMAGUCHI, H. & JENSEN, P. 2010. Safety and exploratory efficacy of the novel thrombin receptor (PAR-1) antagonist SCH530348 for non-ST-segment elevation acute coronary syndrome. *J Atheroscler Thromb,* 17**,** 156-64.

GRAND, R. J., TURNELL, A. S. & GRABHAM, P. W. 1996. Cellular consequences of thrombin-receptor activation. *Biochem J,* 313 (Pt 2)**,** 353-68.

GRANDALIANO, G., VALENTE, A. J. & ABBOUD, H. E. 1994. A novel biologic activity of thrombin: stimulation of monocyte chemotactic protein production. *J Exp Med,* 179**,** 1737-41.

GREENWOOD, S. M. & BUSHELL, T. J. 2010. Astrocytic activation and an inhibition of MAP kinases are required for proteinase-activated receptor-2-mediated protection from neurotoxicity. *J Neurochem,* 113**,** 1471-80.

GRISHINA, Z., OSTROWSKA, E., HALANGK, W., SAHIN-TOTH, M. & REISER, G. 2005. Activity of recombinant trypsin isoforms on human proteinase-activated receptors (PAR): mesotrypsin cannot activate epithelial PAR-1, -2, but weakly activates brain PAR-1. *Br J Pharmacol,* 146**,** 990-9.

GRUBER, C. W., MUTTENTHALER, M. & FREISSMUTH, M. 2010. Ligand-based peptide design and combinatorial peptide libraries to target G protein-coupled receptors. *Curr Pharm Des,* 16**,** 3071-88.

GSCHWEND, T. P., KRUEGER, S. R., KOZLOV, S. V., WOLFER, D. P. & SONDEREGGER, P. 1997. Neurotrypsin, a novel multidomain serine protease expressed in the nervous system. *Mol Cell Neurosci,* 9**,** 207-19.

GUDMUNDSDOTTIR, I. J., LANG, N. N., BOON, N. A., LUDLAM, C. A., WEBB, D. J., FOX, K. A. & NEWBY, D. E. 2008. Role of the endothelium in the vascular effects of the thrombin receptor (protease-activated receptor type 1) in humans. *J Am Coll Cardiol,* 51**,** 1749-56.

GUO, H., LIU, D., GELBARD, H., CHENG, T., INSALACO, R., FERNANDEZ, J. A., GRIFFIN, J. H. & ZLOKOVIC, B. V. 2004. Activated protein C prevents neuronal apoptosis via protease activated receptors 1 and 3. *Neuron,* 41**,** 563-72.

GURBEL, P. A., BLIDEN, K. P., TURNER, S. E., TANTRY, U. S., GESHEFF, M. G., BARR, T. P., COVIC, L. & KULIOPULOS, A. 2016. Cell-Penetrating Pepducin Therapy Targeting PAR1 in Subjects With Coronary Artery Disease. *Arterioscler Thromb Vasc Biol,* 36**,** 189-97.

HAMILTON, J. R., FRAUMAN, A. G. & COCKS, T. M. 2001a. Increased expression of protease-activated receptor-2 (PAR2) and PAR4 in human coronary artery by inflammatory stimuli unveils endothelium-dependent relaxations to PAR2 and PAR4 agonists. *Circ Res,* 89**,** 92-8.

HAMILTON, J. R., MOFFATT, J. D., FRAUMAN, A. G. & COCKS, T. M. 2001b. Protease-activated receptor (PAR) 1 but not PAR2 or PAR4 mediates endothelium-dependent relaxation to thrombin and trypsin in human pulmonary arteries. *J Cardiovasc Pharmacol,* 38**,** 108-19.

HAMM, H. E. 2001. How activated receptors couple to G proteins. *Proc Natl Acad Sci U S A,* 98**,** 4819-21.

HANSON, M. A., ROTH, C. B., JO, E., GRIFFITH, M. T., SCOTT, F. L., REINHART, G., DESALE, H., CLEMONS, B., CAHALAN, S. M., SCHUERER, S. C., SANNA, M. G., HAN, G. W., KUHN, P., ROSEN, H. & STEVENS, R. C. 2012. Crystal structure of a lipid G protein-coupled receptor. *Science,* 335**,** 851-5.

HERNANDEZ, N. A., CORREA, E., AVILA, E. P., VELA, T. A. & PEREZ, V. M. 2009. PAR1 is selectively over expressed in high grade breast cancer patients: a cohort study. *J Transl Med,* 7**,** 47.

HIROTA, C. L., MOREAU, F., IABLOKOV, V., DICAY, M., RENAUX, B., HOLLENBERG, M. D. & MACNAUGHTON, W. K. 2012. Epidermal growth factor receptor transactivation is required for proteinase-activated receptor-2-induced COX-2 expression in intestinal epithelial cells. *Am J Physiol Gastrointest Liver Physiol,* 303**,** G111-9.

HOLLENBERG, M. D. 1999. Protease-activated receptors: PAR4 and counting: how long is the course? *Trends Pharmacol Sci,* 20**,** 271-3.

HOLLENBERG, M. D. & COMPTON, S. J. 2002. International Union of Pharmacology. XXVIII. Proteinase-activated receptors. *Pharmacol Rev,* 54**,** 203-17.

HOLLENBERG, M. D., RENAUX, B., HYUN, E., HOULE, S., VERGNOLLE, N., SAIFEDDINE, M. & RAMACHANDRAN, R. 2008. Derivatized 2-furoyl-LIGRLO-amide, a versatile and selective probe for proteinase-activated receptor 2: binding and visualization. *J Pharmacol Exp Ther,* 326**,** 453-62.

HOLLENBERG, M. D. & SAIFEDDINE, M. 2001. Proteinase-activated receptor 4 (PAR4): activation and inhibition of rat platelet aggregation by PAR4-derived peptides. *Can J Physiol Pharmacol,* 79**,** 439-42.

HOLLENBERG, M. D., SAIFEDDINE, M. & AL-ANI, B. 1996. Proteinase-activated receptor-2 in rat aorta: structural requirements for agonist activity of receptor-activating peptides. *Mol Pharmacol,* 49**,** 229-33.

HONG, J. H., HONG, J. Y., PARK, B., LEE, S. I., SEO, J. T., KIM, K. E., SOHN, M. H. & SHIN, D. M. 2008. Chitinase activates protease-activated receptor-2 in human airway epithelial cells. *Am J Respir Cell Mol Biol,* 39**,** 530-5.

HOPKINS, A. L. & GROOM, C. R. 2002. The druggable genome. *Nat Rev Drug Discov,* 1**,** 727-30.

HOWELLS, G. L., MACEY, M. G., CHINNI, C., HOU, L., FOX, M. T., HARRIOTT, P. & STONE, S. R. 1997. Proteinase-activated receptor-2: expression by human neutrophils. *J Cell Sci,* 110 (Pt 7)**,** 881-7.

HOYLE, G. W., HOYLE, C. I., CHEN, J., CHANG, W., WILLIAMS, R. W. & RANDO, R. J. 2010. Identification of triptolide, a natural diterpenoid compound, as an inhibitor of lung inflammation. *Am J Physiol Lung Cell Mol Physiol,* 298**,** L830-6.

HU, L., XIA, L., ZHOU, H., WU, B., MU, Y., WU, Y. & YAN, J. 2013. TF/FVIIa/PAR2 promotes cell proliferation and migration via PKCalpha and ERK-dependent c-Jun/AP-1 pathway in colon cancer cell line SW620. *Tumour Biol,* 34**,** 2573-81.

HUANG, J. S., DONG, L., KOZASA, T. & LE BRETON, G. C. 2007. Signaling through G(alpha)13 switch region I is essential for protease-activated receptor 1-mediated human platelet shape change, aggregation, and secretion. *J Biol Chem,* 282**,** 10210-22.

HUESA, C., ORTIZ, A. C., DUNNING, L., MCGAVIN, L., BENNETT, L., MCINTOSH, K., CRILLY, A., KUROWSKA-STOLARSKA, M., PLEVIN, R., VAN 'T HOF, R. J., ROWAN, A. D., MCINNES, I. B., GOODYEAR, C. S., LOCKHART, J. C. & FERRELL, W. R. 2016. Proteinase-activated receptor 2 modulates OA-related pain, cartilage and bone pathology. *Ann Rheum Dis,* 75**,** 1989-1997.

HUNG, D. T., WONG, Y. H., VU, T. K. & COUGHLIN, S. R. 1992. The cloned platelet thrombin receptor couples to at least two distinct effectors to stimulate phosphoinositide hydrolysis and inhibit adenylyl cyclase. *J Biol Chem,* 267**,** 20831-4.

HWA, J. J., GHIBAUDI, L., WILLIAMS, P., CHINTALA, M., ZHANG, R., CHATTERJEE, M. & SYBERTZ, E. 1996. Evidence for the presence of a proteinase-activated receptor distinct from the thrombin receptor in vascular endothelial cells. *Circ Res,* 78**,** 581-8.

HYUN, E., ANDRADE-GORDON, P., STEINHOFF, M. & VERGNOLLE, N. 2008. Protease-activated receptor-2 activation: a major actor in intestinal inflammation. *Gut,* 57**,** 1222-9.

HYUN, E., RAMACHANDRAN, R., CENAC, N., HOULE, S., ROUSSET, P., SAXENA, A., LIBLAU, R. S., HOLLENBERG, M. D. & VERGNOLLE, N. 2010. Insulin modulates protease-activated receptor 2 signaling: implications for the innate immune response. *J Immunol,* 184**,** 2702-9.

IABLOKOV, V., HIROTA, C. L., PEPLOWSKI, M. A., RAMACHANDRAN, R., MIHARA, K., HOLLENBERG, M. D. & MACNAUGHTON, W. K. 2014. Proteinase-activated receptor 2 (PAR2) decreases apoptosis in colonic epithelial cells. *J Biol Chem,* 289**,** 34366-77.

IKEHARA, O., HAYASHI, H., WATANABE, Y., YAMAMOTO, H., MOCHIZUKI, T., HOSHINO, M. & SUZUKI, Y. 2010. Proteinase-activated receptors-1 and 2 induce electrogenic Cl-secretion in the mouse cecum by distinct mechanisms. *Am J Physiol Gastrointest Liver Physiol,* 299**,** G115-25.

ISHIHARA, H., CONNOLLY, A. J., ZENG, D., KAHN, M. L., ZHENG, Y. W., TIMMONS, C., TRAM, T. & COUGHLIN, S. R. 1997. Protease-activated receptor 3 is a second thrombin receptor in humans. *Nature,* 386**,** 502-6.

ISHII, K., GERSZTEN, R., ZHENG, Y. W., WELSH, J. B., TURCK, C. W. & COUGHLIN, S. R. 1995. Determinants of thrombin receptor cleavage. Receptor domains involved, specificity, and role of the P3 aspartate. *J Biol Chem,* 270**,** 16435-40.

JACOB, C., YANG, P. C., DARMOUL, D., AMADESI, S., SAITO, T., COTTRELL, G. S., COELHO, A. M., SINGH, P., GRADY, E. F., PERDUE, M. & BUNNETT, N. W. 2005. Mast cell tryptase controls paracellular permeability of the intestine. Role of protease-activated receptor 2 and beta-arrestins. *J Biol Chem,* 280**,** 31936-48.

JACOBY, E., BOUHELAL, R., GERSPACHER, M. & SEUWEN, K. 2006. The 7 TM G-protein-coupled receptor target family. *ChemMedChem,* 1**,** 761-82.

JENKINS, A. L., BOOTMAN, M. D., TAYLOR, C. W., MACKIE, E. J. & STONE, S. R. 1993. Characterization of the receptor responsible for thrombin-induced intracellular calcium responses in osteoblast-like cells. *J Biol Chem,* 268**,** 21432-7.

JIANG, L., LUAN, Y., MIAO, X., SUN, C., LI, K., HUANG, Z., XU, D., ZHANG, M., KONG, F. & LI, N. 2017. Platelet releasate promotes breast cancer growth and angiogenesis via VEGF-integrin cooperative signalling. *Br J Cancer,* 117**,** 695-703.

JOOST, P. & METHNER, A. 2002. Phylogenetic analysis of 277 human G-protein-coupled receptors as a tool for the prediction of orphan receptor ligands. *Genome Biol,* 3**,** Research0063.

JUNGE, C. E., LEE, C. J., HUBBARD, K. B., ZHANG, Z., OLSON, J. J., HEPLER, J. R., BRAT, D. J. & TRAYNELIS, S. F. 2004. Protease-activated receptor-1 in human brain: localization and functional expression in astrocytes. *Exp Neurol,* 188**,** 94-103.

KAHN, M. L., ZHENG, Y. W., HUANG, W., BIGORNIA, V., ZENG, D., MOFF, S., FARESE, R. V., JR., TAM, C. & COUGHLIN, S. R. 1998. A dual thrombin receptor system for platelet activation. *Nature,* 394**,** 690-4.

KANDULSKI, A., KUESTER, D., MONKEMULLER, K., FRY, L., MALFERTHEINER, P. & WEX, T. 2011. Protease-activated receptor-2 (PAR2) in human gastric mucosa as mediator of proinflammatory effects in Helicobacter pylori infection. *Helicobacter,* 16**,** 452-8.

KANEIDER, N. C., LEGER, A. J., AGARWAL, A., NGUYEN, N., PERIDES, G., DERIAN, C., COVIC, L. & KULIOPULOS, A. 2007. 'Role reversal' for the receptor PAR1 in sepsis-induced vascular damage. *Nat Immunol,* 8**,** 1303-12.

KANG, Y., ZHOU, X. E., GAO, X., HE, Y., LIU, W., ISHCHENKO, A., BARTY, A., WHITE, T. A., YEFANOV, O., HAN, G. W., XU, Q., DE WAAL, P. W., KE, J., TAN, M. H., ZHANG, C., MOELLER, A., WEST, G. M., PASCAL, B. D., VAN EPS, N., CARO, L. N., VISHNIVETSKIY, S. A., LEE, R. J., SUINO-POWELL, K. M., GU, X., PAL, K., MA, J., ZHI, X., BOUTET, S., WILLIAMS, G. J., MESSERSCHMIDT, M., GATI, C., ZATSEPIN, N. A., WANG, D., JAMES, D., BASU, S., ROY-CHOWDHURY, S., CONRAD, C. E., COE, J., LIU, H., LISOVA, S., KUPITZ, C., GROTJOHANN, I., FROMME, R., JIANG, Y., TAN, M., YANG, H., LI, J., WANG, M., ZHENG, Z., LI, D., HOWE, N., ZHAO, Y., STANDFUSS, J., DIEDERICHS, K., DONG, Y., POTTER, C. S., CARRAGHER, B., CAFFREY, M., JIANG, H., CHAPMAN, H. N., SPENCE, J. C., FROMME, P., WEIERSTALL, U., ERNST, O. P., KATRITCH, V., GUREVICH, V. V., GRIFFIN, P. R., HUBBELL, W. L., STEVENS, R. C., CHEREZOV, V., MELCHER, K. & XU, H. E. 2015. Crystal structure of rhodopsin bound to arrestin by femtosecond X-ray laser. *Nature,* 523**,** 561-7.

KANKE, T., KABEYA, M., KUBO, S., KONDO, S., YASUOKA, K., TAGASHIRA, J., ISHIWATA, H., SAKA, M., FURUYAMA, T., NISHIYAMA, T., DOI, T., HATTORI, Y., KAWABATA, A., CUNNINGHAM, M. R. & PLEVIN, R. 2009. Novel antagonists for proteinase-activated receptor 2: inhibition of cellular and vascular responses in vitro and in vivo. *Br J Pharmacol,* 158**,** 361-71.

KANKE, T., MACFARLANE, S. R., SEATTER, M. J., DAVENPORT, E., PAUL, A., MCKENZIE, R. C. & PLEVIN, R. 2001. Proteinase-activated receptor-2-mediated activation of stress-activated protein kinases and inhibitory kappa B kinases in NCTC 2544 keratinocytes. *J Biol Chem,* 276**,** 31657-66.

KANKE, T., TAKIZAWA, T., KABEYA, M. & KAWABATA, A. 2005. Physiology and pathophysiology of proteinase-activated receptors (PARs): PAR-2 as a potential therapeutic target. *J Pharmacol Sci,* 97**,** 38-42.

KANTHOU, C., KANSE, S. M., KAKKAR, V. V. & BENZAKOUR, O. 1996. Involvement of pertussis toxin-sensitive and -insensitive G proteins in alpha-thrombin signalling on cultured human vascular smooth muscle cells. *Cell Signal,* 8**,** 59-66.

KATO, Y., KITA, Y., NISHIO, M., HIRASAWA, Y., ITO, K., YAMANAKA, T., MOTOYAMA, Y. & SEKI, J. 1999. In vitro antiplatelet profile of FR171113, a novel non-peptide thrombin receptor antagonist. *Eur J Pharmacol,* 384**,** 197-202.

KATRITCH, V., CHEREZOV, V. & STEVENS, R. C. 2013. Structure-function of the G protein-coupled receptor superfamily. *Annu Rev Pharmacol Toxicol,* 53**,** 531-56.

KAUFMANN, R., JUNKER, U., NUSKE, K., WESTERMANN, M., HENKLEIN, P., SCHEELE, J. & JUNKER, K. 2002. PAR-1- and PAR-3-type thrombin receptor expression in primary cultures of human renal cell carcinoma cells. *Int J Oncol,* 20**,** 177-80.

KAUFMANN, R., RAHN, S., POLLRICH, K., HERTEL, J., DITTMAR, Y., HOMMANN, M., HENKLEIN, P., BISKUP, C., WESTERMANN, M., HOLLENBERG, M. D. & SETTMACHER, U. 2007. Thrombin-mediated hepatocellular carcinoma cell migration: cooperative action via proteinase-activated receptors 1 and 4. *J Cell Physiol,* 211**,** 699-707.

KAWABATA, A., KANKE, T., YONEZAWA, D., ISHIKI, T., SAKA, M., KABEYA, M., SEKIGUCHI, F., KUBO, S., KURODA, R., IWAKI, M., KATSURA, K. & PLEVIN, R. 2004. Potent and metabolically stable agonists for protease-activated receptor-2: evaluation of activity in multiple assay systems in vitro and in vivo. *J Pharmacol Exp Ther,* 309**,** 1098-107.

KAWABATA, A., NISHIKAWA, H., KURODA, R., KAWAI, K. & HOLLENBERG, M. D. 2000. Proteinase-activated receptor-2 (PAR-2): regulation of salivary and pancreatic exocrine secretion in vivo in rats and mice. *Br J Pharmacol,* 129**,** 1808-14.

KAWABATA, A., SAIFEDDINE, M., AL-ANI, B., LEBLOND, L. & HOLLENBERG, M. D. 1999. Evaluation of proteinase-activated receptor-1 (PAR1) agonists and antagonists using a cultured cell receptor desensitization assay: activation of PAR2 by PAR1-targeted ligands. *J Pharmacol Exp Ther,* 288**,** 358-70.

KELSO, E. B., LOCKHART, J. C., HEMBROUGH, T., DUNNING, L., PLEVIN, R., HOLLENBERG, M. D., SOMMERHOFF, C. P., MCLEAN, J. S. & FERRELL, W. R. 2006. Therapeutic promise of proteinase-activated receptor-2 antagonism in joint inflammation. *J Pharmacol Exp Ther,* 316**,** 1017-24.

KEOV, P., SEXTON, P. M. & CHRISTOPOULOS, A. 2011. Allosteric modulation of G protein-coupled receptors: a pharmacological perspective. *Neuropharmacology,* 60**,** 24-35.

KHEDR, M., ABDELMOTELB, A. M., PENDER, S. L. F., ZHOU, X. & WALLS, A. F. 2018. Neutrophilia, gelatinase release and microvascular leakage induced by human mast cell tryptase in a mouse model: Lack of a role of protease-activated receptor 2 (PAR2). *Clin Exp Allergy,* 48**,** 555-567.

KIM, H. Y., GOO, J. H., JOO, Y. A., LEE, H. Y., LEE, S. M., OH, C. T., AHN, S. M., KIM, N. H. & HWANG, J. S. 2012. Impact on inflammation and recovery of skin barrier by nordihydroguaiaretic Acid as a protease-activated receptor 2 antagonist. *Biomol Ther (Seoul),* 20**,** 463-9.

KLAGES, B., BRANDT, U., SIMON, M. I., SCHULTZ, G. & OFFERMANNS, S. 1999. Activation of G12/G13 results in shape change and Rho/Rho-kinase-mediated myosin light chain phosphorylation in mouse platelets. *J Cell Biol,* 144**,** 745-54.

KLEESCHULTE, S., JERRENTRUP, J., GORSKI, D., SCHMITT, J. & FENDER, A. C. 2018. Evidence for functional PAR-4 thrombin receptor expression in cardiac fibroblasts and its regulation by high glucose: PAR-4 in cardiac fibroblasts. *Int J Cardiol,* 252**,** 163-166.

KNECHT, W., COTTRELL, G. S., AMADESI, S., MOHLIN, J., SKAREGARDE, A., GEDDA, K., PETERSON, A., CHAPMAN, K., HOLLENBERG, M. D., VERGNOLLE, N. & BUNNETT, N. W. 2007. Trypsin IV or mesotrypsin and p23 cleave protease-activated receptors 1 and 2 to induce inflammation and hyperalgesia. *J Biol Chem,* 282**,** 26089-100.

KNIAZEFF, J., PREZEAU, L., RONDARD, P., PIN, J. P. & GOUDET, C. 2011. Dimers and beyond: The functional puzzles of class C GPCRs. *Pharmacol Ther,* 130**,** 9-25.

KONG, W., MCCONALOGUE, K., KHITIN, L. M., HOLLENBERG, M. D., PAYAN, D. G., BOHM, S. K. & BUNNETT, N. W. 1997. Luminal trypsin may regulate enterocytes through proteinase-activated receptor 2. *Proc Natl Acad Sci U S A,* 94**,** 8884-9.

KRAMER, R. M., ROBERTS, E. F., HYSLOP, P. A., UTTERBACK, B. G., HUI, K. Y. & JAKUBOWSKI, J. A. 1995. Differential activation of cytosolic phospholipase A2 (cPLA2) by thrombin

and thrombin receptor agonist peptide in human platelets. Evidence for activation of cPLA2 independent of the mitogen-activated protein kinases ERK1/2. *J Biol Chem,* 270**,** 14816-23.

KRISHNAN, A. & SCHIOTH, H. B. 2015. The role of G protein-coupled receptors in the early evolution of neurotransmission and the nervous system. *J Exp Biol,* 218**,** 562-71.

KRUSE, A. C., RING, A. M., MANGLIK, A., HU, J., HU, K., EITEL, K., HUBNER, H., PARDON, E., VALANT, C., SEXTON, P. M., CHRISTOPOULOS, A., FELDER, C. C., GMEINER, P., STEYAERT, J., WEIS, W. I., GARCIA, K. C., WESS, J. & KOBILKA, B. K. 2013. Activation and allosteric modulation of a muscarinic acetylcholine receptor. *Nature,* 504**,** 101-6.

KWONG, K., NASSENSTEIN, C., DE GARAVILLA, L., MEEKER, S. & UNDEM, B. J. 2010. Thrombin and trypsin directly activate vagal C-fibres in mouse lung via protease-activated receptor-1. *J Physiol,* 588**,** 1171-7.

L'ALLEMAIN, G., POUYSSEGUR, J. & WEBER, M. J. 1991. p42/mitogen-activated protein kinase as a converging target for different growth factor signaling pathways: use of pertussis toxin as a discrimination factor. *Cell Regul,* 2**,** 675-84.

LAFFERTY-WHYTE, K., MORMENEO, D. & DEL FRESNO MARIMON, M. 2017. Trial watch: Opportunities and challenges of the 2016 target landscape. *Nat Rev Drug Discov,* 16**,** 10-11.

LAGERSTROM, M. C. & SCHIOTH, H. B. 2008. Structural diversity of G protein-coupled receptors and significance for drug discovery. *Nat Rev Drug Discov,* 7**,** 339-57.

LAM, D. K. & SCHMIDT, B. L. 2010. Serine proteases and protease-activated receptor 2-dependent allodynia: a novel cancer pain pathway. *Pain,* 149**,** 263-72.

LAU, C., LYTLE, C., STRAUS, D. S. & DEFEA, K. A. 2011. Apical and basolateral pools of proteinase-activated receptor-2 direct distinct signaling events in the intestinal epithelium. *Am J Physiol Cell Physiol,* 300**,** C113-23.

LAZARENO, S., POPHAM, A. & BIRDSALL, N. J. 2000. Allosteric interactions of staurosporine and other indolocarbazoles with N-[methyl-(3)H]scopolamine and acetylcholine at muscarinic receptor subtypes: identification of a second allosteric site. *Mol Pharmacol,* 58**,** 194-207.

LEE, E. J., WOO, M. S., MOON, P. G., BAEK, M. C., CHOI, I. Y., KIM, W. K., JUNN, E. & KIM, H. S. 2010. Alpha-synuclein activates microglia by inducing the expressions of matrix metalloproteinases and the subsequent activation of protease-activated receptor-1. *J Immunol,* 185**,** 615-23.

LEE, S. M., BOOE, J. M. & PIOSZAK, A. A. 2015. Structural insights into ligand recognition and selectivity for classes A, B, and C GPCRs. *Eur J Pharmacol,* 763**,** 196-205.

LEESON, P. D. & SPRINGTHORPE, B. 2007. The influence of drug-like concepts on decision-making in medicinal chemistry. *Nat Rev Drug Discov,* 6**,** 881-90.

LIEU, T., SAVAGE, E., ZHAO, P., EDGINGTON-MITCHELL, L., BARLOW, N., BRON, R., POOLE, D. P., MCLEAN, P., LOHMAN, R. J., FAIRLIE, D. P. & BUNNETT, N. W. 2016. Antagonism of the proinflammatory and pronociceptive actions of canonical and biased agonists of protease-activated receptor-2. *Br J Pharmacol,* 173**,** 2752-65.

LIM, S. Y., WAINWRIGHT, C. L., KENNEDY, S. & KANE, K. A. 2009. Activation of protease activated receptor-2 induces delayed cardioprotection in anesthetized mice. *Cardiovasc Drugs Ther,* 23**,** 519-20.

LIPINSKI, C. A., LOMBARDO, F., DOMINY, B. W. & FEENEY, P. J. 2001. Experimental and computational approaches to estimate solubility and permeability in drug discovery and development settings. *Adv Drug Deliv Rev,* 46**,** 3-26.

LIU, J. J., HORST, R., KATRITCH, V., STEVENS, R. C. & WUTHRICH, K. 2012. Biased signaling pathways in beta2-adrenergic receptor characterized by 19F-NMR. *Science,* 335**,** 1106-10.

LOHMAN, R. J., COTTERELL, A. J., BARRY, G. D., LIU, L., SUEN, J. Y., VESEY, D. A. & FAIRLIE, D. P. 2012a. An antagonist of human protease activated receptor-2 attenuates PAR2 signaling, macrophage activation, mast cell degranulation, and collagen-induced arthritis in rats. *Faseb j,* 26**,** 2877-87.

LOHMAN, R. J., COTTERELL, A. J., SUEN, J., LIU, L., DO, A. T., VESEY, D. A. & FAIRLIE, D. P. 2012b. Antagonism of protease-activated receptor 2 protects against experimental colitis. *J Pharmacol Exp Ther,* 340**,** 256-65.

LOUBELE, S. T., SPEK, C. A., LEENDERS, P., VAN OERLE, R., ABERSON, H. L., HAMULYAK, K., FERRELL, G., ESMON, C. T., SPRONK, H. M. & TEN CATE, H. 2009. Activated protein C protects against myocardial ischemia/ reperfusion injury via inhibition of apoptosis and inflammation. *Arterioscler Thromb Vasc Biol,* 29**,** 1087-92.

LUO, J., ZHOU, W., ZHOU, X., LI, D., WENG, J., YI, Z., CHO, S. G., LI, C., YI, T., WU, X., LI, X. Y., DE CROMBRUGGHE, B., HOOK, M. & LIU, M. 2009. Regulation of bone formation and remodeling by G-protein-coupled receptor 48. *Development,* 136**,** 2747-56.

MACFARLANE, S. R., SEATTER, M. J., KANKE, T., HUNTER, G. D. & PLEVIN, R. 2001. Proteinase-activated receptors. *Pharmacol Rev,* 53**,** 245-82.

MACFARLANE, S. R., SLOSS, C. M., CAMERON, P., KANKE, T., MCKENZIE, R. C. & PLEVIN, R. 2005. The role of intracellular Ca2+ in the regulation of proteinase-activated receptor-2 mediated nuclear factor kappa B signalling in keratinocytes. *Br J Pharmacol,* 145**,** 535-44.

MAHAJAN-THAKUR, S., SOSTMANN, B. D., FENDER, A. C., BEHRENDT, D., FELIX, S. B., SCHROR, K. & RAUCH, B. H. 2014. Sphingosine-1-phosphate induces thrombin receptor PAR-4 expression to enhance cell migration and COX-2 formation in human monocytes. *J Leukoc Biol,* 96**,** 611-8.

MAO, Y., ZHANG, M., TUMA, R. F. & KUNAPULI, S. P. 2010. Deficiency of PAR4 attenuates cerebral ischemia/reperfusion injury in mice. *J Cereb Blood Flow Metab,* 30**,** 1044-52.

MARI, B., GUERIN, S., FAR, D. F., BREITMAYER, J. P., BELHACENE, N., PEYRON, J. F., ROSSI, B. & AUBERGER, P. 1996. Thrombin and trypsin-induced Ca(2+) mobilization in human T cell lines through interaction with different protease-activated receptors. *Faseb j,* 10**,** 309-16.

MARTIN, L., AUGE, C., BOUE, J., BURESI, M. C., CHAPMAN, K., ASFAHA, S., ANDRADE-GORDON, P., STEINHOFF, M., CENAC, N., DIETRICH, G. & VERGNOLLE, N. 2009. Thrombin receptor: An endogenous inhibitor of inflammatory pain, activating opioid pathways. *Pain,* 146**,** 121-9.

MARUYAMA, K., KAGOTA, S., MCGUIRE, J. J., WAKUDA, H., YOSHIKAWA, N., NAKAMURA, K. & SHINOZUKA, K. 2015. Enhanced Nitric Oxide Synthase Activation via Protease-Activated Receptor 2 Is Involved in the Preserved Vasodilation in Aortas from Metabolic Syndrome Rats. *J Vasc Res,* 52**,** 232-43.

MARYANOFF, B. E., SANTULLI, R. J., MCCOMSEY, D. F., HOEKSTRA, W. J., HOEY, K., SMITH, C. E., ADDO, M., DARROW, A. L. & ANDRADE-GORDON, P. 2001. Protease-activated receptor-2 (PAR-2): structure-function study of receptor activation by diverse peptides related to tethered-ligand epitopes. *Arch Biochem Biophys,* 386**,** 195-204.

MARYANOFF, B. E., ZHANG, H. C., ANDRADE-GORDON, P. & DERIAN, C. K. 2003. Discovery of potent peptide-mimetic antagonists for the human thrombin receptor, protease-activated receptor-1 (PAR-1). *Curr Med Chem Cardiovasc Hematol Agents,* 1**,** 13-36.

MCCOY, K. L., TRAYNELIS, S. F. & HEPLER, J. R. 2010. PAR1 and PAR2 couple to overlapping and distinct sets of G proteins and linked signaling pathways to differentially regulate cell physiology. *Mol Pharmacol,* 77**,** 1005-15.

MCCULLOCH, K., MCGRATH, S., HUESA, C., DUNNING, L., LITHERLAND, G., CRILLY, A., HULTIN, L., FERRELL, W. R., LOCKHART, J. C. & GOODYEAR, C. S. 2018. Rheumatic Disease: Protease-Activated Receptor-2 in Synovial Joint Pathobiology. *Front Endocrinol (Lausanne),* 9**,** 257.

MCGUIRE, J. J., SAIFEDDINE, M., TRIGGLE, C. R., SUN, K. & HOLLENBERG, M. D. 2004. 2-furoyl-LIGRLO-amide: a potent and selective proteinase-activated receptor 2 agonist. *J Pharmacol Exp Ther,* 309**,** 1124-31.

MCGUIRE, J. J., VAN VLIET, B. N. & HALFYARD, S. J. 2008. Blood pressures, heart rate and locomotor activity during salt loading and angiotensin II infusion in protease-activated receptor 2 (PAR2) knockout mice. *BMC Physiol,* 8**,** 20.

MCINTOSH, K., CUNNINGHAM, M. R., CADALBERT, L., LOCKHART, J., BOYD, G., FERRELL, W. R. & PLEVIN, R. 2010. Proteinase-activated receptor-2 mediated inhibition of TNFalpha-stimulated JNK activation - A novel paradigm for G(q/11) linked GPCRs. *Cell Signal,* 22**,** 265-73.

MILARDI, D. & PAPPALARDO, M. 2015. Molecular dynamics: new advances in drug discovery. *Eur J Med Chem,* 91**,** 1-3.

MIRZA, H., YATSULA, V. & BAHOU, W. F. 1996. The proteinase activated receptor-2 (PAR-2) mediates mitogenic responses in human vascular endothelial cells. *J Clin Invest,* 97**,** 1705-14.

MOLINO, M., BARNATHAN, E. S., NUMEROF, R., CLARK, J., DREYER, M., CUMASHI, A., HOXIE, J. A., SCHECHTER, N., WOOLKALIS, M. & BRASS, L. F. 1997a. Interactions of mast cell tryptase with thrombin receptors and PAR-2. *J Biol Chem,* 272**,** 4043-9.

MOLINO, M., WOOLKALIS, M. J., REAVEY-CANTWELL, J., PRATICO, D., ANDRADE-GORDON, P., BARNATHAN, E. S. & BRASS, L. F. 1997b. Endothelial cell thrombin receptors and PAR-2. Two protease-activated receptors located in a single cellular environment. *J Biol Chem,* 272**,** 11133-41.

MOLLOY, C. J., PAWLOWSKI, J. E., TAYLOR, D. S., TURNER, C. E., WEBER, H. & PELUSO, M. 1996. Thrombin receptor activation elicits rapid protein tyrosine phosphorylation and stimulation of the raf-1/MAP kinase pathway preceding delayed mitogenesis in cultured rat aortic smooth muscle cells: evidence for an obligate autocrine mechanism promoting cell proliferation induced by G-protein-coupled receptor agonist. *J Clin Invest,* 97**,** 1173-83.

MORAES, T. J., MARTIN, R., PLUMB, J. D., VACHON, E., CAMERON, C. M., DANESH, A., KELVIN, D. J., RUF, W. & DOWNEY, G. P. 2008. Role of PAR2 in murine pulmonary pseudomonal infection. *Am J Physiol Lung Cell Mol Physiol,* 294**,** L368-77.

MORAES, T. J., RAFII, B., NIESSEN, F., SUZUKI, T., MARTIN, R., VACHON, E., VOGEL, W., RUF, W., O'BRODOVICH, H. & DOWNEY, G. P. 2009. Protease-activated receptor (Par)1 alters bioelectric properties of distal lung epithelia without compromising barrier function. *Exp Lung Res,* 35**,** 136-54.

MORRIS, R., WINYARD, P. G., BRASS, L. F., BLAKE, D. R. & MORRIS, C. J. 1996. Thrombin receptor expression in rheumatoid and osteoarthritic synovial tissue. *Ann Rheum Dis,* 55**,** 841-3.

MORROW, D. A., BRAUNWALD, E., BONACA, M. P., AMERISO, S. F., DALBY, A. J., FISH, M. P., FOX, K. A., LIPKA, L. J., LIU, X., NICOLAU, J. C., OPHUIS, A. J., PAOLASSO, E., SCIRICA, B. M., SPINAR, J., THEROUX, P., WIVIOTT, S. D., STRONY, J. & MURPHY, S. A. 2012. Vorapaxar in the secondary prevention of atherothrombotic events. *N Engl J Med,* 366**,** 1404-13.

MORROW, D. A., SCIRICA, B. M., FOX, K. A., BERMAN, G., STRONY, J., VELTRI, E., BONACA, M. P., FISH, P., MCCABE, C. H. & BRAUNWALD, E. 2009. Evaluation of a novel antiplatelet agent for secondary prevention in patients with a history of atherosclerotic disease: design and rationale for the Thrombin-Receptor Antagonist in Secondary Prevention of Atherothrombotic Ischemic Events (TRA 2 degrees P)-TIMI 50 trial. *Am Heart J,* 158**,** 335-341.e3.

MYATT, A. & HILL, S. J. 2005. Trypsin stimulates the phosphorylation of p42,44 mitogen-activated protein kinases via the proteinase-activated receptor-2 and protein kinase C epsilon in human cultured prostate stromal cells. *Prostate,* 64**,** 175-85.

NAGUMO, Y., HAN, J., BELLILA, A., ISODA, H. & TANAKA, T. 2008. Cofilin mediates tight-junction opening by redistributing actin and tight-junction proteins. *Biochem Biophys Res Commun,* 377**,** 921-5.

NAKANISHI-MATSUI, M., ZHENG, Y. W., SULCINER, D. J., WEISS, E. J., LUDEMAN, M. J. & COUGHLIN, S. R. 2000. PAR3 is a cofactor for PAR4 activation by thrombin. *Nature,* 404**,** 609-13.

NALDINI, A., PUCCI, A., CARNEY, D. H., FANETTI, G. & CARRARO, F. 2002. Thrombin enhancement of interleukin-1 expression in mononuclear cells: involvement of proteinase-activated receptor-1. *Cytokine,* 20**,** 191-9.

NANTERMET, P. G., BARROW, J. C., LUNDELL, G. F., PELLICORE, J. M., RITTLE, K. E., YOUNG, M., FREIDINGER, R. M., CONNOLLY, T. M., CONDRA, C., KARCZEWSKI, J., BEDNAR, R. A., GAUL, S. L., GOULD, R. J., PRENDERGAST, K. & SELNICK, H. G. 2002. Discovery of a nonpeptidic small molecule antagonist of the human platelet thrombin receptor (PAR-1). *Bioorg Med Chem Lett,* 12**,** 319-23.

NELKEN, N. A., SOIFER, S. J., O'KEEFE, J., VU, T. K., CHARO, I. F. & COUGHLIN, S. R. 1992. Thrombin receptor expression in normal and atherosclerotic human arteries. *J Clin Invest,* 90**,** 1614-21.

NEVEU, I., JEHAN, F., JANDROT-PERRUS, M., WION, D. & BRACHET, P. 1993. Enhancement of the synthesis and secretion of nerve growth factor in primary cultures of glial cells by proteases: a possible involvement of thrombin. *J Neurochem,* 60**,** 858-67.

NGUYEN, C., COELHO, A. M., GRADY, E., COMPTON, S. J., WALLACE, J. L., HOLLENBERG, M. D., CENAC, N., GARCIA-VILLAR, R., BUENO, L., STEINHOFF, M., BUNNETT, N. W. & VERGNOLLE, N. 2003. Colitis induced by proteinase-activated receptor-2 agonists is mediated by a neurogenic mechanism. *Can J Physiol Pharmacol,* 81**,** 920-7.

NGUYEN, N., KULIOPULOS, A., GRAHAM, R. A. & COVIC, L. 2006. Tumor-derived Cyr61(CCN1) promotes stromal matrix metalloproteinase-1 production and protease-activated receptor 1-dependent migration of breast cancer cells. *Cancer Res,* 66**,** 2658-65.

NGUYEN, T. D., MOODY, M. W., STEINHOFF, M., OKOLO, C., KOH, D. S. & BUNNETT, N. W. 1999. Trypsin activates pancreatic duct epithelial cell ion channels through proteinase-activated receptor-2. *J Clin Invest,* 103**,** 261-9.

NHU, Q. M., SHIREY, K., TEIJARO, J. R., FARBER, D. L., NETZEL-ARNETT, S., ANTALIS, T. M., FASANO, A. & VOGEL, S. N. 2010. Novel signaling interactions between proteinase-activated receptor 2 and Toll-like receptors in vitro and in vivo. *Mucosal Immunol,* 3**,** 29-39.

NICHOLS, H. L., SAFFEDDINE, M., THERIOT, B. S., HEGDE, A., POLLEY, D., EL-MAYS, T., VLIAGOFTIS, H., HOLLENBERG, M. D., WILSON, E. H., WALKER, J. K. & DEFEA, K. A. 2012. beta-Arrestin-2 mediates the proinflammatory effects of proteinase-activated receptor-2 in the airway. *Proc Natl Acad Sci U S A,* 109**,** 16660-5.

NICLOU, S., SUIDAN, H. S., BROWN-LUEDI, M. & MONARD, D. 1994. Expression of the thrombin receptor mRNA in rat brain. *Cell Mol Biol (Noisy-le-grand),* 40**,** 421-8.

NIERODZIK, M. L., BAIN, R. M., LIU, L. X., SHIVJI, M., TAKESHITA, K. & KARPATKIN, S. 1996. Presence of the seven transmembrane thrombin receptor on human tumour cells: effect of activation on tumour adhesion to platelets and tumor tyrosine phosphorylation. *Br J Haematol,* 92**,** 452-7.

NIERODZIK, M. L., CHEN, K., TAKESHITA, K., LI, J. J., HUANG, Y. Q., FENG, X. S., D'ANDREA, M. R., ANDRADE-GORDON, P. & KARPATKIN, S. 1998. Protease-activated receptor 1 (PAR-1) is required and rate-limiting for thrombin-enhanced experimental pulmonary metastasis. *Blood,* 92**,** 3694-700.

NIESSEN, F., FURLAN-FREGUIA, C., FERNANDEZ, J. A., MOSNIER, L. O., CASTELLINO, F. J., WEILER, H., ROSEN, H., GRIFFIN, J. H. & RUF, W. 2009. Endogenous EPCR/aPC-PAR1 signaling prevents inflammation-induced vascular leakage and lethality. *Blood,* 113**,** 2859-66.

NIKOLAKOPOULOU, A. M., GEORGAKOPOULOS, A. & ROBAKIS, N. K. 2016. Presenilin 1 promotes trypsin-induced neuroprotection via the PAR2/ERK signaling pathway. Effects of presenilin 1 FAD mutations. *Neurobiol Aging,* 42**,** 41-9.

NIU, Q. X., CHEN, H. Q., CHEN, Z. Y., FU, Y. L., LIN, J. L. & HE, S. H. 2008. Induction of inflammatory cytokine release from human umbilical vein endothelial cells by agonists of proteinase-activated receptor-2. *Clin Exp Pharmacol Physiol,* 35**,** 89-96.

NYSTEDT, S., EMILSSON, K., LARSSON, A. K., STROMBECK, B. & SUNDELIN, J. 1995a. Molecular cloning and functional expression of the gene encoding the human proteinase-activated receptor 2. *Eur J Biochem,* 232**,** 84-9.

NYSTEDT, S., EMILSSON, K., WAHLESTEDT, C. & SUNDELIN, J. 1994. Molecular cloning of a potential proteinase activated receptor. *Proc Natl Acad Sci U S A,* 91**,** 9208-12.

NYSTEDT, S., LARSSON, A. K., ABERG, H. & SUNDELIN, J. 1995b. The mouse proteinase-activated receptor-2 cDNA and gene. Molecular cloning and functional expression. *J Biol Chem,* 270**,** 5950-55.

NYSTEDT, S., RAMAKRISHNAN, V. & SUNDELIN, J. 1996. The proteinase-activated receptor 2 is induced by inflammatory mediators in human endothelial cells. Comparison with the thrombin receptor. *J Biol Chem,* 271**,** 14910-5.

O'CALLAGHAN, K., KULIOPULOS, A. & COVIC, L. 2012. Turning receptors on and off with intracellular pepducins: new insights into G-protein-coupled receptor drug development. *J Biol Chem,* 287**,** 12787-96.

OFFERMANNS, S., LAUGWITZ, K. L., SPICHER, K. & SCHULTZ, G. 1994. G proteins of the G12 family are activated via thromboxane A2 and thrombin receptors in human platelets. *Proc Natl Acad Sci U S A,* 91**,** 504-8.

OFFERMANNS, S., TOOMBS, C. F., HU, Y. H. & SIMON, M. I. 1997. Defective platelet activation in G alpha(q)-deficient mice. *Nature,* 389**,** 183-6.

OGANESYAN, V., OGANESYAN, N., TERZYAN, S., QU, D., DAUTER, Z., ESMON, N. L. & ESMON, C. T. 2002. The crystal structure of the endothelial protein C receptor and a bound phospholipid. *J Biol Chem,* 277**,** 24851-4.

OIKONOMOPOULOU, K., HANSEN, K. K., SAIFEDDINE, M., TEA, I., BLABER, M., BLABER, S. I., SCARISBRICK, I., ANDRADE-GORDON, P., COTTRELL, G. S., BUNNETT, N. W., DIAMANDIS, E. P. & HOLLENBERG, M. D. 2006. Proteinase-activated receptors, targets for kallikrein signaling. *J Biol Chem,* 281**,** 32095-112.

OSSOVSKAYA, V. S. & BUNNETT, N. W. 2004. Protease-activated receptors: contribution to physiology and disease. *Physiol Rev,* 84**,** 579-621.

OSTROWSKA, E. & REISER, G. 2008. The protease-activated receptor-3 (PAR-3) can signal autonomously to induce interleukin-8 release. *Cell Mol Life Sci,* 65**,** 970-81.

OVERINGTON, J. P., AL-LAZIKANI, B. & HOPKINS, A. L. 2006. How many drug targets are there? *Nat Rev Drug Discov,* 5**,** 993-6.

PALCZEWSKI, K., KUMASAKA, T., HORI, T., BEHNKE, C. A., MOTOSHIMA, H., FOX, B. A., LE TRONG, I., TELLER, D. C., OKADA, T., STENKAMP, R. E., YAMAMOTO, M. & MIYANO, M. 2000. Crystal structure of rhodopsin: A G protein-coupled receptor. *Science,* 289**,** 739-45.

PAWLINSKI, R. & MACKMAN, N. 2004. Tissue factor, coagulation proteases, and protease-activated receptors in endotoxemia and sepsis. *Crit Care Med,* 32**,** S293-7.

PEREZ, M., LAMOTHE, M., MARAVAL, C., MIRABEL, E., LOUBAT, C., PLANTY, B., HORN, C., MICHAUX, J., MARROT, S., LETIENNE, R., PIGNIER, C., BOCQUET, A., NADAL-WOLLBOLD, F., CUSSAC, D., DE VRIES, L. & LE GRAND, B. 2009. Discovery of novel protease activated receptors 1 antagonists with potent antithrombotic activity in vivo. *J Med Chem,* 52**,** 5826-36.

PIKE, C. J., VAUGHAN, P. J., CUNNINGHAM, D. D. & COTMAN, C. W. 1996. Thrombin attenuates neuronal cell death and modulates astrocyte reactivity induced by beta-amyloid in vitro. *J Neurochem,* 66**,** 1374-82.

PIN, J. P., GALVEZ, T. & PREZEAU, L. 2003. Evolution, structure, and activation mechanism of family 3/C G-protein-coupled receptors. *Pharmacol Ther,* 98**,** 325-54.

PLANTY, B., PUJOL, C., LAMOTHE, M., MARAVAL, C., HORN, C., LE GRAND, B. & PEREZ, M. 2010. Exploration of a new series of PAR1 antagonists. *Bioorg Med Chem Lett,* 20**,** 1735-9.

PRZYDZIAL, M. J., BHHATARAI, B., KOLETI, A., VEMPATI, U. & SCHURER, S. C. 2013. GPCR ontology: development and application of a G protein-coupled receptor pharmacology knowledge framework. *Bioinformatics,* 29**,** 3211-9.

RALLABHANDI, P., NHU, Q. M., TOSHCHAKOV, V. Y., PIAO, W., MEDVEDEV, A. E., HOLLENBERG, M. D., FASANO, A. & VOGEL, S. N. 2008. Analysis of proteinase-activated receptor 2 and TLR4 signal transduction: a novel paradigm for receptor cooperativity. *J Biol Chem,* 283**,** 24314-25.

RAMACHANDRAN, R., EISSA, A., MIHARA, K., OIKONOMOPOULOU, K., SAIFEDDINE, M., RENAUX, B., DIAMANDIS, E. & HOLLENBERG, M. D. 2012a. Proteinase-activated receptors (PARs): differential signalling by kallikrein-related peptidases KLK8 and KLK14. *Biol Chem,* 393**,** 421-7.

RAMACHANDRAN, R., MIHARA, K., CHUNG, H., RENAUX, B., LAU, C. S., MURUVE, D. A., DEFEA, K. A., BOUVIER, M. & HOLLENBERG, M. D. 2011. Neutrophil elastase acts as a biased agonist for proteinase-activated receptor-2 (PAR2). *J Biol Chem,* 286**,** 24638-48.

RAMACHANDRAN, R., MIHARA, K., MATHUR, M., ROCHDI, M. D., BOUVIER, M., DEFEA, K. & HOLLENBERG, M. D. 2009. Agonist-biased signaling via proteinase activated receptor-2: differential activation of calcium and mitogen-activated protein kinase pathways. *Mol Pharmacol,* 76**,** 791-801.

RAMACHANDRAN, R., NOORBAKHSH, F., DEFEA, K. & HOLLENBERG, M. D. 2012b. Targeting proteinase-activated receptors: therapeutic potential and challenges. *Nat Rev Drug Discov,* 11**,** 69-86.

RASK-ANDERSEN, M., ALMEN, M. S. & SCHIOTH, H. B. 2011. Trends in the exploitation of novel drug targets. *Nat Rev Drug Discov,* 10**,** 579-90.

RASMUSSEN, S. G., CHOI, H. J., ROSENBAUM, D. M., KOBILKA, T. S., THIAN, F. S., EDWARDS, P. C., BURGHAMMER, M., RATNALA, V. R., SANISHVILI, R., FISCHETTI, R. F., SCHERTLER, G. F., WEIS, W. I. & KOBILKA, B. K. 2007. Crystal structure of the human beta2 adrenergic G-protein-coupled receptor. *Nature,* 450**,** 383-7.

RASMUSSEN, S. G., DEVREE, B. T., ZOU, Y., KRUSE, A. C., CHUNG, K. Y., KOBILKA, T. S., THIAN, F. S., CHAE, P. S., PARDON, E., CALINSKI, D., MATHIESEN, J. M., SHAH, S. T., LYONS, J. A., CAFFREY, M., GELLMAN, S. H., STEYAERT, J., SKINIOTIS, G., WEIS, W. I.,

SUNAHARA, R. K. & KOBILKA, B. K. 2011. Crystal structure of the beta2 adrenergic receptor-Gs protein complex. *Nature,* 477**,** 549-55.

REITER, E., AHN, S., SHUKLA, A. K. & LEFKOWITZ, R. J. 2012. Molecular mechanism of beta-arrestin-biased agonism at seven-transmembrane receptors. *Annu Rev Pharmacol Toxicol,* 52**,** 179-97.

RICKS, T. K. & TREJO, J. 2009. Phosphorylation of protease-activated receptor-2 differentially regulates desensitization and internalization. *J Biol Chem,* 284**,** 34444-57.

RINDERKNECHT, H., RENNER, I. G., ABRAMSON, S. B. & CARMACK, C. 1984. Mesotrypsin: a new inhibitor-resistant protease from a zymogen in human pancreatic tissue and fluid. *Gastroenterology,* 86**,** 681-92.

RITCHIE, E., SAKA, M., MACKENZIE, C., DRUMMOND, R., WHEELER-JONES, C., KANKE, T. & PLEVIN, R. 2007. Cytokine upregulation of proteinase-activated-receptors 2 and 4 expression mediated by p38 MAP kinase and inhibitory kappa B kinase beta in human endothelial cells. *Br J Pharmacol,* 150**,** 1044-54.

ROHATGI, T., SEDEHIZADE, F., REYMANN, K. G. & REISER, G. 2004. Protease-activated receptors in neuronal development, neurodegeneration, and neuroprotection: thrombin as signaling molecule in the brain. *Neuroscientist,* 10**,** 501-12.

ROOSTERMAN, D., SCHMIDLIN, F. & BUNNETT, N. W. 2003. Rab5a and rab11a mediate agonist-induced trafficking of protease-activated receptor 2. *Am J Physiol Cell Physiol,* 284**,** C1319-29.

ROSENBAUM, D. M., CHEREZOV, V., HANSON, M. A., RASMUSSEN, S. G., THIAN, F. S., KOBILKA, T. S., CHOI, H. J., YAO, X. J., WEIS, W. I., STEVENS, R. C. & KOBILKA, B. K. 2007. GPCR engineering yields high-resolution structural insights into beta2-adrenergic receptor function. *Science,* 318**,** 1266-73.

ROTHMEIER, A. S. & RUF, W. 2012. Protease-activated receptor 2 signaling in inflammation. *Semin Immunopathol,* 34**,** 133-49.

ROVIEZZO, F., DE ANGELIS, A., DE GRUTTOLA, L., BERTOLINO, A., SULLO, N., BRANCALEONE, V., BUCCI, M., DE PALMA, R., URBANEK, K., D'AGOSTINO, B., IANARO, A., SORRENTINO, R. & CIRINO, G. 2014. Involvement of proteinase activated receptor-2 in the vascular response to sphingosine 1-phosphate. *Clin Sci (Lond),* 126**,** 545-56.

RUDACK, C., STEINHOFF, M., MOOREN, F., BUDDENKOTTE, J., BECKER, K., VON EIFF, C. & SACHSE, F. 2007. PAR-2 activation regulates IL-8 and GRO-alpha synthesis by NF-kappaB, but not RANTES, IL-6, eotaxin or TARC expression in nasal epithelium. *Clin Exp Allergy,* 37**,** 1009-22.

SAIFEDDINE, M., AL-ANI, B., CHENG, C. H., WANG, L. & HOLLENBERG, M. D. 1996. Rat proteinase-activated receptor-2 (PAR-2): cDNA sequence and activity of receptor-derived peptides in gastric and vascular tissue. *Br J Pharmacol,* 118**,** 521-30.

SAIFEDDINE, M., ROY, S. S., AL-ANI, B., TRIGGLE, C. R. & HOLLENBERG, M. D. 1998. Endothelium-dependent contractile actions of proteinase-activated receptor-2-activating peptides in human umbilical vein: release of a contracting factor via a novel receptor. *Br J Pharmacol,* 125**,** 1445-54.

SALAH, Z., MAOZ, M., POKROY, E., LOTEM, M., BAR-SHAVIT, R. & UZIELY, B. 2007. Protease-activated receptor-1 (hPar1), a survival factor eliciting tumor progression. *Mol Cancer Res,* 5**,** 229-40.

SANTULLI, R. J., DERIAN, C. K., DARROW, A. L., TOMKO, K. A., ECKARDT, A. J., SEIBERG, M., SCARBOROUGH, R. M. & ANDRADE-GORDON, P. 1995. Evidence for the presence of a protease-activated receptor distinct from the thrombin receptor in human keratinocytes. *Proc Natl Acad Sci U S A,* 92**,** 9151-5.

SAWADA, K., NISHIBORI, M., NAKAYA, N., WANG, Z. & SAEKI, K. 2000. Purification and characterization of a trypsin-like serine proteinase from rat brain slices that degrades laminin and type IV collagen and stimulates protease-activated receptor-2. *J Neurochem,* 74**,** 1731-8.

SCARBOROUGH, R. M., NAUGHTON, M. A., TENG, W., HUNG, D. T., ROSE, J., VU, T. K., WHEATON, V. I., TURCK, C. W. & COUGHLIN, S. R. 1992. Tethered ligand agonist peptides. Structural requirements for thrombin receptor activation reveal mechanism of proteolytic unmasking of agonist function. *J Biol Chem,* 267**,** 13146-9.

SCHAFFHAUSER, H., ROWE, B. A., MORALES, S., CHAVEZ-NORIEGA, L. E., YIN, R., JACHEC, C., RAO, S. P., BAIN, G., PINKERTON, A. B., VERNIER, J. M., BRISTOW, L. J., VARNEY, M. A. & DAGGETT, L. P. 2003. Pharmacological characterization and identification of amino acids involved in the positive modulation of metabotropic glutamate receptor subtype 2. *Mol Pharmacol,* 64**,** 798-810.

SCHEPIS, A., BARKER, A., SRINIVASAN, Y., BALOUCH, E., ZHENG, Y., LAM, I., CLAY, H., HSIAO, C. D. & COUGHLIN, S. R. 2018. Protease signaling regulates apical cell extrusion, cell contacts, and proliferation in epithelia. *J Cell Biol,* 217**,** 1097-1112.

SCHMIDLIN, F., AMADESI, S., DABBAGH, K., LEWIS, D. E., KNOTT, P., BUNNETT, N. W., GATER, P. R., GEPPETTI, P., BERTRAND, C. & STEVENS, M. E. 2002. Protease-activated receptor 2 mediates eosinophil infiltration and hyperreactivity in allergic inflammation of the airway. *J Immunol,* 169**,** 5315-21.

SCHMIDT, V. A., NIERMAN, W. C., FELDBLYUM, T. V., MAGLOTT, D. R. & BAHOU, W. F. 1997. The human thrombin receptor and proteinase activated receptor-2 genes are tightly linked on chromosome 5q13. *Br J Haematol,* 97**,** 523-9.

SCHROR, K., BRETSCHNEIDER, E., FISCHER, K., FISCHER, J. W., PAPE, R., RAUCH, B. H., ROSENKRANZ, A. C. & WEBER, A. A. 2010. Thrombin receptors in vascular smooth muscle cells - function and regulation by vasodilatory prostaglandins. *Thromb Haemost,* 103**,** 884-90.

SCHUEPBACH, R. A., FEISTRITZER, C., FERNANDEZ, J. A., GRIFFIN, J. H. & RIEWALD, M. 2009. Protection of vascular barrier integrity by activated protein C in murine models depends on protease-activated receptor-1. *Thromb Haemost,* 101**,** 724-33.

SCOTT, G., LEOPARDI, S., PARKER, L., BABIARZ, L., SEIBERG, M. & HAN, R. 2003. The proteinase-activated receptor-2 mediates phagocytosis in a Rho-dependent manner in human keratinocytes. *J Invest Dermatol,* 121**,** 529-41.

SEATTER, M. J., DRUMMOND, R., KANKE, T., MACFARLANE, S. R., HOLLENBERG, M. D. & PLEVIN, R. 2004. The role of the C-terminal tail in protease-activated receptor-2-mediated Ca2+ signalling, proline-rich tyrosine kinase-2 activation, and mitogen-activated protein kinase activity. *Cell Signal,* 16**,** 21-9.

SEEHAUS, S., SHAHZAD, K., KASHIF, M., VINNIKOV, I. A., SCHILLER, M., WANG, H., MADHUSUDHAN, T., ECKSTEIN, V., BIERHAUS, A., BEA, F., BLESSING, E., WEILER, H., FROMMHOLD, D., NAWROTH, P. P. & ISERMANN, B. 2009. Hypercoagulability inhibits monocyte transendothelial migration through protease-activated receptor-1-, phospholipase-Cbeta-, phosphoinositide 3-kinase-, and nitric oxide-dependent signaling in monocytes and promotes plaque stability. *Circulation,* 120**,** 774-84.

SEGAL, L., KATZ, L. S., LUPU-MEIRI, M., SHAPIRA, H., SANDBANK, J., GERSHENGORN, M. C. & ORON, Y. 2014. Proteinase-activated receptors differentially modulate in vitro invasion of human pancreatic adenocarcinoma PANC-1 cells in correlation with changes in the expression of CDC42 protein. *Pancreas,* 43**,** 103-8.

SEITZBERG, J. G., KNAPP, A. E., LUND, B. W., MANDRUP BERTOZZI, S., CURRIER, E. A., MA, J. N., SHERBUKHIN, V., BURSTEIN, E. S. & OLSSON, R. 2008. Discovery of potent and selective small-molecule PAR-2 agonists. *J Med Chem,* 51**,** 5490-3.

SEKIGUCHI, F. 2005. [Development of agonists/antagonists for protease-activated receptors (PARs) and the possible therapeutic application to gastrointestinal diseases]. *Yakugaku Zasshi,* 125**,** 491-8.

SEREBRUANY, V. L., KOGUSHI, M., DASTROS-PITEI, D., FLATHER, M. & BHATT, D. L. 2009. The in-vitro effects of E5555, a protease-activated receptor (PAR)-1 antagonist, on platelet biomarkers in healthy volunteers and patients with coronary artery disease. *Thromb Haemost,* 102**,** 111-9.

SETHI, A. S., LEES, D. M., DOUTHWAITE, J. A. & CORDER, R. 2005. Factor VIIa stimulates endothelin-1 synthesis in TNF-primed endothelial cells by activation of protease-activated receptor 2. *Clin Sci (Lond),* 108**,** 255-63.

SEVIGNY, L. M., ZHANG, P., BOHM, A., LAZARIDES, K., PERIDES, G., COVIC, L. & KULIOPULOS, A. 2011. Interdicting protease-activated receptor-2-driven inflammation with cell-penetrating pepducins. *Proc Natl Acad Sci U S A,* 108**,** 8491-6.

SHAO, F., WANG, G., XIE, H., ZHU, X., SUN, J. & A, J. 2007. Pharmacokinetic study of triptolide, a constituent of immunosuppressive chinese herb medicine, in rats. *Biol Pharm Bull,* 30**,** 702-7.

SHARMA, A., TAO, X., GOPAL, A., LIGON, B., ANDRADE-GORDON, P., STEER, M. L. & PERIDES, G. 2005a. Protection against acute pancreatitis by activation of protease-activated receptor-2. *Am J Physiol Gastrointest Liver Physiol,* 288**,** G388-95.

SHARMA, A., TAO, X., GOPAL, A., LIGON, B., STEER, M. L. & PERIDES, G. 2005b. Calcium dependence of proteinase-activated receptor 2 and cholecystokinin-mediated amylase secretion from pancreatic acini. *Am J Physiol Gastrointest Liver Physiol,* 289**,** G686-95.

SHIN, H., NAKAJIMA, T., KITAJIMA, I., SHIGETA, K., ABEYAMA, K., IMAMURA, T., OKANO, T., KAWAHARA, K., NAKAMURA, T. & MARUYAMA, I. 1995. Thrombin receptor-mediated synovial proliferation in patients with rheumatoid arthritis. *Clin Immunol Immunopathol,* 76**,** 225-33.

SHOCK, D. D., HE, K., WENCEL-DRAKE, J. D. & PARISE, L. V. 1997. Ras activation in platelets after stimulation of the thrombin receptor, thromboxane A2 receptor or protein kinase C. *Biochem J,* 321 (Pt 2)**,** 525-30.

SHPACOVITCH, V., FELD, M., HOLLENBERG, M. D., LUGER, T. A. & STEINHOFF, M. 2008. Role of protease-activated receptors in inflammatory responses, innate and adaptive immunity. *J Leukoc Biol,* 83**,** 1309-22.

SINGH, V. P., BHAGAT, L., NAVINA, S., SHARIF, R., DAWRA, R. K. & SALUJA, A. K. 2007. Protease-activated receptor-2 protects against pancreatitis by stimulating exocrine secretion. *Gut,* 56**,** 958-64.

SOH, U. J., DORES, M. R., CHEN, B. & TREJO, J. 2010. Signal transduction by protease-activated receptors. *Br J Pharmacol,* 160**,** 191-203.

SOKOLOVA, E. & REISER, G. 2007. A novel therapeutic target in various lung diseases: airway proteases and protease-activated receptors. *Pharmacol Ther,* 115**,** 70-83.

STALHEIM, L., DING, Y., GULLAPALLI, A., PAING, M. M., WOLFE, B. L., MORRIS, D. R. & TREJO, J. 2005. Multiple independent functions of arrestins in the regulation of protease-activated receptor-2 signaling and trafficking. *Mol Pharmacol,* 67**,** 78-87.

STEINHOFF, M., BUDDENKOTTE, J., SHPACOVITCH, V., RATTENHOLL, A., MOORMANN, C., VERGNOLLE, N., LUGER, T. A. & HOLLENBERG, M. D. 2005. Proteinase-activated receptors: transducers of proteinase-mediated signaling in inflammation and immune response. *Endocr Rev,* 26**,** 1-43.

STEINHOFF, M., VERGNOLLE, N., YOUNG, S. H., TOGNETTO, M., AMADESI, S., ENNES, H. S., TREVISANI, M., HOLLENBERG, M. D., WALLACE, J. L., CAUGHEY, G. H., MITCHELL, S. E., WILLIAMS, L. M., GEPPETTI, P., MAYER, E. A. & BUNNETT, N. W. 2000. Agonists

of proteinase-activated receptor 2 induce inflammation by a neurogenic mechanism. *Nat Med,* 6**,** 151-8.

STENKAMP, R. E., TELLER, D. C. & PALCZEWSKI, K. 2002. Crystal structure of rhodopsin: a G-protein-coupled receptor. *Chembiochem,* 3**,** 963-7.

STEVENS, R. C., CHEREZOV, V., KATRITCH, V., ABAGYAN, R., KUHN, P., ROSEN, H. & WUTHRICH, K. 2013. The GPCR Network: a large-scale collaboration to determine human GPCR structure and function. *Nat Rev Drug Discov,* 12**,** 25-34.

STOYANOV, B., VOLINIA, S., HANCK, T., RUBIO, I., LOUBTCHENKOV, M., MALEK, D., STOYANOVA, S., VANHAESEBROECK, B., DHAND, R., NURNBERG, B. & ET AL. 1995. Cloning and characterization of a G protein-activated human phosphoinositide-3 kinase. *Science,* 269**,** 690-3.

STRANDE, J. L., HSU, A., SU, J., FU, X., GROSS, G. J. & BAKER, J. E. 2008. Inhibiting protease-activated receptor 4 limits myocardial ischemia/reperfusion injury in rat hearts by unmasking adenosine signaling. *J Pharmacol Exp Ther,* 324**,** 1045-54.

SUEN, J. Y., BARRY, G. D., LOHMAN, R. J., HALILI, M. A., COTTERELL, A. J., LE, G. T. & FAIRLIE, D. P. 2012. Modulating human proteinase activated receptor 2 with a novel antagonist (GB88) and agonist (GB110). *Br J Pharmacol,* 165**,** 1413-23.

SUEN, J. Y., COTTERELL, A., LOHMAN, R. J., LIM, J., HAN, A., YAU, M. K., LIU, L., COOPER, M. A., VESEY, D. A. & FAIRLIE, D. P. 2014. Pathway-selective antagonism of proteinase activated receptor 2. *Br J Pharmacol,* 171**,** 4112-24.

SYEDA, F., GROSJEAN, J., HOULISTON, R. A., KEOGH, R. J., CARTER, T. D., PALEOLOG, E. & WHEELER-JONES, C. P. 2006. Cyclooxygenase-2 induction and prostacyclin release by protease-activated receptors in endothelial cells require cooperation between mitogen-activated protein kinase and NF-kappaB pathways. *J Biol Chem,* 281**,** 11792-804.

TAKIZAWA, T., TAMIYA, M., HARA, T., MATSUMOTO, J., SAITO, N., KANKE, T., KAWAGOE, J. & HATTORI, Y. 2005. Abrogation of bronchial eosinophilic inflammation and attenuated eotaxin content in protease-activated receptor 2-deficient mice. *J Pharmacol Sci,* 98**,** 99-102.

TANAKA, Y., SEKIGUCHI, F., HONG, H. & KAWABATA, A. 2008. PAR2 triggers IL-8 release via MEK/ERK and PI3-kinase/Akt pathways in GI epithelial cells. *Biochem Biophys Res Commun,* 377**,** 622-626.

TAUTERMANN, C. S. 2014. GPCR structures in drug design, emerging opportunities with new structures. *Bioorg Med Chem Lett,* 24**,** 4073-9.

TRICOCI, P., HUANG, Z., HELD, C., MOLITERNO, D. J., ARMSTRONG, P. W., VAN DE WERF, F., WHITE, H. D., AYLWARD, P. E., WALLENTIN, L., CHEN, E., LOKHNYGINA, Y., PEI, J., LEONARDI, S., RORICK, T. L., KILIAN, A. M., JENNINGS, L. H., AMBROSIO, G., BODE, C., CEQUIER, A., CORNEL, J. H., DIAZ, R., ERKAN, A., HUBER, K., HUDSON, M. P., JIANG, L., JUKEMA, J. W., LEWIS, B. S., LINCOFF, A. M., MONTALESCOT, G., NICOLAU, J. C., OGAWA, H., PFISTERER, M., PRIETO, J. C., RUZYLLO, W., SINNAEVE, P. R., STOREY, R. F., VALGIMIGLI, M., WHELLAN, D. J., WIDIMSKY, P., STRONY, J., HARRINGTON, R. A. & MAHAFFEY, K. W. 2012. Thrombin-receptor antagonist vorapaxar in acute coronary syndromes. *N Engl J Med,* 366**,** 20-33.

TRIPATHI, A., LAMMERS, K. M., GOLDBLUM, S., SHEA-DONOHUE, T., NETZEL-ARNETT, S., BUZZA, M. S., ANTALIS, T. M., VOGEL, S. N., ZHAO, A., YANG, S., ARRIETTA, M. C., MEDDINGS, J. B. & FASANO, A. 2009. Identification of human zonulin, a physiological modulator of tight junctions, as prehaptoglobin-2. *Proc Natl Acad Sci U S A,* 106**,** 16799-804.

UEHARA, A., MURAMOTO, K., IMAMURA, T., NAKAYAMA, K., POTEMPA, J., TRAVIS, J., SUGAWARA, S. & TAKADA, H. 2005. Arginine-specific gingipains from

Porphyromonas gingivalis stimulate production of hepatocyte growth factor (scatter factor) through protease-activated receptors in human gingival fibroblasts in culture. *J Immunol,* 175**,** 6076-84.

UNGEFROREN, H., WITTE, D., FIEDLER, C., GADEKEN, T., KAUFMANN, R., LEHNERT, H., GIESELER, F. & RAUCH, B. H. 2017. The Role of PAR2 in TGF-beta1-Induced ERK Activation and Cell Motility. *Int J Mol Sci,* 18.

UUSITALO-JARVINEN, H., KUROKAWA, T., MUELLER, B. M., ANDRADE-GORDON, P., FRIEDLANDER, M. & RUF, W. 2007. Role of protease activated receptor 1 and 2 signaling in hypoxia-induced angiogenesis. *Arterioscler Thromb Vasc Biol,* 27**,** 1456-62.

VACHHARAJANI, N. N., YELESWARAM, K. & BOULTON, D. W. 2003. Preclinical pharmacokinetics and metabolism of BMS-214778, a novel melatonin receptor agonist. *J Pharm Sci,* 92**,** 760-72.

VALANT, C., ROBERT LANE, J., SEXTON, P. M. & CHRISTOPOULOS, A. 2012. The best of both worlds? Bitopic orthosteric/allosteric ligands of g protein-coupled receptors. *Annu Rev Pharmacol Toxicol,* 52**,** 153-78.

VAN BIESEN, T., LUTTRELL, L. M., HAWES, B. E. & LEFKOWITZ, R. J. 1996. Mitogenic signaling via G protein-coupled receptors. *Endocr Rev,* 17**,** 698-714.

VAN DER MERWE, J. Q., HOLLENBERG, M. D. & MACNAUGHTON, W. K. 2008. EGF receptor transactivation and MAP kinase mediate proteinase-activated receptor-2-induced chloride secretion in intestinal epithelial cells. *Am J Physiol Gastrointest Liver Physiol,* 294**,** G441-51.

VANDELL, A. G., LARSON, N., LAXMIKANTHAN, G., PANOS, M., BLABER, S. I., BLABER, M. & SCARISBRICK, I. A. 2008. Protease-activated receptor dependent and independent signaling by kallikreins 1 and 6 in CNS neuron and astroglial cell lines. *J Neurochem,* 107**,** 855-70.

VENKATAKRISHNAN, A. J., DEUPI, X., LEBON, G., TATE, C. G., SCHERTLER, G. F. & BABU, M. M. 2013. Molecular signatures of G-protein-coupled receptors. *Nature,* 494**,** 185-94.

VERGNOLLE, N., CELLARS, L., MENCARELLI, A., RIZZO, G., SWAMINATHAN, S., BECK, P., STEINHOFF, M., ANDRADE-GORDON, P., BUNNETT, N. W., HOLLENBERG, M. D., WALLACE, J. L., CIRINO, G. & FIORUCCI, S. 2004. A role for proteinase-activated receptor-1 in inflammatory bowel diseases. *J Clin Invest,* 114**,** 1444-56.

VERSTEEG, H. H., SCHAFFNER, F., KERVER, M., ELLIES, L. G., ANDRADE-GORDON, P., MUELLER, B. M. & RUF, W. 2008. Protease-activated receptor (PAR) 2, but not PAR1, signaling promotes the development of mammary adenocarcinoma in polyoma middle T mice. *Cancer Res,* 68**,** 7219-27.

VOURET-CRAVIARI, V., BOQUET, P., POUYSSEGUR, J. & VAN OBBERGHEN-SCHILLING, E. 1998. Regulation of the actin cytoskeleton by thrombin in human endothelial cells: role of Rho proteins in endothelial barrier function. *Mol Biol Cell,* 9**,** 2639-53.

VU, T. K., HUNG, D. T., WHEATON, V. I. & COUGHLIN, S. R. 1991. Molecular cloning of a functional thrombin receptor reveals a novel proteolytic mechanism of receptor activation. *Cell,* 64**,** 1057-68.

WACKER, D., WANG, C., KATRITCH, V., HAN, G. W., HUANG, X. P., VARDY, E., MCCORVY, J. D., JIANG, Y., CHU, M., SIU, F. Y., LIU, W., XU, H. E., CHEREZOV, V., ROTH, B. L. & STEVENS, R. C. 2013. Structural features for functional selectivity at serotonin receptors. *Science,* 340**,** 615-9.

WANG, H., MOREAU, F., HIROTA, C. L. & MACNAUGHTON, W. K. 2010. Proteinase-activated receptors induce interleukin-8 expression by intestinal epithelial cells through ERK/RSK90 activation and histone acetylation. *Faseb j,* 24**,** 1971-80.

WANG, H. & REISER, G. 2003. Thrombin signaling in the brain: the role of protease-activated receptors. *Biol Chem,* 384**,** 193-202.

WANG, H., UBL, J. J., STRICKER, R. & REISER, G. 2002. Thrombin (PAR-1)-induced proliferation in astrocytes via MAPK involves multiple signaling pathways. *Am J Physiol Cell Physiol,* 283**,** C1351-64.

WANG, L., LUO, J., FU, Y. & HE, S. 2006a. Induction of interleukin-8 secretion and activation of ERK1/2, p38 MAPK signaling pathways by thrombin in dermal fibroblasts. *Int J Biochem Cell Biol,* 38**,** 1571-83.

WANG, M., AN, S., WANG, D., JI, H., GUO, X. & WANG, Z. 2018. Activation of PAR4 Upregulates p16 through Inhibition of DNMT1 and HDAC2 Expression via MAPK Signals in Esophageal Squamous Cell Carcinoma Cells. *J Immunol Res,* 2018**,** 4735752.

WANG, P. & DEFEA, K. A. 2006. Protease-activated receptor-2 simultaneously directs beta-arrestin-1-dependent inhibition and Galphaq-dependent activation of phosphatidylinositol 3-kinase. *Biochemistry,* 45**,** 9374-85.

WANG, P., KUMAR, P., WANG, C. & DEFEA, K. A. 2007a. Differential regulation of class IA phosphoinositide 3-kinase catalytic subunits p110 alpha and beta by protease-activated receptor 2 and beta-arrestins. *Biochem J,* 408**,** 221-30.

WANG, Y., LUO, W. & REISER, G. 2007b. The role of calcium in protease-activated receptor-induced secretion of chemokine GRO/CINC-1 in rat brain astrocytes. *J Neurochem,* 103**,** 814-9.

WANG, Y., LUO, W., WARTMANN, T., HALANGK, W., SAHIN-TOTH, M. & REISER, G. 2006b. Mesotrypsin, a brain trypsin, activates selectively proteinase-activated receptor-1, but not proteinase-activated receptor-2, in rat astrocytes. *J Neurochem,* 99**,** 759-69.

WARNE, T. & TATE, C. G. 2013. The importance of interactions with helix 5 in determining the efficacy of beta-adrenoceptor ligands. *Biochem Soc Trans,* 41**,** 159-65.

WEI, H., AHN, S., SHENOY, S. K., KARNIK, S. S., HUNYADY, L., LUTTRELL, L. M. & LEFKOWITZ, R. J. 2003. Independent beta-arrestin 2 and G protein-mediated pathways for angiotensin II activation of extracellular signal-regulated kinases 1 and 2. *Proc Natl Acad Sci U S A,* 100**,** 10782-7.

WEINSTEIN, J. R., GOLD, S. J., CUNNINGHAM, D. D. & GALL, C. M. 1995. Cellular localization of thrombin receptor mRNA in rat brain: expression by mesencephalic dopaminergic neurons and codistribution with prothrombin mRNA. *J Neurosci,* 15**,** 2906-19.

WHORTON, M. R., BOKOCH, M. P., RASMUSSEN, S. G., HUANG, B., ZARE, R. N., KOBILKA, B. & SUNAHARA, R. K. 2007. A monomeric G protein-coupled receptor isolated in a high-density lipoprotein particle efficiently activates its G protein. *Proc Natl Acad Sci U S A,* 104**,** 7682-7.

WOJTUKIEWICZ, M. Z., TANG, D. G., BEN-JOSEF, E., RENAUD, C., WALZ, D. A. & HONN, K. V. 1995. Solid tumor cells express functional "tethered ligand" thrombin receptor. *Cancer Res,* 55**,** 698-704.

WONG, P. C., SEIFFERT, D., BIRD, J. E., WATSON, C. A., BOSTWICK, J. S., GIANCARLI, M., ALLEGRETTO, N., HUA, J., HARDEN, D., GUAY, J., CALLEJO, M., MILLER, M. M., LAWRENCE, R. M., BANVILLE, J., GUY, J., MAXWELL, B. D., PRIESTLEY, E. S., MARINIER, A., WEXLER, R. R., BOUVIER, M., GORDON, D. A., SCHUMACHER, W. A. & YANG, J. 2017. Blockade of protease-activated receptor-4 (PAR4) provides robust antithrombotic activity with low bleeding. *Sci Transl Med,* 9.

WU, C. C., HWANG, T. L., LIAO, C. H., KUO, S. C., LEE, F. Y., LEE, C. Y. & TENG, C. M. 2002. Selective inhibition of protease-activated receptor 4-dependent platelet activation by YD-3. *Thromb Haemost,* 87**,** 1026-33.

WU, J., LIU, T. T., ZHOU, Y. M., QIU, C. Y., REN, P., JIAO, M. & HU, W. P. 2017. Sensitization of ASIC3 by proteinase-activated receptor 2 signaling contributes to acidosis-induced nociception. *J Neuroinflammation,* 14**,** 150.

WU, Y., ZHANG, X., ZHOU, H., CHEN, D., XIE, H., MU, Y., WU, B. & YAN, J. 2013. Factor VIIa regulates the expression of caspase-3, MMP-9, and CD44 in SW620 colon cancer cells involving PAR2/MAPKs/NF-kappaB signaling pathways. *Cancer Invest,* 31**,** 7-16.

WYGRECKA, M., DIDIASOVA, M., BERSCHEID, S., PISKULAK, K., TABORSKI, B., ZAKRZEWICZ, D., KWAPISZEWSKA, G., PREISSNER, K. T. & MARKART, P. 2013. Protease-activated receptors (PAR)-1 and -3 drive epithelial-mesenchymal transition of alveolar epithelial cells - potential role in lung fibrosis. *Thromb Haemost,* 110**,** 295-307.

XU, W., LIM, J., GOH, C. Y., SUEN, J. Y., JIANG, Y., YAU, M. K., WU, K. C., LIU, L. & FAIRLIE, D. P. 2015. Repurposing Registered Drugs as Antagonists for Protease-Activated Receptor 2. *J Chem Inf Model,* 55**,** 2079-84.

XU, W. F., ANDERSEN, H., WHITMORE, T. E., PRESNELL, S. R., YEE, D. P., CHING, A., GILBERT, T., DAVIE, E. W. & FOSTER, D. C. 1998. Cloning and characterization of human protease-activated receptor 4. *Proc Natl Acad Sci U S A,* 95**,** 6642-6.

YANG, E., BOIRE, A., AGARWAL, A., NGUYEN, N., O'CALLAGHAN, K., TU, P., KULIOPULOS, A. & COVIC, L. 2009. Blockade of PAR1 signaling with cell-penetrating pepducins inhibits Akt survival pathways in breast cancer cells and suppresses tumor survival and metastasis. *Cancer Res,* 69**,** 6223-31.

YAU, M. K., LIU, L., SUEN, J. Y., LIM, J., LOHMAN, R. J., JIANG, Y., COTTERELL, A. J., BARRY, G. D., MAK, J. Y., VESEY, D. A., REID, R. C. & FAIRLIE, D. P. 2016a. PAR2 Modulators Derived from GB88. *ACS Med Chem Lett,* 7**,** 1179-1184.

YAU, M. K., SUEN, J. Y., XU, W., LIM, J., LIU, L., ADAMS, M. N., HE, Y., HOOPER, J. D., REID, R. C. & FAIRLIE, D. P. 2016b. Potent Small Agonists of Protease Activated Receptor 2. *ACS Med Chem Lett,* 7**,** 105-10.

YONA, S., LIN, H. H., SIU, W. O., GORDON, S. & STACEY, M. 2008. Adhesion-GPCRs: emerging roles for novel receptors. *Trends Biochem Sci,* 33**,** 491-500.

YU, Z., AHMAD, S., SCHWARTZ, J. L., BANVILLE, D. & SHEN, S. H. 1997. Protein-tyrosine phosphatase SHP2 is positively linked to proteinase-activated receptor 2-mediated mitogenic pathway. *J Biol Chem,* 272**,** 7519-24.

ZANNONI, A., BOMBARDI, C., DONDI, F., MORINI, M., FORNI, M., CHIOCCHETTI, R., SPADARI, A. & ROMAGNOLI, N. 2014. Proteinase-activated receptor 2 expression in the intestinal tract of the horse. *Res Vet Sci,* 96**,** 464-71.

ZHANG, C., GAO, G. R., LV, C. G., ZHANG, B. L., ZHANG, Z. L. & ZHANG, X. F. 2012a. Protease-activated receptor-2 induces expression of vascular endothelial growth factor and cyclooxygenase-2 via the mitogen-activated protein kinase pathway in gastric cancer cells. *Oncol Rep,* 28**,** 1917-23.

ZHANG, C., SRINIVASAN, Y., ARLOW, D. H., FUNG, J. J., PALMER, D., ZHENG, Y., GREEN, H. F., PANDEY, A., DROR, R. O., SHAW, D. E., WEIS, W. I., COUGHLIN, S. R. & KOBILKA, B. K. 2012b. High-resolution crystal structure of human protease-activated receptor 1. *Nature,* 492**,** 387-92.

ZHANG, H., JIANG, P., ZHANG, C., LEE, S., WANG, W. & ZOU, H. 2018. PAR4 overexpression promotes colorectal cancer cell proliferation and migration. *Oncol Lett,* 16**,** 5745-5752.

ZHANG, H. C., DERIAN, C. K., ANDRADE-GORDON, P., HOEKSTRA, W. J., MCCOMSEY, D. F., WHITE, K. B., POULTER, B. L., ADDO, M. F., CHEUNG, W. M., DAMIANO, B. P., OKSENBERG, D., REYNOLDS, E. E., PANDEY, A., SCARBOROUGH, R. M. & MARYANOFF, B. E. 2001. Discovery and optimization of a novel series of thrombin

receptor (par-1) antagonists: potent, selective peptide mimetics based on indole and indazole templates. *J Med Chem,* 44**,** 1021-4.

ZHANG, X., WANG, H., MA, Z. & WU, B. 2014. Effects of pharmaceutical PEGylation on drug metabolism and its clinical concerns. *Expert Opin Drug Metab Toxicol,* 10**,** 1691-702.

ZHAO, P., LIEU, T., BARLOW, N., METCALF, M., VELDHUIS, N. A., JENSEN, D. D., KOCAN, M., SOSTEGNI, S., HAERTEIS, S., BARAZNENOK, V., HENDERSON, I., LINDSTROM, E., GUERRERO-ALBA, R., VALDEZ-MORALES, E. E., LIEDTKE, W., MCINTYRE, P., VANNER, S. J., KORBMACHER, C. & BUNNETT, N. W. 2014. Cathepsin S causes inflammatory pain via biased agonism of PAR2 and TRPV4. *J Biol Chem,* 289**,** 27215-34.

ZHAO, P., LIEU, T., BARLOW, N., SOSTEGNI, S., HAERTEIS, S., KORBMACHER, C., LIEDTKE, W., JIMENEZ-VARGAS, N. N., VANNER, S. J. & BUNNETT, N. W. 2015. Neutrophil Elastase Activates Protease-activated Receptor-2 (PAR2) and Transient Receptor Potential Vanilloid 4 (TRPV4) to Cause Inflammation and Pain. *J Biol Chem,* 290**,** 13875-87.

ZOUDILOVA, M., KUMAR, P., GE, L., WANG, P., BOKOCH, G. M. & DEFEA, K. A. 2007. Beta-arrestin-dependent regulation of the cofilin pathway downstream of protease-activated receptor-2. *J Biol Chem,* 282**,** 20634-46.

ZOUDILOVA, M., MIN, J., RICHARDS, H. L., CARTER, D., HUANG, T. & DEFEA, K. A. 2010. beta-Arrestins scaffold cofilin with chronophin to direct localized actin filament severing and membrane protrusions downstream of protease-activated receptor-2. *J Biol Chem,* 285**,** 14318-29.